4-2019

Regulation of Vaccinia Virus Replication: a Story of Viral Mimicry and a Novel Antagonistic Relationship Between Vaccinia Kinase and Pseudokinase

Annabel T. Olson
University of Nebraska-Lincoln, aolson18@huskers.unl.edu

REGULATION OF VACCINIA VIRUS REPLICATION: A STORY OF VIRAL MIMICRY AND A NOVEL ANTAGONISTIC RELATIONSHIP BETWEEN VACCINIA KINASE AND PSEUDOKINASE

by

Annabel T. Olson

A DISSERTATION

Presented to the Faculty of

The Graduate College at the University of Nebraska

In Partial Fulfillment of Requirements

For the Degree of Doctor of Philosophy

Major: Biological Sciences

(Genetics, Cell, and Molecular Biology)

Under the Supervision of Professor Matthew S. Wiebe

Lincoln, Nebraska

April, 2019

SUPERVISORY COMMITTEE SIGNATURES

SUPERVISORY COMMITTEE:

Matt Wiebe, Ph.D. (Primary Advisor)

Deb Brown, Ph.D.

Audrey Atkin, Ph.D.

Luwen Zhang, Ph.D.

Asit Pattnaik, Ph.D.

APPROVED

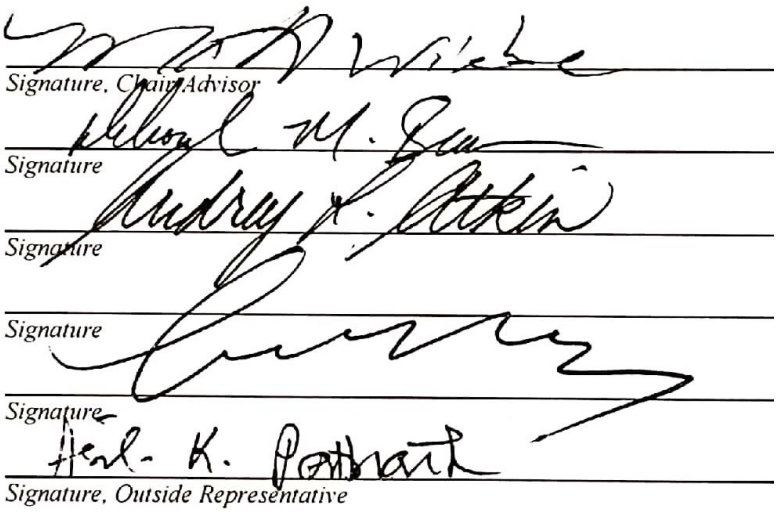

Signature, Chair/Advisor

Signature

Signature

Signature

Signature

Signature, Outside Representative

Final grade for all incomplete dissertation hours: P

Approved: 4.17.19

Signature, Chair/Advisor *Date*

Regulation of vaccinia virus replication: A story of viral mimicry and a novel antagonistic relationship between vaccinia kinase and pseudokinase

Annabel T. Olson, Ph.D.

University of Nebraska, 2019

Advisor: Matthew S. Wiebe

Poxviruses employ sophisticated signaling pathways that thwart cellular defense mechanisms and simultaneously ensure viral factors are modulated properly. Yet, our understanding of these complex signaling networks are incomplete. For example, the vaccinia B1 kinase plays a vital role in inactivating the cellular antiviral factor BAF, and is suggested to orchestrate other pathways. B1 is highly conserved among poxviruses and exhibits a remarkable degree of similarity to VRKs, a family of cellular kinases, suggesting that the viral enzyme has evolved to mimic VRK activity. Indeed, B1 and VRKs have been demonstrated to target a shared substrate, the DNA binding protein BAF, elucidating a signaling pathway important for mitosis and the antiviral response. Our research further characterized the role of B1 during vaccinia infection to gain novel insights into its regulation and integration with cellular signaling pathways.

We began by constructing and characterizing the first B1 deletion virus (ΔB1). Then using this virus, we tested the hypothesis that cellular VRKs can complement B1 function, and discovered a VRK2 role in facilitating DNA replication in the absence of B1. Study of the VRK2 mechanism revealed that B1 and VRK2 mediate DNA replication via an additional pathway that is BAF independent.

We also utilized the ΔB1 virus in an experimental evolution assay to perform an unbiased search for suppressor mutations and identify novel pathways involving B1.

Interestingly, our characterization of the adapted viruses reveals that mutations correlating with a loss of function of the vaccinia B12 pseudokinase provide a striking fitness enhancement to this virus. Next, B12 characterization showed a nuclear localization, unique for poxvirus proteins, that is related to its repressive function. Our data indicate that B12 is not a global repressor, but inhibits vaccinia replication in the absence of the B1 kinase. The mechanism of B12 partially depends on suppression of BAF antiviral activity. However, the parallel B12 pathway to restrict virus replication is less clear. Together, our studies of B1 and B12 present novel evidence that a paralogous kinase-pseudokinase pair can exhibit a unique epistatic relationship in a virus, and orchestrate yet-to-be-discovered nuclear events during infection.

DEDICATION

This doctoral dissertation thesis is dedicated to my parents David and Diana Olson who support me constantly through their love and prayers. By the graces of God my mom is with us today to see me graduate. My mom was diagnosed with stage IV pancreatic cancer in November 2015 and is now in remission since November 2018. She is truly our miracle. God is good.

ACKNOWLEDGMENTS

When they say it takes a village to raise a child, the same can be said for a doctoral recipient. This achievement was not obtained without the support and guidance of many mentors, colleagues/friends and family members.

I feel extremely fortunate to have been advised by Matt Wiebe over my graduate education. His guidance in my personal life, professional development and training as a researcher has greatly contributed to my success as a virologist and growth as an individual. In addition to my training in virology research, learning from Matt's leadership roles in our lab and at the faculty and university levels has been an outstanding example of what a good mentor and colleague looks like. From his example, I will strive to emulate his kindness and insistent drive in order to be a good mentor and colleague to others.

Recognition of my graduate committee members Deb Brown, Audrey Atkin, Asit Pattnaik, and Luwen Zhang is also a necessity for their contributions to my development as a researcher. They challenged my critical thinking skills and ability to articulate my research achievements and proposals. Deb recognized my talent in soft skills and encouraged me to develop this area. She also provided an excellent example of a passionate and skilled educator and researchers who knows the importance of lab community. Each of my committee members welcomed informal meetings and these discussions were some of the best conversations, as I maneuvered through the challenges during my graduate degree.

The previous and current members of the Wiebe lab have been extremely supportive over my time here. I am grateful for the training and patience of Augusta Jamin and April Wicklund during my first years of research in the Wiebe lab and the fellowship of Zhigang Wang, Angela Mercurio, Shawna Fitzwater, Amber Rico, Allie Linville, and Luisa Valencia.

I am grateful for the guidance and friendship of my colleagues Jessica Hargarten, Yen Ahmad Hussin, Kay Kimpston-Burkgren, Nacho Correas, Dane Bowder, Alex Vogel, Anna Lampe, Nicole Bacheller, Eric Noel, Sara Privatt, and the graduate students at the NCV.

The staff members at the NCV have been wonderful to work with, especially Jan Edwards who always greeted me with a warm smile and words of encouragement.

My friends outside of graduate school have also been extremely supportive during this time in graduate school including Grace Regan Reid, Tim Reid, Kelsey Nelson, Allie Klug Dunham, Alicia Wagner Gotto, Katie Johnson Harmelink, Kairsten Nelson, Christie Gleason Lewandoski, and Connor Johnson.

Lastly, my family has been my strong pillar throughout graduate school. I am so thankful for their many visits, long phone conversations and many prayers. The pilgrimages we took together and discussions of God have led me down this current path. Thank you Dad, Mom, Chris, Hailey, Logan, Sophia, Marty, Kathy, and Cordelia for bringing so much happiness and light into my life.

Thank you Lord for all of these people and the ones that are not mentioned, but still impacted by successful achievement of becoming a doctoral recipient.

PREFACE

Chapters 3 and 4, expect section 4.1, have been published in *Journal of Virology*. (Olson, AT. Rico, AB. Wang, Z. Delhon, G. Wiebe, MS. Deletion of the Vaccinia B1 Kinase Reveals Essential Function of this Enzyme Complemented Partly by the Homologous Cellular Kinase VRK2. J Virol. 2017 Jul 12; 91(15). pii: e00635-17. doi: 10.1128/JVI.00635-17)

Chapters 5 and 6, except parts of 5.3, 6.2, and 6.4-6.7, have been published in *PLOS Pathogens*. (Olson, AT. Wang, Z. Rico, AB. Wiebe, MS. A poxvirus pseudokinase represses viral DNA replication via a pathway antagonized by its paralog kinase. PLoS Pathog. 2019 Feb 15;15(2):e1007608. doi: 10.1371/journal.ppat.1007608)

TABLE OF CONTENTS

ABBREVIATIONS LIST

AATI	Advanced Analytical Technical Instruments
AIM2	Absent in melanoma 2
ATP	Adenosine tri-phosphate
BAF	Barrier-to-autointegration factor
BAX	B-cell lymphoma associated X
Bcl-2	B-cell lymphoma 2
Bcl-xL	B-cell lymphoma 2 like 1
BrdU	Bromodeoxyuridine
CRISPR/Cas9	Clustered regularly interspaced short palindromic repeats/CRISPR associated gene 9
CrmA	Cytokine response modifier A
ctrl	Control
Cts	Condit collection of temperature sensitive mutant viruses
DEDs	Death-effector domains
DMEM	Dulbecco's modified Eagle's medium
DNA	Deoxyribonucleic acid
dsDNA	Double-stranded DNA
E. coli	Escherichia coli
EBV	Epstein-Barr Virus
ER	Endoplasmic reticulum
ERK2	Extracellular signal regulated kinase 2
ERp29	Endoplasmic reticulum resident protein 29
FADD	FAS-associated with death domain
FBS	Fetal bovine serum
G-A	Guanine to adenine change
GAPDH	Glyceraldehyde 3-phosphate dehydrogenase
GC	Guanine-cytosine nucleotides
GFP	Green fluorescence protein
Golgi	Golgi apparatus
GSEA	Gene set enrichment analysis
HAP1	Human, near haploid cells
IKK	Inhibitor of κB kinase
IMDM	Iscove's Modified Dulbecco's Medium
indel	Insertion or deletion
IRAK2	Interleukin 1 receptor associated kinase 2
ITRs	Inverted terminal repeats
IκBα	Inhibitor of κBα

kDa	Kilodaltons
MAP	Mitogen-activated protein
MEM	Minimal essential medium
miR	microRNA
MOI	Multiplicity of infection
NF-κB	Nuclear factor kappa beta
OFTu	Ovine fetal turbinate primary cells
ORF	Open reading frame
ORFV	ORF virus
p53	Tumor protein 53
PAMPs	Pathogen associated molecular patterns
PCR	Polymerase chain reaction
PDI	Protein disulfide isomerase
PFAS	Phosphoribosylformylglycinamidine synthetase
PKR	Interferon-inducible RNA-dependent protein kinase
PRRs	Pattern recognition receptors
PyV	Polyomavirus
qPCR	Qunatitative PCR
RACK	Receptor for activated C kinase
RIG-I	Retinoic acid-inducible gene I
RIN	RNA integrity number
RNA	Ribonucleic acid
Ser	Serine
shCtrl	Short hairpin RNA control
siCtrl	Small interfering RNA control
SNP	Single nucleotide polymorphism
SPACA6	Sperm acrosome associated 6
SPI-2	Serine protease inhibitor 2
TA system	Toxin antitoxin system
TCID50	tissue culture infectious dose 50
tet	Tetracycline
Thr	Threonine
TK(-)	Thymidine kinase-negative
TLRs	Toll-like receptors
TRAF6	Tumor necrosis factor receptor-associated factor 6
ts	Temperature sensitive
vGAT	Viral glutamine aminotransferase
VP	Viral protein
VRK	Vaccinia-related kinase
VRK1KO	Vaccinia-related kinase 1 knockout
VRK2KO	Vaccinia-related kinase 2 knockout
WT	Wild type vaccinia virus
ΔB1	B1 kinase deletion vaccinia virus

FIGURES LIST

CHAPTER 1

INTRODUCTION

This Ph.D. dissertation thesis will introduce the vaccinia virus life cycle and recurring themes of viral mimicry of host factors and modulators of vaccinia DNA replication. The aims addressed include 1) Determine how cellular vaccinia-related kinases (VRKs) complement functionally for vaccinia B1 kinase and 2) Identify viral factors capable of regulating the signaling axis of host barrier-to-autointegration factor (BAF) antiviral activity and vaccinia B1 kinase countermeasure to affect DNA replication. Addressing these gaps in knowledge will inform boarder themes of kinase contributions to virus replication and host range specificity, as well as, virus countermeasures to DNA-targeting BAF antiviral activity against virus replication.

1.1. POXVIRIDAE FAMILY

Poxviruses are large double-stranded DNA viruses, which carry out all stages of their lifecycle in the cytoplasm of infected cells (1). Vaccinia virus, the prototypical poxvirus, has a genome 195 kb in size, which encodes approximately 200 proteins (2). These proteins are expressed in a temporally regulated cascade of early, intermediate, and late stages of gene expression. Close to half of poxviral proteins are expressed early in infection and include virally encoded DNA replication machinery and viral transcription factors (2). Also among the early proteins are numerous viral factors capable of interacting with host proteins and modulating host signaling cascades (3). Studies of the host mechanisms targeted by vaccinia proteins have provided fascinating insights into how cellular signaling can be redirected to create an environment favorable to an infecting pathogen.

1.1.A. History

The family *Poxviridae* classifies a group of cytoplasmic replicating viruses with species specific genera in vertebrae and insect hosts. Two subfamilies include viruses that are human pathogens; *Orthopoxvirus variola* and *Mulluscipoxvirus molluscum contagiosum.* The variola virus is the etiological agent of smallpox. The smallpox pathology in humans is characterized by a skin rash. However, at the time of rash presentation the virus had already spread from the typical respiratory site of inoculation into the blood and specific organs before epithelial presentation between 13 - 24 days later. Ulcers form at the mucosal membranes and raised pox on the skin develops. Resolution of the infection occurs for most, although the mortality rate is high, exceeding 30-40%. Predominantly two *Orthopoxviruses,* cowpox virus and vaccinia virus were used to vaccinate against smallpox, and successful eradication was achieved by 1980 following a smallpox eradication program. Despite eradication of variola virus from circulation, instances of zoonosis occur most commonly for monkeypox virus to humans. Additionally, the risk of variola virus use as a bioterrorism threat supports the continued research of poxviruses and development of better protective vaccines against poxviruses.

The historical significance of poxviruses is also attributed to the discovery of vaccinia virus and use of this virus, in conjunction with cowpox virus, for vaccination against smallpox and inform insights into the research of mammalian viruses. Vaccinia virus was the first animal virus seen microscopically, grown in tissue culture, quantified via titration and chemically analyzed. This virus has been used as the prototypical poxvirus and contributed to our understanding of the poxvirus life cycle and many themes including, but not limited to, host-pathogen interaction at the cellular and

molecular levels. Furthermore, use of vaccinia virus and relative, myxoma virus as genetically engineered oncolytic virotherapeutics has immense promise (4). Specifically, myxoma virus has a limited host range that restricts replication in human cells, although permits replication in many cancer cell lines (5) likely due to compromised innate signaling. Attenuated viruses have been generated with a variety of trans genes, yet the most promising direction is the combination of virotherapy and immunotherapy for cancer treatment. Specifically, viruses can be used to deliver a transgene directly to cancer cells and create an immunogenic environment via cell lysis and activation of the immune response cancer cell antigens. Transitioning into the molecular mechanism of host-pathogen interaction, the intracellular signaling pathways that occur during poxvirus infection can be used to inform vaccine and virotherapy design through the study of intracellular pathways that can be manipulated to improve activation of immune cells and antigen presentation.

1.1.B. Genome

The vaccinia virus genome is 195 KB in size, which is considered a large DNA virus. The double-stranded DNA genome is composed of two linear strands of DNA that are joined by AT-rich tandem repeat sequence, termed inverted terminal repeats (ITRs). The ITRs form a loop structure at the terminus of each linear DNA strand, aligning and connecting the two DNA strands and forming a closed loop lacking exposed DNA ends. These ITRs base pair due to the repeat sequence, although there are a number of single or double unpaired bases within this region. It is possible that having unpaired bases in the ITRs contributes to DNA condensation and alternatively a nick DNA site for initiation of DNA replication.

Another contributor of DNA compaction is the percentage of guanine and cytosine base pairs over adenine and thymine pairing, using three or two hydrogen bonds respectively. The human genome has a large range of average GC content between 35% and 60% in a 100 KB fragment (6). The herpes simplex virus dsDNA genome has a relatively high GC content. Lower GC content was identified in intergenic regions and corresponded with enrichment of retrotranspostition events, suggesting that a high GC content may protect viral genes from invasion by mobile genetic elements (7). Viruses within the *Poxviridae* family range in GC content between ~18% and 64% (8). *Orthopoxvirus* genus have about 36% GC richness, while *Parapoxvirus* genus have about 64% genome GC content (8). It is unclear why such a variation in GC content exists for poxviruses or how viral and cellular factors contributing to gene expression and replication may select for higher or lower GC content. To speculate briefly, there is a curious correlation between high GC content in poxviruses and the absence of viral B1 kinase known to regulate DNA condensation factor, BAF. Specifically, B1 may allow for a AT-rich genome, which is favorable for recombination or invading transposons. While poxviruses do differ by much more than solely the presence or absence of the B1 kinase for low and high GC containing viruses, the question of if B1 contributes to a flexible genome and enhanced DNA fragment scavenging is quite a compelling idea.

The coding capacity of poxviruses is quite extensive. The cowpox virus genome includes the core poxvirus genes in addition to all the variable genes in other *Orthopoxviruses.* For this reason, the cowpox virus is thought to be the closest genetic match to the ancestor poxvirus for this genus. The other *Orthopoxviruses* have smaller genomes than cowpox (Fig 1.1) and these genomes are marked with single nucleotide

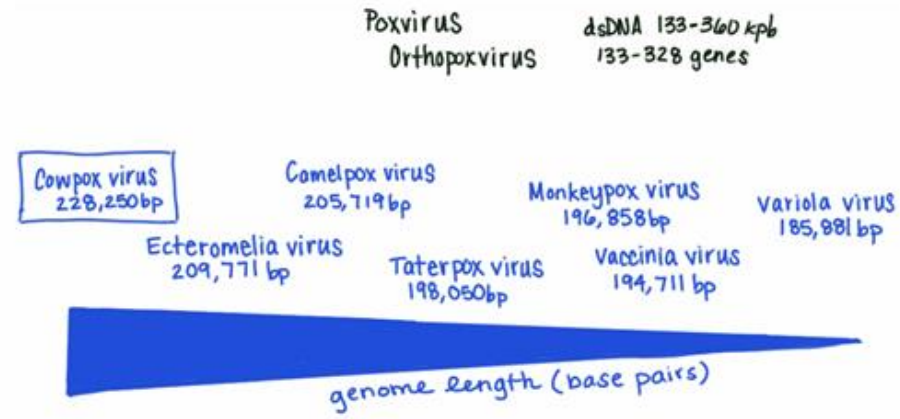

Fig 1.1. Orthopoxvirus genome length. The genome size for a few *Orthopoxviruses* is illustrated to emphasize that cowpox virus contains all conserved core genes and less conserved genes present in all other *Orthopoxviruses.* This indicates that loss of coding sequence has resulted for the other *Orthopoxviruses*, which aligns with preliminary data supporting gene loss as a poxvirus adaptation scheme. The genome sequence lengths were taken from NCBκGenome database.

polymorphisms (SNPs) and gene fragmentations likely caused by insertion/ deletion (indel) mutations and gene deletions (9). Interestingly, ectermelia and camelpox viruses have between 8-10% base pair loss as compared to coxpox virus (Fig 1.1). Taterpox, monkeypox, and vaccinia are reduced by 13-15% coding sequence, while the variola virus genome has 18.6% fewer base pairs than cowpox virus (Fig 1.1). It is tantalizing to ponder why gene loss is observed. Possibly to overcome changes in immune factors between species or utilize cellular factors more efficiently due to initial gene loss events? Gene loss as an adaptive mechanism for poxviruses is indeed supported (9, 10), and begs the question, are poxviruses limited by this adaptation mechanism to a single host with improbable cross species infection?

To argue against restrictive outcome of gene loss adaptation scheme, suppression of growth defective phenotypes for other vaccinia mutants occurs via rapid poxviral gene amplification and gain of function mutations (11, 12). These examples illustrate gene loss or amplification as dynamic mechanisms of poxvirus adaptation, yet the consistent reduction of coding sequence for other *Orthopoxviruses* as compared to cowpox virus could hint at a higher frequency of gene loss over gene amplification adaptation.

1.1.C. Vaccinia virus life cycle

Being the prototypical poxvirus, vaccinia virus life cycle has been well characterized, while gaps in knowledge continue to be studied. Such areas of uncertainty will be indicated throughout this section on the viral life cycle. To begin, the vaccinia virus virion entry into the cell occurs by endocytosis or via a binding and fusion mechanism (Fig 1.2-1) between entry-fusion proteins located on the mature virion membrane and cellular glycosaminoglycans on the plasma membrane. The specific

binding receptors on the cell are not known. However, viral entry does not require tested glycosaminoglycans, suggesting entry mechanisms independent of fusogenic properties exist. Endosomal acidification (13) in combination with actin and ezrin-containing protrusions (14) facilitate entry, indicating an endocytosis mechanism is employed as an alternative entry method. Following entry, the viral core along with viral proteins packaged into the lateral bodies situated on either side of the viral core are released into the cytosol. The core changes in conformation (Fig 1.2-2) and is trafficked along the microtubules of the cell near to the endoplasmic reticulum (15). The core contains the viral genome, a DNA-dependent RNA polymerase, early transcription factors, and other proteins required for transcription. Furthermore, packaging of these proteins is critical, due to early transcription occurring within the viral cores (Fig 1.2-3). These early transcripts, capped and polyadenylated by viral proteins to resemble eukaryotic mRNA, are extruded from the core for translation by the cellular ribosome and translational machinery in the cytoplasm.

Next, the proteins that compose the core are degraded (Fig 1.2-4) in a process referred to as uncoating, which describes the exposure of the viral genome from its protective compartment. Importantly, the uncoating process requires the synthesis of early proteins and coincides with the end of early transcription. Specifically, the core proteins fail to be degraded without early proteins. In addition to uncoating functions, early proteins participate in replication of the viral DNA (16), restriction of immune signaling (17, 18), and transcription of intermediate genes (19). The regulation of gene expression is coordinated by different promoter sequences and

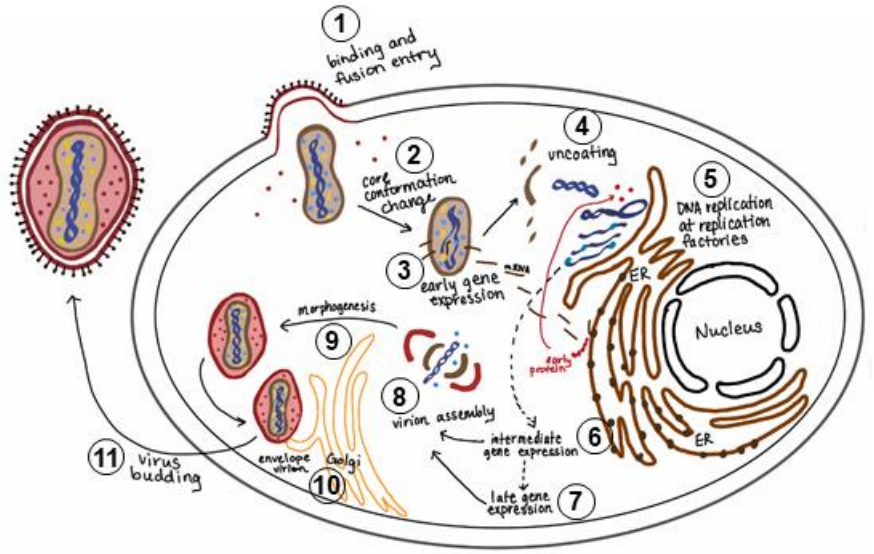

Fig 1.2. Vaccinia virus life cycle. Vaccinia virus entry into a host cell occurs via a binding and fusion action [1]. The core released into the cytoplasm is trafficked along microtubules and undergoes a conformational change [2]. Following this step, early gene expression occurs within the core [3], leading to expression of gene required for uncoating [4]. At this time, the viral genome near ER membranes is incorporated into replication factories. These replication factories are sites of DNA replication [5], intermediate gene expression [6] and late gene expression [7]. Following these stages, the virion is assembled [8], undergoes morphogenesis [9] into a mature virion, which can exit the cell via cell lysis. Alternatively, wrapping of the mature virions in the trans Golgi membrane [10] produces an enveloped mature virion that can bud from the cell [11].

transcription factors, which are synthesized just prior to the requirement for the specific stage of gene expression. Furthermore, rapid mRNA turnover (20, 21) enhances the impact of these specific transcription factors, assisting in the coordinated transition to the next stage of gene expression.

The step following uncoating orients the viral DNA into replication factories near or consisting of ER membranes. Within these replication factories, DNA replication (Fig 1.2-5), intermediate gene expression (Fig 1.2-6), and late gene expression (Fig 1.2-7) occurs. The replication of viral DNA is predicted to initiate at a nick in the DNA, which allows strand displacement DNA replication. However, evidence of smaller DNA-RNA fragments is suggestive of lagging strand synthesis. Recent discoveries of a viral primase (22) and cellular ligase that can complement for viral ligase activity (23) support this alternative lagging strand replication or recombination-dependent mechanism of DNA synthesis. As replication proceeds, concatemeric structures are formed where the synthesized DNA is linked to another DNA strand by a repeat sequence of DNA discussed above as ITRs. The DNA concatemers must be resolved into genome unit molecules to generate progeny virus, but this occurs at a later step.

Transcription of intermediate genes has a less specific promoter sequence than early genes. Alternatively, the late gene promoter region is characterized by an A/T rich core followed by a longer initiator sequence which is unique for late genes. Intermediate genes encode a variety of proteins including late gene transcription factors, and late genes encode proteins important for capsid formation and factors packaged into the virion to support early transcription within the viral core (1).

The membrane that makes the immature virion was shown to be derived from the ER (24-27). Formation of crescent membranes has been observed (Fig 1.2-8) with a dense nucleoprotein mass entering it to form immature virions. Interestingly before the virions change morphologically into mature virions, the concatemeric replicated DNA must be resolved into single genome units (28). At a point following this step, the immature virion undergoes an alteration in morphology from a sphere to a barrel-shaped particle (Fig 1.2-9). Morphogenesis is also characterized by the addition of membrane proteins to the virion exterior and internal core protein processing and reorganization. At this stage the virus can lyse the cell for release or be enveloped (Fig 1.2-10) by the trans Gogli membrane (29, 30) and then bud from the cell (Fig 1.2-11). The budding of an enveloped virion results in a single additional membrane for the enveloped virion as compared to the mature virion. Furthermore, an important step in subsequent infection of mature versus enveloped virions seems to be the removal of the single membrane envelope before association of the virus to the cell membrane. Specifically, proteins that reside on the mature virion membrane must be available to interact with the cell plasma membrane for entry. Overall, the general vaccinia virus life cycle is known. However, the molecular mechanisms to carry out this intricate process are still being revealed. The further study of non-essential genes and identification of cellular complementary proteins aids our discovery of essential or necessary viral protein functions.

1.1.D. Innate immunity

Poxviruses encode a number of proteins to facilitate innate and adaptive immune evasion. This section will specifically address mechanisms of innate immunity evasion. Poxviruses encode homologs of innate immune countermeasures, while also utilizing

alternative mechanisms to evade the host response. The divergence in countermeasures for poxviruses is likely due to adaptation in the various hosts.

The host detects viral DNA, RNA and responds to poxvirus infection through multiple pattern recognition receptors (PRRs). The vaccinia virus counters signaling by toll-like receptors (TLRs) via Bcl-2 like structured proteins (31). Other poxviruses encode homologs to these proteins (32) and likely function to counter innate immune signaling through TLRs as well. Sensing of viral nucleic acid through AIM2 inflammasome (33) and RNA polymerase III (34) intracellular proteins and the latter of the two is restricted by vaccinia E3 protein. Therefore, despite providing pathogen associated molecular patterns (PAMPs), poxviruses counter detection or signaling through TLRs.

Downstream of TLRs, the NF-κB transcription factor complex activates in response to sensed viral infection and coordinates expression of inflammatory genes (35). Poxvirus infection activates NF-κB during infection as shown during infection with a modified vaccinia Ankara virus (36). In contrast to this attenuated virus, wild-type (WT) vaccinia virus expresses proteins that target PKR (37, 38), extracellular signal regulated kinase 2 (ERK2) (39), and TLR adaptor proteins which are upstream viral sensors that activate the NF-κB signaling pathway. The viral countermeasures target multiple proteins of the signaling cascade from the TLR initiating signal. Specifically, a vaccinia virus Bcl-2-like protein prevents TLRs TRAF6 and IRAK2 signaling (40-42), which is upstream of NF-κB activation. Similarly, vaccinia virus and ORFV each express one or more viral proteins that binds directly to IKK, which restricts NF-κB activation (43, 44). Alternatively, molluscum contagiosum encodes a protein the increases IKK degradation

in order to restrict NF-κB activation. Additionally, Ankryin-repeat proteins encoded by vaccinia virus and many *Orthopoxviruses* interact with NF-κB, blocking NF-κB phosphorylation and nuclear translocation. Interestingly, ORFV and myxoma virus both express a protein that mediates this same function, although these proteins lack homology to the *Orthopoxvirus* ankryin-repeat proteins.

Poxviruses also express proteins that coordinate restriction of host apoptosis signaling. This section will highlight both extrinsic and intrinsic apoptotic pathways. The extrinsic pathway began by ligand binding to death receptor on the plasma membrane, signaling cascade to activate caspase 8, and subsequent caspase 3 activation. The intrinsic pathway is mediated by changes in the mitochondria in response to a number of different stimuli including cell cycle dysregulation, DNA damage, pathogen sensing, and hypoxia. The signaling cascade occurs to activate caspase 9, which in turn signals for caspase 3 activation. The execution pathway follows caspase 3 activation and results in the activation of endonuclease and protease activity, cytomorphological changes, and formation of apoptotic bodies as reviewed (45).

The death receptors of the extrinsic apoptosis signaling pathway are inhibited by vaccinia cytokine response modifier A (CrmA) or SPI-2 (46), a viral protein with homology to cellular serine protease inhibitor (SPI) superfamily. *Orthopoxvirus* CrmA/SPI-2 also has a restrictive function on caspase 8 activation (47, 48), downstream of the death receptor signaling. The molluscum contagium virus encodes two proteins with death-effector domains (DEDs), one of which can interact with FADD and caspases (49). Interestingly, despite having restrictive properties on apoptosis, the DED domains were not required for apoptosis restriction (50). Alternatively, interaction with the

inhibitor of κB kinase (IKK) was discovered (51), yet confirmation of this interaction as essential for repressing apoptosis has not been published.

The intrinsic pathway of apoptosis signaling is targeted by viral factors as well. Signaling of apoptosis through the mitochondria includes cytochrome C release from the mitochondria to activate caspase 9. The *Orthopoxvirus* Bcl-2-like proteins discussed in NF-κB countermeasures are also able to restrict cytochrome release in addition to prevent activation of pro-apoptotic proteins, Bak and Bax. Separate from the Bcl-2-like proteins, vaccinia expresses a multifunctional anti-apoptotic protein that can restrict caspase 9 activation and a recent discovery uncovered a role of vaccinia protein to repress the apoptosome and prevent caspase 9 activation (52). Other poxvirus proteins have been shown to restrict induction of apoptosis through both extrinsic and intrinsic pathways, although the specific molecular mechanism is uncharacterized.

Poxviruses, incite proteins from their viral repertoire to counteract host anti-viral signaling through PRRs, NK-κB, apoptosis, and others not summarized here. The interplay between host-virus interactions has fostered evolution of immune response factors and viral countermeasures. Specifically, poxviruses often have redundant countermeasures to antiviral host defense measures as shown by many of these proteins being non-essential when deleted signally and evidence of multiple proteins targeting the same signaling pathway. Furthermore, co-evolution is apparent between virus and host, as poxviruses often mimic host factors in order to bind and restrict host antiviral signaling.

1.1.E. Viral mimicry elicited for counteracting innate immunity

The examples of viral mimicry are most apparent for viral factors that counter the host anti-viral response, although other examples exist. A well characterized group of virus mimics is the Bcl-2 like proteins that modulate apoptosis signaling as recently reviewed (31, 32). Multiple poxviruses encode Bcl-2 like proteins that are not always similar in the amino acid sequence to the mammalian Bcl-2 proteins, however share structurally similar protein folds and conserved domains (53). These Bcl-2 like proteins bind to mammalian Bcl-2 proteins to restrict cell death signaling by pro-apoptotic proteins (54-57). Alternatively, other viral Bcl-2 like proteins restrict signaling through TLRs to activate NF-κB (40, 41, 58-62). This is a clear example of how viral homologs of cellular factors are strategically used to disassemble the host innate immune response to poxvirus infection.

A more recent finding was the molecular mimicry of the cellular inhibitor of κB (IκB)α by a vaccinia virus protein (63). The impact of the viral IκBα mimic is the restricted binding of the cellular factor to the E3 ubiquitin ligase for ubiquitination and degradation. The blocked degradation of IκBα allows for the IκBα-NFκB interaction to be maintained, resulting in retention of NFκB in the cytoplasm and the absence of inflammatory gene expression through NFκB. This viral mimic therefore competes with the cellular homolog for binding to a shared substrate as a countermeasure to the host anti-viral signaling.

Together these viral mimics illustrate how the virus can manipulate the host antiviral response. Specifically, viral proteins with structural or sequence homology and conserved interaction domains as compared to host proteins allows for sequestering of

pro-apoptotic proteins or competition between factors to mediate restricted host responses. Therefore, viral mimicry is a useful mechanism of evading the host immune response.

1.2. VACCINIA B1 KINASE VIRUS MIMICRY OF HOST VACCINIA-RELATED KINASES

Protein kinases regulate the function of a large fraction of cellular proteins, governing numerous molecular processes (64-66). However, much remains unknown about how this class of proteins is regulated and what evolutionary mechanisms may have driven their conservation in all kingdoms of life as well as viruses. Investigation of B1 and F10 kinases and H1 phosphatase encoded by poxviruses has provided fascinating insights into how these factors dysregulate host signaling pathways and orchestrate viral protein function. Expressed early during infection, the product of the vaccinia *B1R* gene encodes the B1 Ser/Thr kinase vital for productive infection with a clear role in impairing at least one facet of the host antiviral response (67-69). B1 homologs are highly conserved within the members of the Poxviridae family that infect mammals, with the only exceptions being the Molluscipoxvirus and Parapoxvirus genera (Fig 1.3). Interestingly, a group of eukaryotic kinases have homology (~40% amino acid identity) to the vaccinia B1 protein (70-73). These proteins are named vaccinia related kinases (VRKs) and have been found to share at least one common substrate with B1, demonstrating that the B1/VRK enzymes represent an intersection of viral and host signaling pathways and an example of viral mimicry of a cellular factor.

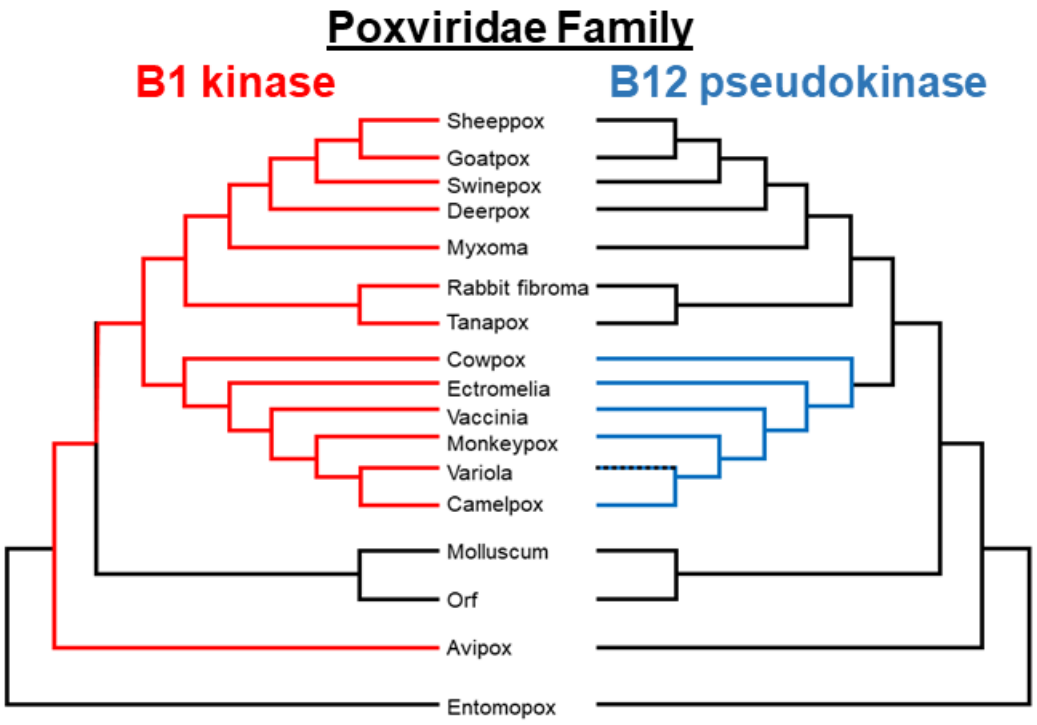

Fig 1.3. Conservation of B1 kinase and B12 pseudokinase in Poxviridae family. The conservation of the *B1R* (red) and *B12R* (blue) genes is overlaid on the Poxviridae family phylogenetic tree generated in Hughes et al (74). A dotted black line is depicted for the variola virus *B12R* gene to illustrate that the 5' end of the gene is present in the virus, despite the 3' end being truncated and not predicted to express a protein.

1.2.A. Vaccinia virus B1 kinase

The vaccinia B1 protein kinase is essential for productive infection and has a clear role in restricting at least one intrinsic immune factor. Much of what we know regarding the function of B1 is based on studies of temperature-sensitive mutant viruses (Cts2 and Cts25) with point mutations in the B1 locus (67, 68). Biochemical and genetic analyses of these mutant viruses and kinases indicates that during infection the altered proteins are expressed, but are considerably more labile than wild-type B1, and have severely reduced catalytic activity (75). Phenotypically, progeny of these B1-deficient viruses are markedly reduced in number during infection at non-permissive temperatures, due to critical defects in viral DNA replication (67, 75). B1 known signaling is summarized (Fig 1.4). Importantly, while wild-type B1 is vital to productive infection in all cell lines tested to date, the severity of the Cts2 virus phenotype is cell type dependent (68, 76, 77). This suggests that functional activity of the mutant B1 protein and/or its substrates may be impacted by host enzymes, which may partially complement for B1 in some cell types.

Furthermore, to ensure replication of the vaccinia genome, it is critical that B1 phosphorylate the cellular protein BAF, encoded by the *BANF1* gene. BAF is a highly conserved DNA-binding protein with essential cellular functions related to maintaining genomic integrity via diverse pathways (78). For example, BAF is capable of intercepting cytoplasmic DNA and assembling higher-order DNA-protein assemblies (79, 80). This allows BAF to strongly inhibit vaccinia virus DNA replication (69) and intermediate transcription (81). Importantly, this host defense activity of BAF against vaccinia virus is dependent on its DNA-binding property, which can be blocked through

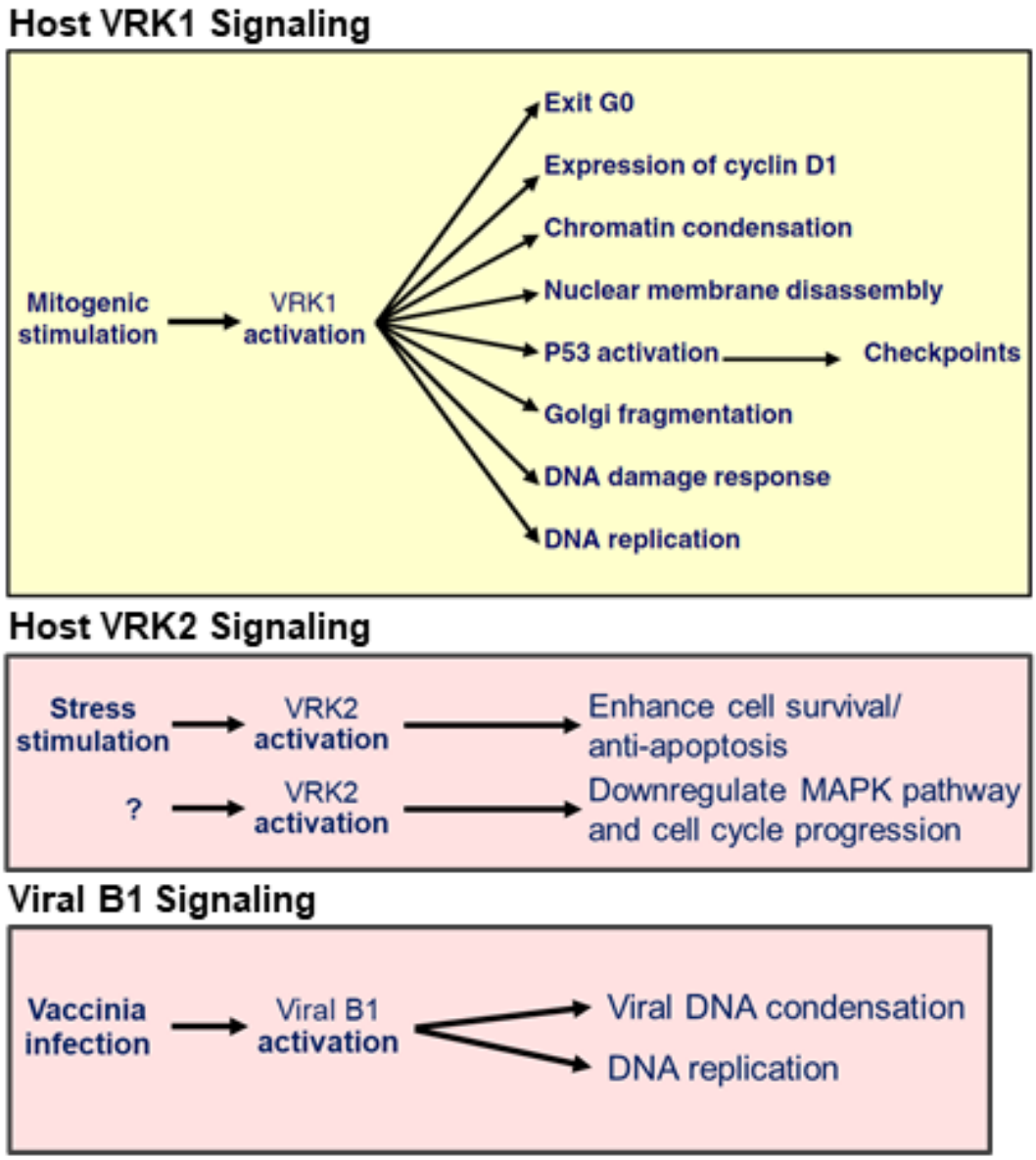

Fig 1.4. Signaling pathways of VRK1, VRK2 and B1 kinases. The signaling pathways for the cellular vaccinia-related kinase 1 and 2 are compared to the vaccinia virus B1 homolog. The VRK1 signaling image was borrowed from a VRK1 review article (82). The VRK2 and B1 signaling pathways were generated from primary literature as referenced specifically in the body of the text.

phosphorylation mediated by B1 (69, 83), thus allowing poxvirus DNA replication to proceed.

Although BAF phosphorylation by B1 clearly enhances viral fitness, genetic and biochemical studies indicate that B1 likely contributes to poxviral replication via other pathways as well. For example, RACK1 (receptor for activated C kinase) is phosphorylated in a B1 dependent manner, triggering a selective advantage for translation of viral RNAs that is postulated to enhance viral fitness late in infection (84). Some other known substrates of the B1 kinase include the ribosomal Sa and S2 proteins (85) as well as the viral H5 multi-functional protein (86, 87), each of which can be directly phosphorylated by B1 in vitro and is modified in a B1-dependent manner in infected cells. However, although it has been known for some time that these proteins are substrates of B1, whether their phosphorylation by B1 is beneficial during the poxvirus lifecycle remains unclear.

1.2.B. Cellular vaccinia-related kinases (VRKs)

The casein family of kinases includes the vaccinia virus related kinases (VRKs) VRK1, VRK2, and VRK3, which are highly conserved in vertebrates and a single VRK protein in *Drosophila melanogaster* and *Caenorhabditis elegans* (88, 89). The discovery that this group of eukaryotic Ser/Thr kinases have homology (~40% identity) to the vaccinia *B1* gene led them to be named vaccinia virus-related kinases (VRKs) (70-72). These kinases are constitutively expressed in a range of cell types (90) and have high sequence conservation between mouse and human homologs (72). These are typical criteria of essential and/or impactful cellular factors as indicated by selected conservation despite changing evolutionary pressures. Furthermore, these kinases have clear sequence

conservation within the domains required for kinase activity (72), potentially indicative of overlapping substrates. Other regions of the VRKs are unique and are responsible for directing distinct subcellular localizations and functions. For example, VRK1 is predominantly located in the nucleus while the major isoform of VRK2 is associated with the endoplasmic reticulum and nuclear envelope (72, 91). Importantly, the divergence of these kinases to localize in separate compartments will also impact the regulation of shared substrates.

The majority of research has focused on the role of VRK1 in the nucleus to regulate factors contributing to cell cycle progression and mediate upstream signaling to inhibit apoptosis as summarized (Fig 1.4). However, there is less known about the role of VRK2 in the cytoplasmic compartment. The signaling pathways regulated by VRK2 are summarized in Fig 1.4. Both VRK1 and VRK2 transcripts were associated with fetal-specific genes upregulated in high proliferative cells (70), indicative of kinase functions during embryonic development. Furthermore, our attempts to deplete VRK1 from a VRK2 knockout cell line resulted in cell death, and single VRK1 knockouts result in infertility (88, 92). Together, research of the VRKs support critical roles for cell growth and organism procreation. Interestingly, both VRK1 and VRK2 possess strong catalytic activity found to modulate cellular processes including mitosis and apoptosis via multiple substrates (89, 93-95). It has also been demonstrated that VRK2 limits cell death during Epstein-Barr Virus (EBV) infection (96) and delays myxoma replication in a breast cancer cell line (97), thus providing other examples that VRKs may regulate pathways important during viral infection.

Importantly, these findings support the model that B1 activity may be complemented in some cells by these host enzymes. Indeed, functional conservation of these viral and cellular kinases has been demonstrated by (i) evidence that VRK1 can rescue the Cts2 viral DNA replication defect when expressed from the Cts2 virus genome under a viral promoter (73), and (ii) the discovery that B1 and VRK1 share the same cellular substrate, BAF (98). Together, the study of VRKs can inform the function of the vaccinia B1 kinase and vice versa to contribute to our interpretation of VRK roles in the host.

1.2.C. Cellular barrier-to-autointegration factor (BAF) substrate

The most well characterized substrate of both B1 and the VRKs is BAF, a highly conserved DNA-binding protein with essential cellular functions. BAF expression is needed for survival and differentiation of both human and mouse embryonic stem cells, and the depletion or knockout of BAF in *Caenorhabditis elegans* and *Drosophila melanogaster* is embryonically lethal (80, 99). BAF has also been implicated in human disease; a point mutation within the BAF-coding region has been identified in two patients presenting with a hereditary progeroid disease called Nestor-Guillermo progeria syndrome (100). The molecular underpinnings of these defects are likely multifactorial (101), as BAF functions during mitosis and other processes integral to maintaining genomic integrity. In addition to these cellular functions, BAF is also capable of strongly inhibiting vaccinia virus DNA replication (69, 83) and intermediate transcription (81). The host defense activity of BAF against vaccinia virus is dependent on its DNA-binding property (Fig 1.5A), where BAF interacts with the phosphate backbone of the virus dsDNA minor groove. A key interaction that is blocked by B1-

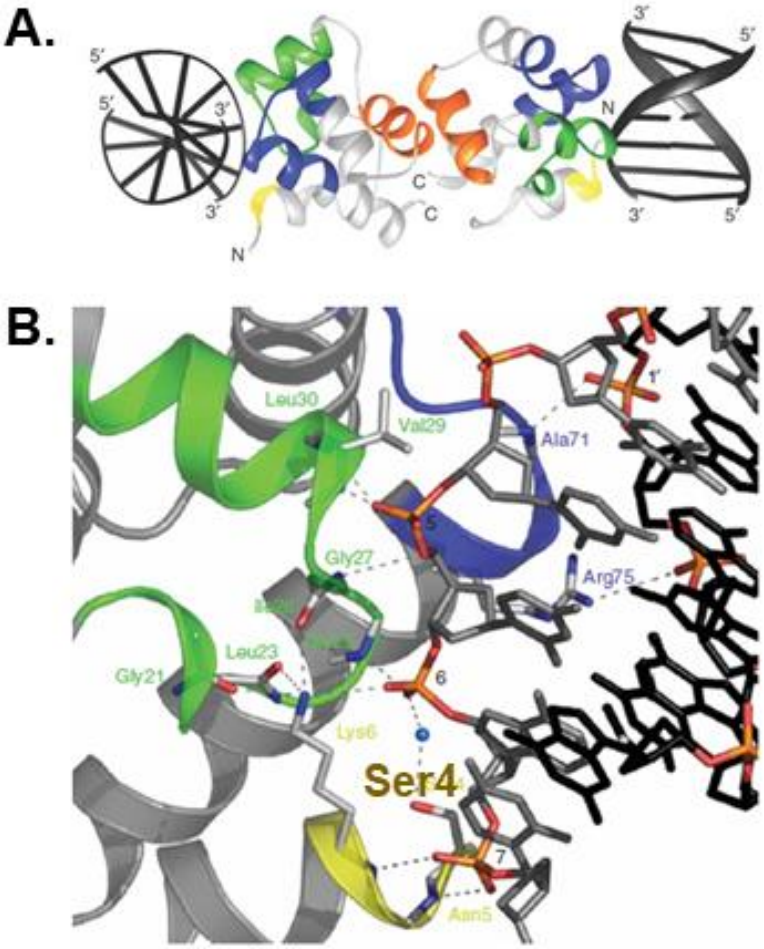

Fig 1.5. Barrier-to-autointegration factor crystal structure with DNA. (A) The three-dimensional crystal structure of BAF bound to DNA is a solved structure. (B) Interactions between multiple residues of a basic region of the BAF molecule interact with the minor groove phosphate backbone of the DNA structure. This interaction includes the Ser4 (yellow) that is shown to be phosphorylated by cellular VRKs and vaccinia B1 kinase, and disrupts BAF-DNA interactions. Images for this figure were borrowed from Bradley et al (79).

mediated phosphorylation is the Ser4 site (Fig 1.5B), which has a direct interaction with the DNA (69, 102). Therefore, the characterization of the B1-BAF signaling axis supports the importance of B1 expression to counteract the cellular BAF antiviral activity during poxvirus DNA replication.

1.3. ENZYME / PSEUDOENZYME MODELS

The discovery of proteins with sequence similarity to enzymes, despite lacking residues required for catalysis was made possible in the age of sequence databases and combined knowledge of bioinformatics, protein structures, and enzyme kinetics. Intriguingly, screening sequence data revealed that most enzyme families contain a catalytic-null protein (103-105), necessitating the characterization of these potential pseudoenzymes. These enzyme families include kinases, phosphatases, proteases, E2 ubiquitin ligases, and phospholipases. The classification of an active protein kinase was first described by Eyers and Murphy, and was based on the characterization of domains required for phosphotransferase activity (106). The requirement of ATP binding was more generally applied to all enzymes for classification as a catalytically active form (107). These transferase-null proteins are referred to as pseudoenzymes or pseudokinases for phosphotrasferase-null proteins. The function of these pseudoenzymes can be appreciated as pseudo-transducers or pseudo-signalers in which the former has an immediate, limited impact while the later has a broader impact on the system (108).

1.3.A. Viral pseudoenzymes and virus required cellular pseudoenzymes

The research on viral pseudoenzymes and viral factors that interact with cellular pseudoenzymes is limited. To explicate what is known about this group of pseudoenzymes and the relationship with virus life cycle modulation, we describe a

specific example of virus hijacking of an enzyme/pseudoenzyme pair, a herpesvirus encoded pseudoenzyme that recruits a cellular paralog, and psuedoenzymes encoded by vaccinia that lack an essential function. Together the primary literature supports virus modulation of host enzyme/pseudoenzyme pairs and provide examples were viruses encoding a catalytic-null protein that is essential for viral function or less clear roles for non-essential psuedoenzymes.

First, an example of virus hijacking a pseduoenzyme/enzyme pair of the host was recently elucidated. The initial discovery of the non-enveloped dsDNA polyomavirus (PyV) requirement of a host catalytic-null protein for the trafficking the virus particle across the ER membrane was quite interesting, especially because this unique mechanism was thought to occur without virion disassembly or budding events. The ER resident protein 29 (ERp29) is an inactive protein disulfide isomerase (PDI). The active PDIs participate in quality control of folding of proteins in the ER lumen via catalysis of disulfide bonds between cysteine residues. The catalytic-null ERp29 is implicated in ER to Golgi apparatus and ER to cytoplasm trafficking. Interestingly, the ERp29 contributes to PyV conformational change that occurs in the ER lumen (109). The cellular pseudoenzyme mediates extension of the VP1 C-terminal arm, which increases the PyV particle binding to the luminal surface of the ER membrane. The PyV particle is then thought to transit through the ER membrane and into the cytosol. Importantly, interaction of the PyV particle with the ER lumen membrane does not occur in the absence of the ERp29. Furthermore, two active proteins from the PDI family also engage and contribute to PyV infection. Intriguingly, the catalytically active ERp57 cooperates with the pseudoenzyme to facilitate VP1 conformational change via a mechanism requiring

catalysis that is not complemented by the other active PDI (110). Therefore, PyV hijacks both cellular pseudoenzyme and catalytic competent PDI for unique transit across the ER membrane and into the cytoplasm without a budding step. Further studies are needed to elucidate the mechanism of virus capture and modulation of this host protein pair.

Second, only one example from the literature was identified for a virus encoding a pseudoenzyme with a characterized essential function during virus infection. Specifically, during gammaherpesvirus infection, the capture of the cellular phosphoribosylformylglycinamidine synthetase (PFAS) occurs via expression of a paralogous, catalytic-null protein, viral glutamine aminotransferase (vGAT), which binds directly to the active enzyme to coordinate function (111). The PFAS-vGAT interaction enables the recruitment of the cellular enzyme and subsequent deamination of RIG-I corresponding to restriction of cytokine production. Therefore, this example illustrates that viruses encoding a pseudoenzyme can be used to manipulate the cellular paralog to evade host immune response.

Third, there are two pseudoenzymes encoded by vaccinia virus that have been studied, but lack a known function during infection. The first is a Ser/Thr catalytic-null B12 (112, 113) encoded by *B12R* under an early promoter (114). This protein has no impact on growth *in vitro* and *in vivo* of a virus as determined by growth studies of a B12 deletion virus (114, 115). Similarly, the serine recombinase predicted catalytic-null F16 protein encoded by the early *F16L* gene was deemed non-essential by unchanged growth kinetics of F16L deletion vaccinia virus (116). Despite the conclusion that both B12R and F16L are non-essential, the *B12R* gene is conserved in all *Orthopoxviruses* (Fig 1.3) and F16L predicted catalytic-null is conserved in the *Chordopoxvirinae* subfamily with the

exception of avipoxviruses and catalytic competent paralog in crocodile poxvirus. Therefore, it is possible that these viral proteins retain function despite a loss of catalytic activity in order for their maintenance throughout evolution, which was shown for vaccinia uracil DNA glycosylase D4R. This protein is essential for DNA replication, although via a catalytic-independent function (117). The importance of these catalytic-null proteins may stem from the presence of viral mimicry of host proteins. It is possible that the requirement of catalytic activity is not required for viral proteins if an active enzyme is expressed by the host. Instead, psedoenzymes may represent a mechanism of modulation of host signaling pathways to enhance virus replication. Additionally, the coding capacity of viruses may impact how viruses utilize pseudoenzymes during infection.

1.3.B. Mechanisms of cellular pseudokinases

From the human kinome, 10% of these proteins are predicted to be catalytically inactive pseudokinases (64) in the canonical sense, but does not account for non-canonical phosphotransferase activity despite mutations predicted to cripple kinase function. Further, the identification of catalytic-null proteins was first described for kinase-like proteins and later applied to other inactive enzymes. To address the mechanisms of pseudoenzymes in cells, we draw from pseudokinase / pseudophosphatase models due to multiple known examples. The molecular mechanisms of pseudokinases and pseudophosphatases have been divided into four categories: modulator, signal integrator, anchor, and competitor (Fig 1.6). Thus far, the characterization of these pseudoenzymes has been linked to one or more of these functional categories (118). Yet,

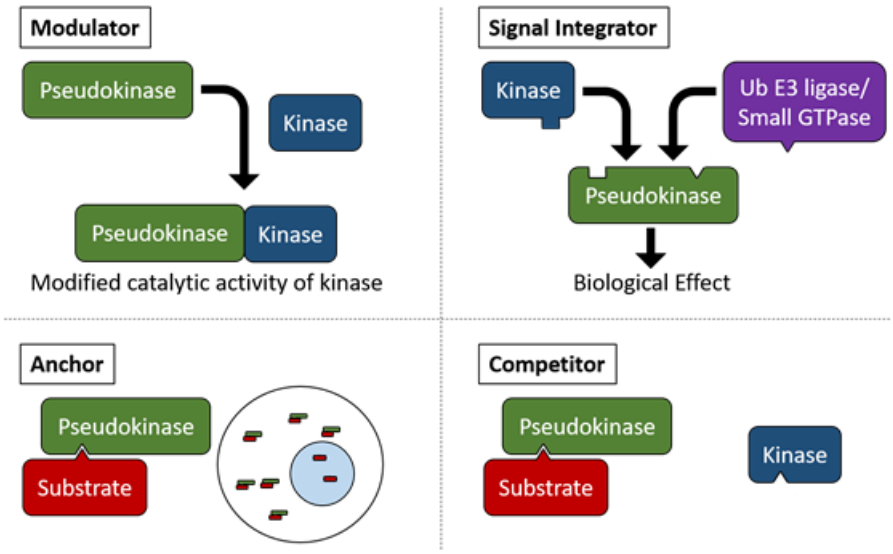

Fig 1.6. Pseudokinase/ pseudophosphatase signaling models. Pseudokinases and pseudophosphatases are categorized functionally into the following groups: modulator, signal integrator, anchor, and competitor. These roles require either direct interaction of the pseudoenzyme with the active enzyme or between the pseudoenzyme and a substrate shared with the enzyme. This illustration was modified from the original graphic in Reiterer et al (118).

as this is a growing area of research alternative mechanisms may exist outside the four models referenced here.

To begin, the modulator function of the catalytic null counterpart 'modulates' catalysis of the active kinase or phosphatase. Examples demonstrate that dimerization of active and catalytic-null proteins can positively regulate catalysis by enhancing binding to specific substrates and/or modify signaling outcomes (119-121). Interestingly, the catalytic dead protein does not completely inhibit catalytic activity of the bound enzyme in these known interactions.

Next, proteins lacking catalytic activity can also behave as scaffolds used to integrate signaling via two or more proteins and are termed 'signal integrators.' Participating as another layer of regulation, these scaffolds can be required for a specific signal to occur (122). Additional pseudoenzymes are predicted to function as scaffolds, however further elucidation of a molecular mechanism is required.

The last two categories include the presence of a shared substrate between a catalytically active and inactive protein. Furthermore, signaling can be modulated by the restriction of a substrate to transit to a different subcellular compartment carrying out the action of a substrate 'anchor' (123). Alternatively, if both proteins reside in the same compartment, a shared binding domain of a substrate can lead to a binding competition between the catalytic active and null proteins (118). It is possible that catalytic dead proteins locked in an open conformation, similar to the open conformation of an active enzyme may participate as efficient competitors for substrate binding. In this example, the pseudoenzyme attenuates the signaling impact of the active enzyme via subcellular localization or occupation of substrate binding site.

These models exemplified by pseudokinase and pseudophosphatases can likely be applied to other pseudoenzymes as the themes of conserved substrate domains and signal transduction can be applied to other transferase activities. Furthermore, the biological relevance of these pseudoenzymes applies to significant cellular processes including, but not limited to, biosynthetic processes, cell migration, innate and adaptive immune signaling, proliferation, differentiation, vesicle transport, and proteasomal signaling (64).

1.4. Aim 1: Determine how cellular VRKs complement functionally for vaccinia B1 kinase.

Despite the fact that the vaccinia B1 kinase and the cellular VRK proteins share similar kinase domains and can all target BAF, it remains to be determined whether the VRK proteins expressed by the cell can regulate BAF antiviral activity or if B1 and the VRKs may share other substrates important for poxviral infection. The purpose of the studies completed in chapters 3 and 4 was to address these and other knowledge gaps in B1 / VRK signal transduction. Herein, we describe the construction and characterization of the first recombinant vaccinia virus in which the entire B1 coding sequence has been deleted (chapter 3). This was achieved using a complementing cell line expressing the B1 protein and allowed us to thoroughly examine the role of B1 independent of any residual hypomorphic activity present for the B1 temperature sensitive mutant proteins. Next, we determined that B1-mediated phosphorylation of BAF is not enhanced by other viral factors, nor does BAF hyperphosphorylation occur during infection in the absence of B1 (chapter 3). Transcriptional analysis of B1 expressing cells also yielded numerous pathways of interest that require validation, but support additional functions for B1 in metabolism, proteolysis, and vesicle transport (chapter 4). Furthermore, using the B1

deletion virus we present evidence that VRK2 and, to a lesser degree, VRK1 can complement for the absence of B1 (chapter 4). Intriguingly, the complementation of the B1 deletion virus by VRK2 appears to occur via a mechanism that is largely independent of BAF (chapter 4), thus indicating that B1 and VRK2 share a novel signaling pathway capable of significantly regulating the poxvirus life cycle. In an effort to understand how poxviruses lacking a B1 kinase replicate, we infected cells deleted of either VRK1 or VRK2 with ORF virus which lacks a B1 kinase (chapter 4).

With no attenuation of viral yield, the ORF virus either uses VRK1 and VRK2 interchangeably or has evolved alternative mechanisms to regulate pathways impacted by B1 during vaccinia virus infection.

1.5. Aim 2: Identify viral factors capable of regulating the B1-BAF signaling axis.

To address this second research aim, in chapter 5 we utilized experimental evolution of the B1 deletion virus to search for novel pathways through which B1 functions. This approach leverages the natural errors that occur during vaccinia DNA replication to introduce variants that can suppress the fitness defect caused by a deleted gene. Whole genome sequencing and analysis of the rescued, adapted B1 deletion viruses revealed an insertion and deletion mutation (indel) within the *B12R* gene (chapter 5). The indel mutation introduced frameshifts into the coding region that led to a truncation of the B12 protein (chapter 5). Previous publications had characterized B12 as a pseudokinase with 36% amino acid similarity to B1 kinase (124, 125). In chapter 5, we present multiple lines of evidence demonstrating that expression of wild-type B12 leads to a striking reduction in fitness of viruses with a defect in B1. Importantly, while mutation or depletion of B12 can rescue the B1 defect in viral DNA replication in

multiple cell types, altering the levels of B12 had no apparent impact on wild-type virus or other mutant viruses. From these data we infer that the inhibitory mechanism executed by B12 is repressed by the B1 kinase.

Additional investigation in search of a mechanism of action for B12 revealed that wild-type B12 primarily localizes to the nucleus, while B12 mutants are diffuse within cells (chapter 6). Together, this indicates that B12 C-terminus is necessary for retention in the nucleus and important for its repressive function on vaccinia DNA replication. Furthermore, the adapted virus containing a B12 mutation exhibits reduced sensitivity to BAF overexpression (chapter 6), suggesting that B12 may function, at least partly, via a BAF dependent mechanism.

The interpretation of how B12-BAF signaling axis modulates DNA replication was aided by the discovery that B12 constitutively colocalizes with chromatin throughout mitosis (chapter 6). BAF also exhibits colocalization with the chromatin, which would place B12 and BAF in close proximity during mitosis. Furthermore, we discovered a B12-VRK1 interaction during infection (chapter 6). When linked with our data that B12 regulates BAF indirectly and previous work characterizing direct VRK1-mediated BAF phosphorylation, a B12-VRK1 interaction may indicate that B12 represses VRK1 phosphorylation of BAF during vaccinia infection. Coming full circle, we showed that when the B1-B12 pair is absent during infection, the cellular VRK1 but not VRK2 contributes to virus replication (chapter 6). This indicates that without the B1-B12 pair, VRK1 plays a more significant role than VRK2 for vaccinia propagation. Therefore, the study of the ΔB1mutB12 virus in cells lacking VRK1 will reveal novel B1/VRK1 signaling pathways necessary for vaccinia replication.

CHAPTER 2

MATERIALS & METHODS

2.1. Reagents. Unless otherwise noted, chemicals were obtained from Sigma Aldrich. Primers were obtained from Integrated DNA Technologies. The complete summary of primers and siRNAs used can be found in table 2.1. The list of antibodies used for experiments is detailed in table 2.2.

Table 2.1 Probes, primers and siRNAs

Name	Sequence
mCherry R Primer (Sanger Seq)	5'-CGCATGAACTCCTTGATGATGGC-3'
mCherry F Primer (Sanger Seq)	5'-GAAGCTGAAGGACGGCGGC-3'
A57 F Primer	5'-GATATGGATGAGGCCAACGAAGC-3'
B2 R Primer	5'-CTCAAACATAGGCAGCAGTGCTCC-3'
B1 ORF R Primer	5'-CTTAGTCCATGGCAAGATACCTCCC-3'
B11R F Primer	5'-TGCTTACTACTAACATGGATACAGA-3'
B13R R Pimer	5'-TCAATACTGACGAGATTGAC-3'
B12R F Primer (Sanger Seq)	5'-CCAGATCTGTATGGAATTGGAGAAACCG-3'
B12R R Primer (Sanger Seq)	5'-CCTCGGTTCTATTTTTCCATGGG-3'
Total VACV DNA (HA) F Primer	5'-CATCATCTGGAATTGTCACTACTAAA-3'
Total VACV DNA (HA) R Primer	5'-ACGGCCGACAATTATAATTAATGC-3'
B1R F Primer (qPCR)	5'-GTGCAAGGCATTTGGTCTATAC-3'
B1R R Primer (qPCR)	5'-CAACATCACCGACCTTTTTGG-3'
B12R Probe	5'-/56-FAM/TTGGAGCAA/ZEN/CAGTTTCAA-3'
B12R F Primer (qPCR)	5'-ACTCACATATAGATTACAACGAGGAC-3'
B12R R Primer (qPCR)	5'-ACCGAACCATTCTATCATGCA-3'
B13R.1 Probe	5'-/56-FAM/AGCTGTTCA/ZEN/GCAGTGGAT-3'
B13R.1 F Primer (qPCR)	5'-CAGCGTCAATCTCGTCAGTAT-3'
B13R.1 R Primer (qPCR)	5'-CCTTATCCATGTTCTCCTCCTTT-3'
B13R.2 Probe	5'-/56-FAM/ACAGAGGTG/ZEN/TTCGGTTCA-3'
B13R.2 F Primer (qPCR)	5'-GGCTCGTATAATCTGGTGGATAC-3'
B13R.2 R Primer (qPCR)	5'-CGTCGACACTCACATCTGAATTA-3'
BamHI-Kozak-HA-B12 F Primer	5'-GAGAGAGGATCCGCCACCATGTATCCCTACGACG-3'
BamHI-Kozak-B12 F Primer	5'-GAGAGAGGATCCGCCACCATGGAAAGCTTCAAGTACTG-3'
B12-BamHI R Primer	5'-GAGAGAGGATCCTTAGTCCTGGATGAACAGCTTCCGC-3'
XhoI-Kozak-HA-B12R F Primer	5'-ATTATCTCGAGGCCACCATGTACCCTTATGATGTGCCAGACTATGCTATGGAATCCTTCAAGTATTGTTTTGATAA
B12R-NheI R Primer	5'-GACTAGCTAGCTCAATCTTGTATAAACAGTTTACGTAGTC-3'
TK-locus L Primer	5'-GGGACTATGGACGCATGATAAG-3'
TK-locus R Primer	5'-ACACTTTCTACACACCGATTGA-3'
TK L Primer	5'-ATACGGAACGGGACTATGGA-3'
B12R F Primer	5'-ACAGTTTCAAGACGAGGAGATTTA-3'
NheI-Kozak-HA-eGFP F Primer	5'-ATTATGCTAGCGCCACCATGTACCCTTATGATGTGCCTGATTATGCAATGGTGAGCAAGGGCGAGG-3'
eGFP-XhoI R Primer	5'-TCACACTCGAGTTACTTGTACAGCTCGTCC-3'
siCtrl (Scramble)	5'-CAGUCGCGUUUGCGACUGGUU-3'
siVRK2 #1	5' -CACAAUAGGUUAAUCGAAAUU- 3'
siVRK2 #2	5' -ACGUUCAGAUCCUCUAUU- 3'
siB12 (siB12-1)	5'-GGUAUAAAGUAUUUGGCUAUU-3'
siB12-2	5'-CAUGAUAACUUCAGGAAAUUU-3'
siB12-3	5'-GGAUAUUGCAUGAUAGAAUUU-3'
siB12-4	5'-UGAUAACGAUGGCAAGAAAUU-3'
siB13-1	5'-AGACAAGAUUGAUGGAUUAUU-3'
siB13-2	5'-GGAUAAGGUUAGCGCUCAAUU-3'

Table 2.2 Antibodies and dilutions			
Antibody	**Company**	**Clone**	**Assay/Dilution**
αBAF (total) (rabbit)	custom	Jamin et al. 2014	IB(1:3,000)
αphospho-BAF (N-terminus phospho-specific) (rabbit)	custom	Jamin et al. 2014	IB(1:1,000)
αGAPDH (mouse)	Santa Cruz Biotechnology		IB(1:200)
αHA.11 (mouse)	BioLegend	16B12	IFA(1:400) / IB(1:1,000)
αI3 (rabbit)	custom		IFA(1:300)
αlaminA/C (mouse)	Cell Signaling		IB(1:2,000)
αmyc (mouse)	Cell Signaling	9B11	IFA(1:100) / IB(1:1,000)
αtubulin (mouse)	Sigma Aldrich	T7816	IB(1:10,000)
αVRK1 (mouse)	Santa Cruz Biotechnology	E-3: sc-390809	IB(1:500)
αVRK2 (mouse)	Santa Cruz Biotechnology	H-5: sc-365199	IB(1:500)
αF18 (rabbit)	custom		IB(1:6,000)
Goat αmouse	BioRad		IB(1:20,000)
Goat αrabbit	BioRad		IB(1:20,000)
Fluor 594 OR 488 conjugated goat αmouse	Life Technologies		IFA(1:400)
Fluor 594 OR 488 conjugated goat αrabbit	Life Technologies		IFA(1:400)

2.2. Cell Culture. African green monkey kidney CV1 cells were obtained from Invitrogen life technologies. African green monkey BSC40, mouse fibroblast L929, human cervix epithelial adenocarcinoma HeLa, human lung epithelial carcinoma A549, and human thymidine kinase-negative 143B osteosarcoma TK(-) cells were purchased and obtained directly from ATCC. These cell lines except A549 cells were maintained in Dulbecco's modified Eagle's medium (DMEM) supplemented with 10% fetal bovine serum (FBS; Atlanta Biologicals) and penicillin-streptomycin in 5% CO_2 at 37˚C. A549 cells were maintained in DME/ Ham's F-12 Nutrient Mixture (1:1) media supplemented with 10% FBS and penicillin-streptomycin in conditions stated above. Human near-haploid fibroblast HAP1 parental, vaccinia-related kinase 1 (VRK1) knockout (VRK1KO), and VRK2KO cells were obtained from Horizon Genomics and maintained in Iscove's Modified Dulbecco's Medium (IMDM; Fisher Scientific) with 10% FBS and penicillin-streptomycin at incubation conditions as stated above. VRK1KO cells (cat# HZGHC000073c014) contain an 11 base pair (bp) deletion in VRK1 exon 5 introduced by CRISPR/Cas9 gene editing and VRK2KO cells (cat# HZGHC000403c006) contain a 7bp deletion in VRK2 exon 2.

Primary ovine fetal turbinate (OFTu) cells were obtained by aseptically removing turbinate tissues from ovine fetuses and were minced in presence of PBS and antibiotics, washed several times with PBS, digested with 0.2% Trypsin at RT for 1-2hr, and gauze-filtered. The cell suspension was centrifuged and pellets were washed twice with PBS and once with growth medium. Cells were maintained in minimal essential medium (MEM) supplemented with 10% fetal bovine serum (FBS), 2 mM of L-glutamine, and 50 μg/mL of gentamicin.

2.3. Generation of stably transduced cell lines. The pHAGE-HYG-MCS-B1myc construct was produced by amplifying a codon optimized myc-tagged B1 ORF using BamHI-Kozak-B1 (5'-AGCAGGATCCGCCACCATGAACTTC-3') forward primer and B1-BamHI (5'-GGCGGATCCTTACAGGTCCTCTTCAG-3') reverse primer set and cloning the product into the BamHI site of the multiple cloning site of the pHAGE-HYG-MCS vector (94). The lentiviruses encapsidating pHAGE-HYG-MCS (126) (control), pHAGE-HYG-B1myc (127), and pHAGE-HYG-3XFlag-BAF (plasmid was generously provided by Dr. Paula Traktman) were produced in 293T cells following transfection with pHAGE-HYG-MCS-B1myc or pHAGE-HYG-MCS (empty vector) in combination with pVSVG, pTat, pREV, and pGag/Pol. Alternatively, a two plasmid helper system was also used to generate lentiviruses encapsidating pHAGE-HYG-MCS (control) or pHAGE-HYG-B1myc. The two plasmid helper system included pVSVG and psPAX2, a gift from Didier Trono (Addgene plasmid # 12260), was combined with the transfer plasmid for transfection of 293T cells. At 15.5hr post transfection, fresh media with 5mM sodium butyrate (EMD Millipore Corp.) was added to cells. At 24hr post transfection, fresh media with 10mM HEPES (Fisher Scientific) was added to cells. At 48hr post

transfection recombinant virus was harvested, polybrene (Fisher Scientific) was added at 10 µg/mL, and stocks were aliquoted for storage at -80˚C. These lentiviruses were used to transduce CV1 cells the day following cell seeding at $3x10^5$ cells in a 35mm well. B1myc and control CV1 cells were selected with 200 µg/mL hygromycin B (Invitrogen) and B1myc expression confirmed with immunoblot using mouse αmyc (Myc-Tag (9B11) Mouse mAb #2276 Cell Signaling) antibody or plaque assay rescue of ΔB1 virus on B1myc expressing CV1 cells.

Lentiviruses expressing BAF-specific short hairpin RNA (shRNA) or control (scrambled) shRNA have been described previously (69), and were used for stable depletion of BAF in CV1 cells and HAP1 VRK2KO cells. Those transduced cells were selected with 10 µg/mL and 500ng/mL of puromycin respectively prior to use in experiments. Lentiviral vector pLenti-C-Myc-DDK expressing myc-tagged human VRK2 (isoform VRK2A, #RC206522L1 OriGene) was used to generate lentivirus as described above.

The lentivirus generation and stable expression of HA-tagged and untagged B12 cells used the pHAGE-HYG-MCS-HA-B12 or pHAGE-HYG-MCS-B12 construct which were produced by PCR amplifying a codon-optimized HA-B12 ORF in the pcDNA3.1 vector purchased from GeneArt (Fig 2.1). The primers used for PCR amplification are found in Table 2.1. HA-B12 or B12 ORF was then cloned into the BamHI site within the pHAGE-HYG-MCS multiple cloning site. Lentivirus generation used the four plasmid helper system (pVSVG, pTat, pREV, pGag/Pol), following the same protocol summarized above for transduction of CV1 cells.

Vaccinia *B12R* codon optimized for mammalian cells (GeneArt)

ATGGAAAGCTTCAAGTACTGCTTCGACAACGACGGCAAGAAGTGGATCATCGGCAACA
CCCTGTACAGCGGCAACAGCATCCTGTACAAAGTGCGGAAGAACTTCACCAGCAGCTT
CTACAACTACGTGATGAAGATCGACCACAAGAGCCACAAGCCTCTGCTGAGCGAGATC
CGGTTCTACATCAGCGTGCTGGACCCTCTGACCATCGACAACTGGACCAGAGAGCGG
GGCATCAAGTACCTGGCCATTCCTGACCTGTACGGCATCGGCGAGACAGACGACTACA
TGTTCTTCGTGATCAAGAACCTGGGCAGAGTGTTCGCCCCTAAGGACACCGAGTCTGT
GTTCGAGGCCTGCGTGACCATGATCAATACCCTGGAATTCATCCACAGCCAGGGCTTC
ACCCACGGCAAGATCGAGCCCAGAAACATCCTGATCCGGAACAAGCGGCTGAGCCTG
ATCGACTACAGCCGGACCAACAAGCTGTACAAGAGCGGCAACTCCCACATCGATTACA
ACGAGGACATGATCACCTCCGGCAACATCAACTATATGTGCGTGGACAACCACCTGGG
CGCCACCGTTTCTAGAAGAGGCGACCTGGAAATGCTGGGCTACTGCATGATCGAGTG
GTTCGGCGGAAAGCTGCCCTGGAAGAACGAGAGCAGCATCAAAGTGATCAAGCAGAA
GAAAGAGTACAAGAAGTTTATCGCCACCTTCTTCGAGGACTGCTTCCCCGAGGGCAAC
GAGCCTCTTGAACTCGTGCGGTACATCGAGCTGGTGTACACACTGGACTACTCTCAGA
CCCCTAACTACGACCGGCTGCGGAAGCTGTTCATCCAGGACTAA

Fig 2.1. Sequence for vaccinia B12R codon optimized for expression in mammalian cells. A vaccinia *B12R* gene codon optimized for expression in mammalian cells was generated by GeneArt.

2.4. Transcriptome analysis. L929 control or B1myc stably expressing cells were transfected with plasmid DNA and harvested 6h post transfection for RNA extraction. Prior to use in RNA sequencing experiments all RNA samples were analyzed with respect to purity and potential degradation. A260/280 ratios were determined using a Nanodrop instrument. Potential degradation was assessed by analysis of 200 ng of the RNA with an Advanced Analytical Technical Instruments (AATI) Fragment Analyzer by the University of Nebraska Medical Center (UNMC) Next Generation Sequencing Core (NGS) Facility. 12 sequencing libraries were generated by the UNMC NGS Core beginning with 1 ug of total RNA from each sample using the TruSeq V2 RNA sequencing library kit from Illumina following recommended procedures. Multiplexed

libraries were sequenced on the HiSeq 2500 (Illumina) and a total of approximately 27 million 50 bp single reads were generated for each sample. Approximately 96 % of the bases >Q30 were achieved with a mean quality score for each sample of Q37. Following sequencing FASTQ files were provided.

The transcriptome analysis was conducted using customized analysis pipeline based on TOPHAT 2.0.13 and CUFFLINKS 2.2.1. The reference genome index and annotation (NCBI build 37.2) were downloaded from Illumina's iGenomes project. The top differentially regulated genes were identified, and the genes were visualized with clustering on both genes and treatments using a R script based on heatmap2 package. Genes differential expressed at a Log_2(fold change) > 1.9 and P-value <0.05 were analyzed in heat map (Fig 4.1B). The transcriptome data was also analyzed for regulation of signaling pathways. First, the transcriptome raw count data was converted to gene symbols. Second, data was analyzed using GSEA program and available gene sets to identify regulated pathways each comparison: B1 with control (Fig 4.2.A), B1/plasmid with control/plasmid (Fig 4.2.B), B1/plasmid with control (Fig 4.3.A), and control/plasmid with control (Fig 4.3.B).

2.5. B1 deletion recombinant virus generation. The B1 deletion recombinant vaccinia virus ΔB1 was generated by infecting B1myc expressing CV1 cells with WT virus (MOI=0.03) and co-transfecting the linear DNA fragment upB1-P11-mCherry-downB1 (Integrated DNA Technologies). This DNA fragment was synthesized to contain the mCherry ORF under the control of the vaccinia p11 promoter (128), and flanked by sequence homologous to the 250bp immediately upstream and downstream of the B1 ORF, thus it was constructed to replace the *B1* ORF with p11mCherry upon homologous

recombination. The infected/transfected cells were incubated for 48hr, harvested and titrated on B1 expressing CV1 cells for isolation of individual plaques. Virus expressing mCherry was purified by serial plaque purification on CV1-B1myc cells until no non-fluorescent plaques (out of 100 plaques) were observed. The ΔB1 virus was plaque purified 6 additional times before being expanded on B1myc expressing CV1 cells and purified using a sucrose cushion. Replacement of the B1 ORF was verified by DNA sequencing and PCR analysis (Table 2.1).

2.6. Serial passage of ΔB1 on CV1 cells for adapted virus generation. The ΔB1mutB12-A1, -A2, -A3 viruses were generated by infecting CV1 cells at a MOI of 0.1 in three independent 10cm plates. Virus was propagated in cells two days at 37˚C before cell harvest. Cells were pelleted and resuspended in 1ml PBS. 100µl cells in PBS were saved for DNA purification and remaining cells were pelleted and resuspended in 900µl 10mM Tris pH 9.0 for virus titration. After freeze/thawing three times, the three independent virus stocks were titrated on B1myc expressing CV1 cells. Using these titers for passage 1 viruses, 10cm plates of CV1 cells were infected at a MOI of 0.1 and allowed to propagate on cells for days at 37˚C. Serial passage of viruses in CV1 cells at a MOI of 0.1 was completed for 7 total passages with either two or three days of propagation before cell harvest. Each passage of virus was titered on complementing, B1myc expressing CV1 cells.

2.7. WT/HA-B12 recombinant virus generation. The recombinant WT/HA-B12 virus expresses an additional vaccinia *B12R* gene with a 5’ HA epitope sequence from the nonessential, thymidine kinase (TK) locus. This virus was generated by homologous recombination using standard protocols and pJS4 variant kindly shared by Paula

Traktman laboratory (69). Briefly, the HA-B12 sequence from the virus was amplified using F and R primers containing XhoI or NheI restriction sites respectively (Table 2.1) and cloned into a pJS4 variant (129) flanking it with regions homologous to the vaccinia TK gene. Next, CV1-B1myc cells were infected with WT virus at MOI = 0.03 followed by transfection 3hpi with 3 µg linear pJS4-HA-B12 per 35mm well. Cells were harvested 48hpi, freeze/thawed three times, and used for virus titrations on CV1-B1myc cells. Recombinant viruses went through two rounds of purification by infecting 143B TK(-)/B1myc cells (lacking cellular expression of thymidine kinase) and treatment with 25 µg/µl bromodeoxyuridine (BrdU) to reduce productive infection of WT virus with an intact TK locus (control infections were completed without BrdU selection). WT/HA-B12 viruses were plaque purified three times and confirmed to be a pure stock using PCR amplification of viral DNA and immunofluorescence detection of HA-B12 protein in 50/50 plaques. An expanded preparation of this virus from a freeze/thawed lysate of infected CV1-B1myc cells was used for immunofluorescence assays.

2.8. Viruses and viral infection assays. Viruses used for experiments include the following: wild-type (WT), B1 deletion (ΔB1) (127), orf virus (130), ΔB1mutB12-A1, ΔB1mutB12-A2, ΔB1mutB12-A3, B1-mutant Cts2 (68), D5-mutant Cts24 (131), E9-mutant Cts42 (132), and WT/HA-B12 WR strain vaccinia viruses. Parapoxvirus orf virus (ORFV; OV-IA82 strain) was isolated, propagated and purified in OFTu cells. Genomic DNA sequencing confirmed homogenous virus stock preparation. ORFV passaged less than 10 times after plaque purification was used for experiments (Fig 4.8C). All other viruses were expanded on BSC40, CV1 or CV1-B1myc cells and purified using a sucrose cushion.

ORFV viral yield was assayed for ORFV infection (MOI=1) of HAP1 control, VRK1KO and VRK2KO cells. Four days post-infection cells were harvested and lysed. Cell debris was pelleted using centrifugation and supernatants containing virus were used to quantitate viral yield by the Spearman-Karber's tissue culture infectious dose 50 method (TCID50/mL), using primary ovine fetal turbinate (Oftu) cells. Viral yield experiment (Fig 4.8C) was performed in experimental duplicate.

Plaque assays were completed using either 200 or 300 plaque forming units (PFU) per well. WT, Cts2 and ΔB1 infections were completed 39.7˚C and fixed/stained 48h post infection. For the ΔB1 adapted virus plaque assays, control or B1myc expressing CV1 cells were infected with WT, ΔB1, or ΔB1 adapted virus A1 for passages 1 through 7. Cells were fixed and stained at 72h post infection. The plaque assay of B12 depletion during WT, ΔB1, and ΔB1mutB12-A3 infection was completed by infecting cells 24h post transfection with siRNA. 72h post infection cells were fixed and stained. The plaque assay on CV1 control or HA-B12 stably expressing cells were fixed 72h post infection with WT or ΔB1mutB12-A3 virus.

For immunofluorescence assays, cell lines were infected with WT or ΔB1 virus at MOI=5 at 37˚C for 7 or 18h prior to fixation with 4% PFA.

Viral growth assays were conducted in multiple cell lines. One-step 24h viral growth assays were completed by infecting a monolayer of CV1, HeLa, A549, L929, or transduced CV1 cells with WT, Cts2, ΔB1, ΔB1mutB12-A1, or ΔB1mutB12-A3 virus at a MOI of 3 and incubated at 37˚C and/or at 37˚C and 39.7˚C (only for studies including temperature sensitive (ts) mutant viruses). At 24h or indicated time post infection cells were harvested for downstream DNA accumulation and viral yield quantification. Half of

the cells harvested were pelleted and resuspended in PBS for DNA purification and qPCR while the other half was resuspended in 10mM Tris pH 9.0, freeze/thawed three times, and serially diluted for titration on CV1-B1myc cells at 37˚C or 31.5˚C (only for experiments including ts mutant viruses). For one-step growth assays with siRNA treated cells, CV1 cells were infected 24h post transfection with siRNA. Viral growth was also measured at multiple time points for CV1 cells infected with WT, ΔB1, or ΔB1mutB12-A3 virus. Cells were infected with a MOI of 3 and harvested at 3, 7, 16, and 24h post infection and used for both DNA accumulation and viral yield quantification. For multi-step growth curves, CV1 cells were infected at a MOI of 0.01 and harvested at 48h post infection for viral yield measurement by titration of samples on CV1-B1myc cells. Multi-step growth assay in siRNA treated cells were carried out at 24h post transfection, with cell harvests at both 7 and 48h post infection for viral yield quantitation.

WT virus was used for infections of cells transfected with pJS4 plasmid constructs. CV1 cells were infected at either a MOI of 3 or 5 and harvested 24h post infection for immunoblot analysis of HA-B12wt and HA-B12ΔA690 expressed from the pJS4 vector late viral promoter.

For detection of early gene expression, CV1 cells were infected with WT, ΔB1, or ΔB1mutB12-A3 at a MOI of 3 and harvested 4h post infection for RNA extraction from cells.

For immunoblotting analysis shown in Fig. 3.3A, CV1 cells were infected with WT or ΔB1 virus at MOI=10 at 37˚C and harvested cells 6hpi. WT, ΔB1, ΔB1mutB12-A1, or ΔB1mutB12-A3 viruses were used for Fig 6.4A BAF blot following the same

conditions. In Fig. 4.4E, HAP1 cell lines were infected with WT or ΔB1 virus at MOI=3 at 37˚C and harvested 7 and 18hpi for early and late protein detection respectively.

2.9. Sequencing. For complete genome sequencing of the WT (from the Wiebe laboratory), ΔB1, ΔB1mutB12-A1, and ΔB1mutB12-A3 viruses 1 ng of viral DNA from each sample was used to construct sequencing libraries. Libraries were constructed using the Nextera XT kit from Illumina per manufacturers suggestions. An aliquot of the resultant multiplexed library of four viral isolates was sequenced on the MiSeq V2 instrument. 150 base pair (bp) paired-end sequencing was performed. The paired reads of 150 bp (trimmed when necessary to remove adaptors and ends of reads with lower QC scores) was provided. Next, Illumina paired-end sequence reads were filtered using the program fastq_quality_filter from FASTX-Toolkit 0.0.14. The read pairs with at least 90% bases having quality of 30 were used to map to reference genome of Vaccinia virus WR (reference genome NC_006998.1). Bowtie2 version 2.2.4 was used for accurate and efficient mapping. Sequence data was uploaded to SRA database (PRJNA490542). The estimated overall coverage of each of the samples (using only the high quality paired reads) is between 800 and 2000x based on a genome size of 220kb.

Sequence data was analyzed for gene duplications, point mutations and insertion or deletion (indel) mutations within protein coding regions of the genome using a self-developed pipeline including samtools/bcftools. Sequence discrepancies that occurred in <5% of the read counts for a single nucleotide call were not included in further analysis. The mapped reads were visualized using Integrated Genome Browser (IGV 2.3.59). Complete genome sequences were aligned for all sequenced viruses and compared to the WT (Wiebe) virus to identify gene duplications. Point mutations were assessed by

comparing WT (Wiebe) to WT WR (reference genome NC_006998.1) in the NCBI database, ΔB1 to WT (Wiebe), and both ΔB1-A1 and ΔB1-A3 to ΔB1 sequenced genome. Lastly, indel mutations were discovered by comparing the indel changes between WT (Wiebe) and WT WR (reference sequence) with the change in indel mutations for ΔB1, ΔB1-A1, or ΔB1-A3 and WT (Wiebe) as in figure 5.2B or by alignment the whole genome sequence for ΔB1-A3 to the WT WR (reference sequence) genome in figure 5.2C. Mutations in greater than 5% of the read counts at a single nucleotide position were considered significant mutations in the mixed population of ΔB1-A1 and ΔB1-A3 viruses.

For *B12R* targeted Sanger sequencing, ΔB1mutB12 virus lineages A1, A2, and A3 were plaque purified twice on CV1 cells. Virus was expanded on CV1 cells and DNA was purified from the resultant viruses using a GeneJET whole-blood genomic DNA purification minikit (Thermo Scientific). Purified DNA samples were subjected to Taq based PCR using 1μM each B11R F and B13R R primers (Table 2.1). Following PCR amplification, B11-B13 products were cleaned using a QIAquick PCR purification kit (Qiagen). PCR products were then submitted for Sanger DNA sequencing (Table 2.1) and analyzed for lesions within *B12R*.

2.10. Plasmid/siRNA/mRNA transfections. Transcriptome analysis of B1 expressing cells with or without control plasmid transfection was completed as follows. L929 control or B1myc stably expressing cells were transfected with 2ug control plasmid pUC-Neo following manufacturer's specifications for a 35mm well. Cells were harvested 6h post transfection for downstream RNA purification. For plasmid transfection for expression of B12 forms, CV1 cells in a 35mm well were transfected with 5μl lipofectamine2000

(Invitrogen) for 5µg pJS4-HA-B12wt or pJS4-HA-B12ΔA690 plasmid DNA following the manufacturer's incubation suggestions. Cells were then infected with WT virus 6h post transfection for expression of HA-B12wt and HA-B12ΔA690 from the pJS4 vector under a late vaccinia virus promoter.

For the transient depletion of VRK2, B12, or B13 mRNA, cells in a 35mm well were transfected with a mixture of 5µl Lipofectamine RNAiMAX (Invitrogen) and 100nM siRNA (Table 2.1) targeting the scramble control, VRK2, B12, or B13 mRNA sequences. During VRK2 depletion, HeLa or A549 cells were transfected and protein depletion was measured by immunoblot analysis at 3 days post transfection. For one-step infections in siCtrl and siVRK2 treated cells, cells were split into a 12-well plate 3 days post transfection and infected 4 days post transfection prior to 24hr DNA accumulation and viral yield assays. For B12 or B13 depletion using siRNA, CV1 transfected cells were incubated 24h at 37˚C before infection of cells for downstream experiments.

In mRNA transfections for immunofluorescence assays, *in vitro* synthesis of GFP or HA-B12 mRNA was conducted following mMessage mMachine^{TM} T7 Ultra manufacturer's recommendations (Invitrogen) with linearized template pcDNA3.1-GFP or pcDNA3.1-HA-B12 (Fig 2.2). GFP was cloned into the pcDNA3.1 vector using primers containing NheI or XhoI restriction sites (Table 2.1). CV1 or CV1-B1myc cells were transfected with 1.5µl Lipofectamine MessengerMax (Invitrogen) and 1µg mRNA per well of a 12-well plate following the manufacturer's protocol. The mRNA transfected cells were fixed or permeabilized the next day for immunofluorescence and prepermeabilization assays.

Vaccinia *B12R* codon optimized for mammalian cells (GenScript)

ATGTACCCTTATGATGTGCCAGATTACGCTATGGAGTCCTTCAAGTATTGCTTCGACAA
CGACGGGAAAAAATGGATTATTGGAAACACACTGTACTCAGGCAACAGCATCCTGTAT
AAGGTGCGCAAGAACTTCACTAGCTCCTTTTACAACTACGTCATGAAGATTGACCACA
AGAGCCATAAACCACTGCTGTCCGAAATCCGATTCTACATTTCCGTGCTGGACCCCCT
GACTATCGATAATTGGACCAGGGAACGCGGGATCAAGTACCTGGCTATTCCTGACCTG
TATGGAATCGGCGAGACTGACGATTACATGTTCTTTGTGATTAAGAACCTGGGAAGGG
TCTTCGCCCCAAAAGATACCGAAAGCGTGTTCGAGGCTTGCGTCACCATGATCAATAC
ACTGGAATTCATTCACAGTCAGGGGTTTACACATGGAAAGATCGAGCCCAGAAACATC
CTGATTCGAAACAAGCGGCTGAGTCTGATTGACTACTCAAGGACTAACAAGCTGTATA
AATCCGGCAACTCTCACATCGACTACAATGAGGATATGATCACCTCTGGAAACATCAAC
TACATGTGCGTGGACAATCATCTGGGCGCAACAGTCAGCCGGAGAGGCGATCTGGAA
ATGCTGGGGTACTGTATGATCGAGTGGTTTGGCGGGAAGCTGCCTTGGAAAAACGAA
TCTAGCATCAAAGTGATCAAGCAGAAGAAAGAATACAAGAAATTCATCGCCACCTTCTT
TGAGGATTGTTTTCCCGAGGGGAATGAACCTCTGGAGCTGGTGCGGTACATTGAGCT
GGTCTATACACTGGATTATTCTCAGACACCCAACTACGATAGACTGCGGAAACTGTTCA
TTCAGGAC

Fig 2.2. Sequence for vaccinia B12R codon optimized for expression in mammalian cells. A vaccinia *B12R* gene codon optimized for expression in mammalian cells was generated by GenScript.

2.11. Immunofluorescence assay. Cells were fixed with 4% paraformaldehyde (Alfa Aesar) in 1X PBS for 15m and permeabilized with 0.2% Triton X-100 (Sigma) in 1X PBS for 10m at room temperature (RT). Primary antibodies were incubated with cells for 2h at RT following dilutions in 1X PBS (Table 2.2). Secondary antibodies with conjugated fluorophore (Table 2.2) were incubated with cells for 1h at RT in the dark. The 4',6-diamidino-2-phenylindole (DAPI) nuclear stain was added to cells at 1:1000 dilution in 1X PBS and incubated with cells for 30m at RT in the dark. All dilutions and washes used 1X DPBS/Modified with Ca+ and Mg+ added (HyClone™ ThermoScientific) for figures 3.1C, 3.2B and 4.5. All other experiments used 1X PBS for

dilutions and washes. Immunofluorescence images were taken using an EVOS® FL Auto Cell Imaging System (Invitrogen) with dual cameras and selected excitation/emission filters GFP (Fluor 488), TxRed (Fluor 594) and DAPI. Using ImageJ software, composites were generated to make minor adjustments to brightness and some images were modified using LUT settings. Images were saved as RGB.tiff or montage.tiff files.

2.12. Prepermeabilization assay. CV1 cells were transfected with HA-GFP, HA-B12 or no mRNA following transfection protocol in section 'Plasmid/siRNA/mRNA transfections'. 24h post transfection with mRNA cells were fixed with 4% paraformaldehyde (Alfa Aesar) in 1X PBS for control 'Fix/Permeabilize Cells' condition or first permeabilized with 0.1% Triton X-100 (Sigma) in 1X PBS for 30s, then fixed for 'Permeabilize/Fix/Permeabilize Cells' condition (133, 134). The following steps were carried out identical to those stated in 'Immunofluorescence assay'.

2.13. Cellular fractionation assay. CV1 control cells or cells stably expressing HA-B12 were fractionated into soluble cytoplasmic (Cyto.), membrane (Memb.), nuclear (Nuc.), chromatin-bound (Chrom.) and cytoskeletal (Cytoskel.) fractions using the Subcellular Protein Fractionation Kit for Cultured Cells (Thermo Scientific #78840) following the manufacturer's instructions with the addition of phosphatase inhibitors. Lamin A/C was used as a nuclear protein control that has soluble fractions and fractions bound to the chromatin and cytoskeleton. GAPDH and BAF are cytosolic and membrane associated protein controls. Additionally, the BAF control protein has a nuclear fraction that is chromatin-bound.

2.14. Immunoblot assay. Protein expression was evaluated by harvesting cells and resuspending cells at 1 X 10^4 or 5 X 10^3 cells/µl in a 2X SDS protein sample buffer

supplemented with either 10U/ml benzonase or 50 units/ml Pierce universal nuclease for cell lysis (Thermo Scientific), trypsin serine protease inhibitor (phenylmethylsulfonyl fluoride), protease inhibitor cocktail (Rocke), and phosphatase inhibitor cocktail (Roche). For detection of tubulin, B1myc, VRK1, VRK2, HA epitope tagged B12 forms, lamin A/C and GAPDH, cells were resolved on a 12% SDS-PAGE gel. Vaccinia F18, total BAF, and phosphorylated BAF protein was detected by resolving cells on an 18% SDS-PAGE gel. Transfer of the proteins to a polyvinylidene difluoride (PVDF) membrane were carried out overnight. Membranes were blocked in 5% milk made in 1X Tris buffer/NaCl/0.05% tween (1X TBST). Primary and secondary antibodies (Table 2.2) added to 1% milk in 1XTBST were incubated with the membrane. Supersignal WestPico chemiluminescent reagents (Thermo Scientific) were incubated with the membranes. Only VRK1 and VRK2 blots were incubated with Supersignal WestFemto Maximum Sensitivity Substrate chemiluminescent reagents (Thermo Scientific). The Bio-Rad ImageLab software was used to quantify chemiluminescence signal. Images were made from film or chemidoc images. Fold B12 protein levels were averaged from 5 independent experiments. Raw values were quantified for HA-B12wt, HA-B12ΔA690, and HA-B12 G-A protein abundance using the volume tool in ImageLab for chemidoc images. Fold values were calculated by setting a standard protein to 1 and determining fold values for HA-B12wt, HA-B12ΔA690, and HA-B12 G-A (Fig 5.6B and C). Relative phospho-BAF protein levels were quantified by dividing raw values for phosphorylated BAF from ImageLab volume tool by total BAF raw values for each experiment (Fig 6.4B-D) and averaged for the three experiments (Fig 6.4E).

2.15. DNA/RNA purification and qPCR. For fold DNA abundance quantified for total VACV DNA and the *B1R* gene specifically, DNA was extracted from WT, ΔB1, ΔB1 adapted viruses A1 passages 1-7, ΔB1 adapted viruses A2 passages 1-7, and ΔB1 adapted viruses A3 passages 1-7 infected CV1 cells (for infection details see section "Viruses and viral infection assays"). The WT and ΔB1 control samples came from one-step infection DNA samples in CV1 cells. DNA was purified using a GeneJET whole-blood genomic DNA purification minikit (#K0782, Thermo Scientific). The Bio-Rad iTaq Universal SYBR Green Supermix was used with quantitative polymerase chain reaction (qPCR) as previously described (102) with the addition of a *B1R* specific primer set. In brief, the WT purified DNA sample was serially diluted to generate a standard curve and determine amplification efficiency of *HA* (total VACV DNA) and *B1R* primer sets (Table 2.1). For WT and ΔB1 controls about 10ng DNA and 1μM primers were combined in a single reaction. Variable amounts of DNA were used for ΔB1-A1, ΔB1-A2, and ΔB1-A3 passages 1-7, although the volume used was constant when combined with 1μM primers per reaction.

The one-step 24h viral DNA accumulation samples were treated similarly to the DNA extraction and purification above. The infection protocol is detailed under one-step viral growth infections in methods section "Viruses and viral infection assays". Samples were subjected to qPCR with the *HA* specific primer set (Table 2.1) in triplicate to determine relative viral DNA accumulation.

For transcriptome analysis, the RNA was extracted from L929 cells following the suggested protocol for the RNeasy Mini Kit (Qiagen). Early viral gene expression was determined by infecting CV1 cells as detailed in methods "Viruses and viral assays"

section and harvested at 4h post infection. RNA was extracted from cells similar to above, using the RNeasy Mini Kit (Qiagen). Reverse transcription of RNA into cDNA was carried out using a high-capacity cDNA reverse transcription kit (Thermo Fisher Scientific, Applied Biosystems). Then using probe and primer sets specific for either B12 or B13 cDNA, qPCR was used to quantify relative mRNA levels for B12 and B13. In a 10ul reaction, probes were used at 0.25nmol and primers for each probe were used at 0.5nmol per reaction (Table 2.1). The single 10ul reaction also included about 40ng cDNA and 10ul of the 2X PrimeTime Gene Expression Master Mix (Integrated DNA Technologies). Each sample was completed in duplicate with three experimental replicates. The WT virus sample was used to generate a standard curved to determine amplification efficiency of the probe/primer sets and this number was factored into the cDNA fold values.

2.16. Statistics. Each experimental question was tested in a minimum of three experimental replicates, unless stated otherwise, and graphed data represent the mean of all experimental replicates. Error bars shown represent standard deviations from the mean. The *P* values indicated were calculated using Excel two-tailed Students t-tests or Prism multiple student *t* test.

CHAPTER 3

GENERATION AND CHARACTERIZATION OF B1 DELETION VIRUS

3.1 Construction of a B1 complementing cell line and B1 deletion vaccinia virus

To gain further insight into the functions of the vaccinia B1 kinase, we initiated construction of a mutant virus in which the B1R ORF is deleted. In light of the previous observation that B1 expression is essential to the viral life cycle (73), we posited that replication of a B1R deletion virus would require a complementing cell line expressing the kinase. Therefore, a lentivirus system was used to stably express a myc-tagged B1 kinase (B1myc), codon optimized for expression in mammalian cells. Transduced CV1 cells were confirmed to have B1myc expression by immunoblot analysis (Fig 3.1A). To determine whether stable expression of B1 resulted in any gross changes in cell fitness, the morphology of the cells was closely monitored, as was their doubling rate over time. We observed no alteration in the morphology of B1myc expressing cells over a period of 3-4 weeks (data not shown). Furthermore, CV1 cells expressing the B1myc protein did not vary significantly from the control cells in regards to apparent doubling time (Fig 3.1B). Finally, we used an immunofluorescence assay to determine the localization of the B1myc protein in transduced cells. We observed that the B1myc protein was present primarily in the cytoplasmic compartment in uninfected cells (Fig 3.1C). Together this data illustrates that we successfully produced a cell line stably expressing the B1myc protein in the cytoplasmic compartment.

To next construct a B1 deletion virus (ΔB1), we utilized a targeting construct in which the mCherry ORF was placed downstream of the vaccinia p11 late promoter and

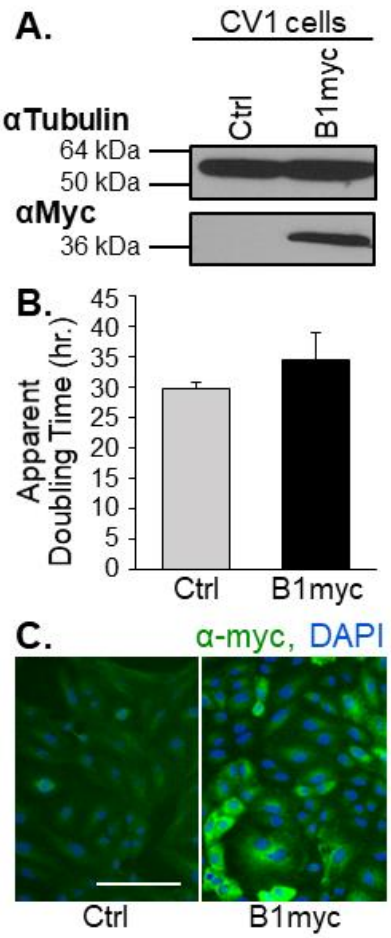

Fig 3.1. Characterization of CV1 cells stably expressing myc-tagged B1 kinase. (A) Representative immunoblot analysis of CV1 whole-cell lysates of control cells or B1myc expressing cells using αmyc or αtubulin primary antibodies. (B) The apparent doubling time of CV1 control (n=2) and B1myc expressing (n=5) cells was calculated. Error bars represent standard deviations. (C) Immunofluorescence analysis of B1myc protein localization in uninfected CV1 control and B1myc transduced cells. The B1myc protein was detected using αmyc primary antibody with appropriate secondary antibody and DAPI was used to detect the cellular nucleus.

flanked by ~250bp homologous to the sequence immediately upstream and downstream of the B1R ORF in the vaccinia WR genome (Fig 3.2A). This targeting construct containing the mCherry ORF was transfected into CV1-B1myc cells infected with WT vaccinia virus, and recombinant progeny were identified using fluorescence microscopy. Virus expressing mCherry was purified by serial plaque purification on CV1-B1myc cells until no non-fluorescent plaques (out of 100 plaques) were observed, and then plaque purified an additional six times. This virus was then expanded on CV1-B1myc cells and replacement of the B1R ORF was verified by PCR using primer sets 1-3 (Fig 3.2A), and DNA sequencing (data not shown). Upon confirmation of the sequence of the newly purified recombinant virus, we began characterization of the B1 deletion virus in immunofluorescence assays and comparative growth studies with the temperature sensitive Cts2 virus detailed below. Microscopy studies using WT and ΔB1 in control CV1 and B1myc expressing cells revealed that replication factories are similar in size and number for WT and ΔB1 viruses in B1 complementing cell lines, but absent for ΔB1 infected control cells (Fig 3.2B, αI3 panel, white arrowheads). Additionally, B1myc localizes to I3 during both WT and ΔB1 infection (Fig 3.2B, white arrowheads) although dispersed in the cytoplasm in the absence of infection (Fig 3.1C). Based on these initial results, ΔB1 behaves similarly to the WT virus in CV1-B1myc cells in relation to the presence of replication foci and B1 recruitment to replication foci.

3.2. B1 expression in CV1 cells rescues viral growth of both Cts2 and ΔB1 to near WT levels.

Next, we characterized ΔB1 using a plaque assay and one-step viral yield assay in CV1 control cells and CV1-B1myc cells. For comparison, the well-characterized

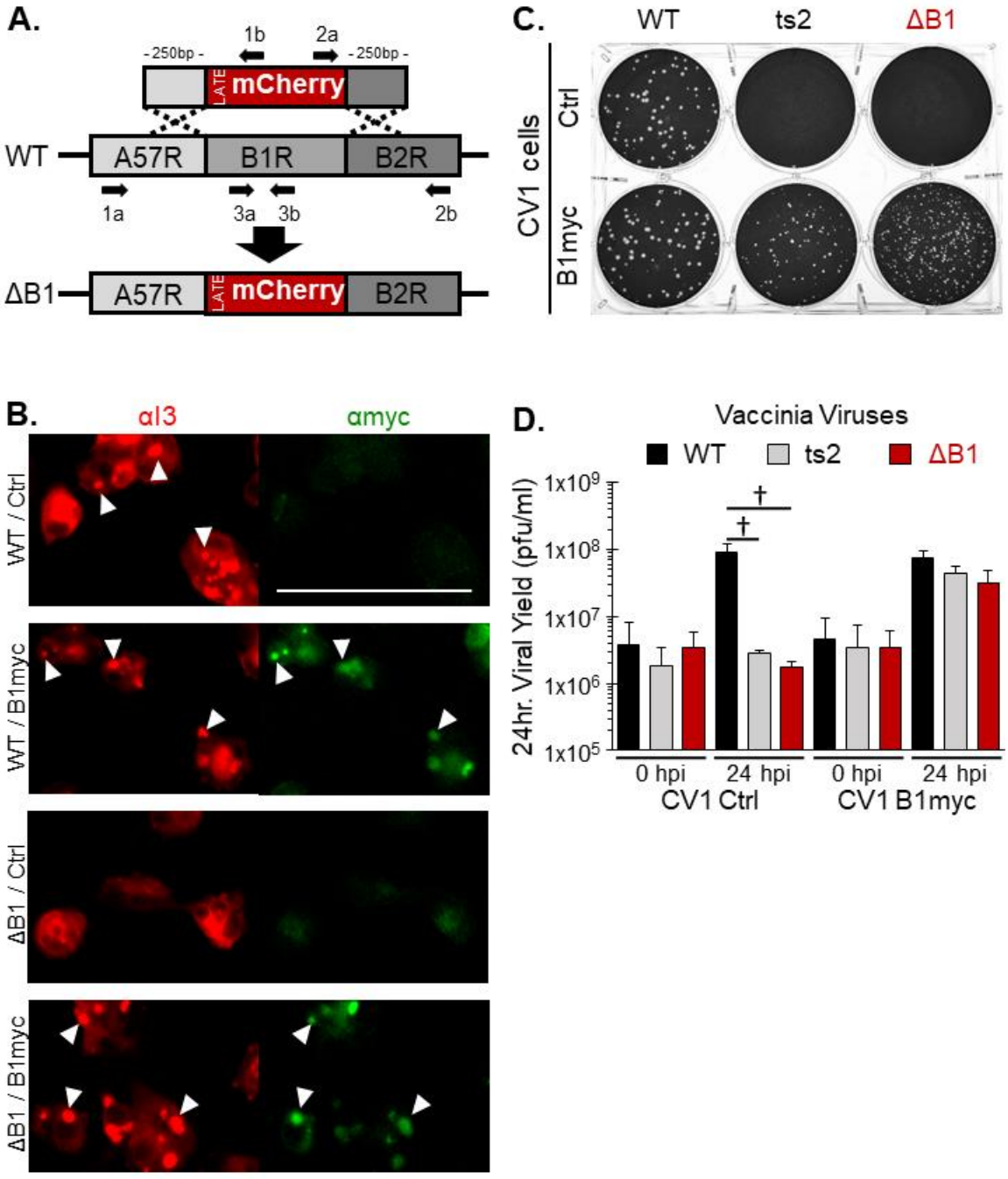
A.
1b
2a
- 250bp -
- 250bp -
LATE
mCherry
WT
A57R
B1R
B2R
1a
3a
3b
2b
ΔB1
A57R
LATE
mCherry
B2R
C.
WT
ts2
ΔB1
CV1 cells
Ctrl
B1myc
B.
αI3
αmyc
WT / Ctrl
WT / B1myc
ΔB1 / Ctrl
ΔB1 / B1myc
D.
Vaccinia Viruses
WT
ts2
ΔB1
24hr. Viral Yield (pfu/ml)
1x10^9
1x10^8
1x10^7
1x10^6
1x10^5
†
†
0 hpi
24 hpi
0 hpi
24 hpi
CV1 Ctrl
CV1 B1myc

Fig 3.2. Knockout strategy and growth characteristics of ΔB1 in CV1 cells. (A) The B1 deletion virus was generated via homologous recombination between the WT WR vaccinia genome and a DNA fragment of the *mCherry* gene with 250bp homologous sequence to the regions flanking the *B1* gene, replacing the *B1* gene with *mCherry* gene under a late viral promoter, p11. Arrows indicate primer sets used to amplify DNA used for sequence confirmation of recombination. **(B)** Immunofluorescence analyses of CV1 control and B1myc cells infected with WT or ΔB1 virus at MOI=5 for 7hr at 37˚C before fixation. Detection of I3 (red) used αI3 primary antibody and B1myc (green) detection used αmyc primary antibody. White arrowheads point to I3 (red) foci representative of DNA replication factories (left panels) and B1myc (green) foci colocalizing with I3 (right panels, B1myc cells only). The late mCherry fluorescent protein produced during ΔB1 infection was not above background levels at 7hpi (data not shown). (C) Plaque assay of control (top row) and B1myc expressing (bottom row) CV1 cells infected with 200PFU per well WT, Cts2, or ΔB1. Cells were incubated for 72hr at 39.7˚C prior to fixation and staining. (D) 24hr viral yield assays were carried out at 39.7˚C for WT (black), Cts2 (grey), and ΔB1 (red) on control (left three bars) and B1myc expressing (right three bars) CV1 cells. Virus titrations were completed on B1myc expressing cells at 31.5˚C. Standard deviation is denoted by error bars and † indicates a p-value < 0.05.

temperature sensitive virus, Cts2, was also included in these assays. Importantly, the Cts2 virus is able to complete the viral life cycle and produce infectious virions at low temperature (31.5˚C), but is inhibited at the stage of DNA replication at high temperature (39.7˚C) (68, 75). In the Cts2 virus, the *B1R* gene contains a single nucleotide substitution that results in expression of a more labile and catalytic-inert protein (75). Therefore, we predicted that the CV1-B1myc cells will complement the Cts2 virus as well as our new recombinant virus, ΔB1. Indeed, B1myc expression rescued the Cts2 virus at non-permissive temperature (39.7˚C) and the ΔB1 at low multiplicity of infection (MOI) as assayed using a plaque assay (Fig 3.2C). Specifically, the number of plaques for Cts2 and the ΔB1 increased from zero to about 200 plaques, although it is noteworthy that the plaque morphology of both Cts2 and ΔB1 produced slightly smaller plaques as compared to the WT virus plaques. Additionally, the WT virus plaque numbers and morphology were not altered by the expression of B1myc in CV1 cells, demonstrating that B1 expression from the cell does not enhance WT viral growth at low MOI.

Production of infectious virus during Cts2 and ΔB1 infection was then assessed through a one-step 24hr infection and titration of virus. In the CV1 control cells (at 39.7˚C) both the Cts2 and ΔB1 viral yield were reduced about 32 and 53 fold respectively in viral yield as compared to WT viral yield (Fig 3.2D). We found that this decrease in yield could be rescued for Cts2 if the assay was done at 31.5°C, but not for the ΔB1 virus (data not shown), thus demonstrating that ΔB1 is not temperature sensitive. Next, the same assays were performed in CV1-B1myc cells. Expression of B1 in these cells did not significantly alter WT viral yield from levels in control cells. However, infections of the CV1-B1myc cells revealed a significant rescue of both the Cts2 and ΔB1 to near WT

levels for viral yield. Specifically, B1myc expression from the cells increased Cts2 and ΔB1 viral yield 16 and 18 fold respectively from viral yield in control cells (Fig 3.2D). Together, these data provide evidence that deletion of B1 from the viral genome results in a severe, temperature-independent loss in viral fitness and that B1 expression from the cell can complement for this defect.

3.3. B1 expression in CV1 cells is necessary and sufficient to hyperphosphorylate BAF independent of other viral factors.

Previous studies of the B1 kinase determined that this kinase is needed to directly regulate the phosphorylation and thus the antiviral activity of BAF, a cellular DNA binding protein. Specifically, hyperphosphorylated BAF has reduced affinity for dsDNA and reduced homodimerization activity, both of which are required to facilitate dsDNA condensation and inhibition of vaccinia DNA replication and intermediate transcription (81, 98, 102, 135). Despite our growing understanding of this B1-BAF signaling axis, it is unknown if the B1 kinase activity mediating BAF phosphorylation in cells is enhanced by other viral factors. To address this gap in knowledge we utilized both the B1myc expressing CV1 cells and ΔB1, to determine if B1myc expression in cells in the absence of infection results in BAF phosphorylation to levels similar to WT infection. First, lysates from uninfected control cells or CV1-B1myc cells were used for an immunoblot analysis of total BAF protein levels and phospho-specific BAF protein levels. Total BAF protein levels were similar between the CV1 control (Fig 3.3A, lane 1, top panel) and CV1-B1myc (lane 2, top panel) transduced cells whereas phospho-specific BAF protein levels were markedly higher in cells stably expressing the B1myc protein than EV (empty vector) transduced cells (Fig 3.3A, compare lanes 1 and 2, bottom panel). Quantitation of

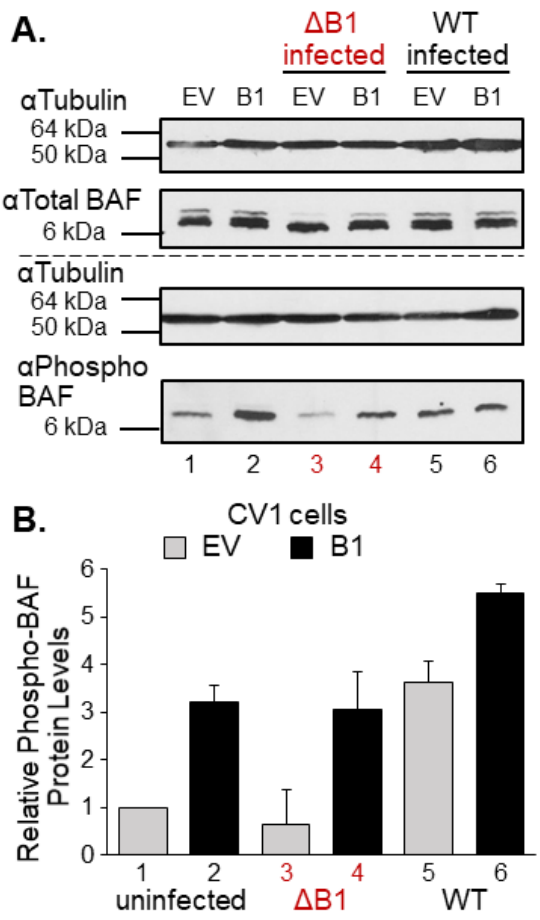

Fig 3.3. B1 is necessary and sufficient to phosphorylate BAF in cultured cells. (A) Whole-cell lysates were harvested from CV1 control (EV) or B1myc expressing (B1) cell lines which were uninfected (lanes 1 and 2) or infected with ΔB1 (lanes 3 and 4, red) or WT (lanes 5 and 6) at MOI=10 for 6hr at 37˚C. Top panel representative immunoblot assayed for tubulin loading control and total BAF protein levels. The same lysates were used to generate the bottom panel of tubulin loading control and phosphorylated BAF form as detected by the phospho-specific BAF antibody. (B) Relative phospho-BAF/ total BAF protein levels were quantified by measuring chemiluminescence using ImageLab software (Bio-Rad) and error bars represent standard deviation (n=4). The uninfected EV sample was set to 1. Numbers under each column correlate to numbering for immunoblot in Fig 3A.

relative phospho-BAF protein levels from four independent experiments are graphed and demonstrate that on average, greater than 3-fold more phosphorylated BAF is found in B1myc-expressing cells than in control cells (Fig 3.3B). These data support the conclusion that B1myc alone is able to upregulate BAF phosphorylation independent of other viral factors.

We next addressed the question of whether other viral factor(s) enhance B1 mediated BAF phosphorylation. CV1 control cells and B1myc expressing cells were infected with either WT virus or ΔB1. Cell lysates isolated at 6hpi were used for analysis of total BAF and phospho-BAF levels. In regard to total BAF protein, we observed similar levels for uninfected and infected cell lysates of both EV (empty vector) and B1myc expressing CV1 cells (Fig 3.3A, top panel). In regard to phosphorylated BAF, ΔB1 infected control CV1 cells consistently showed phospho-BAF levels similar to those in uninfected control CV1 cells (Fig 3.3A, compare lane 1 and 3 in lower panel). In comparison, B1myc expression from cells during ΔB1 infection rescues phospho-BAF levels by approximately 3-fold; similar to fold increase between uninfected CV1-B1myc cells and WT infected control cells (Fig 3.3B, compare column 4 to 1 and 5). WT infected CV1-B1myc cells had on average higher phospho-BAF levels, but no significant change in plaque formation nor viral yield was observed (Fig 3.2B and C). Overall, the findings that no difference is found between BAF phosphorylation in Fig 3.3B (columns 2 and 4) argues against another vaccinia protein enhancing B1 phosphorylation of BAF. Together, these data support previous evidence that B1 kinase is necessary to phosphorylate BAF in cells. Furthermore, our data provide new evidence that this

mechanism occurs independent of other viral factors, as phosphorylation of BAF is not enhanced in the presence of other viral proteins.

3.4. BAF depletion results in a partial rescue of ΔB1 replication.

BAF depletion strongly rescues both viral DNA replication and viral yield during Cts2 infection (69), demonstrating that a primary function of B1 is to inactivate the antiviral activity of BAF. Based on those data, we hypothesized that depletion of BAF would similarly rescue the growth of ΔB1. To test this prediction, lentiviral expression of BAF-specific shRNA was used to deplete endogenous BAF to about 20% of the total BAF protein in CV1 cells (Fig 3.4A). A plaque assay was used to assess viral growth at low MOI in control cells and BAF depleted cells. WT virus maintained plaque size and number independent of BAF depletion, as expected. The Cts2 virus plaque number was rescued by BAF depletion at non-permissive temperature, which is consistent with previous studies utilizing this model. Although, as seen before, the Cts2 plaque size is noticeably smaller than WT (73). Therefore, both B1myc expressing cells (Fig 3.2C) and BAF depleted cells (Fig 3.4B) rescue Cts2 deficiency in plaque number. ΔB1, however, was not rescued by BAF depletion at low MOI infection; no visible plaques were present in either the control or BAF depleted CV1 cells (Fig 3.4B). These results indicate that CV1-B1myc cells (Fig 3.2C) but not BAF depleted cells (Fig 3.4B) rescue the ΔB1 plaque numbers to WT levels at a low MOI infection.

Subsequent studies were conducted at higher MOI to determine DNA replication and viral yield of the ΔB1 in the BAF depleted cells. WT DNA replication remained constant independent of BAF depletion representing control conditions with a functional B1 kinase produced by vaccinia (Fig 3.4C, columns 1 and 4). During Cts2 and ΔB1

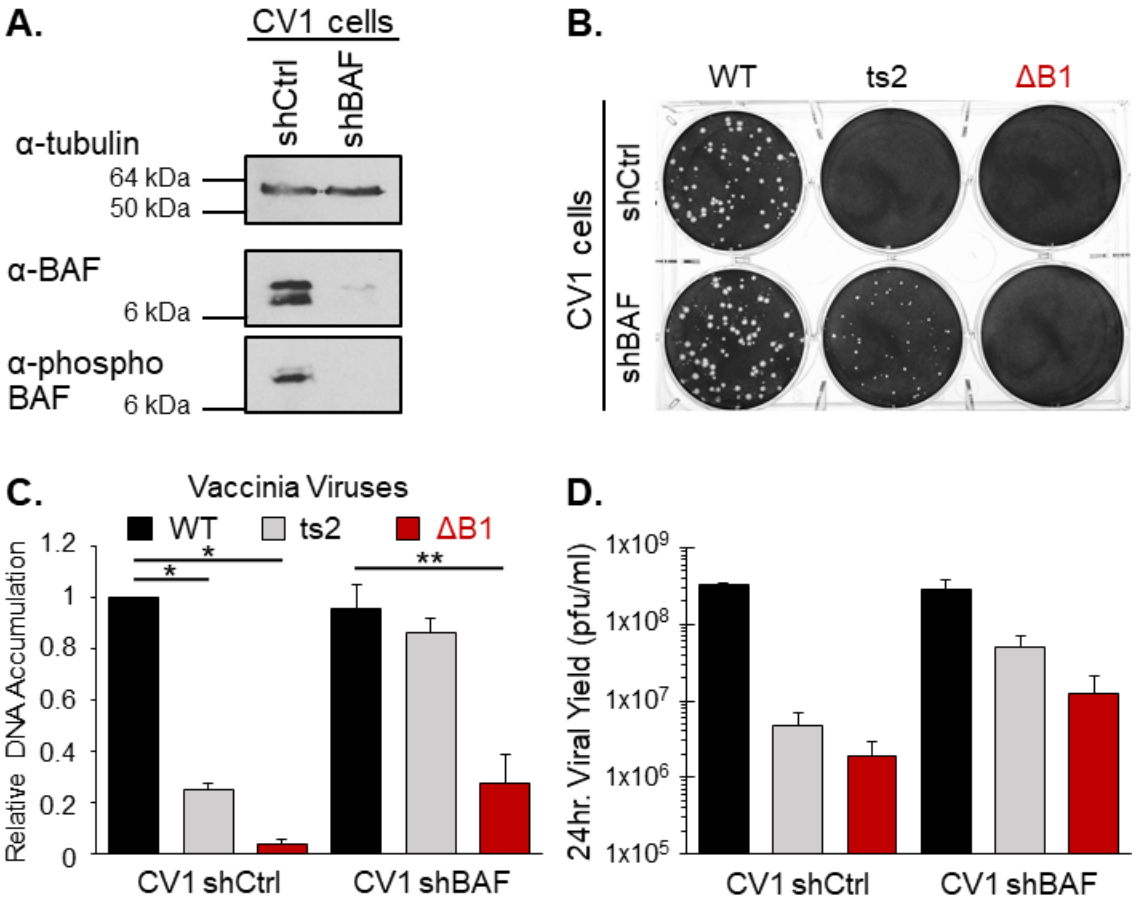

Fig 3.4. Impact of BAF depletion on growth of B1 mutant viruses. (A) Representative immunoblot analysis of BAF in CV1 cells transduced to express shCtrl or shBAF. Detection of tubulin (top panel) was used as a loading control. Total BAF (middle panel) and phospho-BAF (bottom panel) levels were detected using primary antibodies αBAF and αphospho-BAF, respectively. (B) Plaque assay on control (top row) and BAF depleted (bottom row) CV1 cells infected with 200PFU of WT, Cts2, or ΔB1 per well. Cells were incubated for 72hr at 39.7˚C prior to fixation and imaging. One-step (C) DNA accumulation and (D) viral yield assays were completed at 39.7˚C for WT, Cts2, and ΔB1 on shCtrl and shBAF CV1 cells. The WT/CV1 shCtrl sample was set to 1 for relative DNA accumulation. Virus titers were quantified on B1myc expressing cells at 31.5˚C

(Fig 3.4 continued) (permissive temperature for Cts2 virus). Standard deviation is denoted by error bars and p-values * < 0.005, ** < 0.001 (black lines drawn between compared columns).

infections of shCtrl CV1 cells a 75% and 96% reduction of DNA accumulation, respectively, was observed as compared to WT infection of shCtrl cells (Fig 3.4C). In comparison, DNA accumulation during Cts2 infection of BAF depleted CV1 cells was only reduced about 13% from WT, while DNA replication of ΔB1 remained 72% attenuated in BAF depleted cells (Fig 3.4C). Therefore, BAF depletion rescued Cts2 DNA accumulation to near WT levels, but ΔB1 still exhibited attenuation in cells depleted of BAF. To next examine the impact of BAF depletion on production of infectious virus, one-step viral yield assays were undertaken. We observed that the Cts2 and ΔB1 viral yields were reduced 71 and 170 fold as compared to WT during infection of CV1 cells expressing a control shRNA (Fig 3.4D). However, the Cts2 and ΔB1 viruses were about 6 and 23 fold less than WT, respectively, in the BAF depleted cell infections (Fig 3.4D). Therefore, BAF depletion cannot fully rescue ΔB1 DNA replication and viral yield to WT levels. These results revealed an enhanced deficiency of ΔB1 DNA replication and viral yield as compared to the Cts2 virus. It appears that while the B1 mutant protein expressed by Cts2 is highly labile and catalytic-inert at high and low temperatures (75), it still makes a substantial contribution to the viral life cycle either by regulating BAF or possibly through participation in additional, unknown signaling pathways.

3.5. The ΔB1 displays a growth deficient phenotype in multiple cell lines.

We next examined whether ΔB1 exhibited cell-type specific variability in its replication. Previous work using Cts2 and Cts25, another temperature sensitive B1 mutant virus, showed reduced viral growth in the mouse L929 cells when compared to BSC40 cells at non-permissive temperature (68, 75), suggesting that the mutant B1 and/or its substrates may function in a cell type specific manner. If it is the substrates rather than the mutant B1 that is cell-type dependent, then one would predict that ΔB1 would have a similar trend as the Cts2 virus, attenuated viral growth overall and increased deficiency in the mouse L929 cell line. Interestingly, our results showed that the DNA replication was attenuated for the ΔB1 to a similar degree in monkey, mouse and human cell lines with no increased deficiency in the L929 mouse cells as was previously found with Cts2 (75) (Fig 3.5A and C). Virus production was also profoundly diminished, with the ΔB1 viral yield was 448, 176, and 668 fold lower than WT in BSC40, CV1, and L929 cell lines respectively (Fig 3.5B), and 650 fold lower than WT in HeLa cells (Fig 3.5D). Together, these data demonstrate that loss of B1 results in a significantly decrease in viral fitness that can be observed in diverse cell types.

3.6. Chapter 3 Summary

In this chapter we discussed the successful construction of a B1 complementing cell line and B1 deletion vaccinia virus (Fig 3.1 and 3.2). Using this new system to study B1, we determined that B1 in cell culture is sufficient to hyperphosphorylate BAF without additional viral factors (Fig 3.3). We also characterized the phenotype of this ΔB1 virus with the Cts2 B1 mutant virus, which led to a pivotal discovery. Although depletion of BAF rescued the block in DNA replication for the Cts2 B1 mutant virus, only a modest

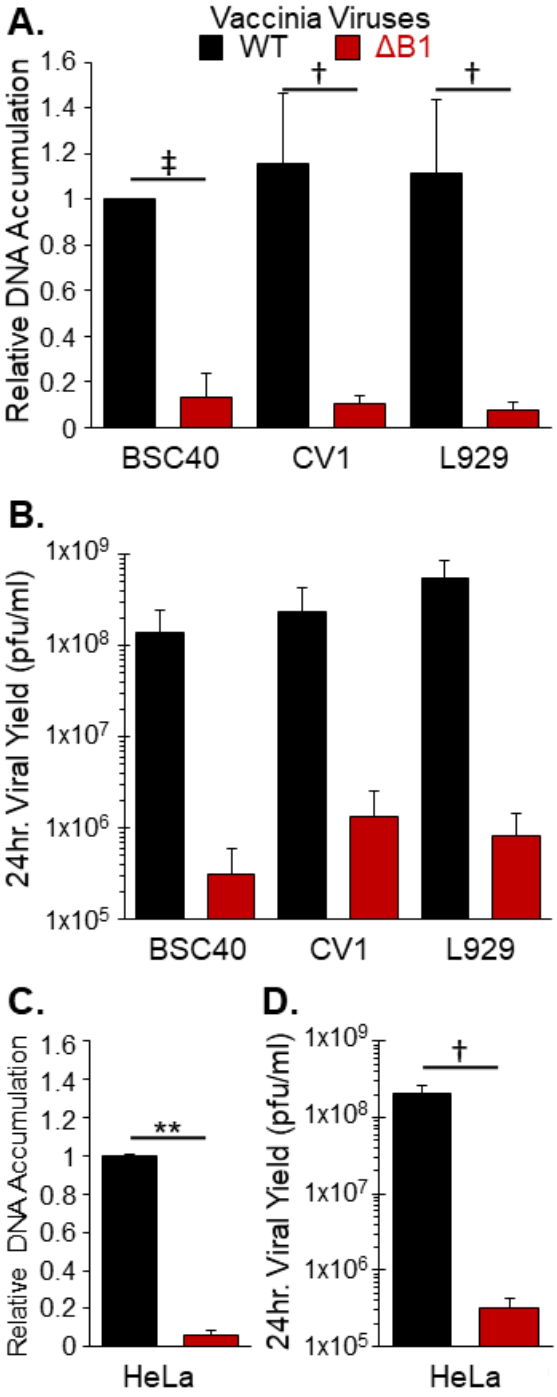

Fig 3.5. Growth of ΔB1 in multiple cell types. One-step infections at MOI=3 for WT (black) or ΔB1 (red) on BSC40, CV1, L929, or HeLa cells incubated at 37˚C. Cells and virus were harvested at 24hpi. (A) DNA accumulation for BSC40, CV1, and L929 cells.

The WT/BSC40 sample was set to 1. (B) Viral yield for infections in BSC40, CV1, and L929 cells. Virus titrations were completed on B1myc expressing CV1 cells. HeLa cell (C) DNA accumulation and (D) viral yield were conducted separately from other cell lines, using an identical protocol. The WT/HeLa sample was set to 1. Viral harvest was titered on CV1-B1myc cells. Standard deviation is denoted by error bars and p-values † < 0.05, ‡ < 0.01, ** < 0.001 (black lines drawn between compared columns).

rescue was observed for the ΔB1 virus (Fig 3.4). Furthermore, the attenuated phenotype of B1 deletion virus was observed in monkey, human and mouse cell lines to similar levels (Fig 3.5). At this point, we predicted that the Cts2 virus expressed a partially functional B1 protein. Although it remained unclear if in the absence of B1, BAF is morepotent than previously appreciated or if B1 also restricts another repressor of viral DNA replication (Fig 3.6).

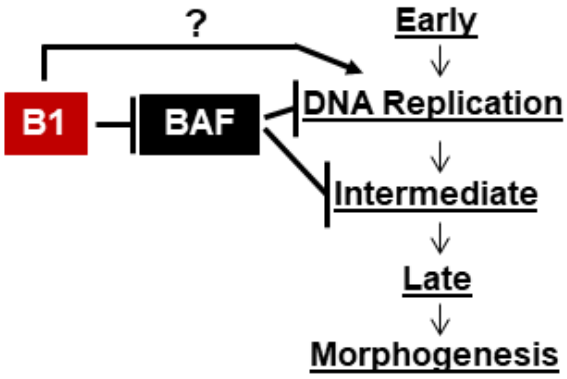

Fig 3.6. B1 regulates DNA replication via a BAF-dependent and independent mechanism. The vaccinia virus life cycle includes stages of early gene expression (early), DNA replication, intermediate gene expression (intermediate), late gene expression (late), and morphogenesis of the assembled virion into a mature virion. In chapter 3 we have confirmed the function of B1 to restrict BAF antiviral activity against vaccinia DNA replication. BAF was previously shown to restrict vaccinia intermediate transcription (81). Our addition to this signaling axis of B1-BAF is a BAF-independent function of B1 to promoted vaccinia DNA replication.

CHAPTER 4

VACCINIA B1 KINASE COMPLEMENTATION BY CELLULAR VRK2

4.1. B1 downregulates gene sets related to immune response signaling.

The vaccinia B1 kinase has a highly promiscuous phosphorylation profile in vitro (98), while also exhibiting conserved phosphorylation of both host (84, 85, 98) and viral (86, 87) proteins in cell culture. Due to the signaling capability of kinases in general and the unrestrained phosphorylation activity of the B1 kinase, we posited that expression of B1 in cells would result in transcriptional modifications. These significantly altered transcripts may provide insight on which pathways the B1 kinase is regulating during infection to promote efficient vaccinia virus replication. We chose to complete our transcriptome analysis of B1 expression in mouse L929 cells due to the available resources to analyze mouse transcriptome changes and signaling pathways. Initially, we assayed for B1 expression in stably transduced L929 cells using immunoblot analysis (Fig 4.1A). Upon confirmation of B1 expression, we transfected control (Ctrl) or B1 expressing cells (B1myc) with 2ug control plasmid or lipofectamine only untransfected with three samples per condition. Cells were harvested 6h post transfection and RNA was extracted and purified. The RNA integrity number (RIN) score was 10, which certified excellent RNA quality, for each sample as measured using the Advanced Analytical Technical Instruments (AATI) Fragment Analyzer (data not shown). Importantly, RNA quality scores below 6 have a drastic, negative impact on the confidence of differential gene expression trends observed due to RNA degradation unrelated to experimental conditions. Sequencing libraries for each sample were generated and followed by RNA

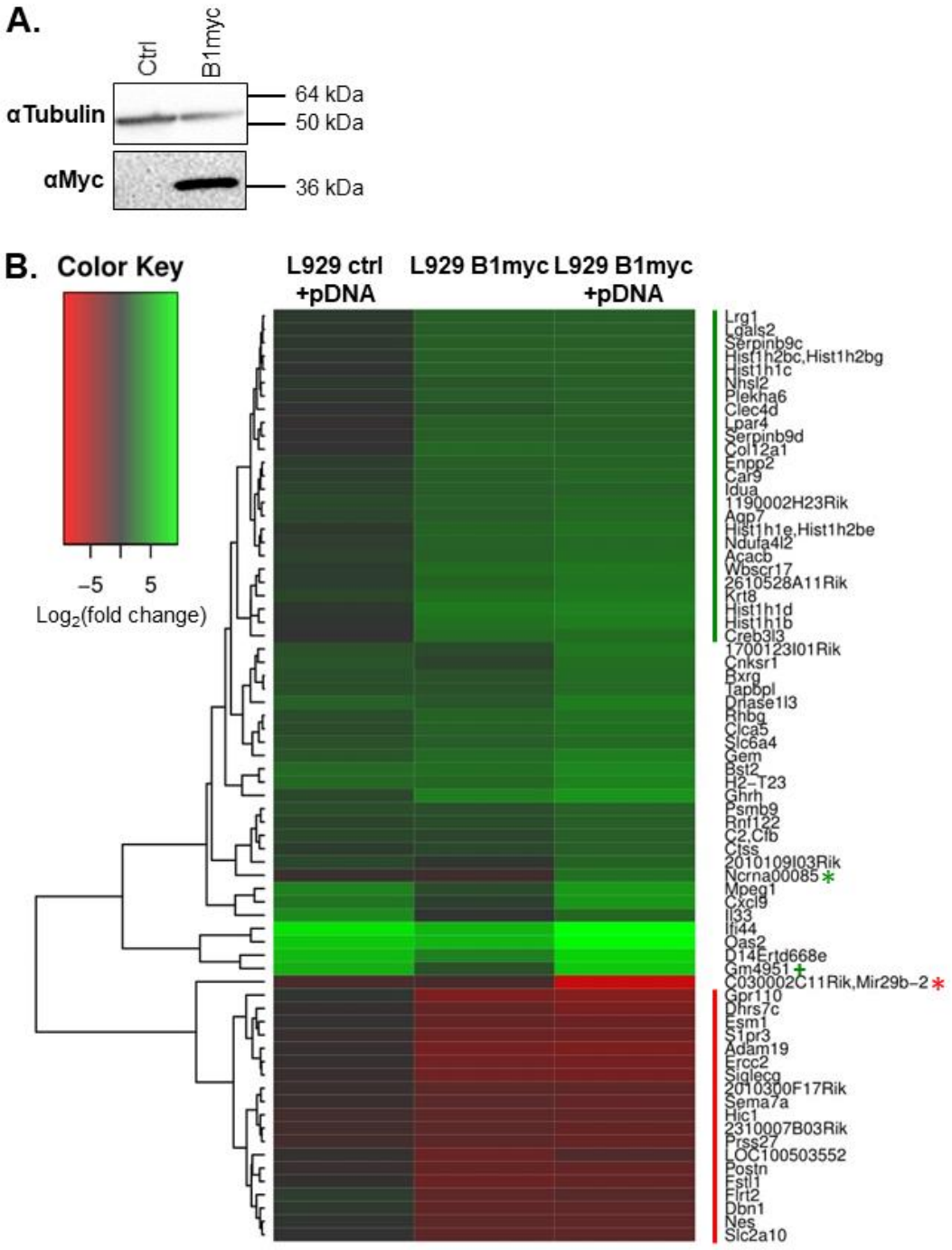
A.
Ctrl
B1myc
αTubulin
αMyc
64 kDa
50 kDa
36 kDa
B. Color Key
−5
5
Log2(fold change)
L929 ctrl +pDNA
L929 B1myc
L929 B1myc +pDNA
Lrg1
Lgals2
Serpinb9c
Hist1h2bc,Hist1h2bg
Hist1h1c
Nhsl2
Plekha6
Clec4d
Lpar4
Serpinb9d
Col12a1
Enpp2
Car9
Idua
1190002H23Rik
Aqp7
Hist1h1e,Hist1h2be
Ndufa4l2
Acacb
Wbscr17
2610528A11Rik
Krt8
Hist1h1d
Hist1h1b
Creb3l3
1700123I01Rik
Cnksr1
Bxrg
Tapbpl
Dnase1l3
Rhbg
Clca5
Slc6a4
Gem
Bst2
H2−T23
Ghrh
Psmb9
Rnf122
C2,Cfb
Ctss
2010109I03Rik
Ncrna00085
Mpeg1
Cxcl9
Il33
Ifi44
Oas2
D14Ertd668e
Gm4951
C030002C11Rik,Mir29b−2
Gpr110
Dhrs7c
Esm1
S1pr3
Adam19
Ercc2
Siglecg
2010300F17Rik
Sema7a
Hic1
2310007B03Rik
Prss27
LOC100503552
Postn
Fstl1
Flrt2
Dbn1
Nes
Slc2a10

Fig 4.1. Transcriptional modulation of host genes during B1 expression. (A) Control or B1myc stably expressing L929 cell lysates were subjected to immunoblot analysis using αTubulin and αMyc primary antibodies to detect tubulin (loading control) and B1myc protein. (B) Transcriptome data was analyzed for the following comparisons as presented in a heat map: L929 control/plasmid DNA to L929 control, L929 B1myc to L929 control, and L929 B1myc/plasmid DNA to L929 control. Gene transcripts that were reduced as compared to L929 control gene transcripts (red) and increased (green) are included in the heat map for data (P-value <0.05). The green or red bar next to the gene names represents >1.9 fold increase (green) or decrease (red) in transcripts for L929 B1myc comparison to L929 control cells. Asterisks and plus sign highlight genes of interest: Ncrna00085 (green asterisk), Gm4951 (green plus sign), and [C030002C11 Rik, miR-29b-2, miR-29c] (red asterisk).

sequencing. The RNA sequencing quality was greater than 30, with a mean core of 37. Transcriptome analysis was completed by comparing sample RNA sequencing data with the mouse transcriptome. Under B1 expression, transcription of 242 genes out of 28,902 total murine genes were significantly changed from control cells (P-value <0.05). A subset of these genes had a Log_2(fold change) > 1.9. Specifically, 25 genes were upregulated (Fig 4.1B, L929 B1myc column, green line) and 19 genes were downregulated (Fig 4.1B, L929 B1myc column, red line) as compared to L929 control cells. Ncrna00085 also known as sperm acrosome associated 6 (SPACA6) protein mRNA is upregulated in L929 B1myc cells with plasmid DNA but not in L929 with plasmid DNA nor in L929 B1myc cells (Fig 4.1B, green * and Table 4.1). The SPACA6 protein

Table 4.1 Transcriptome details of genes of interest				Log2(fold change) as compared to L929 cells			Gene Ontology (Provided by Mouse Genome Informatics)			
Gene	**Gene name**	**NCBI ID**	**Gene Type**	**L929 with pDNA**	**L929 B1myc**	**L929 B1myc with pDNA**	**Function**	**Process**	**Component**	**Comments**
Ncrna00085	Sperm acrosome associated 6	75202	protein coding	**-0.248089**	**-0.584388**	**2.92541**	Molecular function	Fusion of sperm to egg plasma membrane involved in single fertilization	Integral component of membrane, Membrane	A male-infertile transgenic mouse, BART97b, has a deletion of the *Spaca6* gene which encodes an uncharacterized Immunoglobulin Superfamily (IgSF) protein. The murine *Spaca6* encodes an evolutionary conserved IgSF protein. PMID: 24275887
C030002C11Rik, Mir29b-2,Mir29c	non-coding RNA gene region			**-1.17196**	**-0.974089**	**-6.96485**				
C030002C11Rik	RIKEN cDNA A330023F24	320977	long non-coding RNA				N/A	N/A	N/A	
Mr29b-2	microRNA 29b-2	723963	non-coding RNA				N/A	Cellular hyperosmotic salinity response Cellular response to leukemia inhibitor factor Cellular reponse to lipopolysaccharide Long-term synaptic potentiation Negative regulation of gene expression Sensory perception of sound Tissue remodeling	N/A	
Mr29c	microRNA 29c	387224	non-coding RNA				N/A	Cellular hyperosmotic salinity response Cellular response to amino acid stimulus Cellular response to ethanol Cellular response to leukemia inhibitor factor Negative regulation of gene expression Tissue remodeling	N/A	Linkage between miRNA29c and immune response modulation to viruses. PMID: 24953694 & 28063705
Gm4951	Interferon-gamma-inducible GTPase 2 (Ifgga2)	240327	protein coding	**5.78962**	**1.51303**	**6.95206**	GTPase activity	Cellular response to interferon-beta Defense response	endoplasmic reticulum membrane	

is essential for male murine fertility, specifically in the ability of sperm to fuse with the egg plasma membrane (136). The next gene region of interest includes the following three genes, which were grouped together; C030002C11 Rik, miR-29b-2, and miR-29c. This gene cluster was significantly reduced in expression particularly in L929 B1myc cells with plasmid DNA (Fig 4.1B, red * and Table 4.1). Interestingly, the miR-29c is related to modulation of innate and adaptive immunity signaling in response to viruses (137, 138). Lastly, Gm4951 transcripts were increased in all samples as compared to L929 cells, and B1myc expression with plasmid DNA seemed to have an additive impact on transcription levels (Fig 4.1B, green + and Table 4.1). The *Gm4951* gene is also referred to as interferon-gamma-inducible GTPase 2, which is based on functional predictive methods based on gene sequence.

Another method was taken to analyze this data utilizing gene ontology tools. First, the transcriptome raw count data was converted to gene symbols. Second, GSEA was used to identify regulated pathways for B1 expression and/or plasmid DNA transfection with L929 cell control condition. In cells expressing B1, there was a trend of low expression values for gene sets related to immune response/ stress signaling (Fig 4.2A). A comparison between plasmid transfected L929 and L929 B1myc cells had gene sets with higher expression values for pathways associated with endoplasmic reticulum (ER), Golgi apparatus, and vesicle transport signaling as well as proteolysis activity signaling, signal transduction and immune signaling for the L929 B1myc plasmid transfected condition (Fig 4.2B). Analysis of gene set enrichment differences between L929 cells and L929 B1myc cells transfected with plasmid DNA showed lower gene expression for gene set for immune response/ stress signaling, proteolysis activity signaling, ER/Golgi

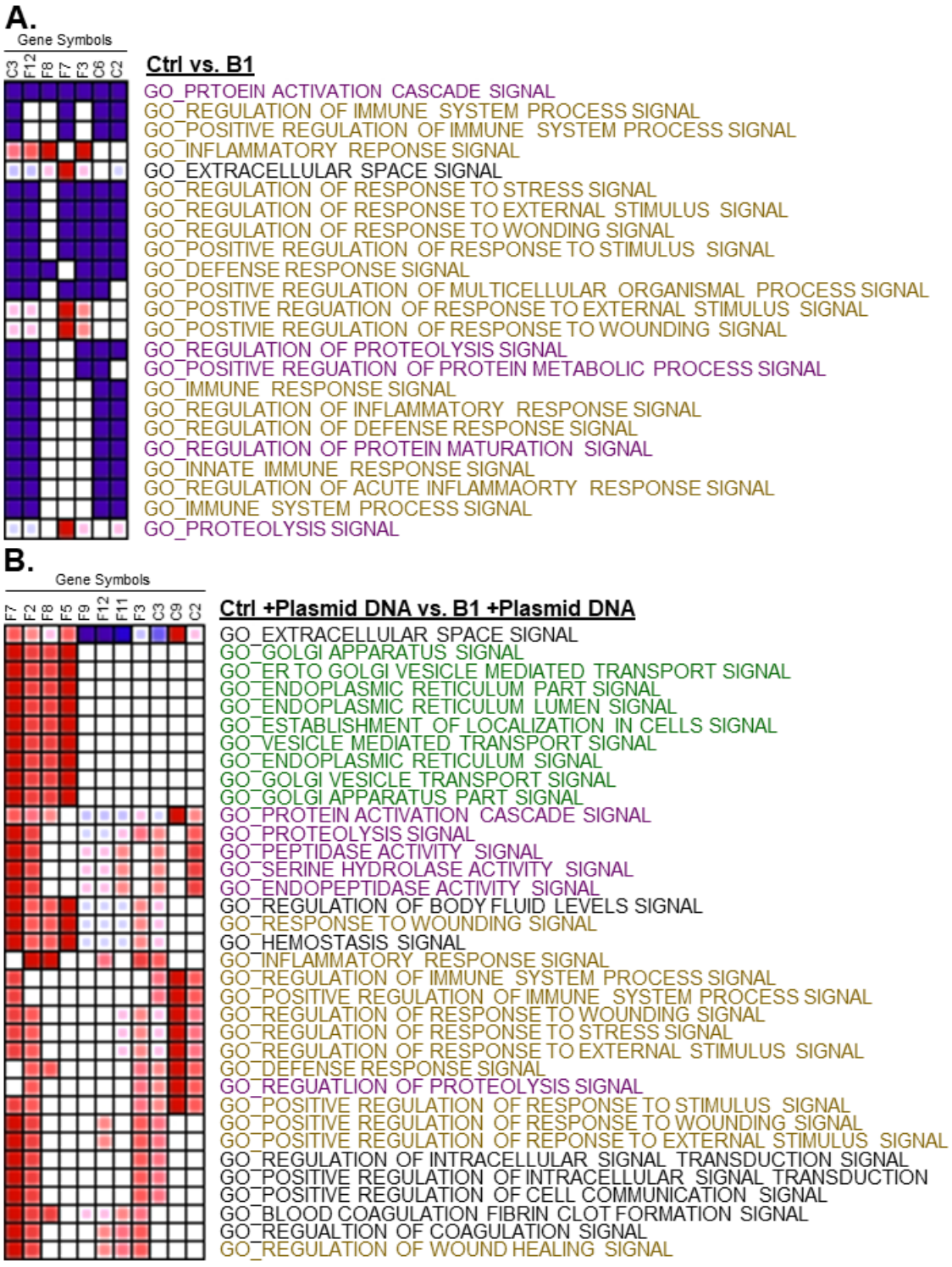
A.
Gene Symbols
C3 F12 F8 F7 F3 C6 C2
Ctrl vs. B1
GO_PRTOEIN ACTIVATION CASCADE SIGNAL
GO_REGULATION OF IMMUNE SYSTEM PROCESS SIGNAL
GO_POSITIVE REGULATION OF IMMUNE SYSTEM PROCESS SIGNAL
GO_INFLAMMATORY REPONSE SIGNAL
GO_EXTRACELLULAR SPACE SIGNAL
GO_REGULATION OF RESPONSE TO STRESS SIGNAL
GO_REGULATION OF RESPONSE TO EXTERNAL STIMULUS SIGNAL
GO_REGULATION OF RESPONSE TO WONDING SIGNAL
GO_POSITIVE REGULATION OF RESPONSE TO STIMULUS SIGNAL
GO_DEFENSE RESPONSE SIGNAL
GO_POSITIVE REGULATION OF MULTICELLULAR ORGANISMAL PROCESS SIGNAL
GO_POSTIVE REGUATION OF RESPONSE TO EXTERNAL STIMULUS SIGNAL
GO_POSTIVIE REGULATION OF RESPONSE TO WOUNDING SIGNAL
GO_REGULATION OF PROTEOLYSIS SIGNAL
GO_POSITIVE REGUATION OF PROTEIN METABOLIC PROCESS SIGNAL
GO_IMMUNE RESPONSE SIGNAL
GO_REGULATION OF INFLAMMATORY RESPONSE SIGNAL
GO_REGULATION OF DEFENSE RESPONSE SIGNAL
GO_REGULATION OF PROTEIN MATURATION SIGNAL
GO_INNATE IMMUNE RESPONSE SIGNAL
GO_REGULATION OF ACUTE INFLAMMAORTY RESPONSE SIGNAL
GO_IMMUNE SYSTEM PROCESS SIGNAL
GO_PROTEOLYSIS SIGNAL
B.
Gene Symbols
F7 F2 F8 F5 F9 F12 F11 F3 C3 C9 C2
Ctrl +Plasmid DNA vs. B1 +Plasmid DNA
GO_EXTRACELLULAR SPACE SIGNAL
GO_GOLGI APPARATUS SIGNAL
GO_ER TO GOLGI VESICLE MEDIATED TRANSPORT SIGNAL
GO_ENDOPLASMIC RETICULUM PART SIGNAL
GO_ENDOPLASMIC RETICULUM LUMEN SIGNAL
GO_ESTABLISHMENT OF LOCALIZATION IN CELLS SIGNAL
GO_VESICLE MEDIATED TRANSPORT SIGNAL
GO_ENDOPLASMIC RETICULUM SIGNAL
GO_GOLGI VESICLE TRANSPORT SIGNAL
GO_GOLGI APPARATUS PART SIGNAL
GO_PROTEIN ACTIVATION CASCADE SIGNAL
GO_PROTEOLYSIS SIGNAL
GO_PEPTIDASE ACTIVITY SIGNAL
GO_SERINE HYDROLASE ACTIVITY SIGNAL
GO_ENDOPEPTIDASE ACTIVITY SIGNAL
GO_REGULATION OF BODY FLUID LEVELS SIGNAL
GO_RESPONSE TO WOUNDING SIGNAL
GO_HEMOSTASIS SIGNAL
GO_INFLAMMATORY RESPONSE SIGNAL
GO_REGULATION OF IMMUNE SYSTEM PROCESS SIGNAL
GO_POSITIVE REGULATION OF IMMUNE SYSTEM PROCESS SIGNAL
GO_REGULATION OF RESPONSE TO WOUNDING SIGNAL
GO_REGULATION OF RESPONSE TO STRESS SIGNAL
GO_REGULATION OF RESPONSE TO EXTERNAL STIMULUS SIGNAL
GO_DEFENSE RESPONSE SIGNAL
GO_REGUATLION OF PROTEOLYSIS SIGNAL
GO_POSITIVE REGULATION OF RESPONSE TO STIMULUS SIGNAL
GO_POSITIVE REGULATION OF RESPONSE TO WOUNDING SIGNAL
GO_POSITIVE REGULATION OF REPONSE TO EXTERNAL STIMULUS SIGNAL
GO_REGULATION OF INTRACELLULAR SIGNAL TRANSDUCTION SIGNAL
GO_POSITIVE REGULATION OF INTRACELLULAR SIGNAL TRANSDUCTION
GO_POSITIVE REGULATION OF CELL COMMUNICATION SIGNAL
GO_BLOOD COAGULATION FIBRIN CLOT FORMATION SIGNAL
GO_REGUALTION OF COAGULATION SIGNAL
GO_REGULATION OF WOUND HEALING SIGNAL

Fig 4.2. Gene ontology for cells expressing vaccinia B1 kinase. L929 transcriptome data was used to identify signaling pathways differentially regulated under the following conditions: (A) L929 B1myc to L929 control and (B) L929 B1myc/plasmid DNA to L929 control/plasmid DNA. Gene symbols represent a set of genes from the GSEA consortium. The heat map indicates gene sets denoted by a specific gene symbol with high expression (red), low expression (blue) or no change (white) for the experimental condition as compared to control. Gene ontology (GO) terms were color coded to represent broad signaling categories: stress/immune response (gold), protein activation/proteolysis (purple), vesicle trafficking (green), and intracellular/extracellular signaling/signal transduction (black).

apparatus/vesicle transport signaling (Fig 4.3A). There were also a few gene sets with higher gene expression for pathways involving signal transduction and cell-to-cell communication (Fig 4.3A). Lastly, plasmid transfected cells as compared to L929 untransfected cells had lower gene set expression values for pathways related to proteolysis activity signaling and immune/stress signaling (Fig 4.3B). Together, this transcriptome analysis of B1 expressing cells with and without the presence of foreign DNA identified many genes of interest, particularly miR-29c, which will require further analysis for relevant genes of interest and functional ramifications during vaccinia virus infection. Furthermore, the gene ontology analysis of altered pathways during B1 expression suggests a function of B1 that reduces immune and stress responses, which would be beneficial in the context of vaccinia virus induction of immune and stress sensors.

A.

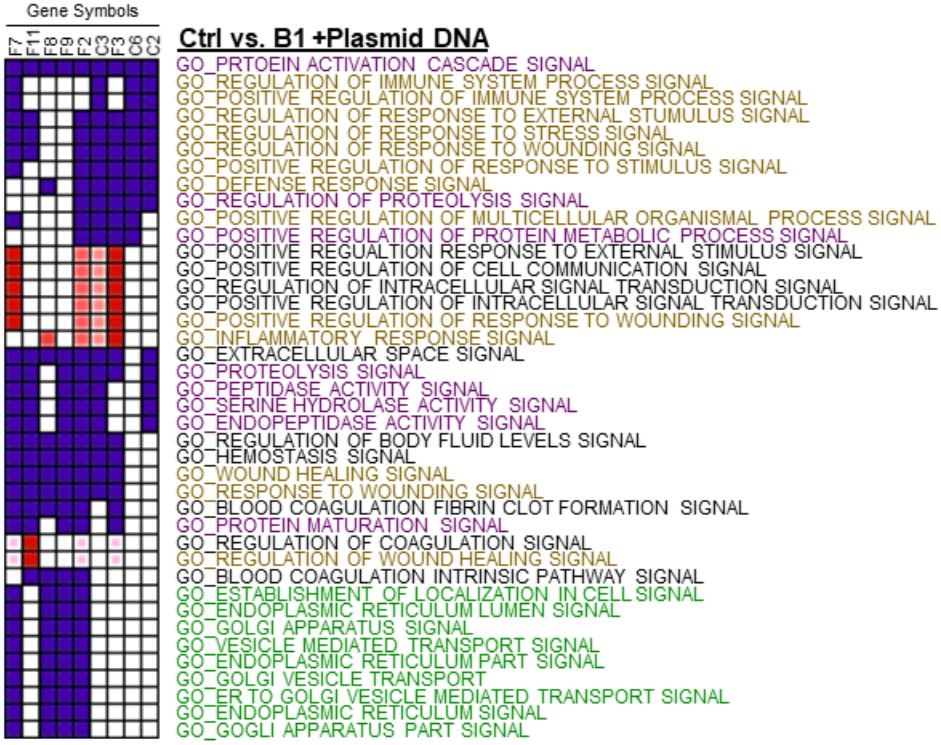
Gene Symbols
F7
F11
F8
F9
F2
C3
F3
C6
C2
Ctrl vs. B1 +Plasmid DNA
GO_PRTOEIN ACTIVATION CASCADE SIGNAL
GO_REGULATION OF IMMUNE SYSTEM PROCESS SIGNAL
GO_POSITIVE REGULATION OF IMMUNE SYSTEM PROCESS SIGNAL
GO_REGULATION OF RESPONSE TO EXTERNAL STUMULUS SIGNAL
GO_REGULATION OF RESPONSE TO STRESS SIGNAL
GO_REGULATION OF RESPONSE TO WOUNDING SIGNAL
GO_POSITIVE REGULATION OF RESPONSE TO STIMULUS SIGNAL
GO_DEFENSE RESPONSE SIGNAL
GO_REGULATION OF PROTEOLYSIS SIGNAL
GO_POSITIVE REGULATION OF MULTICELLULAR ORGANISMAL PROCESS SIGNAL
GO_POSITIVE REGULATION OF PROTEIN METABOLIC PROCESS SIGNAL
GO_POSITIVE REGUALTION RESPONSE TO EXTERNAL STIMULUS SIGNAL
GO_POSITIVE REGULATION OF CELL COMMUNICATION SIGNAL
GO_REGULATION OF INTRACELLULAR SIGNAL TRANSDUCTION SIGNAL
GO_POSITIVE REGULATION OF INTRACELLULAR SIGNAL TRANSDUCTION SIGNAL
GO_POSITIVE REGULATION OF RESPONSE TO WOUNDING SIGNAL
GO_INFLAMMATORY RESPONSE SIGNAL
GO_EXTRACELLULAR SPACE SIGNAL
GO_PROTEOLYSIS SIGNAL
GO_PEPTIDASE ACTIVITY SIGNAL
GO_SERINE HYDROLASE ACTIVITY SIGNAL
GO_ENDOPEPTIDASE ACTIVITY SIGNAL
GO_REGULATION OF BODY FLUID LEVELS SIGNAL
GO_HEMOSTASIS SIGNAL
GO_WOUND HEALING SIGNAL
GO_RESPONSE TO WOUNDING SIGNAL
GO_BLOOD COAGULATION FIBRIN CLOT FORMATION SIGNAL
GO_PROTEIN MATURATION SIGNAL
GO_REGULATION OF COAGULATION SIGNAL
GO_REGULATION OF WOUND HEALING SIGNAL
GO_BLOOD COAGULATION INTRINSIC PATHWAY SIGNAL
GO_ESTABLISHMENT OF LOCALIZATION IN CELL SIGNAL
GO_ENDOPLASMIC RETICULUM LUMEN SIGNAL
GO_GOLGI APPARATUS SIGNAL
GO_VESICLE MEDIATED TRANSPORT SIGNAL
GO_ENDOPLASMIC RETICULUM PART SIGNAL
GO_GOLGI VESICLE TRANSPORT
GO_ER TO GOLGI VESICLE MEDIATED TRANSPORT SIGNAL
GO_ENDOPLASMIC RETICULUM SIGNAL
GO_GOGLI APPARATUS PART SIGNAL

B.

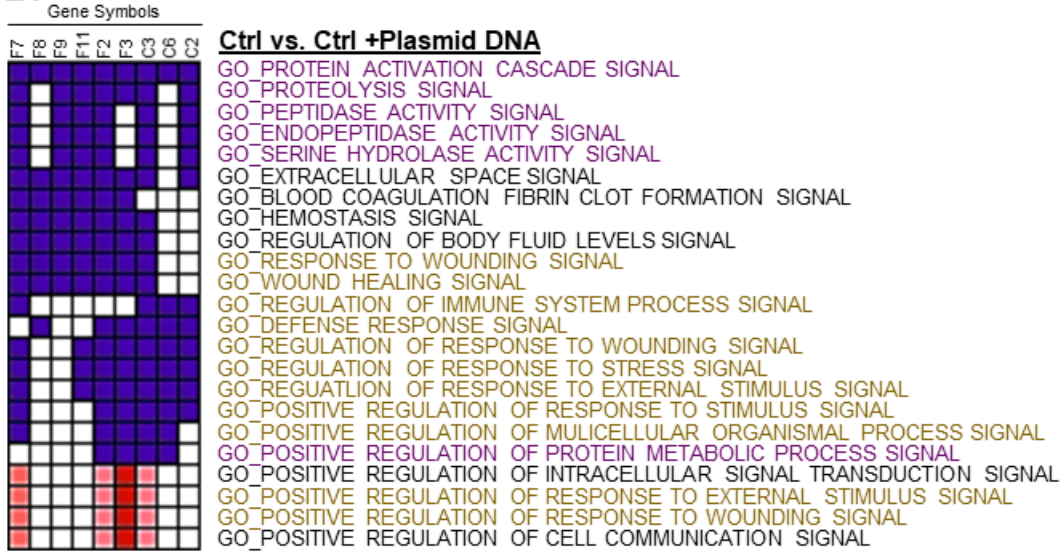
Gene Symbols
F7
F8
F9
F11
F2
F3
C3
C6
C2
Ctrl vs. Ctrl +Plasmid DNA
GO_PROTEIN ACTIVATION CASCADE SIGNAL
GO_PROTEOLYSIS SIGNAL
GO_PEPTIDASE ACTIVITY SIGNAL
GO_ENDOPEPTIDASE ACTIVITY SIGNAL
GO_SERINE HYDROLASE ACTIVITY SIGNAL
GO_EXTRACELLULAR SPACE SIGNAL
GO_BLOOD COAGULATION FIBRIN CLOT FORMATION SIGNAL
GO_HEMOSTASIS SIGNAL
GO_REGULATION OF BODY FLUID LEVELS SIGNAL
GO_RESPONSE TO WOUNDING SIGNAL
GO_WOUND HEALING SIGNAL
GO_REGULATION OF IMMUNE SYSTEM PROCESS SIGNAL
GO_DEFENSE RESPONSE SIGNAL
GO_REGULATION OF RESPONSE TO WOUNDING SIGNAL
GO_REGULATION OF RESPONSE TO STRESS SIGNAL
GO_REGUATLION OF RESPONSE TO EXTERNAL STIMULUS SIGNAL
GO_POSITIVE REGULATION OF RESPONSE TO STIMULUS SIGNAL
GO_POSITIVE REGULATION OF MULICELLULAR ORGANISMAL PROCESS SIGNAL
GO_POSITIVE REGULATION OF PROTEIN METABOLIC PROCESS SIGNAL
GO_POSITIVE REGULATION OF INTRACELLULAR SIGNAL TRANSDUCTION SIGNAL
GO_POSITIVE REGULATION OF RESPONSE TO EXTERNAL STIMULUS SIGNAL
GO_POSITIVE REGULATION OF RESPONSE TO WOUNDING SIGNAL
GO_POSITIVE REGULATION OF CELL COMMUNICATION SIGNAL

Fig 4.3. Gene ontology for B1/DNA and DNA control. L929 transcriptome data was used to identify signaling pathways differentially regulated under the following conditions: (A) L929 B1myc/plasmid DNA to L929 control and (B) L929 control/plasmid DNA to L929 control. Gene symbols represent a set of genes from the GSEA consortium. The heat map indicates gene sets denoted by a specific gene symbol with high expression (red), low expression (blue) or no change (white) for the experimental condition as compared to control. Gene ontology (GO) terms were color coded to represent broad signaling categories: stress/immune response (gold), protein activation/proteolysis (purple), vesicle trafficking (green), and intracellular/extracellular signaling/signal transduction (black).

4.2. VRK2 is required in HAP1 cells for optimal DNA replication of ΔB1.

The vaccinia B1 kinase has ~40% sequence identity to a family of conserved cellular genes called vaccinia related kinases (VRKs) from which it likely evolved (70). VRKs have essential roles within cells, one of which is to mediate BAF regulation during mitosis. *In vivo,* VRK1 regulates BAF function in the nucleus via phosphorylation (89) and *in vitro,* both VRK1 and VRK2 are able to phosphorylate BAF (98). Complementation studies for B1 kinase were completed previously, using VRK1 recombined into the Cts2 virus. In those studies, VRK1 expressed under a viral promoter in the cytoplasmic compartment rescued viral DNA replication deficiency of the Cts2 virus to greater than WT levels, although plaque morphology was smaller for Cts2-VRK1 recombinant virus than for the WT control (73). These studies confirmed complementation under conditions which circumvent the nuclear restriction of

endogenous VRK1. Therefore, we hypothesized that endogenous VRKs would compensate for the absence of the viral B1 kinase during infection. To test this hypothesis, we used a human, near haploid (HAP1) cell line control and VRK1 or VRK2 knockout (KO) HAP1 cell lines to evaluate the requirement of VRK1 or VRK2 during infection with the ΔB1. First, we confirmed the loss of expression of either VRK1 or VRK2 from the knockout HAP1 cell lines by immunoblot analysis (Fig 4.4A). Second, although VRKs are known to regulate the cell cycle (139-143), we observed no significant variability in apparent doubling time between the control and the knockout HAP1 cell lines (Fig 4.4B). Third, we examined viral DNA accumulation to determine VRK1 or VRK2 complementation of B1 function. WT and ΔB1 viruses have similar levels of relative DNA present at 3hpi in HAP1 control, VRK1KO, and VRK2KO cell lines indicative of viral entry, but minimal if any DNA replication at this time point (Fig 4.4C, left). At 7hpi DNA accumulation increased for both viruses but showed a consistent lag during ΔB1 infection as compared to WT virus in HAP1 control, VRK1KO, and VRK2KO cells (Fig 4.4C, right) demonstrating the importance of B1 for DNA replication in these cells. Interestingly, by 24hpi, the amount of ΔB1 DNA detected was similar to WT virus in the HAP1 control cells, indicating that although ΔB1 lags at 7hpi it can recover if given enough time (Fig 4.4D). However, ΔB1 DNA was not as abundant in the VRK1KO or VRK2KO HAP1 cells lines at 24hpi. Infected VRK1KO cells exhibited a 52% reduction in relative DNA accumulated for ΔB1 as compared to the WT virus (Fig 4.4D). A striking difference was observed in the VRK2KO cells, which showed further reduction in DNA accumulation during ΔB1 infection, reaching levels of only 3% DNA accumulation as compared to WT total levels. Next, we analyzed expression of a

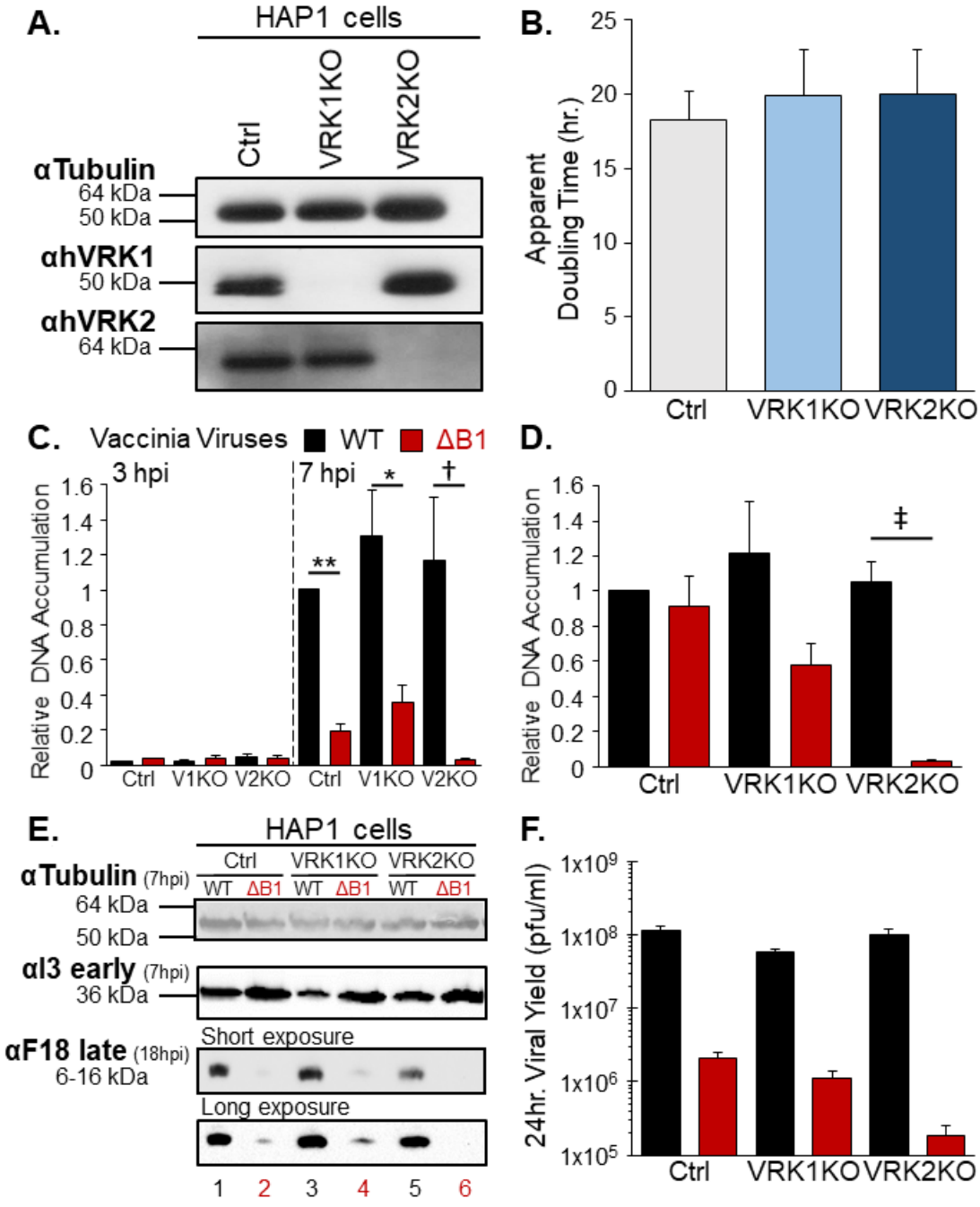
A.
HAP1 cells
Ctrl
VRK1KO
VRK2KO
αTubulin
64 kDa
50 kDa
αhVRK1
50 kDa
αhVRK2
64 kDa
B.
Apparent Doubling Time (hr.)
25
20
15
10
5
0
Ctrl
VRK1KO
VRK2KO
C.
Vaccinia Viruses
WT
ΔB1
3 hpi
7 hpi
*
†
**
Relative DNA Accumulation
1.6
1.4
1.2
1
0.8
0.6
0.4
0.2
0
Ctrl
V1KO
V2KO
Ctrl
V1KO
V2KO
D.
‡
Relative DNA Accumulation
Ctrl
VRK1KO
VRK2KO
E.
HAP1 cells
Ctrl
VRK1KO
VRK2KO
WT
ΔB1
WT
ΔB1
WT
ΔB1
αTubulin (7hpi)
64 kDa
50 kDa
αI3 early (7hpi)
36 kDa
αF18 late (18hpi)
6-16 kDa
Short exposure
Long exposure
1
2
3
4
5
6
F.
24hr. Viral Yield (pfu/ml)
1x10^9
1x10^8
1x10^7
1x10^6
1x10^5
Ctrl
VRK1KO
VRK2KO

Fig 4.4. VRK2, and to a lesser extent VRK1, complement B1 roles in DNA replication and viral yield production of ΔB1. (A) HAP1 cell lysates from control, VRK1KO, and VRK2KO cells were subjected to immunoblot analysis using αtubulin, αVRK1, or αVRK2 primary antibody. (B) The apparent doubling time was calculated for each HAP1 cell line. Standard deviation is denoted by error bars (n= 5). (C) DNA accumulation for 3hpi (left of dotted line) and 7hpi (right of dotted line) for WT (black) or ΔB1 (red) in HAP1 control, VRK1KO, or VRK2KO cells. The 3hpi WT/Ctrl sample was set to 1. (D) DNA accumulation and (F) viral yield measured for WT (black) or ΔB1 (red) at 24hpi in HAP1 cell lines; control, VRK1KO, or VRK2KO cells. The WT/Ctrl sample was set to 1 for DNA accumulation. Standard deviation is denoted by error bars and p-values † < 0.05, ‡ < 0.01, * < 0.005, ** < 0.001. (E) Whole-cell lysates from control (lanes 1 and 2), VRK1KO (lanes 3 and 4), and VRK2KO (lanes 5 and 6) were infected with either WT (lanes 1, 3, and 5) or ΔB1 (lanes 2, 4, and 6) and harvested for immunoblot analysis for both early gene expression (αI3) at 7hpi and late gene expression (αF18) at 18hpi. Cell loading control, tubulin, was detected from 7hpi cell lysates. The F18-specific blot shown at both a short (top) and long (bottom) exposure time.

representative early and late gene to determine if loss of B1 affected these stages of the virus life cycle in HAP1 cells. Early gene expression, as assayed by I3 protein level at 7hpi via immunoblot analysis, was present at similar to slightly higher levels for ΔB1 as compared to WT in HAP1 control, VRK1KO, and VRK2KO cell lines (Fig 4.4E). This early gene expression is consistent with unaltered early transcription despite the loss of B1. Late gene expression, as measured by detection of late protein F18 at 18hpi (Fig 4.4E), was markedly reduced during ΔB1 as compared to the WT infection in HAP1 control and VRK1KO cells lines, although a low level of expression could be detected in these two cell lines. Importantly, no visible F18 late protein was observed for the ΔB1 in the VRK2KO HAP1 cells. These data are consistent with a model in which the replication of ΔB1 DNA in control and VRK1 KO cells allows for weak late gene expression; whereas the severely impaired DNA replication in VRK2 KO cells results in a complete block of late gene expression. Finally, we tested the effects of VRK1 and VRK2 absence on viral yield for the ΔB1. Consistent with the late gene expression data, the viral yield was almost 53-fold less for ΔB1 than for the WT virus in the HAP1 control cells (Fig 4.4F). The ΔB1 viral yield during infection of VRK1KO cells exhibited a 52-fold reduction as compared to WT infections, similar to the trend observed in HAP1 control cells (Fig 4.4F). As observed for the viral DNA replication data (Fig 4.4D), an additional reduction in viral fitness occurred in the VRK2KO cells. The viral yield of the ΔB1 in the VRK2KO cells was 550 fold lower than WT viral yield under the same cellular conditions (Fig 4.4F). Lastly, we used an immunofluorescence assay to assess early (I3) and late (P11mCherry) protein expression for ΔB1 in each HAP1 cell line. The uninfected cells represent the negative controls for I3 and mCherry viral protein

expression (Fig 4.5, panels 1 and 5). At 7hpi the I3 early protein is expressed in ΔB1 infected parental HAP1 cells and forms foci indicative of replication factories (Fig 4.5, panel 2), which is consistent with both 7hpi I3 protein levels (Fig 4.4E) and DNA accumulation results (Fig 4.4C). Interestingly, while I3 was expressed in VRK1KO and VRK2KO cells, the number of concentrated foci formed by I3 decreases in the VRK1KO cell line and are quite rare in VRK2KO cells as compared to ΔB1 infected HAP1 control cells (Fig 4.5, top row, panels 3 and 4).

Next, late protein expression was assayed through detection of the mCherry protein, in which gene expression is regulated by the P11 late viral promoter. mCherry protein expression followed a similar trend as observed for ΔB1 F18 immunoblot (Fig 4.4E); almost all cells express mCherry during ΔB1 infection of HAP1 control cells, about half in VRK1KO cells and very few VRK2KO cells express mCherry protein (Fig 4.5, panels 6-8). In summary, VRK2 absence and to a lesser extent VRK1 absence resulted in a marked deficiency of ΔB1 DNA replication, 24hr viral yield, 7hpi replication factory formation, and 18hpi late expression of mCherry. These data indicate that endogenous VRK2 can partly compensate for the absence of the B1 kinase during infection of HAP1 cells, specifically during viral DNA replication. Furthermore, endogenous VRK1 was also able to complement B1 roles during DNA replication, although to a much lesser degree than VRK2 in these studies.

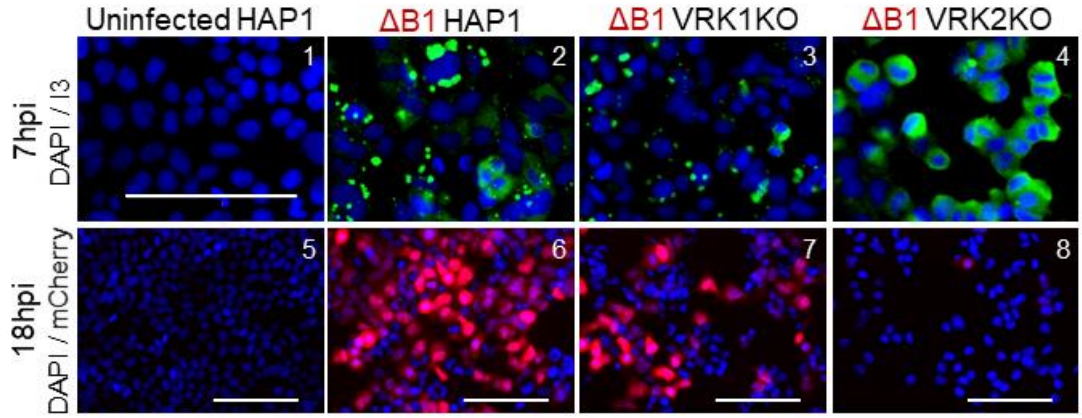

Fig 4.5. Characterization of ΔB1 DNA replication factory formation, and late mCherry protein levels in HAP1 control, VRK1KO and VRK2KO cell lines. Immunofluorescence analyses of uninfected HAP1 control cells (panels 1 and 5), and ΔB1 infected HAP1 control (panels 2 and 6), VRK1KO (panels 3 and 7), and VRK2KO (panels 4 and 8) at MOI=5 and incubated at 37˚C. Early I3 protein was detected using αI3 primary antibody at 7hpi (panels 2-4) and late mCherry fluorescent protein was imaged from cells at 18hpi (panels 6-8). Uninfected HAP1 control cells were also incubated with αI3 primary antibody and appropriate secondary antibody. All cells were incubated with DAPI stain used to detect nuclei.

4.3. VRK2 reconstitution in VRK2 knockout HAP1 cells rescues ΔB1 DNA replication.

To confirm the necessity of VRK2 during ΔB1 infection we generated a lentivirus expressing the wild type human *VRK2* gene, tagged at its C-terminus with the myc epitope. Stable expression of exogenous VRK2myc was achieved in both HAP1 control cells and VRK2KO HAP1 cells (Fig 4.6A). Exogenous VRK2myc (gray arrow) protein levels in the transduced VRK2KO HAP1 cells were similar to protein levels of endogenous VRK2 (black arrow) in HAP1 control cells (Fig 4.6A, lanes 1 and 4). Exogenous VRK2myc protein expression in the transduced HAP1 control cells was less than exogenous VRK2myc levels in the VRK2KO HAP1 cells, although detectable at a longer exposure (Fig 4.6A, lanes 2 and 4). Relative DNA accumulation measurements were used to determine if addition of exogenous VRK2myc could rescue the deficiency of the ΔB1 during infection of the VRK2KO HAP1 cell line (Fig 4.6B). Exogenous VRK2myc expression in HAP1 control cells did not alter the WT or ΔB1 relative DNA accumulation (Fig 4.6B, lanes 1-4). Importantly, the reconstitution of VRK2 protein in the VRK2KO HAP1 cells resulted in a rescue of ΔB1 relative DNA accumulation 16 fold above that in VRK2KO cells (compare bars 6 and 8). These data confirm that the ΔB1 DNA replication deficiency in the VRK2KO HAP1 cells is due to an absence of VRK2. This is the first demonstration that VRK2 specifically complements for the loss of B1 kinase during viral DNA replication carried out in HAP1 cells.

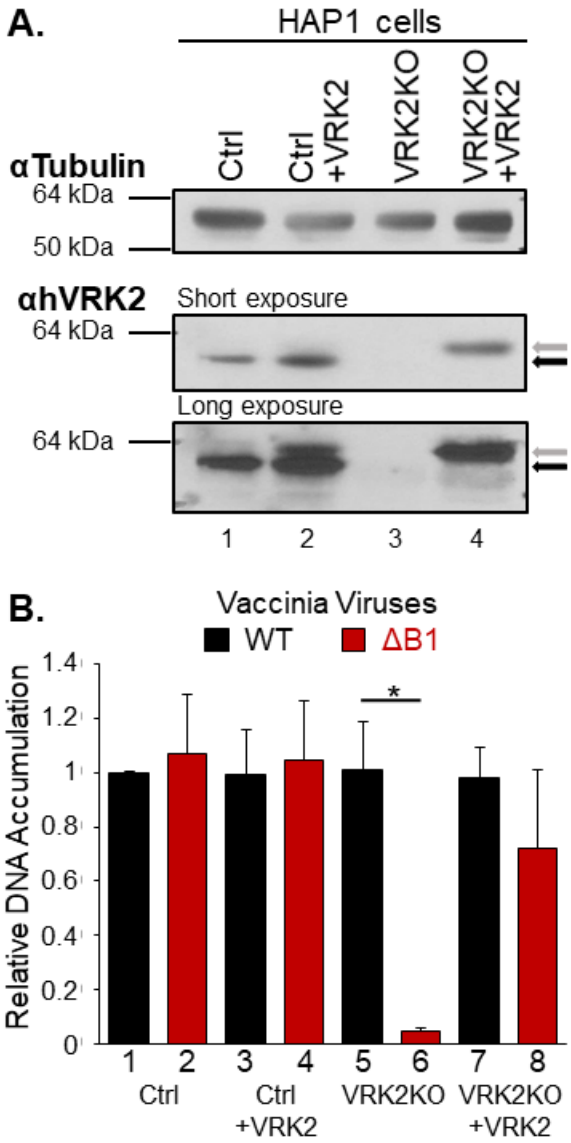

Fig 4.6. VRK2 reconstitution rescues ΔB1 deficiency in HAP1 VRK2KO cells. A) HAP1 control (lanes 1 and 2) and VRK2KO (lanes 3 and 4) cells were transduced with a lentivirus expressing human myc-tagged VRK2 to generate HAP1 control/ VRK2myc (lane 2) and VRK2KO/ VRK2myc (lane 4) cells. Immunoblot analysis of endogenous VRK2 (black arrow, 58kDa) and exogenous VRK2myc (grey arrow) for each transduced cell line. **B)** DNA accumulation was measured after 24hr one-step infection with WT

(Fig 4.6 continued) (black) or ΔB1 (red) in control cells (columns 1 and 2), exogenous VRK2myc expressing control cells (columns 3 and 4), VRK2KO cells (columns 5 and 6), and exogenous VRK2myc expressing VRK2KO cells (columns 7 and 8). The WT/Ctrl sample was set to 1. Standard deviation is denoted by error bars and * p-value is <0.005 (black lines drawn between compared columns).

4.4. Impact of VRK2 depletion on ΔB1 DNA replication in HeLa and A549 cells.

Our above studies indicate that HAP1 cells are somewhat unique from other cell lines tested (Fig 3.5A-D) in that vaccinia virus DNA replication is delayed during ΔB1 infection, but approaches WT levels by 24hpi (Fig 4.4C and D). Therefore, significant reductions in DNA accumulation during ΔB1 infection of HAP1 cells can be measured effectively, as illustrated in VRK2KO HAP1 cells (Fig 4.4C and D). To further examine the requirement of VRK2 during vaccinia virus infection in the absence of B1 we utilized two other human cancer cell lines, HeLa and A549, which express similar protein levels of VRK2 to HAP1 cells (Fig 4.7A). First, we used siRNA to deplete VRK2 from either HeLa or A549 cells, using siRNAs targeting VRK2 mRNA. HeLa cells were depleted of VRK2 using two different siRNAs designed to target different sites on the VRK2 mRNA. The siVRK2#1 achieved a better depletion than siVRK2#2 resulting in about 20% remaining endogenous VRK2 (Fig 4.7B). WT 24hpi DNA accumulation was not affected by VRK2 depletion in HeLa cells (Fig 4.7C). Notably, ΔB1 displayed a statistically significant, although modest, decrease in DNA replication during infection of VRK2 depleted HeLa cells as compared to infection of siCtrl HeLa cells. The viral yield of WT virus was not altered while ΔB1 was modestly reduced during infection of VRK2

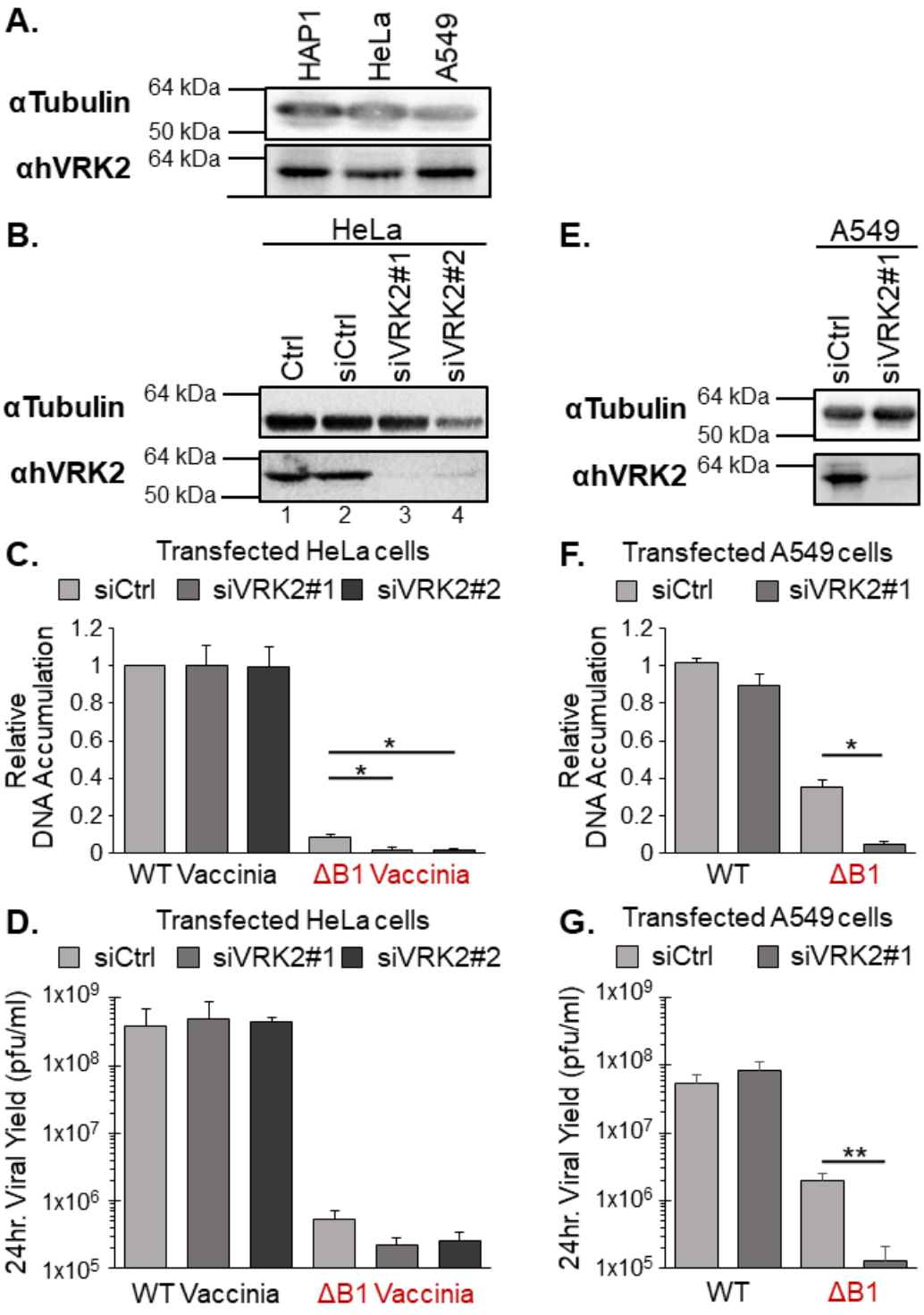
A.
HAP1
HeLa
A549
αTubulin
64 kDa
50 kDa
αhVRK2
64 kDa
B.
HeLa
Ctrl
siCtrl
siVRK2#1
siVRK2#2
αTubulin
64 kDa
αhVRK2
64 kDa
50 kDa
1 2 3 4
E.
A549
siCtrl
siVRK2#1
αTubulin
64 kDa
50 kDa
αhVRK2
64 kDa
C.
Transfected HeLa cells
siCtrl
siVRK2#1
siVRK2#2
Relative DNA Accumulation
1.2
1
0.8
0.6
0.4
0.2
0
*
*
WT Vaccinia
ΔB1 Vaccinia
F.
Transfected A549 cells
siCtrl
siVRK2#1
Relative DNA Accumulation
1.2
1
0.8
0.6
0.4
0.2
0
*
WT
ΔB1
D.
Transfected HeLa cells
siCtrl
siVRK2#1
siVRK2#2
24hr. Viral Yield (pfu/ml)
1x10^9
1x10^8
1x10^7
1x10^6
1x10^5
WT Vaccinia
ΔB1 Vaccinia
G.
Transfected A549 cells
siCtrl
siVRK2#1
24hr. Viral Yield (pfu/ml)
1x10^9
1x10^8
1x10^7
1x10^6
1x10^5
**
WT
ΔB1

Fig 4.7. Effect of VRK2 depletion on ΔB1 growth in human HeLa and A549 cells. (A) Immunoblot analysis of HAP1 control, HeLa, and A549 human cell lysates using αtubulin and αVRK2 primary antibodies as shown. (B) Endogenous VRK2 was depleted in HeLa cells by transfection of cells with two different siRNAs targeting human VRK2 mRNA. Immunoblot analysis for tubulin loading control and αhuman VRK2 protein was completed for whole-cell lysates of untransfected HeLa cell control (lane 1), siRNA scrambled as siCtrl (lane 2), siVRK2#1 (lane 3), or siVRK2#2 (lane 4) transfected HeLa cells. (C) DNA accumulation and (D) 24hr viral yield assays were completed in siCtrl (light grey bars), siVRK2#1 (grey bars), and siVRK2#2 (dark grey bars) transfected HeLa cells for WT and ΔB1 infected cells. The WT/HeLa siCtrl sample was set to 1 for DNA accumulation. (E) Endogenous VRK2 was depleted in human A549 cells by transfection of cells with siVRK2#1. Immunoblot analysis of siCtrl and siVRK2#1 transfected A549 cell lysates for detection of tubulin loading control and human VRK2 protein. (F) DNA accumulation and (G) viral yield assays were completed in siCtrl (light grey bars) and siVRK2#1 (grey bars) transfected CV1 cells for WT (left two columns) and ΔB1 (right two columns) infected cells. The WT/A549 siCtrl sample was set to 1 for DNA accumulation. Standard deviation is denoted by error bars and * p-value < 0.005, ** < 0.001 (black lines drawn between compared columns).

depleted HeLa cells. (Fig 4.7D). Next, endogenous VRK2 was depleted in A549 cells using siVRK2#1. Depletion of VRK2 in A549 cells resulted in <20% remaining endogenous VRK2 as assayed using immunoblot (Fig 4.7E). WT virus relative DNA accumulation (Fig 4.7F) and viral yield (Fig 4.7G) were not significantly altered by reduction of endogenous VRK2 from A549 cells. Yet, we observed a significant decrease for ΔB1 DNA accumulation (Fig 4.7F) and viral yield (Fig 4.7G) in the VRK2 depleted A549 cells. This outcome mirrored the attenuation of ΔB1 in HAP1 VRK2KO cells (Fig 4.4D and F). These data indicate that HAP1 and A549 are cell lines in which ΔB1 can attain elevated levels of DNA accumulation, enabling us to quantify a significant attenuation during the absence or depletion of VRK2. Moreover, the sufficiency of VRK2 to compensate for B1 during ΔB1 infection appears to be cell type dependent, as suggested by the differing magnitude of the results in HeLa cells versus HAP1 and A549 cells

4.5. BAF depletion in HAP1 cells lacking VRK2 results in a small increase in ΔB1 DNA replication.

Our next goal was to explore the mechanism through which VRK2 complements for the lack of the B1 viral kinase in ΔB1. Based on *in vitro* studies confirming VRK2 ability to phosphorylate BAF (98), we hypothesized that, like B1, VRK2 may regulate BAF antiviral function in cells; therefore, BAF depletion would rescue ΔB1 growth in VRK2KO cells. To test this prediction, we transduced HAP1 control and VRK2KO cells to express a BAF-specific shRNA. We then measured viral DNA accumulation during WT virus and ΔB1 infection in these transduced VRK2KO cells. We found that in cells infected with WT virus, DNA replication was not affected by BAF depletion, consistent

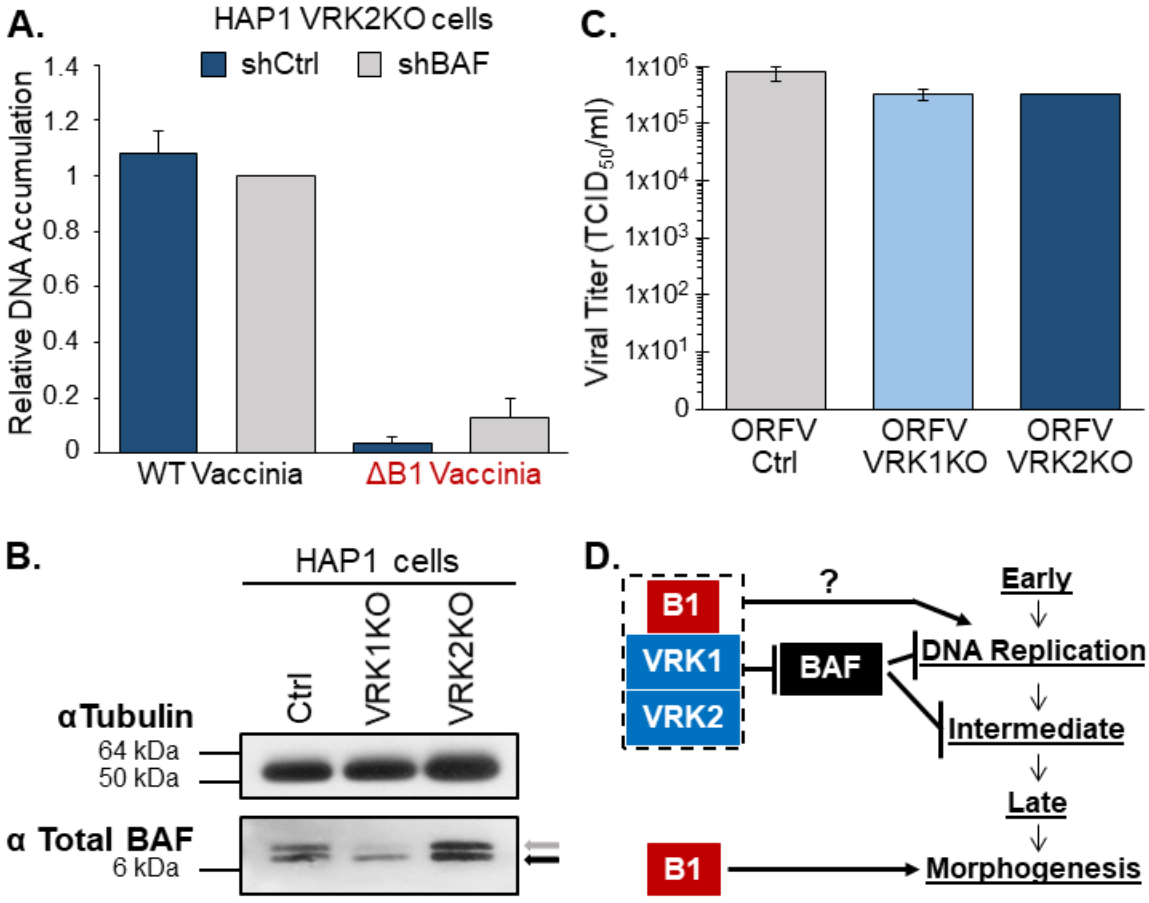

Fig 4.8. VRK2 rescues ΔB1 DNA replication primarily through a BAF independent mechanism. ORFV life cycle occurs independent of either VRK1 or VRK2 expression from HAP1 cells. (A) DNA accumulation was measured at 24hpi for WT (left two columns) and ΔB1 (right two columns) in control or BAF depleted cells HAP1 VRK2KO cells. The WT/HAP1 VRK2KO shCtrl sample was set to 1. (B) Immunoblot analysis of HAP1 control (lane 1), VRK1KO (lane 2), and VRK2KO (lane 3) cell lysates using αtubulin and αBAF primary antibodies as shown. (C) HAP1 control, VRK1KO, and VRK2KO cells were infected with parapoxvirus, orf virus (ORFV) at MOI =1 for four days. Cell and virus were harvested and titrated on primary ovine fetal turbinate (Oftu) cells and quantified by the Spearman-Karber's tissue culture infectious dose 50

method (TCID50/mL). Viral titer values are an average of 2 replicates and error bars indicate standard deviation between replicates. (D) Working model of B1 and VRK regulated vaccinia virus life cycle stages based on this study and previous reports.. We identified a B1-VRK2 shared function in BAF regulation and a BAF-independent mechanism, both affecting vaccinia DNA replication. B1 was also previously shown to contribute to vaccinia morphogenesis.

with other cell lines (69, 81, 83). In comparison, when measuring ΔB1 DNA accumulation in the VRK2KO shCtrl cells and BAF depleted cells, a 3.5 fold rescue is observed (Fig 4.8A). This increase from 4% to 12% DNA accumulation as compared to WT infection of VRK2KO shCtrl cells is modest, but is similar to earlier results for ΔB1 DNA accumulation in BAF depleted CV1 cells (Fig 3.4C). We therefore posit that VRK2 enhances ΔB1 DNA replication partially through a BAF dependent mechanism, but also to a significant degree through a BAF independent mechanism.

To examine whether loss of VRK2 impacts BAF expression levels or phosphorylation status, we then performed immunoblot analysis of BAF in HAP1 control, VRK1KO, and VRK2KO cells (Fig 4.8B). The antibody employed detects both phosphorylated BAF (grey arrow), which migrates more slowly in the gel, and the more rapidly migrating unphosphorylated form of BAF (black arrow). In control HAP1 cells, both forms are detected at similar levels. In VRK1KO cells there is a clear loss of the upper band representing phosphorylated BAF. This data is consistent with numerous other studies that VRK1 plays an important part in modifying BAF phospho-status in the nucleus (89, 94, 98, 144). Interestingly, in VRK2KO cell lysates there is no apparent loss

of the upper form of BAF. This lack of a measurable impact of VRK2 on BAF phosphorylation indicates that VRK1 is the dominant BAF kinase in HAP1 cells when measured in whole cell lysates and leads us to speculate that VRK2 mediated complementation for B1 occurs via a BAF independent mechanism.

4.6. The viral life cycle of ORF virus, naturally lacking the B1 kinase, is not affected by the absence of either cellular VRK1 or VRK2.

Our observation that VRK2 can partly complement during infection with ΔB1 raised the question of whether other viruses lacking a B1 homolog may depend on VRK1 or VRK2 for replication. The orf virus (ORFV) is a Poxviridae family member; however, it is classified under the *Parapoxvirus* genus (1) and lacks a B1-like kinase (130). To explore the role of VRK1 and VRK2 during ORFV infection we performed a viral growth assay in HAP1 control, VRK1KO, and VRK2KO cells. Interestingly, no significant difference was observed for ORFV viral titer between the control HAP1 cells and either VRK1KO or VRK2KO HAP1 cells (Fig 4.8C). These results indicate that VRK1 or VRK2 are not required for the viral life cycle of ORFV and that this pathogen has evolved alternative mechanisms to replicate without B1. Consistent with this reasoning, ORFV infection of CV1-B1myc cells did not exhibit enhanced viral fitness when compared to control CV1 cells (data not shown). This suggests that ORFV may not rely on cellular VRK1 or VRK2, possibly due to a divergence in evolution from *Orthopoxviruses*. Alternatively, it is plausible that the ORFV is capable of utilizing either VRK1 or VRK2 interchangeably in order to replicate its viral DNA. Future production of a VRK1/VRK2 double knockout cell line will be needed to test this possibility.

4.7. Chapter 4 Summary

To this point we know that the vaccinia B1 kinase regulates the antiviral activity of BAF and has additional substrates with no known associated function. To fill this gap in knowledge of B1 roles, this chapter 1) identified cellular pathways differentially regulated during B1 expression and 2) characterized cooperative activity between B1 and cellular VRK homologs. Together, we identified potential regulatory roles of B1 on stress/immune response, metabolism, signal transduction, proteolysis and vesicle transport. Mediation of stress/immune response as well as signal transduction are known for B1 function, yet the other pathways present novel pathways related to B1 regulation. Furthermore, we show in this chapter the redundant function of VRK2 with the B1 kinase and discover that this shared function between B1 and VRK2 is largely BAF independent (Fig 4.8D). Lastly, we determined that the necessary role of B1 and the VRKs was specific for vaccinia virus but not ORFV, supporting a model where *Parapoxvirus* divergence and absence of a B1 kinase does not increase the requirement of both cellular VRKs.

CHAPTER 5

VACCINIA B1 KINASE AND B12 PSEUDOKINASE ARE GENETICALLY AND FUNCTIONALLY LINKED

5.1. Fitness gains observed following adaption of the ΔB1 virus correlate with an indel mutation within the *B12R* gene.

The vaccinia virus B1 kinase is a critical positive regulator of vaccinia DNA replication. Specifically, B1 inhibits the BAF antiviral factor, which can otherwise restrict viral DNA replication and subsequent gene expression (69); however, much remains unknown about how B1 may regulate other viral factors during infection. In a recent study of B1 function, our laboratory generated a mutant vaccinia virus (ΔB1 virus) in which the *B1R* gene was deleted by homologous recombination (127). As expected, without this viral kinase, growth of the ΔB1 virus was severely impaired compared to WT virus. Intriguingly, the fact that some progeny virus could be isolated following infection with the ΔB1 virus suggested to us that it may be amenable for use in a screen for second site suppressors using an experimental evolution protocol. If successful, this approach could reveal novel genetic linkages between *B1R* and other viral genes.

The experimental evolution of ΔB1 was conducted by iterative passage of the virus at a low multiplicity of infection (MOI) of 0.1 on non-complementing CV1 cells. Each infection was allowed to proceed for three to four days prior to harvest. After each passage the viral yield was determined by plaque assay titration on complementing, B1 expressing CV1 (CV1-B1myc) cells characterized previously (127). Virus titrations on the CV1-B1myc cells allowed for accurate quantification of serially passaged ΔB1 virus, while no visible plaques could form on the non-complementing CV1 cells. The process of

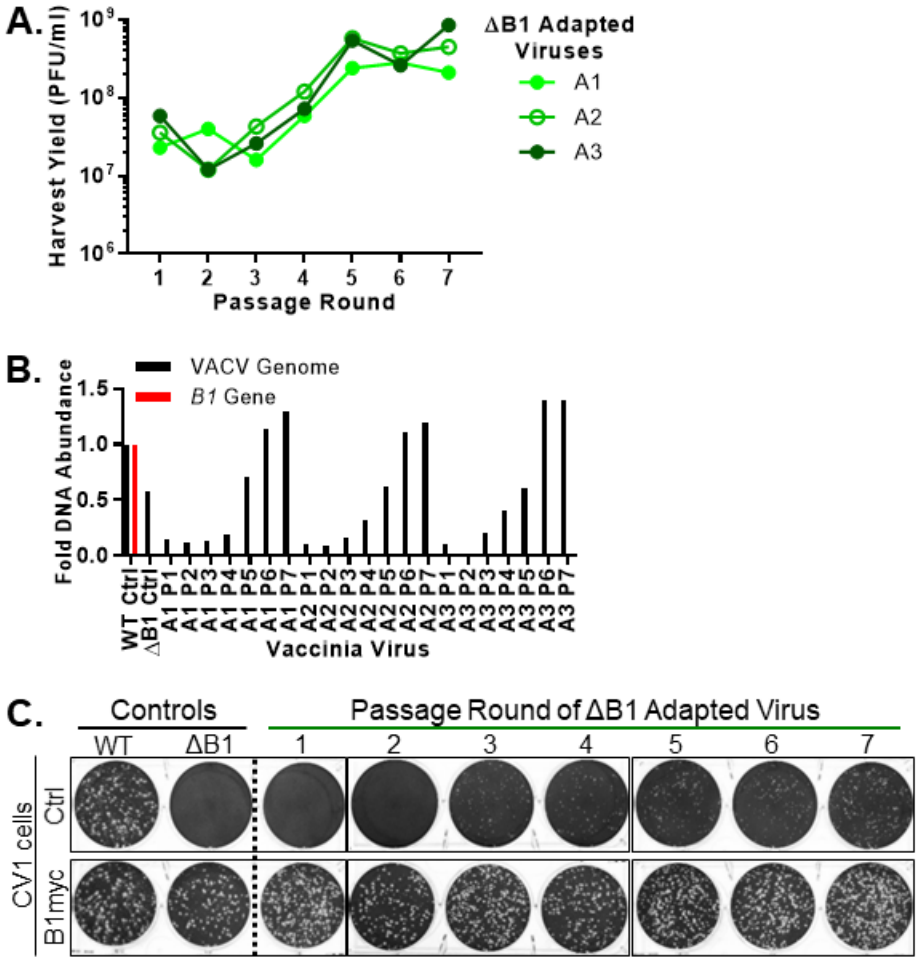

Fig 5.1. Adaptation of ΔB1 virus. (A) ΔB1 virus was serially passaged in CV1 cells in triplicate and named A1-A3 for adapted ΔB1 viruses. Virus harvested at each passage was titrated on CV1-B1myc cells. (B) Fold DNA abundance was quantified using qPCR and primers designed to vaccinia *HA* or *B1* genes for total viral DNA or B1 specific DNA. DNA was isolated from CV1 cells infected with WT, ΔB1, ΔB1-A1 passages 1-7, ΔB1-A2 passages 1-7, or ΔB1-A3 passages 1-7 viruses at a MOI of 3 and harvested 24h post infection. (C) Plaque assay of CV1 control or B1myc expressing cells infected with WT, ΔB1 and ΔB1-A1 virus from passages 1-7 at 200 PFU/well. Cells were fixed 72h post infection.

harvesting, titration on CV1-B1myc cells, and reinfection of CV1 cells at low MOI was carried out for seven passage rounds. Virus yield at each passage was graphed for the A1, A2, and A3 lineages of adapted ΔB1 virus (Fig 5.1A). During these serial passages, the yield of the ΔB1 virus showed a notable 10-fold increase in titer between passage rounds 3 and 5, suggesting the emergence of a rescued virus in all three, independent replicates. Using quantitative PCR we verified that the *B1R* gene remained undetected in our serially passaged viruses (Fig 5.1B), thus confirming that reintroduction of B1 is not responsible for the rescue of the passaged ΔB1 virus.

Next, we predicted that the 10-fold increase in viral yield may be sufficient to permit spread through non-complementing cells and allow plaque formation. To test this prediction, we infected CV1 control cells and CV1-B1myc cells with 200 plaque forming units (PFU) per well of WT, ΔB1, and each passage of adapted ΔB1 virus from lineage A1, then fixed and stained the cells at 72h post infection. Starting at passage three, the adapted cultures contained virus that formed plaques which were smaller than WT, but clearly visible on non-complementing CV1 cells (Fig 5.1C, top row). As expected, adapted ΔB1 virus plaque size was increased in cells expressing B1 in trans (Fig 5.1C, bottom row). These data confirm the rescue of the adapted ΔB1 virus in non-complementing CV1 cells, although the smaller plaque phenotype of the adapted ΔB1 virus suggests that it is less fit than the WT virus in this assay.

With three independently adapted ΔB1 viruses in hand, we sought to identify significant genetic alterations within the adapted viruses as compared to the ΔB1 virus. To this end, DNA isolated from the WT (Wiebe laboratory), ΔB1, and adapted ΔB1 viruses A1 and A3 (passage round 7) were subjected to 150 base pair paired end

sequencing using a MiSeq V2 instrument. Following guided assembly, WT (Wiebe), ΔB1, ΔB1-A1, and ΔB1-A3 sequences were compared to the WT Western Reserve reference genome (NC_006998.1) in the NCBI database. One previously characterized mechanism of virus adaptation involves the development of genomic 'accordions' in which gene amplifications occur for a specific locus, permitting a dose dependent compensation by a complementary gene (11, 12). However, the ΔB1-A1 and ΔB1-A3 virus sequence data lacked evidence of genomic accordions, which would have been identified by large increases of sequence read counts for a particular region in the adapted genomes compared to WT and ΔB1 controls. Instead we observed a consistent read count depth across the entire genome for both adapted and control viruses. We also analyzed the specific read calls at each nucleotide position in the complete genome for evidence of single nucleotide polymorphisms (SNPs). For this analysis we made sequence comparisons between WT (Wiebe) to WT WR (reference sequence), ΔB1 to WT (Wiebe), and ΔB1mutB12 to ΔB1. From the genome analyses of ΔB1-A1 and ΔB1-A3 viruses, only one non-synonymous mutation was identified, which was found solely in the ΔB1-A1 virus. This mutation identified in ΔB1-A1 is a G to A substitution expected to cause a Gly115 to Asp mutation within the *B12R* coding region. Based on the read depth for this specific nucleotide location, we determined that this point mutation is present in 18% of the reads from the ΔB1-A1 virus (Fig 5.2A and Table 5.1). Finally, we quantified reads containing insertion/deletion (indel) mutations across the entire genome for ΔB1, ΔB1-A1, and ΔB1-A3 as compared to the changes in WT (Wiebe) from the WT WR (reference sequence) genome. To present the locations of indels graphically, comparisons of indel read counts are plotted along the y-axis for ΔB1 to WT (Fig 1B,

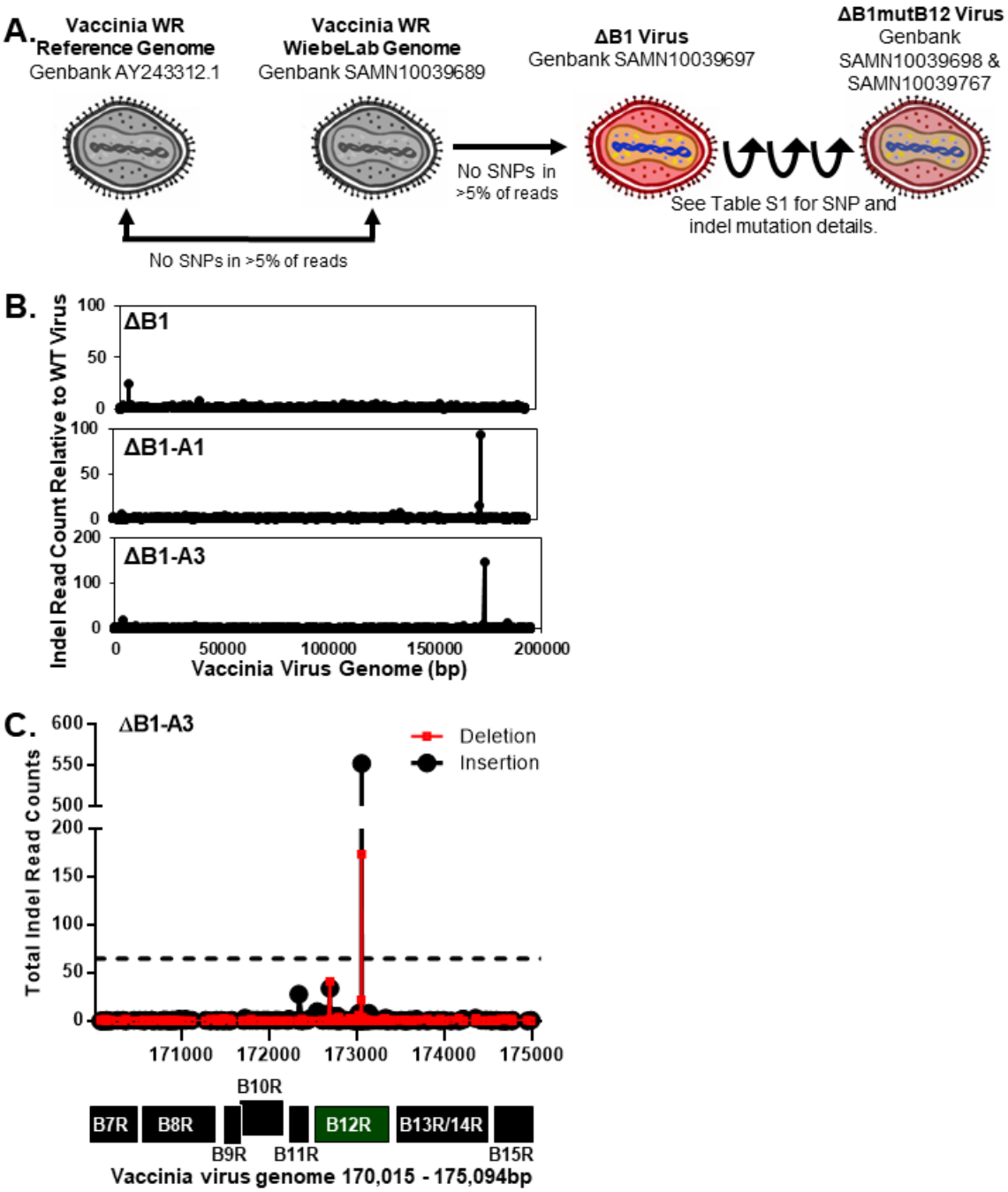
A.
Vaccinia WR
Reference Genome
Genbank AY243312.1
Vaccinia WR
WiebeLab Genome
Genbank SAMN10039689
ΔB1 Virus
Genbank SAMN10039697
ΔB1mutB12 Virus
Genbank
SAMN10039698 &
SAMN10039767
No SNPs in
>5% of reads
See Table S1 for SNP and
indel mutation details.
No SNPs in >5% of reads
B.
Indel Read Count Relative to WT Virus
ΔB1
ΔB1-A1
ΔB1-A3
Vaccinia Virus Genome (bp)
C.
ΔB1-A3
Deletion
Insertion
Total Indel Read Counts
B10R
B7R
B8R
B9R
B11R
B12R
B13R/14R
B15R
Vaccinia virus genome 170,015 - 175,094bp

Fig 5.2. Characterization of ΔB1 viruses serially passaged on CV1 cells and identification of mutation within the *B12R* gene. (A) Experimental evolution depiction with genome reference identification numbers. There were no single nucleotide polymorphisms (SNPs) in >5% of the nucleotide read counts for the coding regions of vaccinia WR reference compared to WiebeLab virus genome, and WiebeLab compared to ΔB1 virus genome. (B) Deep sequencing data for WT (Wiebe), ΔB1, ΔB1-A1, and ΔB1-A3 viruses was used to graph insertion/deletion mutations at each nucleotide site for the entire vaccinia genome when comparing ΔB1, ΔB1-A1, and ΔB1-A3 viruses to the change in indel mutations of the WT (Wiebe) compared to the WT WR (reference sequence). (C) Graphed insertion/deletion mutations for ΔB1-A3 compared to WT WR (reference sequence) for reads 170,015-175,094bp. The dotted line indicates indel mutations that occur in 5% of the total reads at a single nucleotide. Indel mutations above 5% were considered significant mutations in the mixed ΔB1 adapted virus population. Locations of encoded genes are labeled below, corresponding to the base pairs on the x-axis of the graph.

Table 5.1. Sequencing data from adapted ΔB1 viruses

Whole Genome Illumina Sequencing Data (Mutations >5%)

Vaccinia Virus	Mutation Type	WT WR Ref.[c]	B12R[d]	Read Depth	Mutation	Mutation %[e]	A.A. Sequence Change[f]	Notes
ΔB1-A1[a]	SNP	173172 bp	644 bp	1077	G → A	18.15%	G → D at 215 a.a.	Mutation not detected in ΔB1-A3 virus (read depth: 1146)
ΔB1-A1[a]	Indel	172854 bp	326 bp	1667	+ C	2.52%	Premature STOP at 113 a.a.	Indel occurs in a run of four cytosines
					- C	2.46%	Premature STOP at 122 a.a.	Indel occurs in a run of four cytosines
ΔB1-A3[b]				1794	+ C	1.90%	Premature STOP at 113 a.a.	Indel occurs in a run of four cytosines (under 5% threshold)
					- C	2.29%	Premature STOP at 122 a.a.	Indel occurs in a run of four cytosines (under 5% threshold)
ΔB1-A1[a]	Indel	173217 bp	689 bp	973	+ A	36.07%	Premature STOP at 234 a.a.	Indel occurs in a run of eight adenines
					- A	11.92%	Premature STOP at 237 a.a.	Indel occurs in a run of eight adenines
ΔB1-A3[b]				1104	+ A	50.09%	Premature STOP at 234 a.a.	Indel occurs in a run of eight adenines
					- A	15.76%	Premature STOP at 237 a.a.	Indel occurs in a run of eight adenines

Targeted *B12R* Sanger Sequencing Data

Virus	Isolate	Mutation Type	WT WR Ref.[c]	B12R[d]	Mutation	A.A. Sequence Change[f]	Notes
ΔB1-A1	**1**	Indel	173217 bp	689 bp	+ A	Premature STOP at 234 a.a.	Indel occurs in a run of eight adenines
ΔB1-A1	**2**				- A	Premature STOP at 237 a.a.	Indel occurs in a run of eight adenines
ΔB1-A2	**1**	Indel	172942 bp	414 bp	+ A[g]	Premature STOP at 147 a.a.	Indel occurs in a run of five adenines
ΔB1-A2	**2**	Indel	173217 bp	689 bp	+ A	Premature STOP at 234 a.a.	Indel occurs in a run of eight adenines
ΔB1-A2	**3**				+ A		Indel occurs in a run of eight adenines
ΔB1-A2	**4**				+ A		Indel occurs in a run of eight adenines
ΔB1-A2	**5**				- A	Premature STOP at 237 a.a.	Indel occurs in a run of eight adenines
ΔB1-A3	**1**	Indel	172854 bp	326 bp	+ C[g]	Premature STOP at 113 a.a.	Indel occurs in a run of four cytosines
ΔB1-A3	**2**	Indel	173217 bp	689 bp	+ A	Premature STOP at 234 a.a.	Indel occurs in a run of eight adenines
ΔB1-A3	**3**				- A	Premature STOP at 237 a.a.	Indel occurs in a run of eight adenines

[a] ΔB1-A1 Genome (Genbank SAMN10039698)

[b] ΔB1-A3 Genome (Genbank SAMN10039767)

[c] Site of nucleotide mutation within the WT WR Reference Genome (Genbank AY243312.1)

[d] Site of nucleotide mutation within the *B12R* gene relative to the ATG start site (NC_006998.1)

[e] Mutation percentage is calculated by dividing nucleotide reads containing a mutation by the read depth at the specific nuclotide site.

[f] Premature STOP results in an amino acid sequnce less than the full length 283 a.a. B12 protein.

[g] Isolate lacks insertion/deletion mutation at 689 bp site within the *B12R* gene.

top), ΔB1-A1 to WT (middle), and ΔB1-A3 to WT (bottom) and the nucleotide numbers of the reference genome along the x-axis. Strikingly, indel mutations were identified at identical nucleotide positions in the ΔB1-A1 and ΔB1-A3 comparisons to WT (Fig 5.2B, middle and bottom graph), but not for ΔB1 sequence comparison to WT (Fig 5.2B, top graph). Narrowing the x-axis to focus on the region of interest, we graphed the total number of indel mutations found between 170,015 and 175,094 base pairs for the ΔB1-A3 alignment to the ΔB1 genome (Fig 5.2C). The genes labeled below the x-axis indicate the genes encoded at the specific base pair regions. This graph depicts that the ΔB1-A3 virus population contains a significant spike in insertion and deletion mutations within the *B12R* gene. This spike of indel mutations corresponds to adenine 689 in the *B12R* gene, which is the start of an eight adenine sequence (Table 5.1). This single site of indel mutations is present in approximately 48% and 65% of the reads for the ΔB1-A1 and ΔB1-A3 virus, respectively (Table 5.1). Interestingly, either an insertion or deletion of an adenine at this site alters the predicted reading frame of the gene and thereby introduces a premature stop codon, resulting in a truncated B12 protein. In addition to the Illumina sequencing of mixed viral populations, targeted Sanger sequencing of the B12 locus was performed on 10 isolated plaques chosen from the three adapted cultures after two rounds of plaque purification. As a result, we found that all ten isolated plaques contain either an indel mutation at B12 nucleotide 689 or an indel at another earlier position in *B12R* (Table 5.1). Together these results highlight the significant frequency of mutations within the *B12R* gene, leading it to become our top candidate for a ΔB1 second site suppressor mutation.

The B12 protein is 283 amino acids in length and shares 36% amino acid identity to the vaccinia B1 kinase (124, 125). Akin to the B1 kinase, the B12 protein is homologous to the cellular vaccinia related kinases (VRKs). Furthermore, the viral *B12R* gene is expressed early in infection, like the B1 kinase, but differs from the B1 kinase in that it lacks catalytic activity (114, 124). Proteins that possess sequence and structural similarity to active kinases, but lack phosphotransferase activity due to alterations in key catalytic residues are abundant in all forms of life and are commonly referred to as pseudokinases. Although B12 is a pseudokinase and B1 paralog, the function of B12 during infection remains an enigma to date, as previous studies revealed no phenotypic defect for a mutant vaccinia virus missing 83% of the *B12* gene (114, 115).

5.2. The ΔB1mutB12 virus exhibits rescued DNA replication and viral yield in multiple cell lines.

As described above, the adapted ΔB1 virus (hereafter referred to as the ΔB1mutB12 virus) exhibited a visible plaque phenotype not observed for the ΔB1 virus. To investigate the extent of the ΔB1mutB12 rescued phenotype, we measured both DNA accumulation and viral yield during a single round of vaccinia virus replication in noncomplementing cells. Following synchronous infections at a MOI of 3, viral genome replication was measured by qPCR. Compared to the ΔB1 virus, the ΔB1mutB12-A1 (light green bars) and the ΔB1mutB12-A3 (dark green bars) viruses exhibit increased DNA accumulation at 24h, exceeding ΔB1 (red bars) levels by >5-fold in monkey CV1 cells (Fig 5.3A) and >18-fold in human HeLa cells (Fig 5.3B). Increases were also

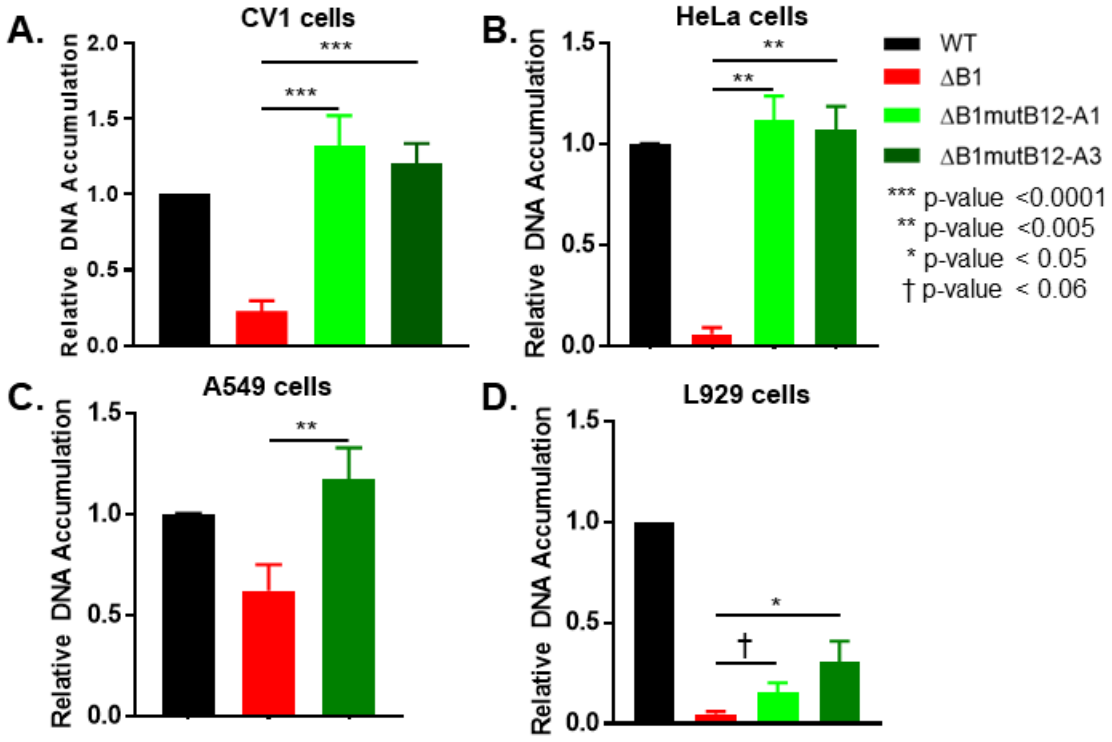

Fig 5.3. Rescued DNA replication block for ΔB1mutB12 virus in multiple cells. (A) CV1, (B) HeLa, (C) A549, and (D) L929 cells infected with WT (black), ΔB1 (red), ΔB1mutB12-A1 (light green), ΔB1mutB12-A3 (dark green) at a MOI of 3 were harvested 24h post infection for qPCR of relative DNA accumulation.

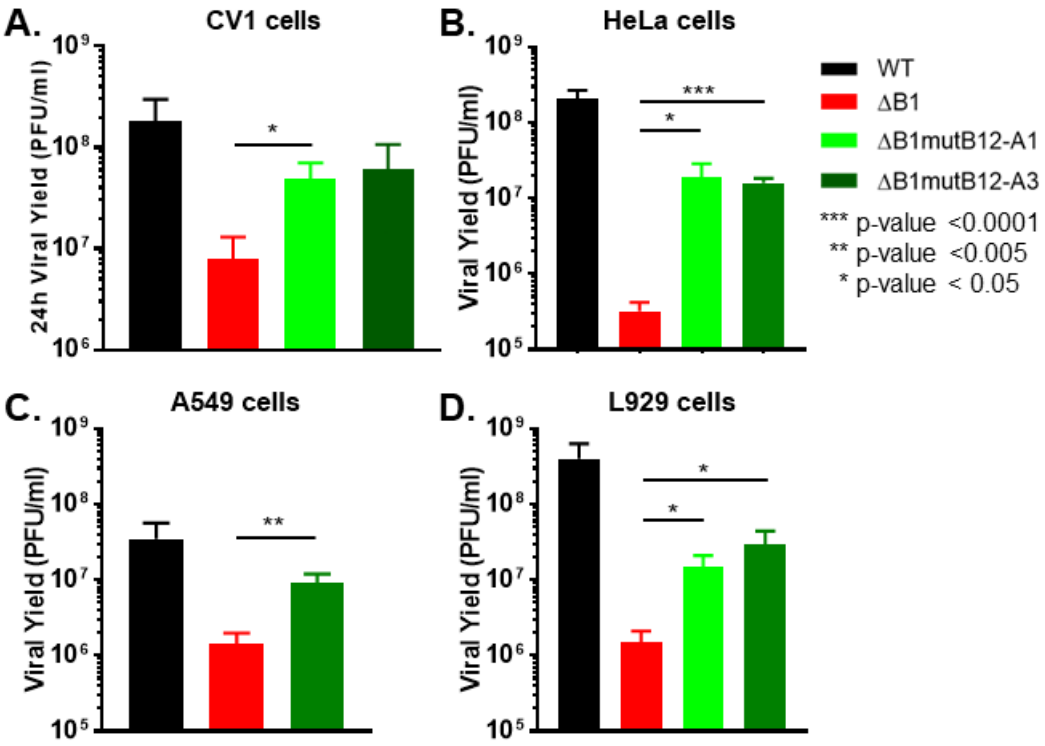

Fig 5.4. Rescued viral yield for ΔB1mutB12 virus in multiple cells. (A) CV1, (B) HeLa, (C) A549, and (D) L929 cells infected with WT (black), ΔB1 (red), ΔB1mutB12-A1 (light green), ΔB1mutB12-A3 (dark green) at a MOI of 3 were harvested 24h post infection for titration on CV1-B1myc cells for viral yield.

observed in human A549 cells (Fig 5.3C) and mouse L929 cells (Fig 5.3D), although to a lesser degree.

Regarding viral progeny, the ΔB1mutB12-A1 (light green bars) and ΔB1mutB12-A3 (dark green bars) exhibit rescued viral yield phenotypes in multiple cell lines when compared to the ΔB1 (red bars) virus. Specifically, the viral yields for ΔB1mutB12-A1 and -A3 viruses compared to ΔB1 levels were increased >6-fold in monkey CV1 cells (Fig 5.4A), >50-fold in human HeLa cells (Fig 5.4B), >6-fold in human A549 cells (Fig 5.4C), and >12-fold in mouse L929 cells (Fig 5.4D). Notably, despite a >50-fold rescue over the ΔB1 viral yield, the ΔB1mutB12-A1 and -A3 viruses remained at 11-fold (p-value = 0.0056) and 13-fold (p-value = 0.0051) lower levels than WT yields in HeLa cells (Fig 5.4B). Similarly, the ΔB1mutB12-A1 virus was 28-fold (p-value = 0.0474) lower than WT viral yield in L929 cells (Fig 5.4D), despite showing a >12-fold increase from ΔB1 levels. These results demonstrate a rescued viral yield phenotype for ΔB1mutB12-A1 and -A3 over ΔB1 levels in all cell lines, while remaining attenuated compared to WT virus.

To examine ΔB1mutB12-A3 virus yield at earlier time points, CV1 cells infected with WT (black line), ΔB1 (red line) or ΔB1mutB12-A3 (green line) virus were harvested early during infection to monitor input DNA (3hpi) and initial DNA replication (7hpi), while later time points were selected for the completion of DNA replication (16hpi) and the completion of vaccinia virus replicative cycle (24hpi). DNA accumulation at each time point demonstrated that the ΔB1mutB12-A3 virus replicated its genome at a rate similar to WT (Fig 5.5A). Next, virus samples were titrated on CV1-B1myc complementing cells to quantify viral yield at each time point. At early time points the

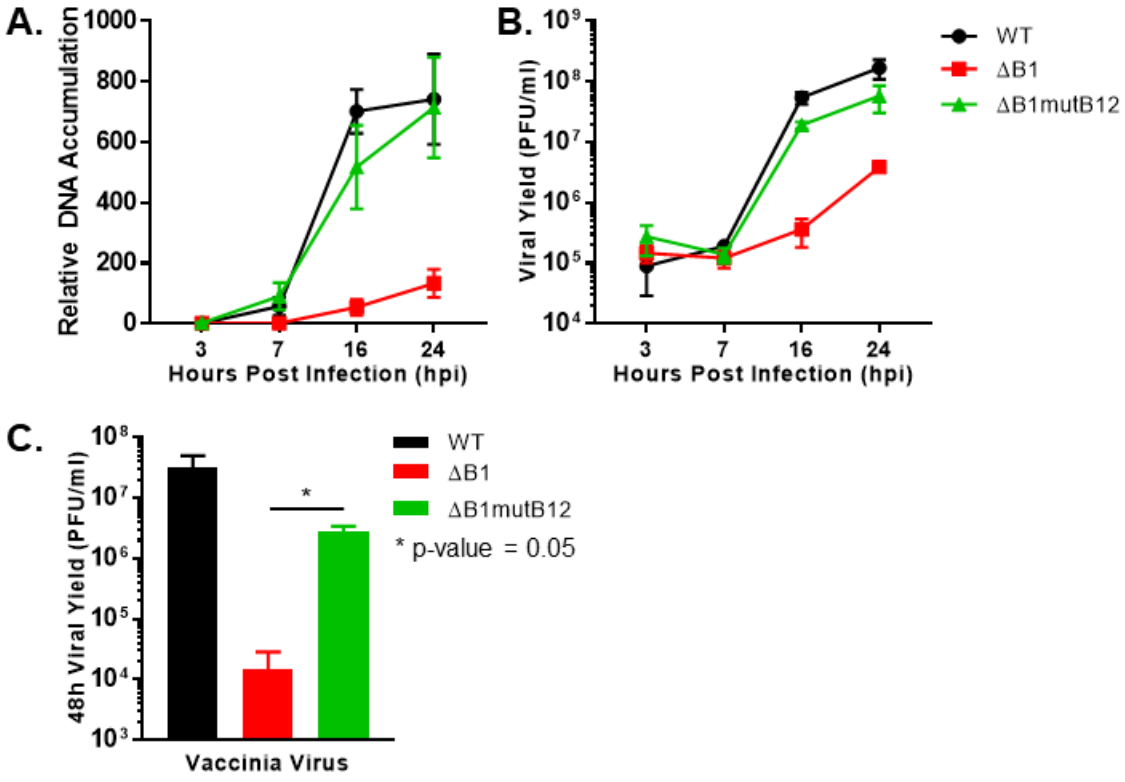

Fig 5.5. Viral growth kinetics of ΔB1mutB12 is similar to WT virus. (A) WT (black), ΔB1 (red), or ΔB1mutB12-A3 (green) infections of CV1 cells were performed at a MOI of 3 and harvested at 3, 7, 16, or 24h post infection for relative DNA accumulation or (B) viral yield quantification on CV1-B1myc cells. (C) A multi-step viral yield assay was completed by infecting CV1 cells at a MOI of 0.01 with WT (black), ΔB1 (red) or ΔB1mutB12-A3 (green) and harvested at 48h post infection for titration on CV1-B1myc cells.

ΔB1mutB12 viral yield levels were identical to WT levels. Similar to the 24h only data (Fig 5.4A), the ΔB1mutB12-A3 virus exhibited an almost 3-fold reduction in viral yield as compared to WT virus at late time points, although these differences were not statistically different (Fig 5.5B, 16 and 24hpi). Therefore, the WT virus and ΔB1mutB12 virus have only modest growth difference with respects to DNA accumulation and viral yield output in CV1 cells under these conditions.

The similar growth profiles of WT and ΔB1mutB12 viruses in CV1 cells at a MOI of 3 led us to question whether the same was true at lower concentrations of virus. For this next assay, cells were infected with a low MOI of 0.01 and allowed to propagate, spreading cell-to-cell, for 48h before harvest and titration on CV1-B1myc cells. From these infections, ΔB1mutB12 (green bar) viral yield was >180-fold higher than ΔB1 (red bar) virus (Fig 5.5C). Interestingly, the ΔB1mutB12-A3 (green bars) virus was attenuated 12-fold (p-value = 0.09) as compared to the WT (black bars) virus viral yield (Fig 5.5C). In summary, the ΔB1mutB12 virus exhibits a rescued DNA accumulation phenotype compared to ΔB1 in multiple species cell lines. The viral yield of the ΔB1mutB12 virus also indicates a recovered growth phenotype as compared to ΔB1 levels for all cell lines tested. Yet, the extent of ΔB1mutB12 attenuation compared to WT viral yield differed depending on the cell line and amount of virus used for infection.

5.3. The B12ΔA690 protein is truncated and accumulates to lower levels than the wild-type B12 protein.

The sequencing data for the ΔB1mutB12 viruses revealed a prevalent indel mutation within the 3’ end of the *B12R* gene that leads to a frame shift. This frameshift introduces a premature stop codon into the mRNA, which is predicted to translate into a

protein missing about 45 amino acids from the C-terminus, about 16% of the total polypeptide. Studies on VRK1, a cellular homolog of B12 determined that removal of 18% of the protein from the C-terminus produces a protein that cannot be purified from *E. coli* (145) suggesting that this region is necessary for protein folding and/or stability. The only nonsynonymous point mutation in greater than 5% of the read counts also occurred within the *B12R* gene and encoded a glycine (G) to aspartate (D) change at amino acid 215 (Table 5.1). Interestingly, the temperature sensitive (ts) B1 mutant virus, ts25, has a lesion within the *B1R* gene that results in glycine at amino acid 227 to change to aspartate. This glycine aligns with the mutated glycine in the B12 protein sequence of the ΔB1 adapted virus. Analysis of the ts25 virus growth supports that the lesion in *B1R* results in a catalytic null, labile B1 protein (73). Based on these supporting information and B12 sequence analysis, we hypothesized that the indel mutation within the *B12R* gene will lead to a truncated protein with reduced protein accumulation, and B12 amino acid G to D mutation would reduce B12 protein stability similarly resulting in decreased protein abundance. To test this hypotheses, we PCR amplified the wild-type *B12R* vaccinia gene from the WT vaccinia virus and generated two *B12R* mutants. The first *B12R* mutant was a single adenine deletion at nucleotide 690, corresponding to the site of the indel in ΔB1mutB12. The second *B12R* mutant contained a SNP at nucleotide G215 to A for representation of the point mutant in the ΔB1mutB12-A1 virus, Next, we cloned the vaccinia virus *B12R* gene or the *B12R* mutants with a HA epitope tag sequence at the 5' end of the gene into the pJS4 vaccinia expression vector. CV1 cells were transfected with pJS4-HA-B12wt, pJS4-HA-B12ΔA690, or pJS4-HA-B12 G-A plasmid DNA, synchronously infected with WT virus at a MOI of 3 and harvested 24h post infection to

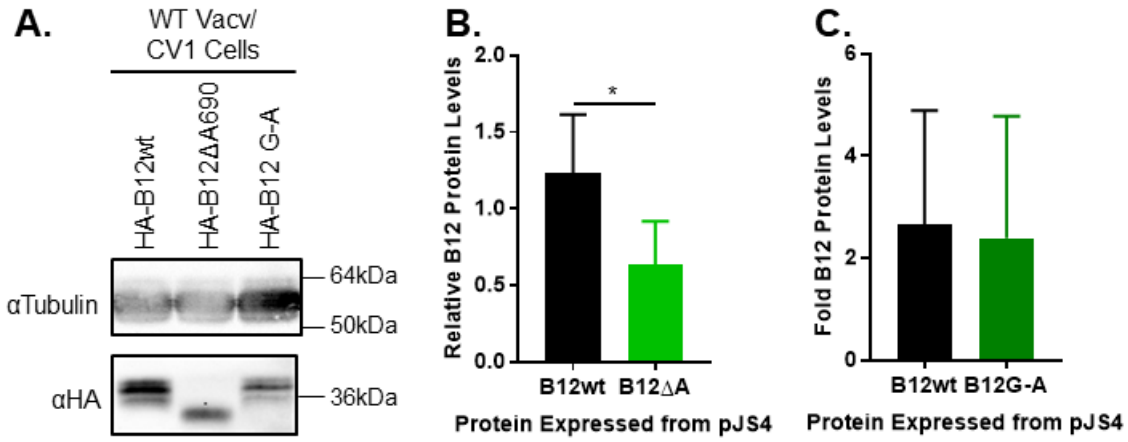

Fig 5.6. Adapted virus B12ΔA690 mutant is truncated and less abundant than wild-type B12 protein. (A) CV1 cells were transfected with pJS4-HA-B12wt, pJS4-HA-B12ΔA690 or pJS4-HA-B12 G-A plasmid and infected 6h post transfection with WT virus at a MOI of 3. 24h post infection cells were harvested for immunoblot analysis. The HA-B12Δ690 represents the indel mutation and HA-B12 G-A represents the point mutation within the ΔB1mutB12 virus *B12R* gene. (B) B12 proteins were expressed from the pJS4 vector during WT infection (representative immunoblot in Fig 1A). Protein abundance was averaged for HA-B12wt and HA-B12ΔA690 or for (C) HA-B12wt and HA-B12 G-A from five independent experiments.

allow for saturation of late gene expression. Following immunoblot analysis, the tubulin control shows equal loading of protein, while the HA blot shows HA-B12ΔA690 protein band has a smaller molecular weight as shown by a faster migrating band than the HA-B12wt and HA-B12 G-A protein bands (Fig 5.6A). As predicted, the HA-B12ΔA690 protein has reduced protein abundance, almost 2 fold lower than HA-B12wt protein (Fig 5.6B). However, the HA-B12 G-A mutant protein was not significantly lower than HA-B12wt protein abundance and averages at 90% of the wild-type protein (Fig 5.6C). Together, these results support the hypothesis that deletion of the adenine at nucleotide position 690 within the *B12R* gene results in a truncated protein and reduced protein levels as compared to the wild-type B12 protein. While similar protein levels between HA-B12wt and HA-B12 G-A supports that the mutant protein is not inherently less stable, the population of ΔB1 adapted viruses containing this mutation suggests that this residue or region may be critical for B12 function.

5.4. Loss of B12 through depletion rescues the ΔB1 and ts2 growth phenotype, but not other viruses with restricted DNA replication phenotypes.

The results thus far confirm that HA-B12ΔA690 is both truncated and may be less stable than the HA-B12wt protein. We posited two possible scenarios to explain how the enhanced replication of ΔB1mut12 may be mediated by the truncation and reduced abundance of B12. Either a proviral activity of B12 is increased in ΔB1mutB12 due to the absence of a regulatory domain lost after truncation, or wild-type B12 is capable of a repressive activity that is no longer present in the ΔB1mutB12 virus. To distinguish between these gain of function versus loss of function scenarios for the *B12R* indel mutation, we decided to test how ΔB1 growth was impacted by B12 depletion mediated

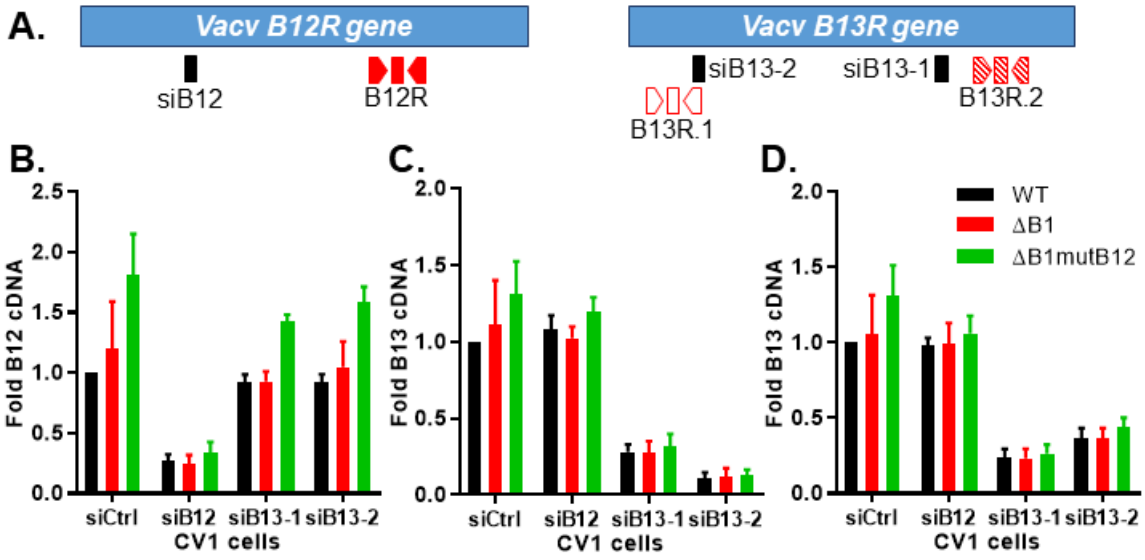

Fig 5.7. Depletion of B12 or B13 mRNA impact on neighboring gene expression. (A) Depiction of *B12R* and *B13R* general regions targeted by siRNA for mRNA depletion and probe/primer set binding of cDNA to quantify relative early gene expression using qPCR. (B) CV1 cells were transfected with siRNA for 24h then infected with WT (black), ΔB1 (red), or ΔB1mutB12-A3 (green) at a MOI of 3 and harvested 4h post infection for mRNA isolation. The cDNA generated from harvested mRNA samples was used with probe/primer sets in panel (A) to quantify early gene expression for *B12R* (B) and *B13R* using either the probe/primers B13R.1 set (C) or B13R.2 set (D).

by siRNA targeting of B12 mRNA. First, as controls, B12 mRNA levels for WT (black bars), ΔB1 (red bars), and ΔB1mutB12 (green bars) were quantified at 4h post infection in CV1 cells. Purified RNA was reverse transcribed to cDNA for qPCR quantitation of relative B12 mRNA levels using a specific primer and probe set (Fig 5.7A). Each virus expressed similar levels of relative B12 mRNA (Fig 5.7B, siCtrl). Second, we determined the level of B12 depletion using siRNA targeting B12 mRNA. Transfection of CV1 cells with siB12 prior to infection reduced relative B12 mRNA to <28% for each virus as compared to control cells (Fig 5.7B). We also verified that downstream *B13R* gene expression was not altered for the ΔB1mutB12 virus or during B12 mRNA depletion (Fig 5.7C and D) using two different B13 primer/probe sets (Fig 5.7A). We further validated that these primer probe sets were specific for B13 by demonstrating that they were sensitive to siRNAs specific to B13 (Fig 5.7C and D).

Upon successful B12 depletion using siRNA, we addressed the question of whether B12 loss of function rescues the ΔB1 growth phenotype. To test the rescue of ΔB1 plaque formation by depletion of B12, a plaque assay was carried out on CV1 siCtrl and siB12 (four different siRNAs targeting the B12 mRNA) treated cells during WT, ΔB1, and ΔB1mutB12 virus infections at 200 PFU/well (Fig 5.8A). We observed that WT and ΔB1mutB12 viruses can form plaques on CV1 siCtrl cells and similarly on CV1 siB12 cells. Strikingly, the ΔB1 virus that is unable to form plaques on CV1 siCtrl cells was able to form plaques in CV1 siB12 cells that were of a similar size as those present in the wells infected with ΔB1mutB12. To quantify this rescue in viral yield, CV1 cells were infected with WT, ΔB1, or ΔB1mutB12 virus at a low MOI of 0.01 for a multi-step growth assay. Infected cells were harvested at 7h and 48h post infection. At 7h post

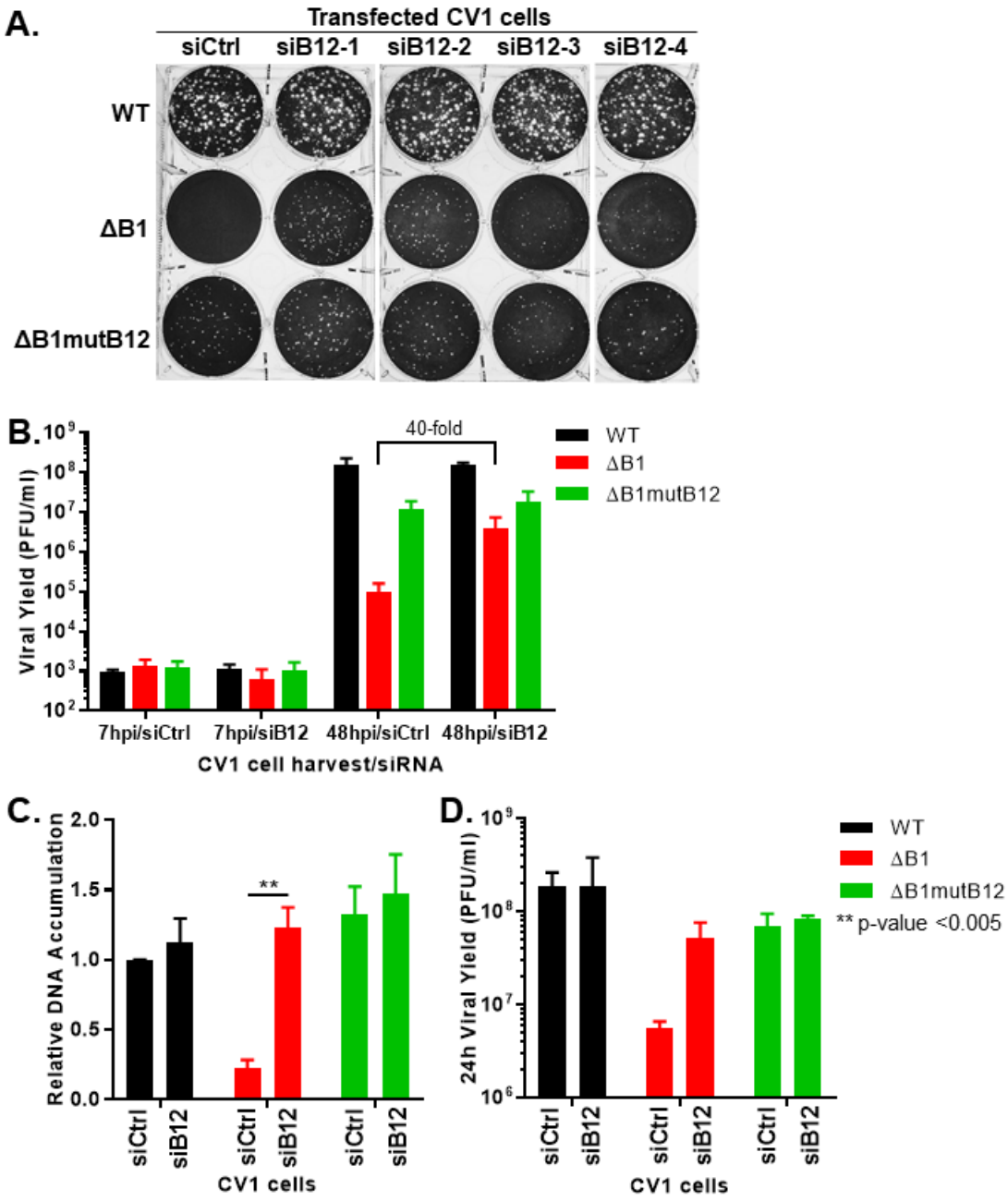
A.
Transfected CV1 cells
siCtrl
siB12-1
siB12-2
siB12-3
siB12-4
WT
ΔB1
ΔB1mutB12
B.
Viral Yield (PFU/ml)
40-fold
WT
ΔB1
ΔB1mutB12
7hpi/siCtrl
7hpi/siB12
48hpi/siCtrl
48hpi/siB12
CV1 cell harvest/siRNA
C.
Relative DNA Accumulation
**
siCtrl
siB12
CV1 cells
D.
24h Viral Yield (PFU/ml)
WT
ΔB1
ΔB1mutB12
** p-value <0.005
CV1 cells

Fig 5.8. Depletion of B12 rescues ΔB1 virus growth in CV1 cells. (A) 200PFU/well WT, ΔB1, or ΔB1mutB12-A3 infections were carried out on CV1 cells 24h following transfection with siCtrl or siB12. Cells were fixed 72h post infection. (B) Multi-step viral yield assay was conducted in siCtrl or siB12 CV1 cells for WT (black), ΔB1 (red), and ΔB1mutB12-A3 (green) infections at a MOI of 0.01. Cells were harvested at 7h or 48h post infection and titration on CV1-B1myc cells. (C) Growth assays on siCtrl or siB12 transfected CV1 cells were completed for WT (black), ΔB1 (red), and ΔB1mutB12 (green) viruses at a MOI of 3 for relative DNA accumulation and (D) viral yield titration on CV1-B1myc cells.

infection, each virus shows similar amounts of viral yield in CV1 siCtrl-treated cells and CV1 siB12-treated cells (Fig 5.8B). This measurement at 7h post infection is indicative of input virus. At 48h post infection, WT (black bars) and ΔB1mutB12 (green bars) yields remain constant between control and B12 depletion (Fig 5.8B). By comparison, the ΔB1 (red bar) virus increases 40-fold in the CV1 siB12 cells as compared to CV1 siCtrl cells (Fig 5.8B).

Next, we quantified the rescue of DNA accumulation and viral yield following B12 depletion during ΔB1 infection using a one-step viral growth assay. Both WT and ΔB1mutB12 DNA accumulation levels are not significantly increased during infection of CV1 siB12 cells as compared to CV1 siCtrl cells (Fig 5.8C). However, DNA accumulation of ΔB1 increases 5.4-fold in CV1 siB12 cells compared to CV1 siCtrl cells. Similarly, the viral yield for WT and ΔB1mutB12 viruses remains constant between CV1 siCtrl and siB12 infected cells while ΔB1 yields an increase of about 9-fold in CV1 siB12

cells as compared to siCtrl treated cells (Fig 5.8D). In summary, the replication assays of ΔB1 virus during B12 depletion indicate that the loss of B12 function rescues the ΔB1 phenotype. This siRNA study also refutes the gain of function scenario outlined earlier. Specifically, if the indel mutation within *B12R* resulted in a gain of function, then the depletion of the B12 mutant during ΔB1mutB12 infections should have restored the attenuated ΔB1 phenotype during these infections, but it did not (Fig 5.8C and D, compare siB12 ΔB1mutB12 to siCtrl ΔB1). Together, these data are consistent with the model that the *B12R* indel mutation in ΔB1mutB12 causes a loss of B12 function, leading us to infer that full length B12 is a repressor of ΔB1 growth.

It was interesting that siB12 treatment does not impact WT growth, but is only apparent in the absence of the B1 kinase, indicating that the B12 repressive function may not be active in the presence of B1. To explore this possibility further, we examined whether B12 depletion would increase DNA accumulation of other replication deficient vaccinia viruses, such as those with lesions in the D5 primase/helicase or E9 DNA polymerase. We posited that if B12 inhibition is directly linked to a B1 mediated pathway of promoting DNA replication, then depleting B12 will only rescue B1 mutant or deletion viruses (Fig 5.9A). Alternatively, depletion of B12 may also rescue growth of other replicative deficient viruses such as D5 or E9 mutant viruses, which would indicate that B12 inhibits DNA replication via a more general mechanism of action (Fig 5.9A). In order to determine which model fits B12 repressive function, we depleted B12 during infection with WT or mutant viruses and assayed for DNA accumulation. Viruses used for this assay included WT, ΔB1, a temperature sensitive B1 mutant (ts2) virus (68), a temperature sensitive D5 primase/helicase mutant (ts24) virus (131), and a temperature

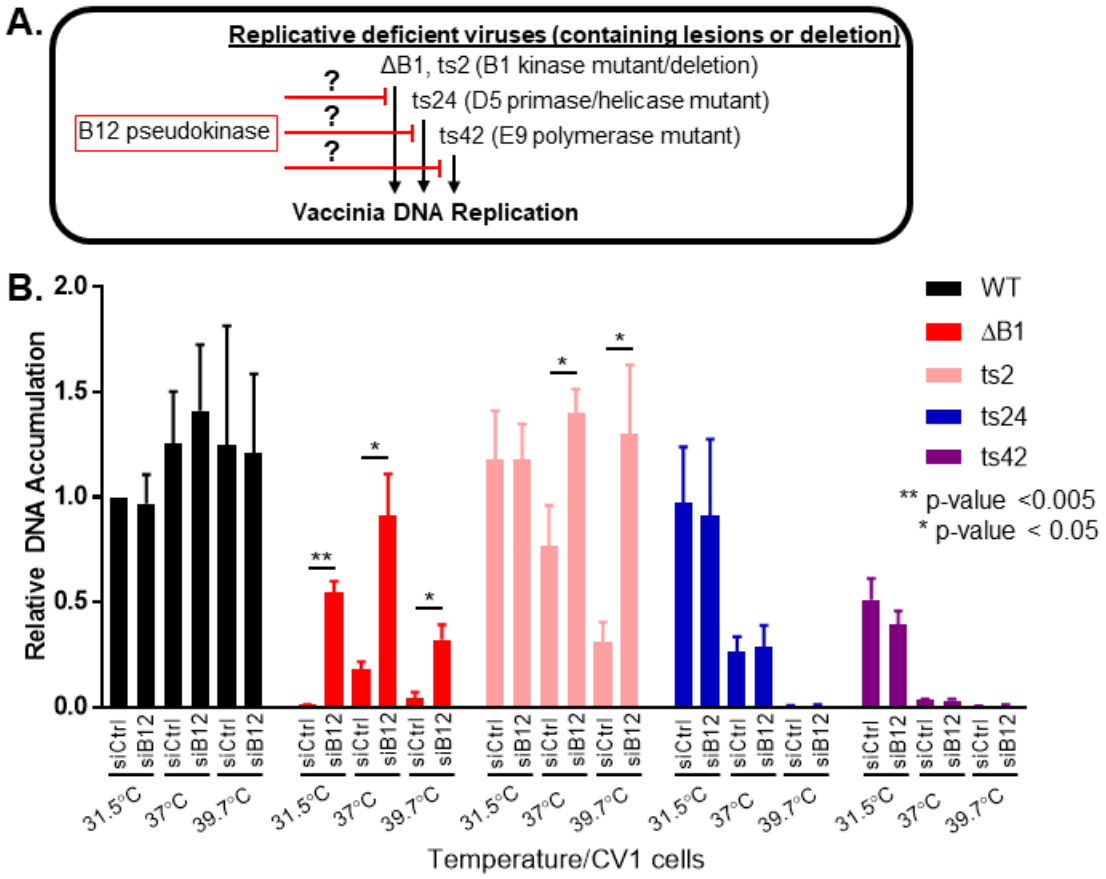

Fig 5.9. Rescue of DNA replication block using siB12 is specific for viruses lacking a functional B1. (A) Diagram of hypothesis that B12 is either a general inhibitor of DNA replication or specific to B1 kinase mutant viruses. (B) CV1 cells treated with siCtrl or siB12 were infected with WT (black), ΔB1 (red), ts2 B1 mutant (pink), ts24 D5 mutant (blue), or ts42 E9 mutant (purple) at a MOI of 3 and harvested 24h post infection for quantification of relative DNA accumulation. Infections were carried out at 31.5˚C, 37˚C or 39.7˚C to provide permissive, semi-nonpermissive and nonpermissive temperatures respectively for the temperature sensitive mutant viruses.

sensitive E9 DNA polymerase mutant (ts42) virus (132). Infections were performed at permissive temperature (31.5˚C), semi-permissive temperature (37˚C), and nonpermissive temperature (39.7˚C). DNA accumulation was quantified using qPCR during a synchronous infection of siCtrl or siB12 treated CV1 cells. The 24h DNA accumulation for WT virus remains constant at all three temperatures, independent of siB12 pre-treatment of cells (Fig 5.9B, black bars). The ΔB1 virus DNA accumulation was attenuated compared to WT in siCtrl cells as previously published (127). Pre-treatment with siB12 rescues the ΔB1 DNA accumulation 58-fold, 5-fold, and >9-fold as compared to the siCtrl at 31.5˚C, 37˚C, and 39.7˚C respectively (Fig 5.9B, red bars). The temperature sensitive ts2 B1 mutant virus follows a similar trend to the ΔB1 virus. Specifically, at non-permissive temperatures the siB12 treated cells have increased DNA accumulation 2-fold at 37˚C and >4-fold at 39.7˚C as compared to siCtrl cells for the ts2 virus (Fig 5.9B, pink bars). At permissive temperature the ts2 virus has similar DNA accumulation as the WT virus as expected. Importantly, the rescue in DNA accumulation observed for ΔB1 at all temperatures and for ts2 at non-permissive temperatures was not observed for the other two viruses with restricted DNA accumulation. Explicitly, the ts24 (blue bars) and ts42 (purple bars) viruses have similar restricted DNA accumulation at 37˚C and 39.7˚C temperatures for CV1 siCtrl cells compared to CV1 siB12 cells (Fig 5.9B). In summary, these data demonstrate that the depletion of B12 specifically rescues B1 mutant/deletion viruses, while B12 depletion does not enhance DNA replication for temperature sensitive D5 (ts24) and E9 (ts42) mutant viruses.

5.5. Reconstitution of B12 in CV1 cells represses ΔB1 and ΔB1mutB12 replication.

At this point we have shown that siRNA-directed loss of B12 rescues the ΔB1 and ts2 virus growth, specifically by increasing DNA replication. This supports a model in which B12 carries out a repressive function on DNA replication in the absence of a functional B1 kinase. To complement our above B12 depletion studies, we next hypothesized that expression of B12 from the cellular genome would be sufficient to inhibit replication of viruses lacking B1. To test this hypothesis, we began by generating cells stably expressing a HA-tagged or untagged codon optimized B12 (GeneArt). Codon optimization for mammalian cells allows for enhanced expression of the gene by mammalian cells and in our system codon optimized B12 is resistant to the siB12 used to deplete B12 mRNA expressed by the virus. Expression of HA-B12 was confirmed using immunoblot analysis of whole cell lysates from both control and HA-B12 lentivirus transduced and selected CV1 cells (Fig 5.10A).

To test the repressive activity of reconstituted B12, we transfected control or HA-B12 expressing CV1 cells with siCtrl or siB12 for 24h and then infected cells with WT, ΔB1, or ΔB1mutB12 virus at a MOI of 3. The cells were harvested at 24h post infection and relative DNA accumulation of each vaccinia virus was quantified using qPCR. Using a combination of siB12 treatment during a ΔB1 infection and separately using the ΔB1mutB12 virus allows us to test B12 repressive activity via restoration on two different systems in which the viral B12 has been inactivated. First, we compared results from cells treated with the control siRNA. In cells transfected with siCtrl, the DNA accumulation for the WT virus is not altered by reconstitution of HA-B12 (Fig 5.10C, siCtrl, black solid and striped bars). In contrast, the ΔB1 virus exhibited a 2.7-fold

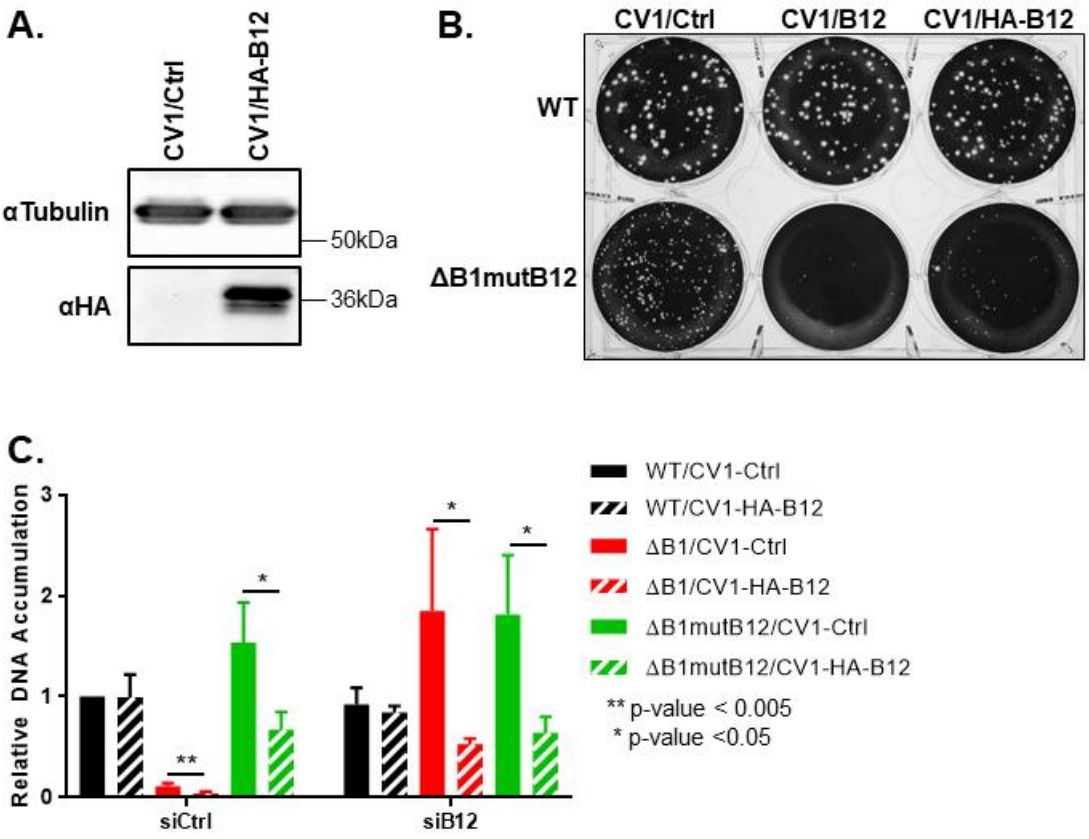

Fig 5.10. B12 reconstitution during infection with B1 and B12 naïve viruses repressed vaccinia replication. (A) Immunoblot analysis of control or HA-B12 (GeneArt) lentivirus transduced CV1 cells was completed to detect tubulin (loading control) and HA (HA-tagged B12). (B) CV1 control cells or cells stably expressing B12 or HA-tagged B12 were infected with WT or ΔB1mutB12-A3 at 300PFU/well and fixed 72h post infection. (C) 24h relative DNA accumulation quantification was completed for CV1 control or HA-B12 expressing cells transfected with siCtrl or siB12 and infected with WT (black), ΔB1 (red), or ΔB1mutB12-A3 (green) at a MOI of 3.

reduction in relative DNA accumulation in CV1-HA-B12 cells as compared to CV1-Ctrl cells (Fig 5.10C, siCtrl, red solid and striped bars). Similarly, the relative DNA accumulation for ΔB1mutB12 virus was 2.3-fold lower in HA-B12 expressing cells than control cells (Fig 5.10C, siCtrl, green solid and striped bars).

Next, we compared cells in which viral B12 was depleted. In siB12 transfected cells, the WT virus DNA accumulation was not altered by HA-B12 expression in cells (Fig 5.10C, siB12, black solid and striped bars). Consistent with our model of B12 repressive activity during vaccinia virus infection in the absence of a functional B1 kinase, the DNA accumulation for the ΔB1 virus was 3.4-fold lower in HA-B12 expressing cells than control cells under siB12 conditions (Fig 5.10C, siB12, red solid and striped bars). Lastly, the ΔB1mutB12 replication in HA-B12 expressing cells was reduced 2.8-fold relative to control cells for siB12 transfected cells (Fig 5.10C, siB12, green solid and striped bars). Importantly, B12 expression from the cell was sufficient to inhibit DNA replication for both the ΔB1/siB12 and ΔB1mutB12 systems. These data further support a model in which B12 can downregulate vaccinia virus DNA accumulation in the absence of a functional B1 kinase.

Previously we demonstrated that depletion of B12 during a ΔB1 infection allows the virus to carry out productive infection as measured by the formation of plaques on CV1 cells (Fig 5.8A). To determine how reconstitution of wild-type B12 affects vaccinia productive infection, we carried out a plaque assay of either WT or ΔB1mutB12 infected control, B12 expressing, or HA-B12 expressing CV1 cells. Cells were fixed three days post infection. The WT virus plaque number and size was unchanged by the expression of B12 or HA-B12 in cells as compared to the control CV1 cells (Fig 5.10B,

top row). Strikingly, after infection with the ΔB1mutB12 virus there was a consistent reduction in number and in size of plaques in both the B12 and HA-B12 expressing cells compared to control CV1 cells (Fig 5.10B, bottom row). Thus, the addition of the wild-type B12 decreases ΔB1mutB12 productive infection, providing additional evidence that B12 can impair poxvirus replication in the absence of B1.

5.6. Chapter 5 Summary

These studies in chapter 5 extend our understanding of B1 roles to promote DNA replication by identifying viral factors that can contribute to vaccinia DNA replication in the absence of the essential B1 kinase. Using experimental evolution of the B1 deletion vaccinia virus we identified two significant mutations in only the *B12R* gene out of the entire viral genome that rescued the viral fitness of ΔB1. We characterized the B12ΔA690 mutant as a truncated protein, reduced 2-fold in abundance and the B12 G-A mutant to have similar protein levels as the wild-type B12. Significantly. we also determined that B12 loss rescued the replicative defect in the absence of the B1 kinase (Fig 5.11). Furthermore, the role of B12 to repress DNA replication is not a dominant phenotype when a functional B1 kinase is expressed (Fig 5.11).

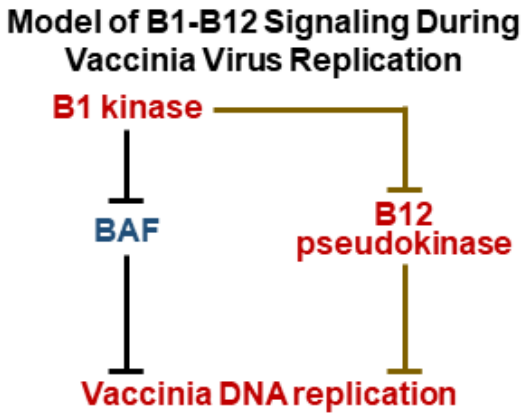

Fig 5.11. Model of B1-B12 signaling during vaccinia virus replication. The contributes of this chapter to our working model includes the discovery that vaccinia B12 pseudokinase restricts vaccinia DNA replication and is regulated by vaccinia B1 kinase.

CHAPTER 6

B12 MEDIATES RESTRICTION OF VACCINIA DNA REPLICATION VIA INTERACTIONS WITH NUCLEAR FACTORS

6.1. B12 is predominantly nuclear and solubilizes separate from chromatin-bound proteins.

To provide insight into the function of the B12 protein, we examined the subcellular localization of transiently expressed HA-tagged B12 (GenScript) in CV1 cells. One day after transfection, cells were fixed, incubated with αHA primary antibody with corresponding secondary antibody and stained with DAPI for immunofluorescence imaging of cells. The HA-B12 expressing cells show a clear nuclear localization as compared to control cells (Fig 6.1A, top row). By comparison, the B1 kinase localizes to the cytoplasm (Fig 6.1A, bottom row), as published previously (127). Next, we tested whether B1 expression in cells could alter B12 subcellular localization by examining transiently expressed HA-B12 in cells expressing the myc-tagged B1 protein. The top panels show that HA-B12 still exhibits a nuclear localization in cells expressing the B1 kinase (Fig 6.1B, top row). Additionally, the B1 kinase does not have altered localization in the presence of HA-B12 expression and nuclear localization (Fig 6.1B, bottom row). Therefore, B1 expression does not detectably redirect B12 localization in this assay.

Although B12 localized to the nucleus in uninfected cells, it is possible that B12 localization is different during vaccinia infection. To address this question, homologous recombination within the nonessential viral TK locus was used to generate a WT/HA-B12 recombinant virus expressing the transgene under an early and leaky late viral promoter (Fig 6.1C). This inducible system also allows for increased HA-B12 late

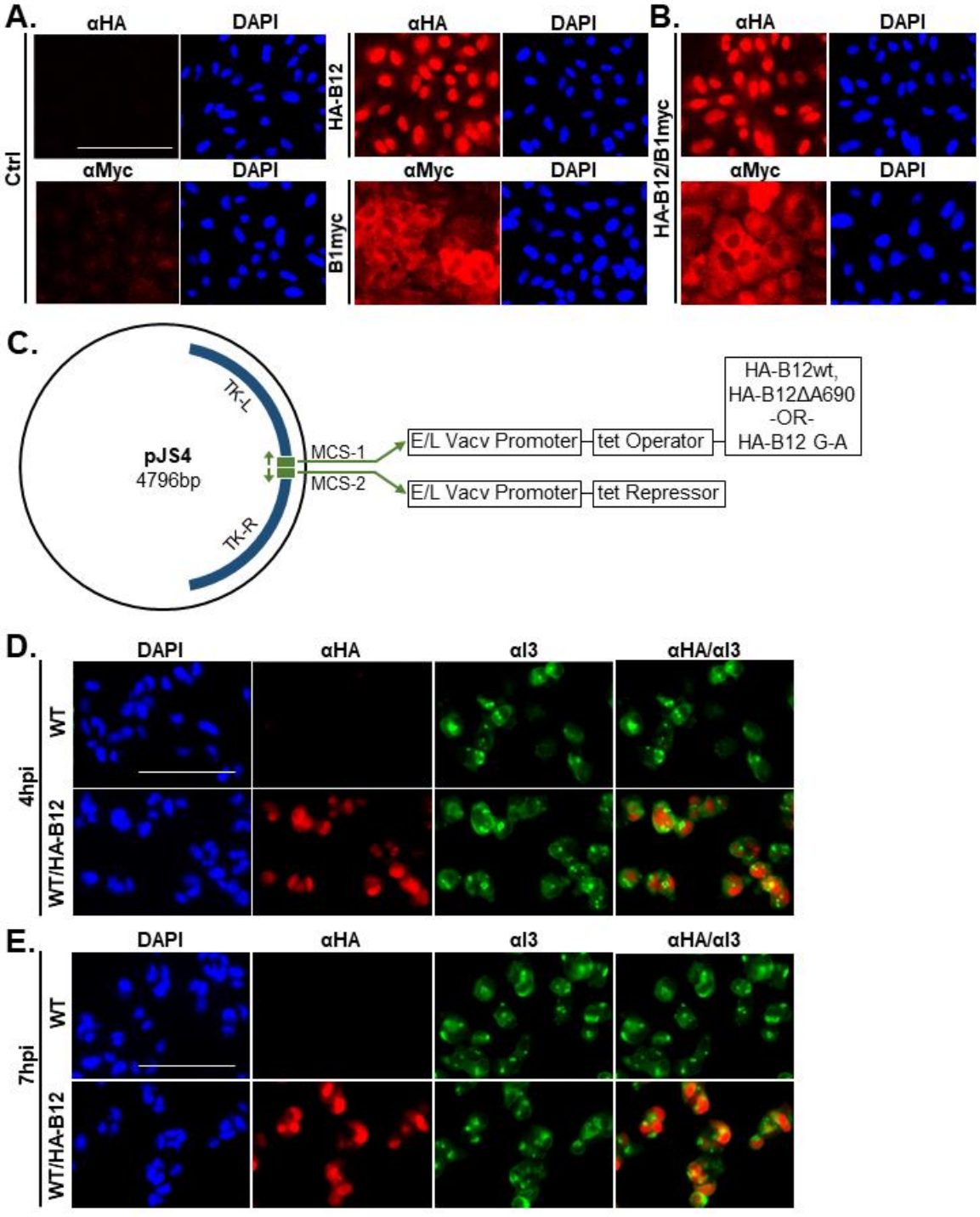
A.
αHA
DAPI
αHA
DAPI
Ctrl
HA-B12
αMyc
DAPI
αMyc
DAPI
B1myc
B.
αHA
DAPI
HA-B12/B1myc
αMyc
DAPI
C.
TK-L
pJS4
4796bp
TK-R
MCS-1
MCS-2
E/L Vacv Promoter
tet Operator
HA-B12wt,
HA-B12ΔA690
-OR-
HA-B12 G-A
E/L Vacv Promoter
tet Repressor
D.
DAPI
αHA
αI3
αHA/αI3
4hpi
WT
WT/HA-B12
E.
DAPI
αHA
αI3
αHA/αI3
7hpi
WT
WT/HA-B12

Fig 6.1. B12 exhibits a nuclear localization in uninfected and infected cells. (A) CV1 cells with or without HA-B12 (GenScript) mRNA transfection were used for immunofluorescence detection of HA-tagged B12 (red, top row). CV1 control and CV1-B1myc expressing cells were incubated with αmyc for B1myc detection (red, bottom row). All cells were stained with DAPI nuclear stain (blue). (B) B1myc expressing CV1 cells were also transfected with HA-B12 (GenScript) mRNA and separately incubated with a primary antibody to detect HA-tagged B12 (αHA, top red image) or myc-tagged B1 (αmyc, bottom red image) and DAPI (blue) nuclear stain. (C) Plasmid schematic of HA-B12 forms cloned into pJS4 vector under an early/late promoter and a leaky tetracycline repressor. (D) CV1 cells were infected with WT or WT/HA-B12 virus at a MOI of 5 and fixed at 4hpi or (E) 7hpi for immunofluorescence analysis of HA-B12 detection (red), I3 ssDNA binding protein (green) and DAPI nuclear stain (blue).

expression, occurring outside of the virion core, during doxycycline treatment which restricts tetracycline (tet) repressor binding to the tet operator (Fig 6.1C). To assess HA-B12 localization during infection, CV1 cells were infected with WT or WT/HA-B12 virus at a MOI of 5 and fixed at either 4 or 7hpi, chosen to coincide with times of peak early gene expression and DNA replication. Interestingly, virus expressed HA-B12 exhibited a predominantly nuclear localization at 4 and 7hpi, (Fig 6.1D and E, αHA panel) similar to that observed in uninfected cells. Furthermore, HA-B12 nuclear localization was distinct from the viral, cytoplasmic replication factories as indicated by puncta formation of vaccinia I3 single-stranded DNA binding protein (Fig 6.1D and E, αI3 and αHA/αI3 panels). To further characterize HA-B12 nuclear localization, we

examined B12 solubility in two separate assays. First using an immunofluorescence based approach, we utilized a protocol in which cells are briefly treated with detergent prior to fixation to separate highly soluble proteins from those more strongly tethered to nucleic acids or cytoskeletal elements in the cell (133, 134, 146-150). Cells transiently expressing HA-B12 or HA-GFP were either fixed then permeabilized or first prepermeabilized (0.1% Triton X-100), followed by fixing cells and a second permeabilization (0.2% Triton X-100) step. In CV1 cells fixed prior to permeabilization, the control cells (top row) had low background after αHA incubation, the HA-B12 (middle row) had a nuclear localization, and HA-GFP expressing cells (bottom row) showed diffuse localization of that protein (Fig 6.2A). For CV1 cells that were prepermeabilized, the αHA columns for control cells (top row) had low background, HA-B12 expressing cells (middle row) continued to exhibit bright, nuclear localization, while HA-GFP expressing cells (bottom row) exhibited only background levels of green fluorescence similar to the control cells (Fig 6.2B). In summary, pre-permeabilization of cells was sufficient to solubilize HA-GFP from cells while HA-B12 was retained in the nucleus under the same conditions. Together, these data suggest that B12 not only localizes to the nucleus of uninfected or infected cells, but also interacts with unknown binding partners there.

For comparison to the immunofluorescence based solubilization assay, we also examined the B12 fractionation profile following sequential treatment with a commercially optimized panel of extraction buffers. Following fractionation of control CV1 and CV1-HA-B12 cells, western blot analysis was performed using equal proportions of each fraction (Fig 6.2C). In addition to HA-B12, we examined the

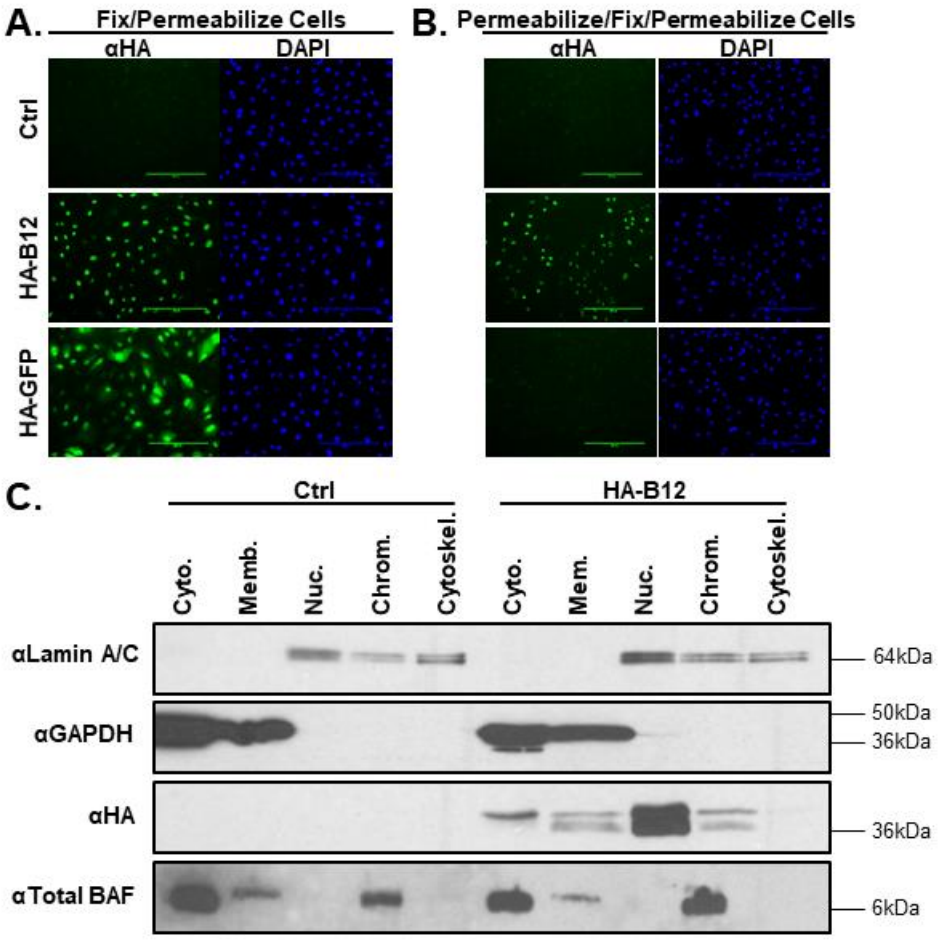

Fig 6.2. B12 nuclear localization is distinct from chromatin bound proteins. (A) CV1 cells were transfected with no mRNA, HA-GFP mRNA, or HA-B12 (GenScript) mRNA. Cells were either fixed then permeabilized to detect HA-tagged proteins or (B) prepermeabilized, fixed and then permeabilized again for detection of HA-tagged proteins remaining in cells following washes to remove unbound protein. The DAPI nuclear stain (blue) and αHA antibody (green) for detection of HA-GFP and HA-B12 were used. (C) Subcellular fractionation of CV1 control or HA-B12 (GeneArt) stably expressing cells was completed to separate cells into cytoplasmic extract (Cyto.), membrane extract (Memb.), soluble nuclear extract (Nuc.), chromatin-bound extract

(Fig 6.2 continued) (Chrom.), and cytoskeleton extract (Cytoskel.). Lamin A/C, GAPDH and BAF protein detection were used as fractionation controls and HA was used to detect HA-tagged B12 protein.

abundance of GAPDH, lamin A/C, and BAF in each fraction. As expected, GAPDH was most enriched in the cytoplasm with some also detected in the membrane fraction, but not in the other fractions. Lamin A/C was enriched in fractions expected to contain nuclear components and cytoskeleton. Previous studies have demonstrated that BAF is present both in the nucleus, where it binds chromatin, and free in the cytoplasm as summarized in a recent review article (151). Our results here are consistent with those data and show BAF to be primarily present in a soluble form in the cytoplasmic fraction, and in a chromatin-bound fraction. Interestingly, the HA-B12 protein was found primarily in the soluble nuclear fraction. Detectable HA-B12 was also present in the cytoplasmic, membrane and chromatin-bound extracts albeit at much lower levels. Together in concert with the immunofluorescence assays, these studies indicate that B12 localizes predominantly to the nucleus where it fractionates distinctly from BAF and likely other chromatin associated proteins.

6.2. Wild-type B12 predominant nuclear localization correlates with B12 repressive function.

To this point we have shown that B12 predominantly localizes to the nucleus even during infection with the WT virus. However, it is unclear if nuclear localization is necessary for B12 repressive activity on vaccinia DNA replication. To characterize the connection between B12 nuclear localization and repressive activity we took two

different approaches. The first approach was to test if B12 remained nuclear in infected cells lacking the B1 kinase. Our current data support a regulatory function of the B1 kinase to defuse B12 repressive activity (Fig 5.9). Therefore, it is possible that in the absence of the B1 kinase during infection, the B12 protein may carry out an abnormal function, inconsistent with the phenotype during WT infection. For this experiment, CV1 cells were transfected with *in vitro* synthesized HA-B12 (GenScript), infected 24h post transfection with WT, ΔB1, or ΔB1mutB12 at a MOI of 5, and fixed for immunofluorescence analysis at 7h post infection. Primary antibodies for I3 single-stranded DNA binding protein (green) and HA epitope (red) were used to visualize replication factories and HA-B12 respectively. During WT and ΔB1mutB12 infections replication factories are visible at 7h post infection and are highlighted with white arrow heads (Fig 6.3A, left and right columns), while the ΔB1 virus does not form replication factories (Fig 6.3A, middle columns) consistent with a replicative block as shown previously (Fig 3.2B and D). HA-B12 is predominantly nuclear in WT infected cells (Fig 6.3B, left columns) as shown with the WT/HA-B12 recombinant virus (Fig 6.1D and E). Consistent with this phenotype, HA-B12 is also predominantly nuclear in ΔB1 and ΔB1mutB12 infected cells (Fig 6.3B, middle and right columns). However, a striking reduction in replication factories was observed in ΔB1mutB12 infected cells expressing HA-B12 (Fig 6.3B, right columns), which was rescued in cells expressing both HA-B12 and B1myc (Fig 6.3C). It is important to note that HA-B12 protein may have localized to the nucleus before viral infection. Despite this possibility, the ΔB1mutB12 virus still exhibited an attenuated phenotype as visualized by a reduction in replication factories for this experiment. One additional limitation of this experiment was the variability in HA-

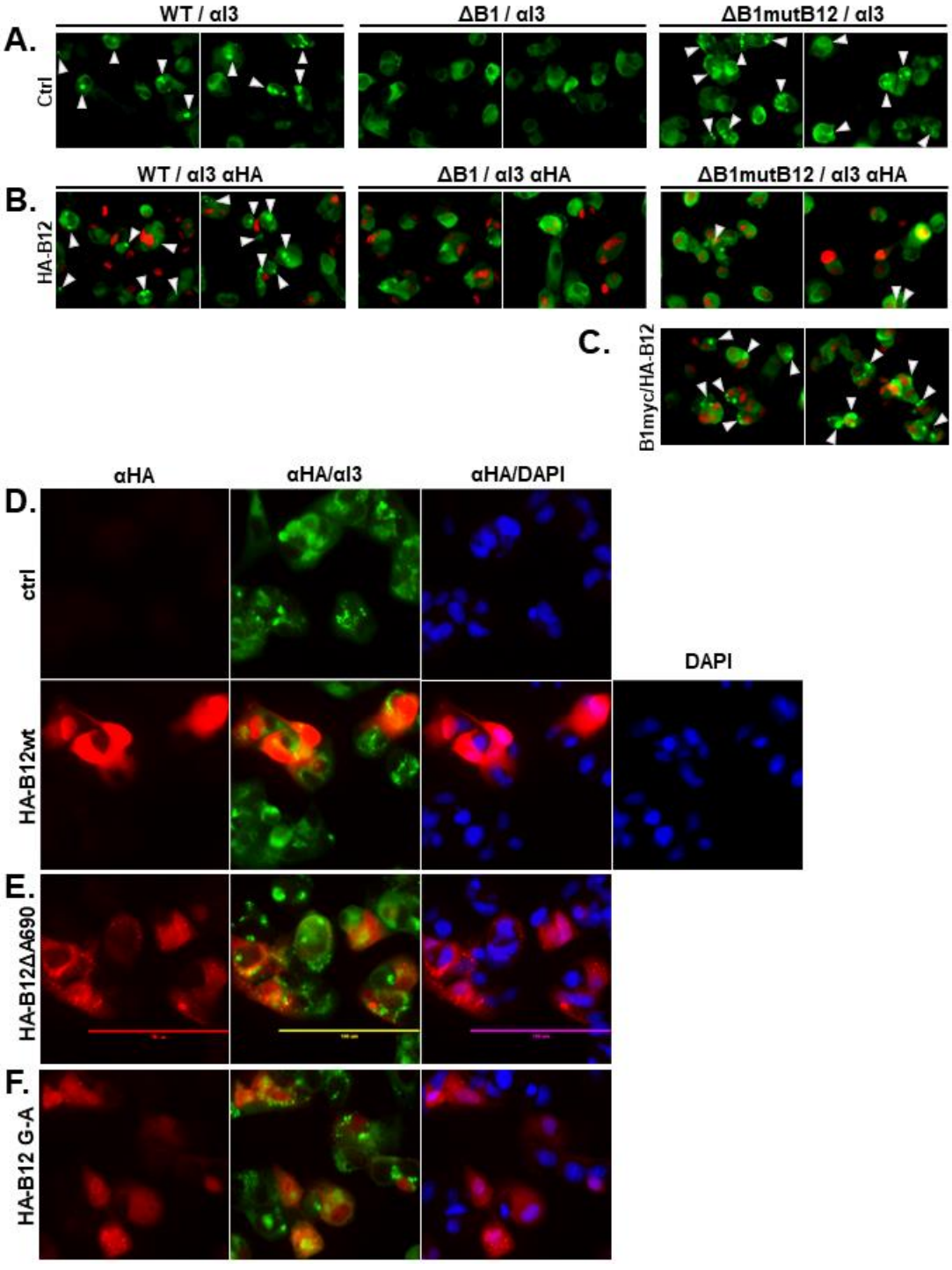
A.
WT / αI3
ΔB1 / αI3
ΔB1mutB12 / αI3
Ctrl
B.
WT / αI3 αHA
ΔB1 / αI3 αHA
ΔB1mutB12 / αI3 αHA
HA-B12
C.
B1myc/HA-B12
αHA
αHA/αI3
αHA/DAPI
D.
ctrl
DAPI
HA-B12wt
E.
HA-B12ΔA690
F.
HA-B12 G-A

Fig 6.3. Wild-type B12 is nuclear during infection and mutant B12 proteins are diffuse. (A) CV1 cells control or (B) transfected with HA-B12 (GenScript) mRNA and (C) stable B1myc expressing cells were used for immunofluorescence detection of HA-tagged B12 (red) during infection with WT, ΔB1, or, ΔB1mutB12 virus at an MOI of 5 and assayed for I3 (green) representing replication factories. (D) CV1 cells were transfected with pJS4-HA-B12wt, (E) pJS4-HA-B12ΔA690 or (F) pJS4-HA-B12 G-A plasmid and infected with WT virus at a MOI of 5 and fixed at 24h post infection for immunofluorescence analysis of HA-B12 form (red), I3 (green), or nucleic acid stain DAPI (blue).

B12 mRNA quality. This was inferred by differences observed in HA-B12 intensity when assayed in immunofluorescence assays and inconsistent results in repression assays where HA-B12 mRNA transfection was carried out to determine B12 repressive function on I3 puncta formation during ΔB1mutB12 infection. Therefore, an alternative method of HA-B12 expression may be necessary to clearly conclude that B12 is absent from replication factories in the cytoplasm.

The second approach was to discern if the adapted virus mutations of *B12R* altered B12 predominant nuclear localization. As we are unable to visualize B12 localization at replication factories or in the cytoplasm during infection with replicative deficient B1 deletion viruses, it is possible that B12 nuclear localization is important for its repressive function. The B12 protein is small enough to diffuse into the nucleus and our data supports a B12 interaction with a host, nuclear factor to restrict diffusion of B12 out of the nucleus (Fig 6.2A and B). Therefore, we predicted that ΔB1 adapted virus

mutations, ΔA690 and G215-to-A215, within *B12R* may alter B12 predominant nuclear localization if B12 mutants lack a nuclear interacting partner. To determine the localization of the mutant B12 proteins, CV1 cells were transfected with pJS4-HA-B12wt, pJS4-HA-B12ΔA690, or pJS4-HA-B12 G-A plasmid DNA for expression of an HA-tagged B12 protein under a late viral promoter. At 6h post transfection, cells were infected with WT virus at a MOI of 5 and fixed 16h post infection for immunofluorescence analysis. The HA-B12wt protein is predominantly nuclear with some diffusion into the cytoplasm (6.3D), identical to the WT/HA-B12 recombinant virus phenotype (Fig 6.1D and E). A striking change to diffuse cellular localization was visualized for both the HA-B12ΔA690 (Fig 6.3E) and HA-B12 G-A (Fig 6.3F) mutant proteins. These two approaches support a correlation between B12 predominant nuclear localization and B12-mediated repressive activity. Due to incomplete repression of the ΔB1mutB12 virus in HA-B12 add back experiments, it seems unlikely that undetectable levels of HA-B12 in the cytoplasm are sufficient for repression of viral replication in the absence of a function B1 kinase.

6.3. The ΔB1mutB12 virus is less sensitive to BAF antiviral activity than the ΔB1 virus correlating with altered BAF regulation.

The vaccinia virus B1 kinase regulates the antiviral protein BAF via phosphorylation of its N-terminus, which inactivates BAF binding to dsDNA (98) and repression of vaccinia virus DNA replication (69). To investigate whether a link exists between BAF and the rescued growth phenotype of ΔB1mutB12, we measured both phosphorylated BAF levels during ΔB1mutB12 infection and DNA replication of the ΔB1mutB12 virus in cells overexpressing BAF. First for immunoblot analysis of BAF,

CV1 cells were infected with WT, ΔB1, and ΔB1mutB12 viruses at a MOI of 10. Infected cells were harvested at 6h post infection along with an uninfected control sample, lysed in the presence of phosphatase and protease inhibitors and subjected to immunoblot analysis. BAF specific antibodies recognizing either total BAF (phospho-BAF upper band and unphosphorylated BAF lower band) or only phosphorylated BAF were used to detect protein levels under each condition. The total BAF levels were similar between uninfected and each infected sample in multiple experiments (Fig 6.4A, top row). Regarding phosphorylated BAF levels, lysates from WT infected cells contained increased levels of modified BAF as compared to the uninfected control (Fig 6.4A, αPhospho BAF, compare lanes 1 and 2). In contrast, the ΔB1 infected cells show a consistent reduction in phospho-BAF levels as compared to both uninfected and WT infected cells (Fig 6.4A, αPhospho BAF, compare lane 3 with lanes 1 and 2). Surprisingly, the ΔB1mutB12-A1 and ΔB1mutB12-A3 viruses had phospho-BAF amounts that were repeatedly higher than the ΔB1 infected cells (Fig 6.4A, αPhospho BAF, compare lanes 4 and 5 with lane 3), but not to the same level as those in WT infected lysates. Consistent with this representative immunoblot, infection with ΔB1mutB12-A1 or ΔB1mutB12-A3 virus clearly correlates with elevated phosphorylated BAF as compared to ΔB1 infected cells in multiple biological replicates (Fig 6.4B-E). This suggests that the absence of a functional B12 protein during ΔB1 infection correlates with increased BAF phosphorylation and consequently may affect BAF's antiviral activity.

The intermediate level of BAF modification in ΔB1mutB12 lysates compared to WT and ΔB1 infected lysates may impact BAF's capacity to block viral DNA replication.

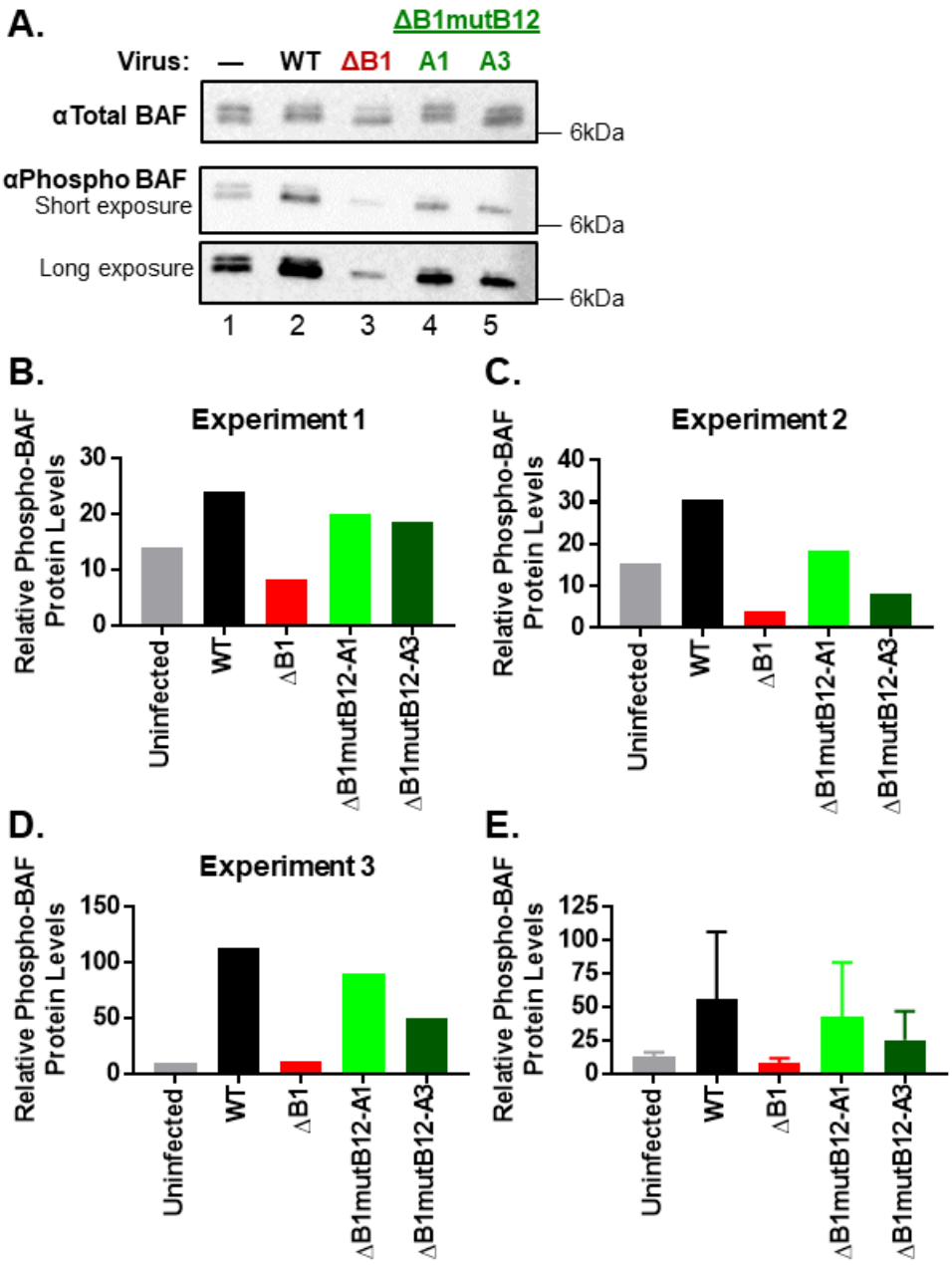
A.
ΔB1mutB12
Virus: — WT ΔB1 A1 A3
αTotal BAF
6kDa
αPhospho BAF
Short exposure
6kDa
Long exposure
6kDa
1 2 3 4 5
B.
Experiment 1
Relative Phospho-BAF Protein Levels
30
20
10
0
Uninfected
WT
ΔB1
ΔB1mutB12-A1
ΔB1mutB12-A3
C.
Experiment 2
Relative Phospho-BAF Protein Levels
40
30
20
10
0
Uninfected
WT
ΔB1
ΔB1mutB12-A1
ΔB1mutB12-A3
D.
Experiment 3
Relative Phospho-BAF Protein Levels
150
100
50
0
Uninfected
WT
ΔB1
ΔB1mutB12-A1
ΔB1mutB12-A3
E.
Relative Phospho-BAF Protein Levels
125
100
75
50
25
0
Uninfected
WT
ΔB1
ΔB1mutB12-A1
ΔB1mutB12-A3

Fig 6.4. ΔB1mutB12 virus infection enhances BAF phosphorylation as compared to ΔB1 virus infection. (A) Immunoblot analysis of total BAF protein (top panel) or phosphorylated BAF (bottom panel) in CV1 cells uninfected or infected with WT, ΔB1, ΔB1mutB12-A1, or ΔB1mutB12-A3 at a MOI of 10. Cells were collected at 6h post infection. (B) Immunoblot analysis in three biological replicates were used to quantify total BAF protein and phosphorylated BAF in CV1 cells uninfected (grey) or infected with WT (black), ΔB1 (red), ΔB1mutB12-A1 (light green), or ΔB1mutB12-A3 (dark green). Protein levels were determined by chemiluminescence quantification using ImageLab on chemidoc images and raw values were used to calculate phospho-BAF over total BAF levels for biological replicate experiment 1, experiment 2 (C), and experiment 3 (D). (E) The phospho-BAF levels relative to total BAF levels were averaged for all three experiments.

If true, one would predict that the ΔB1mutB12 virus may remain sensitive to BAF levels, but to a lesser degree than the ΔB1 virus. To test this model, cells stably overexpressing 3XFlag-tagged BAF protein (~10-12 fold increased BAF protein as compared to endogenous BAF levels) or control cells were infected with WT, ΔB1, or ΔB1mutB12-A3 virus at a MOI of 3 and levels of DNA accumulation measured. The DNA accumulation for WT, ΔB1, and ΔB1mutB12-A3 infected cells was reduced by 1.3-fold, 26-fold, and 7.5-fold respectively in Flag-BAF cells as compared to control CV1 cells (Fig 6.5A). This data demonstrates a significant attenuation of both ΔB1 and ΔB1mutB12 DNA accumulation, but not WT virus, when BAF levels are increased. Furthermore, the viral yield of WT, ΔB1, and ΔB1mutB12-A3 viruses were 5.8-fold, >51-fold and >10-

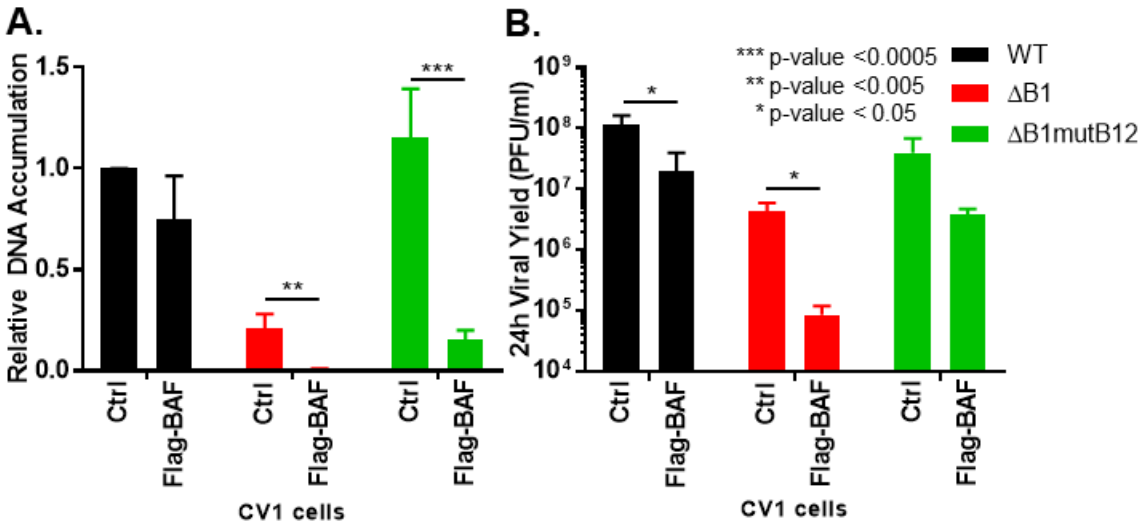

Fig 6.5. The ΔB1mutB12 virus restriction of BAF antiviral activity is greater than the ΔB1 virus. (A) Control or CV1 cells expressing 3XFlag-tagged BAF in excess were infected with WT (black), ΔB1 (red), or ΔB1mutB12 (green) at a MOI of 3 and harvested at 24h post infection for analysis of relative DNA accumulation or (B) viral yield titration on CV1-B1myc cells.

fold reduced in Flag-BAF cells than control CV1 cells (Fig 6.5B). It is interesting to note that in the presence of increased BAF, the ΔB1mutB12 DNA accumulation and viral yield levels are 19-fold and 45-fold higher respectively than the ΔB1 virus (Figs 6.5A and B, compare green bars to red bars from cells expressing Flag-BAF). Combined, these assays demonstrate a correlation between loss of B12 function and increased phosphorylated BAF levels, and support the conclusion that ΔB1mutB12 virus represents an intermediate sensitivity to BAF's antiviral activity as compared to the ΔB1 and WT viruses.

6.4. B12-mediated regulation of BAF phosphorylation activity is through an indirect mechanism.

The B12 protein is known to be catalytically inactive (112). Therefore, mediation of BAF phosphorylation levels may occur through a direct binding and sequestering from a host kinase or through indirect regulation of a kinase or pseudokinase to act on the BAF protein. In order to dissect a direct versus an indirect mechanism of B12-mediated regulation of BAF phosphorylation levels, we tested B12 interaction with BAF in two different assays. To begin, we used immunoprecipitation of αHA in HA-B12 expressing cells and immunoblot of endogenous or FLAG-tagged BAF. From this assay we did not show a significant enrichment of BAF bound to HA-B12 as compared to background binding to HA conjugated beads incubated with FLAG-BAF cell lysate (data not shown). For the reciprocal αFLAG immunoprecipitation, no HA-B12 was detected (data not shown). Under these lysis conditions, a B12-BAF interaction is not strongly supported.

It is possible that the lysis conditions are too stringent to preserve the interaction between B12 and BAF. Therefore, we postulated that if BAF interaction with B12

tethered the pseudokinase to the nucleus we could observed a requirement of BAF for B12 nuclear retention. To test this theory, we stably depleted BAF to ~14% endogenous BAF levels using a lentiviral system packaging a shRNA for a non-specific/Ctrl target or BAF targeted depletion (Fig 6.6A). CV1-shCtrl and –shBAF cells were transfected with HA-B12 *in vitro* synthesized mRNA and either fixed at 24h post transfection (Fig 6.6B) or permeabilized first followed by fixing of cells (Fig 6.6C) and immunofluorescence analysis. Consistent with the tethered phenotype of B12 localization even following pre-permeabilization (Fig 6.2A and B), both CV1-shCtrl (Fig 6.6B) and CV1-shBAF (Fig 6.6C) cells retained nuclear B12 following pre-permeabilization. Therefore, under conditions in which B12 is retained in the nucleus due to a predicted interaction with a host factor, depletion of BAF does not impact B12 nuclear retention. The immunoprecipitation and immunofluorescence data do not support a B12-BAF interaction.

6.5. B12 localizes to the chromatin during mitosis.

We have now shown that B12 regulates BAF phosphorylation, likely through an indirect mechanism. The nuclear localized BAF is diffuse in non-dividing cells and interacts with inner nuclear membrane proteins and DNA during mitosis (89, 152, 153). In order to understand the role of B12-mediated regulation of BAF we asked if B12 expression could modulate nuclear inner membrane proteins and if B12, similar to BAF, localized to the chromatin in dividing cells. First, to determine the impact of HA-B12 expression on the integrity of the nuclear membrane, we used immunofluorescence analysis of emerin nuclear membrane protein and the nuclear pore complex proteins which are imbedded in the nuclear membrane. CV1 cells were transfected with either

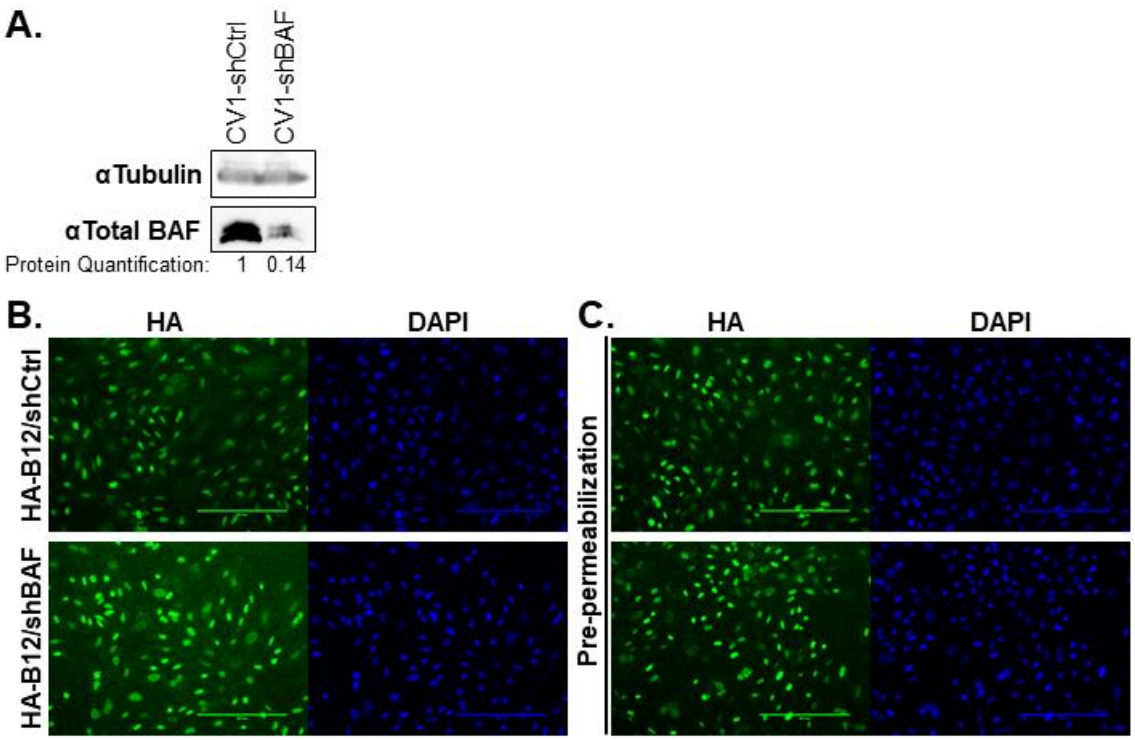

Fig 6.6. B12 nuclear localization is not disrupted by BAF depletion. (A) CV1 cells were transduced with shCtrl or BAF for stable depletion and harvested for immunoblot analysis of tubulin and total BAF. (B) CV1 control or shBAF transduced cells transfected with no mRNA or HA-B12 (GenScript) mRNA. Cells were either fixed then permeabilized to detect HA-tagged proteins or (C) prepermeabilized, fixed and then permeabilized again for detection of HA-tagged proteins remaining in cells following washes to remove unbound protein. The DAPI nuclear stain (blue) and αHA antibody (green) for detection of HA-B12 were used.

HA-GFP or HA-B12 mRNA. 24h post transfection the cells were fixed, permeabilized and incubated with HA, emerin, and nuclear pore complex (NPC) primary antibodies and corresponding secondary antibodies. The HA antibody has low background in the control well where no mRNA was added, diffuse HA-GFP detection throughout the cells, and nuclear localization of HA-B12 (Fig 6.7A, left panels). Both emerin and NPC were unaltered by HA-GFP or HA-B12 expression and remained localized to the nuclear membrane and nuclear space in all conditions (Fig 6.7A, middle and right panels). Therefore, the expression of HA-B12 in cells does not disrupt the nuclear membrane shape or integrity of cells not going through mitosis. Next, we asked if B12 localized to the chromatin during mitosis as we have shown diffuse localization in non-dividing cells. For this immunofluorescence assay, CV1 cells were transfected with HA-B12 mRNA and fixed 24h post transfection. DAPI nuclear stain and HA primary antibodies were used to visualize DNA and HA-B12 respectively. Control cells not expressing HA-B12 had very low background when incubated with the HA primary antibody and corresponding fluorescent secondary antibody (data not shown). During prophase, HA-B12 is diffuse within the nucleus corresponding to the DAPI stain (Fig 6.7B, Prophase). The nuclear envelop disassembles at the end of prophase, yet HA-B12 maintains colocalization with the chromatin from prometaphase to telophase (Fig 6.7B). BAF has been shown to localize to the chromatin during late anaphase and telophase to contribute to the exit of mitosis and reformation of the nuclear envelop (89, 94, 154). Interestingly, we did not observe dysregulation of emerin localization during telophase (Fig 6.7C), which we would expect if BAF interaction with emerin was disrupted. Nonetheless, obtaining higher resolution images may be required to confirm that emerin disruption is not

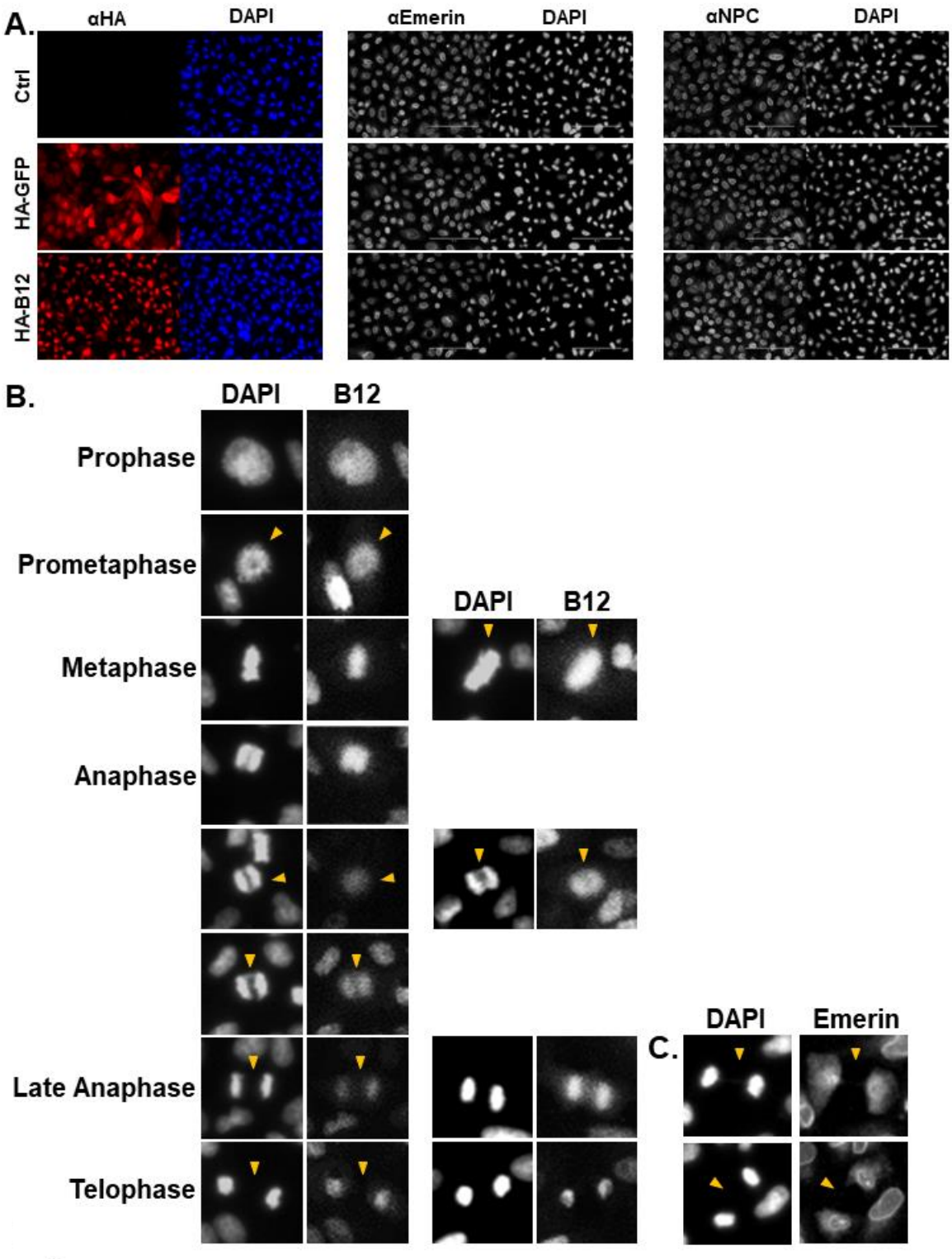
A.
αHA
DAPI
αEmerin
DAPI
αNPC
DAPI
Ctrl
HA-GFP
HA-B12
B.
DAPI
B12
Prophase
Prometaphase
Metaphase
Anaphase
Late Anaphase
Telophase
DAPI
B12
C.
DAPI
Emerin

Fig 6.7. B12 is constitutively colocalized to cellular chromatin during mitosis. (A) CV1 cells were transfected with no mRNA, HA-GFP mRNA, or HA-B12 (GenScript) mRNA and fixed for immunofluorescence analysis of HA (red), emerin, nuclear pore complex (NPC), and DAPI (blue). (B) HA-B12 mRNA transfected CV1 cells were fixed for immunofluorescence analysis of nucleic acid stain DAPI (left column) and HA (right column) of HA-B12 protein throughout mitosis, or (C) emerin during late anaphase and telophase. Yellow arrowheads indicate the cell corresponding to the listed cell division stage. Mitotic cells were manually selected from wide field images containing many cells.

occurring in B12 expressing cells. Therefore, the B12-mediated regulation of BAF phosphorylation levels may result in BAF retention on the chromosomes as observed during VRK1 depletion (94). Further characterization of B12 impact on inner nuclear membrane proteins is needed, preferably using high resolution imaging of protein localization throughout mitosis and telophase.

6.6. B12 pseudokinase interacts with host VRK1.

In order to provide insight into potential cellular proteins interacting with B12 in the nucleus we decided to optimize for HA-tagged B12 immunoprecipitation during infection coupled with mass spectrometry analysis of B12-bound proteins. In an effort to increase HA-B12 expression in infected cells we chose to use the WT/HA-B12 recombinant virus which expresses HA-B12 under an early/late, inducible promoter (Fig 6.1C). First, we wanted to determine the relative levels of B12 proteins expressed by the WT/HA-B12 recombinant virus as compared to the WT virus and from the WT/HA-B12

virus utilizing doxycycline to induce higher expression B12 levels. Many early vaccinia proteins are expressed at low levels and antibodies specific to these viral proteins are not sensitive enough to detect the protein at such low abundances. For this reason, we used whole cell proteomics to determine relative B12 quantities for WT, WT/HA-B12, and WT/HA-B12 with doxycycline at 7h post infection. CV1 cells were infected with virus at a MOI of 10, harvested using RIPA buffer, and subjected to whole cell mass spectrometry. WT/HA-B12 recombinant virus expressed B12 at levels 3.4-fold more abundance than WT levels (Fig 6.8A). Addition of doxycycline during WT/HA-B12 infection increased B12 levels by 18-fold as compared to WT infection with doxycycline treatment and 4-fold as compared to WT/HA-B12 without doxycycline (Fig 6.8A).

Using this inducible, WT/HA-B12 recombinant virus for increased expression of the HA-B12 protein during infection, we asked if immunoprecipitation of B12 pulled down any unique bands. CV1 cells were infected with WT, WT/HA-B12 or WT/HA-B12 with 50ng/ml doxycycline treatment at a MOI of 5 and harvested at 7h post infection. The 7h time point was selected to correspond with the start of peak vaccinia DNA replication. This experiment was carried out in duplicate with one set of samples being used for a silver stain of total protein bound to the immunoprecipitated HA-B12 and the other set of samples for an immunoblot. The silver stain of the WT, WT/HA-B12 and WT/HA-B12 plus doxycycline treatment eluent samples showed a unique ~50kDa band for the WT/HA-B12 viruses with and without doxycycline treatment that was not in the WT sample. Intriguingly, the host VRK1 protein is 50kDa in size and localizes to the nuclear compartment. Therefore, in addition to assaying for the HA-B12 protein in the immunoblot we also assayed for VRK1 protein. Similar to the whole cell proteomics

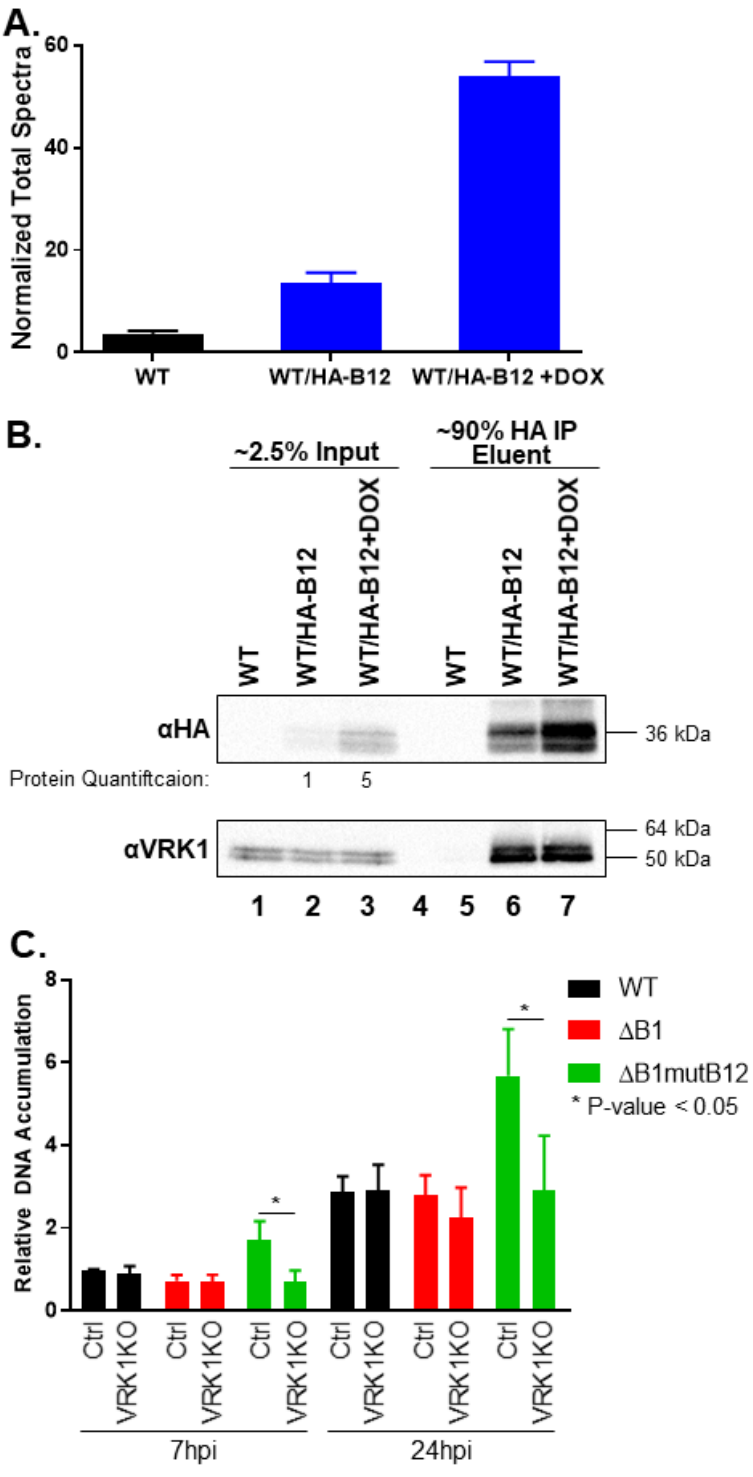
A.
Normalized Total Spectra
60
40
20
0
WT
WT/HA-B12
WT/HA-B12 +DOX
B.
~2.5% Input
~90% HA IP Eluent
WT
WT/HA-B12
WT/HA-B12+DOX
WT
WT/HA-B12
WT/HA-B12+DOX
αHA
36 kDa
Protein Quantiftcaion:
1
5
αVRK1
64 kDa
50 kDa
1 2 3 4 5 6 7
C.
Relative DNA Accumulation
8
6
4
2
0
WT
ΔB1
ΔB1mutB12
* P-value < 0.05
*
*
Ctrl
VRK1KO
7hpi
24hpi

Fig 6.8. B12 immunoprecipitation identified VRK1 interaction and VRK1 is proviral during ΔB1mutB12 infection. (A) CV1 cells were infected with WT (black bar), WT/HA-B12, or WT/HA-B12 with 50ng/ml doxycycline treatment (blue bars). B12 normalized total spectra were graphed. (B) Cells were also harvested for immunoprecipitation of HA-B12 and immunoblot of HA for HA-B12 or cellular VRK1. (C) HAP1 control or VRK1 knockout cells were infected with WT (black), ΔB1 (red), or ΔB1mutB12 (green) at MOI of 3 and harvested 24h post infection for DNA accumulation quantification.

data, the input HA-B12 protein levels are 5-fold higher in doxycycline treated cells infected with WT/HA-B12 than untreated cells (Fig 6.8B, compare αHA lanes 2 and 3). Slightly greater HA-B12 protein levels are immunoprecipitated from WT/HA-B12 with doxycycline lysates than without doxycycline treatment (Fig 6.8B, compare lanes 6 and 7). Protein levels of cellular VRK1 are similar for infected cells for input samples (Fig 6.8B, αVRK1 lanes 1-3). Enrichment of VRK1 protein was detected only in HA-B12 protein containing lysates and not for the WT infected control lysates, indicating a B12-VRK1 interaction (Fig 6.8B, compare lanes 6 and 7 to lane 5). Importantly, this interaction can be detected from lysates during WT/HA-B12 infection without doxycycline.

6.7. VRK1 has pro-viral activity in the absence of the B1 kinase and B12 pseudokinase.

With the discovery of a nuclear factor that interacts with the viral B12 pseudokinase, we asked if the function of VRK1 is upstream or downstream of B12

signaling to repress vaccinia DNA replication. We hypothesized that if the rescued DNA replication and viral yield of the ΔB1mutB12 virus was VRK1 dependent then we would observe a reduction in viral growth in VRK1 knockout cells. On the opposing side, if VRK1 participated in a function upstream of B12 repressive activity, then we would predict reduced viral DNA replication for the ΔB1 virus and not for the ΔB1mutB12 virus in the absence of VRK1. To test these hypotheses, we carried out a one-step viral yield assay in HAP1 control and VRK1KO cells during WT, ΔB1 or ΔB1mutB12 infection at a MOI of 3. Cells were harvested 24h post infection. Neither WT nor ΔB1mutB12 viral DNA accumulation was affected by VRK1 absence at 7 and 24h post infection (Fig 6.8C). Intriguingly, the ΔB1mutB12 virus had ~2-fold lower relative DNA accumulation in VRK1 knockout cells than in control cells at both 7 and 24h time points (Fig 6.8C). This data supports VRK1 working downstream of B12, mediating a pro-viral function in the absence of both the viral B1 kinase and B12 pseudokinase.

6.8. Chapter 6 Summary

These data summarized in this chapter addressed questions pertaining to B12 molecular mechanism in both infected and uninfected cells. In brief, we discovered B12 localizes predominantly to the nucleus of infected and uninfected cells (Fig 6.1). This nuclear presence is due to a tight interaction with a nuclear factor, likely distinct from a direct B12-DNA interaction (Fig 6.2) and B12 nuclear localization is likely necessary for its repressive function (Fig 6.3). An intriguingly observation that links B12 to the antiviral protein BAF was the correlation between the presence of the wild-type B12 protein and reduced phosphorylated BAF levels (Fig 6.4). The B12 protein seems to move between a diffuse nuclear localization in non-dividing cells and localize constitutively to the

chromatin throughout mitosis (Fig 6.7). Furthermore, we identified a B12-VRK1 interaction and determined that the rescue of the ΔB1mutB12 virus is dependent on VRK1 in the HAP1 cells (Fig 6.8). Together, this chapter of data contributes the discovery of an indirect, B12-mediated restriction of BAF phosphorylation. In our model of BAF antiviral effect on vaccinia DNA replication, more dephosphorylated BAF would increase BAF antiviral activity (Fig 6.9). Additionally, VRK1 is also a part of B12 mediated regulation of vaccinia DNA replication (Fig 6.9). Although, VRK1 seems to play a proviral function in the absence of B1 and B12.

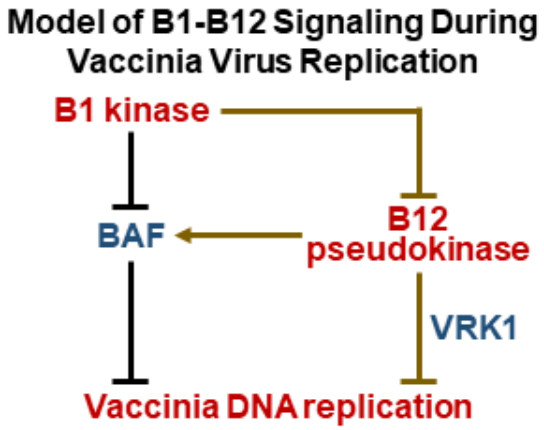

Fig 6.9. Working model of B1/B12/BAF signaling during vaccinia infection. The B1 kinase participates in restriction of BAF's antiviral function against vaccinia DNA replication in the cytoplasm, while also repressing B12 negative regulation of vaccinia DNA replication through an unknown mechanism that is partly mediated via BAF regulation. Direct interactions and/or signaling through additional factors may be required for B1-B12 signaling and B12-BAF signaling, and are depicted using gold lines. B1-BAF interaction and BAF binding to dsDNA are direct interactions and denoted in black lines. VRK1 contributes to a proviral function that is restricted by the B12 pseudokinase.

CHAPTER 7

DISCUSSION

The sequence identity between the poxvirus B1 protein and the eukaryotic VRKs is striking; approaching 40% within their respective catalytic domains (72). While genes encoding protein kinases are present in other DNA viruses (65), none exhibit this level of sequence identity to any host kinase. Viral mimicry of host signaling components is often an indication of which cellular pathways are manipulated during the course of infection. Thus, our working hypothesis is that B1 and VRKs share substrates important to poxviral replication. This avenue of study has been fruitful in the past, leading to the identification of BAF as a target of both VRKs and B1 (98) and revealing a novel function for BAF in antiviral defense (69). In chapters 3 and 4, we characterize a B1-expressing cell line and B1-deletion virus, which provide new insights into the function and regulation of this critical viral protein. We then explore the impact of B1 deletion on viral DNA replication in various cell types, focusing our efforts on the question of whether the cellular VRK proteins can complement for the loss of B1 when they are expressed at endogenous levels by the cell.

7.1. The severe replicative deficiency of ΔB1 revealed a BAF-independent function for the B1 kinase.

Previous biochemical and genetic studies of the vaccinia B1 kinase utilizing temperature sensitive viruses uncovered a pivotal role for this protein during genome replication (75). Furthermore, earlier efforts to delete the B1 gene using homologous recombination were unsuccessful (73), indicating that the fitness cost of B1 deletion is severe. In this study, we have revisited the goal of constructing a B1 knockout virus,

relying on a complementing cell line for B1 expression during the isolation of the new virus. The stable expression of B1 in these cells also presented us with an opportunity to characterize B1 in the absence of other viral proteins. We did not observe any difference in growth rate or morphology of cells stably expressing B1, suggesting that expression of this viral kinase is not toxic to CV1 cells. We also found that B1 was present throughout the cytoplasm in uninfected cells, consistent with the fact that it does not possess a sequence predicted to direct localization to the nucleus or other organelles. Interestingly, in infected cells B1 colocalizes with I3, the viral ssDNA binding protein and well-established marker of viral replication factories. This recapitulates previous evidence that B1 is present at viral factories (113); however, as B1 is expressed by the cell in our assay, this new data suggests that B1 is actively recruited to sites of vaccinia DNA replication. If this is indeed the case, we speculate that recruitment is driven by the ability of B1 to interact with another protein, such as the viral H5 protein rather than viral DNA; B1 has been previously demonstrated to interact with H5 in multiple assays (86, 155), but B1 does not have any domains predicted to directly bind to DNA. Recruitment of B1 to viral factories may enhance its ability to phosphorylate important target proteins, such as the fraction of cellular BAF that is nearest to viral DNA and thus the most imminent threat to the virus. Importantly however, we found that BAF phosphorylation increases in B1-expressing cells in a manner independent of infection. This extends previous *in vitro* data indicating that other viral proteins are not needed for B1 phosphorylation of BAF (98), but it remains possible that phosphorylation of other B1 substrates depends more heavily on B1 localization to factories.

Our characterization of the B1 deletion virus included direct comparison with the Cts2 virus in multiple assays. As with Cts2, in CV1 cells the ΔB1 virus exhibits a marked loss in viral progeny and impairment of viral DNA replication, although in both regards the phenotype of the ΔB1 virus was more severe than Cts2. A significant advantage of studying the ΔB1 virus is that the phenotype is also robust at 37˚C, allowing us to examine B1 function in cell types that cannot tolerate higher temperatures needed for the Cts2 phenotype. Depletion of BAF rescued replication of both Cts2 and the ΔB1 viruses, reaffirming the B1-BAF signaling axis; although the increase observed during the ΔB1 infection was notably reduced as compared to Cts2. This observation either demonstrates that BAF remains a potent antiviral even after depletion or suggests that other important B1 signaling pathways are being disrupted in the complete absence of this kinase.

Positing that the ΔB1 virus may exhibit some host tropism, due to either cell type specific complementing kinases or downstream targets, we next examined the ability of this mutant virus to carry out DNA replication and produce new virus in a variety of cell lines. As a result of these studies it was clear that B1 is vital for production of new infectious virus in all cell types. However, in regard to DNA accumulation, the cell lines could be grouped into two categories. In BSC40, CV1, L929, and HeLa cells there was a severe decrease in DNA replication; even when assayed late in infection the viral DNA from a ΔB1 infection was 10% or less of the WT virus. In contrast, in HAP1 and A549 cells gross DNA accumulation was slower than WT, but was significant and by 24hr approached WT levels.

Together, chapter 3 data emphasizes the importance of utilizing both temperature sensitive mutant viruses, such as Cts2, and single gene deletion viruses, ΔB1, in order to provide insight into protein function. Herein, we added evidence to support a BAF-independent function of the B1 kinase to promote vaccinia DNA replication (Fig 3.6).

7.2. B1 is a viral mimic of host VRK2 as shown by partial complementation of B1 function by endogenously expressed VRK2.

The B1 kinase was shown to have a promiscuous phosphorylation activity *in vitro*, which was in contrast to its cellular homolog VRK1 (98). To understand how B1 expression in cells changes the cellular environment to promote vaccinia replication upon infection, we postulated that transcriptome analysis of B1 expressing cells would reveal insights into which cellular pathways B1 modulates. Not surprisingly, B1 expression in cells downregulated transcription of genes involved in immune and stress responses (Fig 7.1).

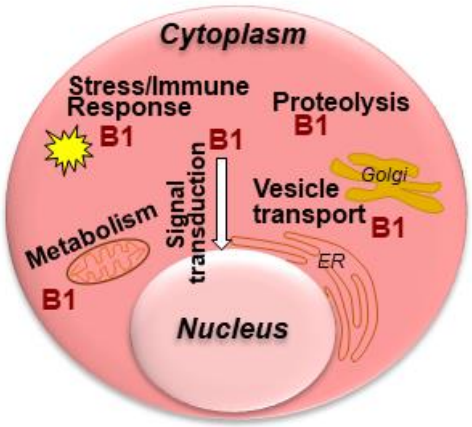

Fig 7.1. Biological processes transcriptionally regulated by B1 expression. B1 expression in cells transcriptionally regulates stress/immune response, metabolism, signal transduction, proteolysis, and vesicle transport in uninfected cells.

An interesting finding from this data was B1 association with modulation of transport signaling of the endoplasmic reticulum (ER) and Golgi apparatus (Fig 7.1).

Vaccinia replication factories are thought to form near ER membranes, and utilize the membrane to partition the replication factory environment from the cytoplasm (156, 157). Furthermore, envelopment of mature virions following morphogenesis contains membranes originating from endosomes (158) or the trans Golgi organelle (29, 30) and utilizes retrograde transport from the early endosomes to the trans Golgi network for membrane wrapping (159). Therefore, a role of B1 to support replication and envelopment of the virus by modulating trafficking of proteins and vesicles is an intriguing idea. From the analysis of changes in specific gene expression profiles, we identified a role for B1 to upregulate expression of the sperm acrosome associated 6 gene, which is shown to be important for fusion of sperm with an egg during fertilization (136). It is possible that vaccinia virus utilities this same protein to facilitate envelopment of the mature virion or for budding from the cell. However, confirmation of transcriptional regulation during infection is required before addressing questions of possible utility by the virus during replication.

As referenced above, we characterized in chapter 4 a moderate replicative defect of ΔB1 in HAP1 and A549 cell lines. To address the question of viral mimicry of host kinases, we next hypothesized that cellular VRK activity may allow for genome replication in HAP1 and A549 cell lines. To test this theory, we acquired HAP1 cell lines altered at either the *VRK1* or *VRK2* gene using CRISPR/Cas9 mediated gene editing. Immunoblot analysis using antibodies specific for each VRK failed to detect VRK1 or VRK2 in the cell line in which that gene had been edited, thus validating these

as single knockouts for either VRK1 or VRK2. We also monitored the rate of cell growth for both the knockout and control cells and found they were very similar. This was a surprising observation, as previous studies have demonstrated that depletion of VRK1 can severely impair growth of MCF10a and MDA-MB-231 cells, while also causing mitotic defects linked to reduced BAF phosphorylation (94). Indeed, immunoblot of BAF levels present in VRK1KO cells reveal a clear reduction in the slower migrating phosphorylated form of BAF as compared to control HAP1 cell, consistent with a decrease in BAF phosphorylation in these cells. Future investigation will be needed to determine why HAP1 cells tolerate the loss of VRK1 during mitosis. Possible mechanisms include the activity of VRK2 or other kinases in the cell, which may substitute for VRK1 in these cells.

Using these HAP1 cell lines, we next compared relative DNA accumulation, protein expression and productive viral yield during infection with the WT and ΔB1 viruses. These studies indicated that loss of VRK1 in HAP1 cells has no effect on the WT virus and only a minimal impact during ΔB1 infection. In comparison, loss of VRK2 had no significant effect during WT infection, but had a striking effect on the ΔB1 life cycle. Specifically, while early gene expression in ΔB1 infected cells is unchanged, no DNA accumulation nor late gene expression is observed in VRK2KO cells. This robust block in DNA replication culminates in an additional 10-fold inhibition of virus production as compared to the ΔB1 infected HAP1 control cells. Importantly, VRK2 depletion in A549 cells also decreases ΔB1 DNA replication and viral yield while having no impact on WT infection, which supports the model that VRK2 functionally overlaps with B1 in these cell lines.

The seminal observation made by Boyle and Traktman that VRK1 can rescue Cts2 replication if expressed from the viral genome laid the groundwork for the discovery of BAF phosphorylation, which is now understood to be a regulator of that protein's antiviral defense and mitotic function. Interestingly, here we show that loss of VRK2 does not result in a discernable change in BAF phosphorylation in HAP1 cells and BAF depletion has only a very modest effect on DNA replication in ΔB1 infected VRK2KO cells. Together, these data are consistent with the working model depicted in Fig 4.8D). We suggest that VRK2 complements for the loss of B1 via a novel mechanism, likely involving phosphorylation of an important substrate other than BAF. While previous studies from our lab indicate that B1 is needed for a step late in the viral life cycle in U2OS cells (77), the data presented here provide a clear indication that B1 is needed at the stage of DNA replication not only to inactivate BAF but also for other reasons in some cells. Furthermore, the functions of B1 cannot be rescued completely by VRKs during vaccinia virus life cycle.

7.3. Experimental evolution of ΔB1 exposed a DNA replication restrictive function for proposed non-functional vaccinia B12 pseudokinase.

A growing body of evidence indicates that vaccinia kinases modulate multiple signaling pathways, although which of these are consequential for viral fitness is less well understood (160-165). A primary function of B1 is to inactivate the host defense activity of BAF and allow DNA replication to proceed (69). Notably, in chapter 3 we describe an incomplete rescue of a B1 deletion virus following shRNA-mediated depletion of BAF, suggesting that additional important functions for B1 exist. To expand our current understanding of B1 driven signaling we subjected the B1 deletion virus to experimental

evolution. When coupled with whole genome sequencing, this allowed us to identify a vaccinia mutation correlating with marked suppression of the fitness defect caused by the deletion of the *B1R* gene. Experiments using this approach to investigate mechanisms of poxvirus adaption after deletion of other genes have been performed previously, revealing that these pathogens can undergo rapid genetic expansions to form an 'accordion' of copies of a compensating gene to enhance virus production (11, 12). Other adaptation studies have demonstrated that alterations in a small number of amino acids may be sufficient to detectably compensate for the loss of a gene (10, 166). In contrast to these examples exploiting gain of function mutations to improve the fitness of a mutant virus, the data presented here indicate that a divergent mechanism involving the rapid disruption of a suppressor gene, *B12R*, is sufficient for enhancement of ΔB1 virus replication.

The initial evidence of a link between B1 and the mutation of *B12R* was quite compelling, as greater than 48% of the read counts included an indel at the identical nucleotide site in two independently adapted ΔB1 viruses. The evidence that B12 mutation is linked to viral adaptation was further supported through targeted Sanger sequencing of DNA isolated from individual plaques from all three adapted viral stocks. A fascinating aspect of the major indel mutation is its location in a homopolymeric run of eight adenines. Indeed, each of the less prevalent indel sites mapped via Sanger sequencing was also within a homopolymeric run of 4-5 nucleotides. Such sites of repeated sequence may cause polymerase stuttering and favor indel introduction, perhaps contributing to how quickly the virus was able to adapt in our assay (167-170). Thus, independent of our goal to discover novel interactions between B1 and other vaccinia

A.

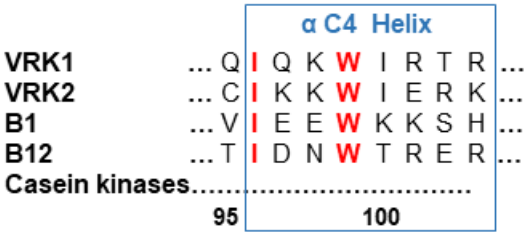

B.

Kinase Name	Amino acid length	Identity to B12
B12 Ser/thr kinase Vaccinia virus	283	--
B1 Ser/thr kinase Vaccinia virus	300	36%
VRK1 Ser/thr kinase Homo sapiens	396	32%
VRK2 Ser/thr kinase Homo sapiens	508	29%
VRK3 Pseudokinase Homo sapiens	473	28%
Casein kinase Pandoravirus salinus	371	27%
Casein kinase 1 γ 2 Homo sapiens	415	27%

Fig 7.2. Vaccinia B12 pseudokinase has homology to vaccinia B1 kinase and cellular vaccinia-related kinases. (A) Vaccinia B1, B12, VRK1, and VRK2 proteins have a conserved αC4 helix, which distinguishes these proteins from related casein kinases. (B) Amino acid length and sequence identity of B1, VRKs and casein kinases as compared to vaccinia B12 pseudokinase.

genes, this study is insightful as an experimental model of reductive evolution during poxvirus adaptation. Indeed, rigorous sequence comparisons of gene maps within members of the Orthopoxvirus genus have led to the theory that gene loss has played a defining role in adapting family members to specific hosts (9). Notably, these bioinformatics analyses predicted that indels introduced at simple sequence repeats within viral ORFs are likely a common molecular mechanism for gene fragmentation (9). Our data now provide strong experimental evidence that indel introduction can indeed occur rapidly at homopolymeric sequence repeats during viral replication, causing gene loss. Of further significance, it is clear that reductive evolution can lead to substantial fitness gains for these pathogens and may be a stronger selective pressure on viruses than previously appreciated.

Upon discovering the frame-shifting indel present within the *B12R* gene we compared the amino acid sequence identity with other casein kinases, including a small group that contained a unique αC4 helix (Fig 7.2A). Similar to previous comparisons, the vaccinia B12 is most similar to vaccinia B1, yet also exhibits 32% shared identity with the cellular VRK1 (Fig 7.2B). As stated before, B12 is a catalytic-null protein (114). Specifically, the three critical domains required for phosphotranserase activity form a catalytic pocket as highlighted in yellow on the VRK1 crystal structure (Fig 7.3A). Both B1 and VRK1 have these domains required for ATP binding, phosphotransfer, and catalysis conserved (Fig 7.3B). However, B12 is missing or has amino acid changes at each of these specified domains (Fig 7.3B). Therefore, it is unlikely that B12 is complementing the absence of B1 via a canonical phosphotransferase mechanism. Thus

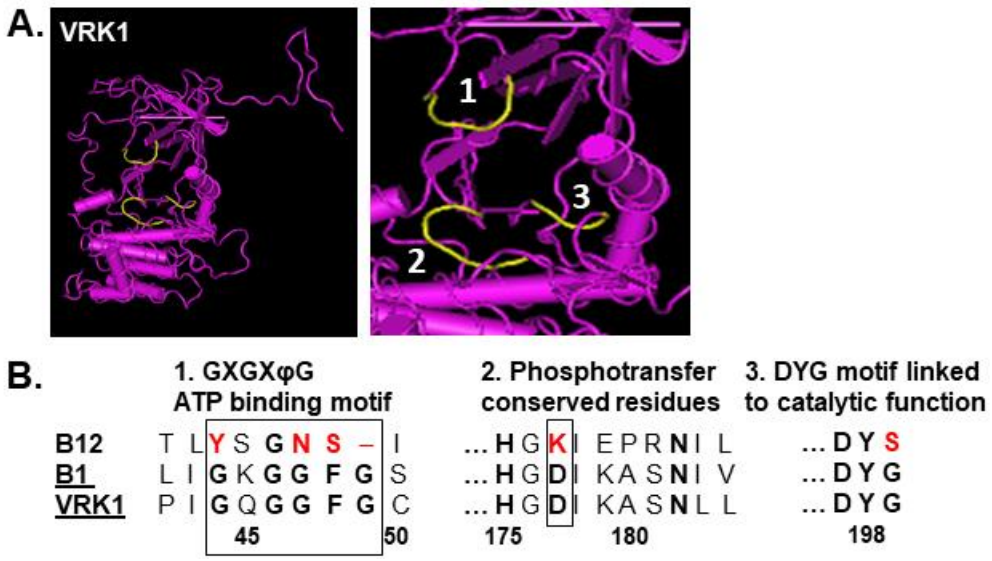

Fig 7.3. Domains required for B1 and VRK1 catalytic activity are missing in the B12 amino acid sequence. (A) The crystal structure of VRK1 with highlighted domains required for catalysis (1-3) the kinase pocket. (B) Amino acid residues required for catalytic activity are present in B1 and VRK1, but absent from B12 sequence.

speculated that a non-canonical mechanism of phosphotransferase activity could be enhanced by the indel mutation observed in the adapted virus *B12R.*

Alternatively, a loss of function could also result from the frameshift induced by the indel within *B12R.* To support this hypothesis, VRK1 truncation studies determined that removal of the most C-terminal alpha helix results in an insoluble protein when expressed in *E. coli* (145), which is highlight in blue (Fig 7.4A, VRK1). Using a modeling website, we constructed the predicted three-dimensional structure of vaccinia B1 and B12 in order to map the adenine indel (red) and SNP (pink) onto the B12 protein with reference to the C-terminal αhelix (blue) in figure 7.4A and B. These models illustrate a further truncation of the B12 protein beyond the C-terminal alpha helix, suggesting if B12 has similar structural requirements as VRK1 we could expect this protein to be unfolded. Furthermore, the SNP is located in a loop structure, known to have increased flexibility than structured beta sheets and alpha helices. It is possible that this mutation affects the nearby alpha helix, however functional studies are required to make this conclusion. With these two possible outcomes in mind, we were curious to learn how the adapted virus mutations altered B12 protein function.

We posited that the truncation of B12 may enhance viral fitness either via a loss of B12 function or a gain of function, the latter scenario possible if the truncation removed a theoretical autoinhibitory domain from the protein. Experiments employing siRNA to deplete B12 led to three important observations, allowing these two possibilities to be distinguished. First, in the presence of siB12, the replication of ΔB1 virus DNA and yield of progeny virus increased to levels very similar to that observed with the adapted ΔB1mutB12 virus in most cell lines tested. This outcome supports the

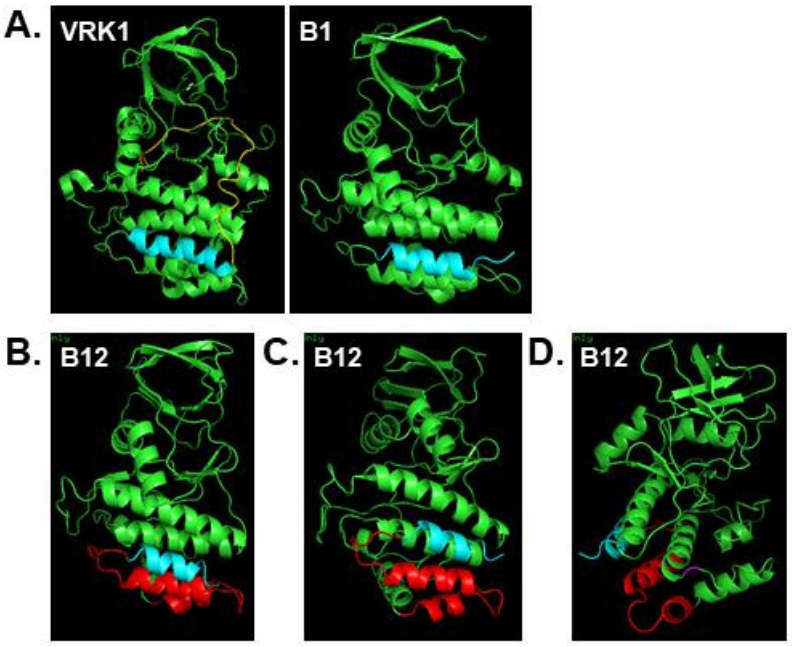

Fig 7.4. B12 predicted three-dimensional structure. (A) Crystal structure of VRK1 with highlighted helix (blue) corresponding to the truncated, insoluble protein and predicted vaccinia B1 kinase with the same C-terminal helix highlighted as VRK1. (B-D) B12 predicted vaccinia B12 psuedokinase with C-terminal helix highlighted (blue) and helices removed during B12 mutations from ΔB1mutB12 viruses (red). (D) The point mutation in B12 from the ΔB1mutB12 virus is highlighted (pink).

loss of B12 function scenario. Second, while siB12 treatment led to the same decrease in B12 mRNA from the ΔB1 virus and the ΔB1mutB12 virus, there was no reduction in DNA accumulation or viral yield from the ΔB1mutB12 virus with siB12 treatment arguing against a gain of function mutation. Third, while siB12 enhanced the replication of the temperature sensitive Cts2 B1 mutant virus, it did not affect the WT virus or other mutant viruses that exhibited reduced DNA replication at less permissive temperatures because of defects in the vaccinia polymerase or primase/helicase proteins. This third point emphasizes that the repressive function of B12 is controlled by the B1 kinase. Together, these assays demonstrate that loss of B12 can suppress the fitness defects of B1 mutant viruses, but does not enhance replication of viruses containing a wild-type *B1R* gene.

These genetic data are consistent with a model in which the B12 pseudokinase is capable of acting as a repressor of vaccinia replication in a B1-dependent manner. The inference that B12 function is masked by B1 is also consistent with previous single gene knockout studies of B12. Specifically, thorough examination of a virus lacking the majority of the *B12R* gene revealed no detectable change in viral fitness in cell culture or mouse pathology as compared to WT virus controls (114, 115). Those results led to B12 being designated as one of the nonessential genes of vaccinia, which is also supported by the fact that although the *B12R* gene is present in all members of the Orthopoxvirus genus, the closely related taterpoxvirus and variola virus have a nonsense or deletion mutation, respectively, in their B12 homolog (167). However, our studies demonstrate that while nonessential, B12 pseudokinase is not without function. Furthermore, our work adds to a growing body of evidence indicating that poxvirus genes categorized as

nonessential in tissue culture and *in vivo* studies based on single gene deletions should be investigated in multigenic knockout backgrounds, especially if they belong to gene families (171).

7.4. B12 nuclear localization and interactions contribute to the replicative defect of ΔB1.

To understand the possible ramifications of our B1/B12 model we find it informative to draw from virology as well as potentially analogous systems in the broader scientific literature. For example, the signaling relationship exhibited by B1 and B12 demonstrates similarity to features of toxin-antitoxin (TA) systems common in bacteria or poison-antidote modules more recently uncovered in higher organisms (172-180). While TA systems proceed via diverse and often poorly understood molecular mechanisms, they are generally comprised of two genes, one of which is capable of decreasing the overall fitness of the organism and is referred to as the toxin. Critically however, the toxin's repressive activity is inhibited in cells expressing a cognate antitoxin gene product. In some instances, the TA system is regulated by upstream signals that can influence antitoxin stability and/or activity, thus potentially benefiting an organism by slowing its growth in response to stress (172, 173, 175, 181). However, in other examples, TA modules provide little or no known benefit for their host, instead behaving as a type of 'selfish' genetic element, perhaps to ensure their conservation in an organism by addicting the organism to an antidote against the TA encoded 'poison' protein (176, 177, 182). As described herein, some attributes of toxin-antidote genetic elements also apply to the B1 and B12 pair. Consideration of parallels between B1/B12 signaling and TA systems has implications beyond poxviruses; this viral kinase and pseudokinase

exhibit high sequence similarity to a family of mammalian proteins known as the VRKs (vaccinia related kinases) also containing kinase and pseudokinase domains (70, 72, 124). Thus, it is conceivable that the mammalian VRK family members and possibly some of the other numerous kinase-pseudokinase pairs in nature exhibit features of TA modules as well.

Returning to our data of B12 repressive activity, we have begun to dissect the B12 mechanism of action. Due to the apparent antagonism of B12-mediated repression in the presence of B1, we were interested in examining where B12 localized in cells with respect to the B1 kinase. We hypothesized that B12 may be localized to the cytoplasm where the B1 kinase is found in both uninfected and infected cells (113, 127). However, we were somewhat surprised to find that B12 is found predominately in the cell nucleus, even in cells expressing the B1 kinase in the cytoplasm and in vaccinia infected cells. Solubilization studies suggest that B12 is tethered to an unknown partner protein in the nucleus; it is tempting to hypothesize that identifying this partner may provide a clue as to B12's mechanism of action.

Our data support a nuclear function for B12 to restrict virus DNA replication. However, we were curious if B12 would localize to viral DNA at cytoplasmic replication factories in viruses lacking the B1 kinase. Strikingly, we observed B12 nuclear localization in HA-B12 mRNA transfected cells infected with ΔB1mutB12 virus in conjunction with reduced formation of replication factories. We next hypothesized that if B12 nuclear localization was necessary for its repressor function, we would observe disrupted nuclear localization with the mutant forms of B12 from the adapted ΔB1 viruses. The mutant B12 proteins, B12ΔA690 and B12 G-A, had a diffuse localization in

infected cells. Therefore, all our data to this point indicate an indirect function of B12-mediated restriction of virus DNA replication via mechanisms that initiate in the nucleus.

We can only speculate as to the function of B12 in the nucleus at this time. Other poxviral proteins including C4 (183), C6 (184), C16 (185), B14 (186), K7 (187), N2 (188), F16 (116), and E3 (189) can be detected in the nucleus and have been found to impact innate immune signaling in most cases. However, there is no precedent to date for a nuclear poxviral protein affecting viral DNA replication. Intriguingly, the B12 connection to B1 may also partly incorporate BAF. This B1-regulated antiviral host factor is prevalent in both the nucleus and cytoplasm (Fig 7.5A). For this reason, we investigated how the presence of B12 affects the ability of BAF to act as a host defense against vaccinia. Measurement of phosphorylated BAF levels in infected cells demonstrated that WT virus led to a clear increase in BAF phosphorylation when compared to ΔB1 infected cells, as has been previously published (127). Interestingly, BAF phosphorylation in ΔB1mutB12 infected cells was greater than in ΔB1 infected cells, albeit not to the same levels as during WT virus infection. Parallel studies of viral yield in cells overexpressing BAF demonstrated that inhibition by BAF was strongest on the ΔB1 virus and, while still observed during ΔB1mutB12 infection, BAF affected this adapted virus to a lesser degree. These data suggest a model in which B12 functions via a BAF dependent mechanism, albeit only in part. Specifically, our previously published data that BAF-depletion only modestly rescues the ΔB1 phenotype (127) leads us to propose that B12 is also working through a distinct and BAF-independent pathway (Fig 6.9). It is provocative to consider that this pathway may be executed or triggered by B12 from within the nucleus.

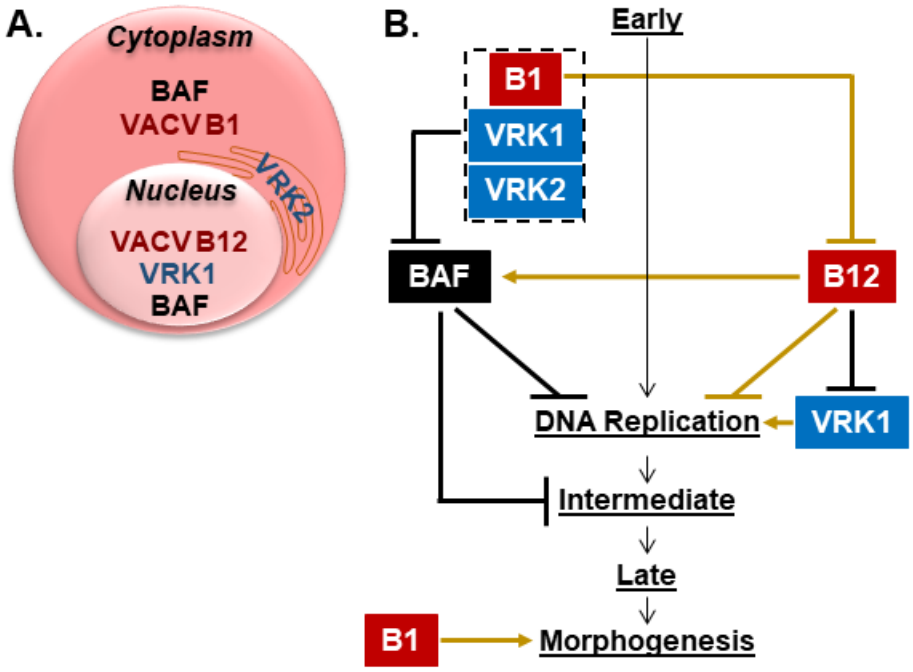

Fig 7.5. Subcellular localization and working signaling model of vaccinia B1 kinase and B12 pseudokinase. (A) The vaccinia virus B1 kinase is predominantly cytoplasmic with BAF and VRK2 bound to the ER membrane. BAF also have a nuclear fraction with cellular VRK1 and vaccinia B12 pseudokinase. (B) Vaccinia proteins (red) and cellular kinases (blue) regulate the host BAF antiviral activity and vaccinia virus DNA replication. B12 repressive function on DNA replication is mediated via a BAF dependent and independent pathway. VRK1 was also shown to promote DNA replication in the absence of the B1 kinase, but is restricted or modulated by the B12 protein.

In order elucidate how B12 regulates BAF phosphorylation levels, we utilized immunoprecipitation of HA-B12 to assay for an interaction between B12 and BAF. We were surprised to observed no enrichment of BAF from HA-B12 eluents as compared to background control. Therefore, our data does not support a direct interaction between B12 and BAF. In cells, BAF is known to play important roles to mediate efficient exit from mitosis and nuclear envelope reformation via interactions with inner nuclear membrane proteins and chromosomes (89, 152, 153). It is possible that B12 regulates BAF indirectly, through modulation of factors that regulate or interact with BAF. For this reason, we chose to ask if B12 expression in cells results in changes to the nuclear membrane structure. No changes were observed. However, BAF also interacts with inner nuclear proteins and chromatin during late anaphase and telophase stages of mitosis. To elucidate at what stage during the cell cycle B12 may impact BAF phosphorylation levels the most we turned to the images of cells going through mitosis. Shockingly B12, despite lacking a DNA binding domain, remains colocalized with the chromatin throughout all of mitosis (Fig. 6.7B). The cellular paralog of B12, VRK1, is known to interact with histones (93) and transcription factors (142, 190-192) on the chromatin but releases from the chromatin during metaphase and anaphase (193). Alternatively, the AURKB is a kinase regulator of mitosis that phosphorylates histone proteins (194). This kinase similarly releases from the chromatin during anaphase of mitosis (193). Intriguingly, BAF is shown to be diffuse and then bind to chromatin during anaphase and telophase (154). The constitutive localization of B12 with the chromatin during mitosis is unclear, and will require further study for functional validation.

As a final step in these current studies to determine a function for the B12 protein, we strove to identify host and viral protein interactors. We were able to identify a strong interaction between B12 and the cellular VRK1 protein during infection (Fig 6.8B). The VRK1 protein is known to phosphorylate BAF in the nucleus to regulate chromatin condensation (89, 94, 98). This kinase is also known to regulate cell division at multiple levels (93, 98, 142, 143), modulate Gogli fragmentation (140), and DNA damage response (190, 195, 196). Furthermore, it is possible that VRK1 modulates B12 as an upstream component of signaling and B12 regulation. Alternatively, VRK1 could participate in a downstream function related to repression of vaccinia virus DNA replication. By using the VRK1 knockout HAP1 cells, we discovered that VRK1 activity contributes to the rescue of the ΔB1mutB12 virus replication. This data supports a function of VRK1 downstream of B12, and suggests that B12 may be restrictive of VRK1 activity which results in virus replicative deficiency in the absence of the B1 kinase. To speculate on the impact of this data, we predict that VRK1 may complement for a B1 function for viral DNA replication. However, the B12 pseudokinase may restrict VRK1 activity in a WT infection to mediate evasion of innate immunity or another yet to be determined function.

7.5. Conclusion

The findings discussed in this PhD dissertation thesis can be summarized into three major discoveries as summarized (Fig 7.5A and B). 1) VRK2 partially complements the function of the vaccinia B1 kinase during infection. 2) The B1 kinase and vaccinia B12 pseudokinase represent a digenic relationship of genetic and functional linkage. 3) The B12 psuedokinase is a negative regulator of vaccinia DNA replication via BAF-

independent and dependent pathways. These discoveries highlight the interconnectedness of the cellular VRKs and the viral kinase/pseudokinase pair, providing insight into viral mimicry and our ongoing question of how poxviruses lacking a B1 protein replicate.

As in the case of the B1-BAF axis where parallel study of VRK1 was insightful, future study of VRK2 and B1 will likely yield clues regarding which other pathways are modulated by the B1 kinase. Published research of VRK2 provides a list of candidate signaling cascades which may be involved. For example, VRK2 has been reported to modulate MAP kinase signaling pathways at the ER, in part via interaction with the KSR scaffolding protein (197, 198). Additionally, VRK2 appears to act as an apoptosis regulator in some studies, inhibiting cell death via interaction with Bcl-xL or by altering BAX gene expression (95). An investigation of these pathways in conjunction with structure / function studies of VRK2 are ongoing in our lab. Yet, the most promising link between VRK2 and B1 seems to be a shared regulation of vaccinia B12. Future studies will shed light on the molecular mechanisms underlying VRK2 and B1 shared functions, providing greater insight into how host and viral signaling converge during poxviral infection.

Our continued study of the vaccinia B1 kinase using the ΔB1 virus has yielded numerous unexpected insights into poxvirus adaptation pathways and signal transduction circuitry. Our results evince that B1 contributes to viral fitness via antagonism of BAF and B12 proteins, and raise new questions regarding the underlying mechanism of action for this pseudokinase and how it is governed by B1. The findings of B12-VRK1 interaction and VRK1 requirement for maintenance of the ΔB1mutB12 rescued phenotype, distinguishes a dependence on VRK1 in the absence of B1 and B12.

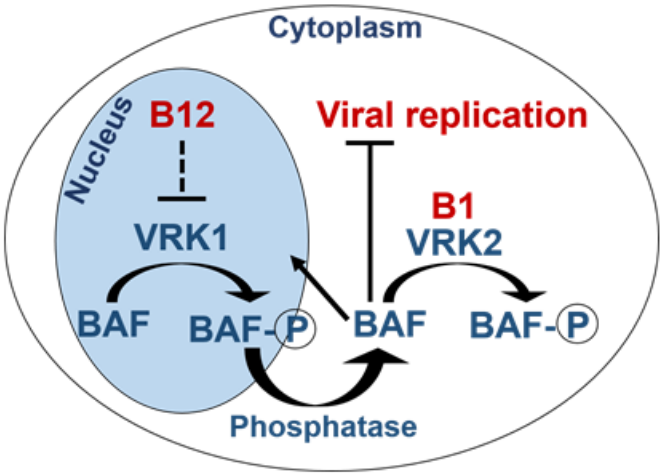

Fig 7.6. Working model of BAF regulation by cellular and viral kinases and pseudokinase. Vaccinia B1 kinase and cellular VRK2 proteins phosphorylate BAF in the cytoplasm to restrict BAF antiviral activity against vaccinia DNA replication. The vaccinia B12 pseudokinase restricts host VRK1-mediated phosphorylation of BAF in the nucleus. VRK1 inhibition retains BAF in the nucleus in an unphosphorylated form that would otherwise traffic to the cytoplasm, dephosphorylated, and mediate antiviral activity against viral DNA.

To speculate briefly, B12 restriction of BAF phosphorylation could occur in order to retain BAF in the nucleus (Fig 7.6). In the absence of B12, VRK1 contributes to the phosphorylation of BAF and BAF cycling between the nucleus and the cytoplasm (Fig 7.6). However, if this model is correct we would expect VRK1 to inhibit vaccinia DNA replication when both B1 and B12 are absent. Specifically, VRK1 phosphorylated BAF would rapidly move from the nucleus to the cytoplasm where it is dephosphorylated and ready to restrict vaccinia replication. Is this model flawed or simply incomplete? It is possible that VRK1 signaling of other pathways buffers the negative impact of BAF antiviral activity. Therefore, manipulation of pathways known to be regulated by VRK1 is of interest to identify which pathways are necessary for ΔB1mutB12 propagation.

Another interesting aspect of this research is the result that B1 requirement is in part to neutralize B12 repressive activity during vaccinia replication. Future investigation of whether the inhibitory action of B12 extends to other poxviruses including those lacking a B1 kinase, and perhaps even other pathogens, will be particularly intriguing. Finally of broader relevance, pseudokinase domains are prevalent in diverse eukaryotic organisms (118, 199), however this is the first example of a function for a viral pseudokinase. The study of B12 pseudokinase and paralog B1 kinase will likely be of broad biological interest.

7.7. Future Directions

We recently discovered that vaccinia encodes a self-repressor, B12 pseudokinase, that modulates host VRK1 to inhibit vaccinia DNA replication. The cellular factor, VRK1, is known to promote proliferation and metastasis of some cancers (139, 200, 201), while mutations or deletions of VRK1 cause microcephaly among other

neurological deficiencies (141, 202, 203) and infertility (88, 92), respectively. We have identified a novel system to study VRK1 roles during vaccinia virus replication by elucidating the mechanism of action for a viral pseudokinase that modulates VRK1 function. At this time, we have not characterized the mechanism of how B12 pseudokinase modulates VRK1 activity to restrict virus DNA replication. However, this gap in knowledge will provide insight not only to viral DNA replication, but also generally to aspects of chromosomal maintenance in proliferating cancer cells, fetal neuronal developmental, and particular signaling pathways regulated by VRK1. Specifically, the findings from studying this system will contribute to our understanding of how the viral pseudokinase regulates VRK1 and through which signaling pathways VRK1 complements the essential mechanism of viral DNA replication. Furthermore, unveiling novel methods of VRK1 regulation is translatable to treatment of certain cancers and will enhance our understanding of VRK1 roles during infertility and neurological development deficiencies. Our **long-term goal** is to identify B1-VRK shared signaling pathways that are required for vaccinia virus efficient DNA replication. In order to achieve this goal and fill the current gap in knowledge, our overall **objective** is to elucidate the mechanism how B12 modulates VRK1 activity and determine how VRK1 regulates vaccinia virus DNA replication in the absence of functional B1 and B12 proteins.

The **central hypothesis** is that VRK1 and B1 kinase have a shared function to regulate vaccinia DNA replication. VRK1 and B1 are known to regulate a shared substrate, BAF (98). Additionally, human VRK1 expressed by the virus can rescue the growth deficiency of a B1 mutant virus (73), supporting an overlapping regulation of

signaling pathways necessary for vaccinia DNA replication. Importantly, multiple lines of evidence detailed in this thesis dissertation support a primarily BAF-independent mechanism in which VRK1 complements vaccinia DNA replication when expressed from its endogenous locus in the cell (chapters 3 and 6). Therefore, the rationale of addressing this central hypothesis is to extend our understanding of vaccinia DNA replication modulators and clarify our interpretation of how these viral and cellular homologs regulate each other and participate in shared or divergent signaling pathways.

Aim 1: Determine how B12 modulates VRK1 signaling activity. We hypothesize that B12 acts as an adaptor protein to VRK1 to regulate interactions with specific substrates thus modulating VRK1 kinase activity.

Experiment 1: Does B12 restrict VRK1 catalytic activity in vitro? In vitro analysis of VRK1 catalytic activity was completed with heat inactivated lysates and showed VRK1 auto-phosphorylation and BAF phosphorylation (98). We predict that addition of B12 to this assay will show restriction of BAF phosphorylation typically mediated by VRK1, and enhanced phosphorylation of novel VRK1 substrates.

Experiment 2: Does B12 inhibit VRK1-mediated phosphorylation of BAF in cell culture? Based on our previous studies that B12 expression during ΔB1 infection leads to less phospho-BAF (chapter 3 and 6) and the dependence on VRK1 for ΔB1mutB12 virus rescued phenotype (chapter 6), we predict that B12 restricts VRK1-mediated phosphorylation of BAF. Therefore, we expect VRK1 knockout cells or VRK1 depletion will reduce phosphorylated BAF levels during a ΔB1mutB12 infection as compared to cells expressing endogenous levels of VRK1.

Experiment 3: Does B12 modulate VRK1 colocalization with chromatin during mitosis? VRK1 is known to bind and phosphorylate histones (93), and similar to B12, colocalizes with chromatin during prophase, prometaphase, and telophase stages of cell division (93, 193). However, our recent studies revealed that unlike VRK1, B12 remains localized to the chromatin throughout mitosis (chapter 6). Intriguingly, we noticed two instances where B12 expressing cells in late anaphase stages contained chromatin bridges, which were not observed for GFP expressing control cells (data not shown). The presence of chromatin bridges indicates compromised chromosomal integrity during segregation (204-206). With these pieces of data in mind, we predict that B12 nuclear presence will dysregulate VRK1 chromatin localization during mitosis.

Aim 2: Determine how VRK1 complements vaccinia virus DNA replication in the absence of the B1-B12 digenic pair. Our hypothesis is that VRK1 phosphorylation of key substrates, particularly those involved in DNA damage response and mitosis, allow for both host and virus DNA replication.

Experiment 1: Is VRK1 catalytic activity required for rescued fitness of the ΔB1mutB12 virus? Almost all of VRK1 cellular functions require catalytic activity. The sole catalytic-independent function of VRK1 is during neuronal migration (141). Furthermore, B1 regulation of vaccinia virus DNA replication is kinase dependent (68, 73, 75). Based on these data, we predict that catalytic activity is required to promote ΔB1mutB12 virus replication. We will test this question using VRK1 kinase dead protein expression in VRK1 knockout cells and assay for ΔB1mutB12 virus DNA replication as compared to VRK1 knockout cells.

Experiment 2: Does depletion of BAF rescue the attenuation of ΔB1mutB12 in VRK1 knockout cells? We have not directly tested this, however our indirect evidence indicates that B12-VRK1 repression of B1 deletion vaccinia virus replication is only modestly BAF dependent (chapters 3 and 6). For this reason, we predict that depletion of BAF will only modestly rescue the growth defect of ΔB1mutB12 in VRK1 knockout cells.
Experiment 3: Does restriction of the DNA damage response negate the requirement of VRK1 for ΔB1mutB12 replication? As mentioned above, there were two instances were cells expressing B12 had chromatin bridges connecting the segregated chromosomes during late anaphase (data not shown). It is therefore possible that changes to the cellular DNA, including subtle changes less extreme than chromatin bridging in late anaphase, activate the DNA damage response. Therefore, during infection both host and viral DNA replication would be susceptible to DNA damage signaling. Therefore, we predict that suppression of the DNA damage response during ΔB1mutB12 infection of VRK1 knockout cells will enhance viral DNA replication.

The findings of these proposed studies will impact our interpretation of virus mimicry of host proteins and determine the extent of overlapping pathways for these cellular and viral kinase homologs. The signaling mechanisms elucidated inform which cellular pathways can be targeted by the virus using catalytically active and dead proteins, articulating how viral pseudoenzymes modulate the host environment. Furthermore, understanding how the cellular VRK1 is regulated by vaccinia B12 pseudokinase will determine the translation potential of B12 as a drug to target VRK1 and/or use as a tool for manipulation of VRK1 in different disease models.

CHAPTER 8

REFERENCES

1. **Moss, B.** 2013. Poxviridae, p. 2129. *In* D. M. Knipe and P. M. Howley (eds.), Fields Virology, 6th ed., vol. 2. Lippincott Williams and Wilkins, Philadelphia, PA.

2. **Yang, Z., S. Cao, C. A. Martens, S. F. Porcella, Z. Xie, M. Ma, B. Shen, and B. Moss.** 2015. Deciphering Poxvirus Gene Expression by RNA Sequencing and Ribosome Profiling. Journal of Virology. **89:**6874-6886. doi: 1128/JVI.00528-15.

3. **Bratke, K. A., A. McLysaght, and S. Rothenburg.** 2013. A survey of host range genes in poxvirus genomes. Infect. Genet. Evol. **14:**406-425. doi: 10.1016/j.meegid.2012.12.002 [doi].

4. **Chan, W. M., and G. McFadden.** 2014. Oncolytic Poxviruses. Annu. Rev. Virol. **1:**119-141. doi: 10.1146/annurev-virology-031413-085442 [doi].

5. **Chan, W. M., M. M. Rahman, and G. McFadden.** 2013. Oncolytic myxoma virus: the path to clinic. Vaccine. **31:**4252-4258. doi: 10.1016/j.vaccine.2013.05.056 [doi].

6. **Lander, E. S., et al, and International Human Genome Sequencing Consortium.** 2001. Initial sequencing and analysis of the human genome. Nature. **409:**860-921. doi: 10.1038/35057062 [doi].

7. **Brown, J. C.** 2007. High G+C Content of Herpes Simplex Virus DNA: Proposed Role in Protection Against Retrotransposon Insertion. Open Biochem. J. **1:**33-42. doi: 10.2174/1874091X00701010033 [doi].

8. **Moss, B.** 2007. Poxviruses, p. 2947-2961. *In* D. M. Knipe, P. M. Howley, D. E. Griffin, M. A. Martin, R. A. Lamb, B. Roizman, and S. E. Straus (eds.), Fields Virology, Fifth ed., . Lippincott Williams & Wilkins, a Wolters Kluwer Business, Philadelphia, PA.

9. **Hatcher, E. L., R. C. Hendrickson, and E. J. Lefkowitz.** 2014. Identification of nucleotide-level changes impacting gene content and genome evolution in orthopoxviruses. J. Virol. **88:**13651-13668. doi: 10.1128/JVI.02015-14 [doi].

10. **Brennan, G., J. O. Kitzman, J. Shendure, and A. P. Geballe.** 2015. Experimental Evolution Identifies Vaccinia Virus Mutations in A24R and A35R That Antagonize the Protein Kinase R Pathway and Accompany Collapse of an Extragenic Gene Amplification. Journal of Virology. **89:**9986-9997. doi: 10.1128/JVI.01233-15.

11. **Elde, N. C., S. J. Child, M. T. Eickbush, J. O. Kitzman, K. S. Rogers, J. Shendure, A. P. Geballe, and H. S. Malik.** 2012. Poxviruses deploy genomic accordions to adapt rapidly against host antiviral defenses. Cell. **150:**831-841. doi: 10.1016/j.cell.2012.05.049 [doi].

12. **Brennan, G., J. O. Kitzman, S. Rothenburg, J. Shendure, and A. P. Geballe.** 2014. Adaptive gene amplification as an intermediate step in the expansion of virus host range. PLoS Pathog. **10:**e1004002. doi: 10.1371/journal.ppat.1004002 [doi].

13. **Bengali, Z., A. C. Townsley, and B. Moss.** 2009. Vaccinia virus strain differences in cell attachment and entry. Virology. **389:**132-140. doi: 10.1016/j.virol.2009.04.012.

14. **Locker, J. K., A. Kuehn, S. Schleich, G. Rutter, H. Hohenberg, R. Wepf, and G. Griffiths.** 2000. Entry of the two infectious forms of vaccinia virus at the plasma membane is signaling-dependent for the IMV but not the EEV. Mol. Biol. Cell. **11:**2497-2511. doi: 10.1091/mbc.11.7.2497 [doi].

15. **Tolonen, N., L. Doglio, S. Schleich, and J. K. Locker.** 2001. Vaccinia Virus DNA Replication Occurs in Endoplasmic Reticulum-enclosed Cytoplasmic Mini-Nuclei. Molecular Biology of the Cell. **12:**2031-2046. doi: 10.1091/mbc.12.7.2031.

16. **Moss, B.** 2013. Poxvirus DNA Replication. Cold Spring Harbor Perspectives in Biology. **5**. doi: 10.1101/cshperspect.a010199.

17. **Bidgood, S. R., and J. Mercer.** 2015. Cloak and Dagger: Alternative Immune Evasion and Modulation Strategies of Poxviruses. Viruses. **7:**4800-4825. doi: 10.3390/v7082844 [doi].

18. **Nichols, D. B., W. De Martini, and J. Cottrell.** 2017. Poxviruses Utilize Multiple Strategies to Inhibit Apoptosis. Viruses. **9:**10.3390/v9080215. doi: E215 [pii].

19. **Broyles, S. S.** 2003. Vaccinia virus transcription. Journal of General Virology. **84:**2293-2303. doi: 10.1099/vir.0.18942-0.

20. **K. Oda, W. K. J.** 1967. **Hybridization and sedimentation studies on early and late vaccinia messenger RNA**. J Mol Biol. **27:**395-419.

21. **Sebring, E. D., and N. P. Salzman.** 1967. Metabolic properties of early and late vaccinia virus messenger ribonucleic acid. J. Virol. **1:**550-558.

22. **De Silva, F. S., W. Lewis, P. Berglund, E. V. Koonin, and B. Moss.** 2007. Poxvirus DNA primase. Proc. Natl. Acad. Sci. U. S. A. **104:**18724-18729. doi: 10.1073/pnas.0709276104.

23. **Paran, N., F. S. De Silva, T. G. Senkevich, and B. Moss.** 2009. Cellular DNA Ligase I Is Recruited to Cytoplasmic Vaccinia Virus Factories and Masks the Role of the Vaccinia Ligase in Viral DNA Replication. Cell Host Microbe. **6:**563-569. doi: 10.1016/j.chom.2009.11.005.

24. **Chlanda, P., M. A. Carbajal, M. Cyrklaff, G. Griffiths, and J. Krijnse-Locker.** 2009. Membrane rupture generates single open membrane sheets during vaccinia virus assembly. Cell. Host Microbe. **6:**81-90. doi: 10.1016/j.chom.2009.05.021.

25. **Maruri-Avidal, L., A. S. Weisberg, and B. Moss.** 2011. Vaccinia virus L2 protein associates with the endoplasmic reticulum near the growing edge of crescent precursors of immature virions and stabilizes a subset of viral membrane proteins. J. Virol. **85:**12431-12441. doi: 10.1128/JVI.05573-11 [doi].

26. **Maruri-Avidal, L., A. S. Weisberg, H. Bisht, and B. Moss.** 2013. Analysis of viral membranes formed in cells infected by a vaccinia virus L2-deletion mutant suggests their origin from the endoplasmic reticulum. J. Virol. **87:**1861-1871. doi: 10.1128/JVI.02779-12 [doi].

27. **Maruri-Avidal, L., A. S. Weisberg, and B. Moss.** 2013. Direct formation of vaccinia virus membranes from the endoplasmic reticulum in the absence of the newly characterized L2-interacting protein A30.5. J. Virol. **87:**12313-12326. doi: 10.1128/JVI.02137-13 [doi].

28. **Garcia, A. D., and B. Moss.** 2001. Repression of vaccinia virus Holliday junction resolvase inhibits processing of viral DNA into unit-length genomes. J. Virol. **75:**6460-6471. doi: 10.1128/JVI.75.14.6460-6471.2001 [doi].

29. **Hiller, G., and K. Weber.** 1985. Golgi-derived membranes that contain an acylated viral polypeptide are used for vaccinia virus envelopment. J. Virol. **55:**651-659.

30. **Schmelz, M., B. Sodeik, M. Ericsson, E. J. Wolffe, H. Shida, G. Hiller, and G. Griffiths.** 1994. Assembly of vaccinia virus: the second wrapping cisterna is derived from the trans Golgi network. J. Virol. **68:**130-147.

31. **Gonzalez, J., and M. Esteban.** 2010. A poxvirus Bcl-2-like gene family involved in regulation of host immune response: sequence similarity and evolutionary history. Virol J. **7:**59.

32. **Kvansakul, M., S. Caria, and M. G. Hinds.** 2017. The Bcl-2 Family in Host-Virus Interactions. Viruses. **9:**10.3390/v9100290. doi: E290 [pii].

33. **Rathinam, V. A., Z. Jiang, S. N. Waggoner, S. Sharma, L. E. Cole, L. Waggoner, S. K. Vanaja, B. G. Monks, S. Ganesan, E. Latz, V. Hornung, S. N. Vogel, E. Szomolanyi-Tsuda, and K. A. Fitzgerald.** 2010. The AIM2 inflammasome is essential for host defense against cytosolic bacteria and DNA viruses. Nat. Immunol. **11:**395-402. doi: 10.1038/ni.1864.

34. **Valentine, R., and G. L. Smith.** 2010. Inhibition of the RNA polymerase III-mediated dsDNA-sensing pathway of innate immunity by vaccinia virus protein E3. J. Gen. Virol. **91:**2221-2229. doi: 10.1099/vir.0.021998-0 [doi].

35. **Mitchell, S., J. Vargas, and A. Hoffmann.** 2016. **Signaling via the NFκB system.** Wiley Interdiscip Rev Syst Biol Med. **8:**227-247.

36. **Martin, S., and J. L. Shisler.** 2009. Early viral protein synthesis is necessary for NF-kappaB activation in modified vaccinia Ankara (MVA)-infected 293 T fibroblast cells. Virology. **390:**298-306. doi: 10.1016/j.virol.2009.05.014 [doi].

37. **Davies, M. V., H. W. Chang, B. L. Jacobs, and R. J. Kaufman.** 1993. The E3L and K3L vaccinia virus gene products stimulate translation through inhibition of the double-stranded RNA-dependent protein kinase by different mechanisms. J. Virol. **67:**1688-1692.

38. **Sharp, T. V., F. Moonan, A. Romashko, B. Joshi, G. N. Barber, and R. Jagus.** 1998. The vaccinia virus E3L gene product interacts with both the regulatory and the substrate binding regions of PKR: implications for PKR autoregulation. Virology. **250:**302-315. doi: S0042-6822(98)99365-5 [pii].

39. **Gedey, R., X. Jin, O. Hinthong, and J. L. Shisler.** 2006. Poxviral Regulation of the Host NF-κB Response: the Vaccinia Virus M2L Protein Inhibits Induction of NF-κB Activation via an ERK2 Pathway in Virus-Infected Human Embryonic Kidney Cells. Journal of Virology. **80:**8676-8685. doi: 10.1128/JVI.00935-06.

40. **Bowie, A., E. Kiss-Toth, J. A. Symons, G. L. Smith, S. K. Dower, and L. A. O'Neill.** 2000. A46R and A52R from vaccinia virus are antagonists of host IL-1 and toll-like receptor signaling. Proc. Natl. Acad. Sci. U. S. A. **97:**10162-10167. doi: 10.1073/pnas.160027697.

41. **Harte, M. T., I. R. Haga, G. Maloney, P. Gray, P. C. Reading, N. W. Bartlett, G. L. Smith, A. Bowie, and L. A. J. O'Neill.** 2003. The Poxvirus Protein A52R Targets Toll-like Receptor Signaling Complexes to Suppress Host Defense. The Journal of Experimental Medicine. **197:**343-351. doi: 10.1084/jem.20021652.

42. **Schroder, M., M. Baran, and A. G. Bowie.** 2008. Viral targeting of DEAD box protein 3 reveals its role in TBK1/IKKepsilon-mediated IRF activation. Embo J. **27:**2147-2157. doi: 10.1038/emboj.2008.143.

43. **DiPerna, G., J. Stack, A. G. Bowie, A. Boyd, G. Kotwal, Z. Zhang, S. Arvikar, E. Latz, K. A. Fitzgerald, and W. L. Marshall.** 2004. Poxvirus protein N1L targets the I-kappaB kinase complex, inhibits signaling to NF-kappaB by the tumor necrosis factor superfamily of receptors, and inhibits NF-kappaB and IRF3 signaling by toll-like receptors. J. Biol. Chem. **279:**36570-36578. doi: 10.1074/jbc.M400567200.

44. **Qin, Y., M. Li, S. Zhou, W. Yin, Z. Bian, and H. Shu.** 2017. SPI-2/CrmA inhibits IFN-ß induction by targeting TBK1/IKKe. Sci Rep. **7:**10495.

45. **Elmore, S.** 2007. Apoptosis: a review of programmed cell death. Toxicol. Pathol. **35:**495-516. doi: 779478428 [pii].

46. **Tian, T., K. Dubin, Q. Jin, A. Qureshi, S. King, L. Liu, X. Jiang, G. Murphy, T. Kupper, and R. Fuhlbrigge.** 2012. Disruption of TNF-a/TNFR1 function in resident skin cells impairs host immune response against cutaneous vaccinia virus infection. J Invest Dermatol. **132:**1425-1434.

47. **Dobbelstein, M., and T. Shenk.** 1996. Protection against apoptosis by the vaccinia virus SPI-2 (B13R) gene product. Journal of Virology. **70:**6479-6485.

48. **Macen, J., A. Takahashi, K. B. Moon, R. Nathaniel, P. C. Turner, and R. W. Moyer.** 1998. Activation of Caspases in Pig Kidney Cells Infected with Wild-Type and CrmA/SPI-2 Mutants of Cowpox and Rabbitpox Viruses. Journal of Virology. **72:**3524-3533.

49. **Bertin, J., R. C. Armstrong, S. Ottilie, D. A. Martin, Y. Wang, S. Banks, G. H. Wang, T. G. Senkevich, E. S. Alnemri, B. Moss, M. J. Lenardo, K. J. Tomaselli, and J. I. Cohen.** 1997. Death effector domain-containing herpesvirus and poxvirus proteins inhibit both Fas- and TNFR1-induced apoptosis. Proc. Natl. Acad. Sci. U. S. A. **94:**1172-1176.

50. **Garvey, T. L., J. Bertin, R. M. Siegel, G. H. Wang, M. J. Lenardo, and J. I. Cohen.** 2002. Binding of FADD and caspase-8 to molluscum contagiosum virus MC159 v-FLIP is not sufficient for its antiapoptotic function. J. Virol. **76:**697-706.

51. **Randall, C., J. Jokela, and J. Shisler.** 2012. The MC159 protein from the molluscum contagiosum poxvirus inhibits NF-κB activation by interacting with the IκB kinase complex. J Immunol. **188:**2371-2379.

52. **Ryerson, M. R., M. M. Richards, M. Kvansakul, C. J. Hawkins, and J. L. Shisler.** 2017. Vaccinia Virus Encodes a Novel Inhibitor of Apoptosis That Associates with the Apoptosome. J. Virol. **91:**10.1128/JVI.01385-17. Print 2017 Dec 1. doi: e01385-17 [pii].

53. **Neidel, S., C. Maluquer de Motes, D. S. Mansur, P. Strnadova, G. L. Smith, and S. C. Graham.** 2015. Vaccinia virus protein A49 is an unexpected member of the B-cell Lymphoma (Bcl)-2 protein family. J. Biol. Chem. **290:**5991-6002. doi: 10.1074/jbc.M114.624650 [doi].

54. **Wasilenko, S. T., L. Banadyga, D. Bond, and M. Barry.** 2005. The vaccinia virus F1L protein interacts with the proapoptotic protein Bak and inhibits Bak activation. J. Virol. **79:**14031-14043. doi: 79/22/14031 [pii].

55. **Postigo, A., J. R. Cross, J. Downward, and M. Way.** 2006. Interaction of F1L with the BH3 domain of Bak is responsible for inhibiting vaccinia-induced apoptosis. Cell Death Differ. **13:**1651-1662. doi: 10.1038/sj.cdd.4401853.

56. **Fischer, S. F., H. Ludwig, J. Holzapfel, M. Kvansakul, L. Chen, D. C. Huang, G. Sutter, M. Knese, and G. Häcker.** 2006. Modified vaccinia virus Ankara protein F1L is a novel BH3-domain-binding protein and acts together with the early viral protein E3L to block virus-associated apoptosis. Cell Death Differ. **13:**109-118.

57. **Cooray, S., M. W. Bahar, N. G. Abrescia, C. E. McVey, N. W. Bartlett, R. A. Chen, D. I. Stuart, J. M. Grimes, and G. L. Smith.** 2007. Functional and structural studies of the vaccinia virus virulence factor N1 reveal a Bcl-2-like anti-apoptotic protein. J. Gen. Virol. **88:**1656-1666. doi: 88/6/1656 [pii].

58. **Stack, J., I. R. Haga, M. Schröder, N. W. Bartlett, G. Maloney, P. C. Reading, K. A. Fitzgerald, G. L. Smith, and A. G. Bowie.** 2005. Vaccinia virus protein A46R targets multiple Toll-like–interleukin-1 receptor adaptors and contributes to virulence. The Journal of Experimental Medicine. **201:**1007-1018. doi: 10.1084/jem.20041442.

59. **Perdiguero, B., and M. Esteban.** 2009. The interferon system and vaccinia virus evasion mechanisms. J. Interferon Cytokine Res. **29:**581-598. doi: 10.1089/jir.2009.0073.

60. **Keating, S. E., G. M. Maloney, E. M. Moran, and A. G. Bowie.** 2007. IRAK-2 Participates in Multiple Toll-like Receptor Signaling Pathways to NFκB via Activation of TRAF6 Ubiquitination. Journal of Biological Chemistry. **282:**33435-33443. doi: 10.1074/jbc.M705266200.

61. **Stack, J., and A. G. Bowie.** 2012. Poxviral protein A46 antagonizes Toll-like receptor 4 signaling by targeting BB loop motifs in Toll-IL-1 receptor adaptor proteins to disrupt receptor:adaptor interactions. J Biol Chem. **287:**22672-22682. doi: 10.1074/jbc.M112.349225.

62. **Fedosyuk, S., I. Grishkovskaya, E. J. de Almeida Ribeiro, and T. Skern.** 2014. Characterization and structure of the vaccinia virus NF-κB antagonist A46. J Biol Chem. **289:**3749-3762.

63. **Mansur, D., C. Maluquer de Motes, L. Unterholzner, R. Sumner, B. Ferguson, H. Ren, P. Strnadova, A. Bowie, and G. Smith.** 2013. Poxvirus targeting of E3 ligase β-TrCP by molecular mimicry: a mechanism to inhibit NF-κB activation and promote immune evasion and virulence. PLoS Pathog. **9:**e1003183.

64. **Manning, G., D. B. Whyte, R. Martinez, T. Hunter, and S. Sudarsanam.** 2002. The protein kinase complement of the human genome. Science. **298:**1912-1934. doi: 10.1126/science.1075762.

65. **Jacob, T., C. Van den Broeke, and H. W. Favoreel.** 2011. Viral serine/threonine protein kinases. J. Virol. **85:**1158-1173. doi: 10.1128/JVI.01369-10.

66. **Roskoski, R.,Jr.** 2015. A historical overview of protein kinases and their targeted small molecule inhibitors. Pharmacol. Res. **100:**1-23. doi: 10.1016/j.phrs.2015.07.010 [doi].

67. **Condit, R. C., A. Motyczka, and G. Spizz.** 1983 Jul 30. Isolation, characterization, and physical mapping of temperature-sensitive mutants of vaccinia virus. Virol. **128:**429-443.

68. **Rempel, R. E., M. K. Anderson, E. Evans, and P. Traktman.** 1990. Temperature-sensitive vaccinia virus mutants identify a gene with an essential role in viral replication. J. Virol. **64:**574-583.

69. **Wiebe, M. S., and P. Traktman.** 2007. Poxviral B1 kinase overcomes barrier to autointegration factor, a host defense against virus replication. Cell. Host Microbe. **1:**187-197. doi: 10.1016/j.chom.2007.03.007.

70. **Nezu, J., A. Oku, M. H. Jones, and M. Shimane.** 1997. Identification of two novel human putative serine/threonine kinases, VRK1 and VRK2, with structural similarity to vaccinia virus B1R kinase. Genomics. **45:**327-331.

71. **Zelko, I., R. Kobayashi, P. Honkakoski, and M. Negishi.** 1998 Apr 1. Molecular Cloning and Characterization of a Novel Nuclear Protein Kinase in Mice. Arch. Biochem. Biophys. **352:**31-36. doi: 10.1006/abbi.1998.0582.

72. **Nichols, R. J., and P. Traktman.** 2004. Characterization of three paralogous members of the Mammalian vaccinia related kinase family. J. Biol. Chem. **279:**7934-7946. doi: 10.1074/jbc.M310813200.

73. **Boyle, K. A., and P. Traktman.** 2004. Members of a novel family of mammalian protein kinases complement the DNA-negative phenotype of a vaccinia virus ts mutant defective in the B1 kinase. J. Virol. **78:**1992-2005.

74. **Hughes, A. L., S. Irausquin, and R. Friedman.** 2010. The evolutionary biology of poxviruses. Infect. Genet. Evol. **10:**50-59. doi: 10.1016/j.meegid.2009.10.001.

75. **Rempel, R. E., and P. Traktman.** 1992. Vaccinia virus B1 kinase: phenotypic analysis of temperature-sensitive mutants and enzymatic characterization of recombinant proteins. J. Virol. **66:**4413-4426.

76. **Kovacs, G. R., N. Vasilakis, and B. Moss.** 2001. Regulation of viral intermediate gene expression by the vaccinia virus B1 protein kinase. J. Virol. **75:**4048-4055. doi: 10.1128/JVI.75.9.4048-4055.

77. **Jamin, A., N. Ibrahim, A. Wicklund, K. Weskamp, and M. S. Wiebe.** 2015. Vaccinia B1 kinase is required for post-replicative stages of the viral lifecycle in a BAF-independent manner in U2OS cells. Journal of Virology. **89:**10247-59. doi: 10.1128/JVI.01252-15.

78. **Jamin, A., and M. S. Wiebe.** 2015. Barrier to Autointegration Factor (BANF1): interwoven roles in nuclear structure, genome integrity, innate immunity, stress responses and progeria. Curr. Opin. Cell Biol. **34:**61-68. doi: 10.1016/j.ceb.2015.05.006 [doi].

79. **Bradley, C. M., D. R. Ronning, R. Ghirlando, R. Craigie, and F. Dyda.** 2005. Structural basis for DNA bridging by barrier-to-autointegration factor. Nat. Struct. Mol. Biol. **12:**935-936. doi: 10.1038/nsmb989.

80. **Zheng, R., R. Ghirlando, M. S. Lee, K. Mizuuchi, M. Krause, and R. Craigie.** 2000. Barrier-to-autointegration factor (BAF) bridges DNA in a discrete, higher-order nucleoprotein complex. Proc. Natl. Acad. Sci. U. S. A. **97:**8997-9002. doi: 10.1073/pnas.150240197.

81. **Ibrahim, N., A. Wicklund, A. Jamin, and M. S. Wiebe.** 2013. Barrier to autointegration factor (BAF) inhibits vaccinia virus intermediate transcription in the absence of the viral B1 kinase. Virology. **444:**363-373. doi: 10.1016/j.virol.2013.07.002; 10.1016/j.virol.2013.07.002.

82. **Valbuena, A., M. Sanz-García, I. López-Sánchez, F. M. Vega, and P. A. Lazo.** 2011. Roles of VRK1 as a new player in the control of biological processes required for cell division. Cell. Signal. **23:**1267-1272. doi: 10.1016/j.cellsig.2011.04.002.

83. **Ibrahim, N., A. Wicklund, and M. S. Wiebe.** 2011. Molecular characterization of the host defense activity of the barrier to autointegration factor against vaccinia virus. J. Virol. **85:**11588-11600. doi: 10.1128/JVI.00641-11.

84. **Jha, S., M. G. Rollins, G. Fuchs, D. J. Procter, E. A. Hall, K. Cozzolino, P. Sarnow, J. N. Savas, and D. Walsh.** 2017. Trans-kingdom mimicry underlies ribosome customization by a poxvirus kinase. Nature. **546:**651-655. doi: 10.1038/nature22814 [doi].

85. **Banham, A. H., D. P. Leader, and G. L. Smith.** 1993. Phosphorylation of ribosomal proteins by the vaccinia virus B1R protein kinase. FEBS Lett. **321:**27-31.

86. **Beaud, G., R. Beaud, and D. P. Leader.** 1995. Vaccinia virus gene H5R encodes a protein that is phosphorylated by the multisubstrate vaccinia virus B1R protein kinase. Journal of Virology. **69:**1819-1826.

87. **Brown, N. G., D. Nick Morrice, G. Beaud, G. Hardie, and D. P. Leader.** 2000. Identification of sites phosphorylated by the vaccinia virus B1R kinase in viral protein H5R. BMC Biochem. **1:**2.

88. **Cullen, C. F., A. L. Brittle, T. Ito, and H. Ohkura.** 2005. The conserved kinase NHK-1 is essential for mitotic progression and unifying acentrosomal meiotic spindles in Drosophila melanogaster. J. Cell Biol. **171:**593-602. doi: 10.1083/jcb.200508127.

89. **Gorjanacz, M., E. P. Klerkx, V. Galy, R. Santarella, C. Lopez-Iglesias, P. Askjaer, and I. W. Mattaj.** 2007. Caenorhabditis elegans BAF-1 and its kinase VRK-1 participate directly in post-mitotic nuclear envelope assembly. Embo J. **26:**132-143. doi: 10.1038/sj.emboj.7601470.

90. **Blanco, S., L. Klimcakova, F. M. Vega, and P. A. Lazo.** 2006. The subcellular localization of vaccinia-related kinase-2 (VRK2) isoforms determines their different effect on p53 stability in tumour cell lines. FEBS Journal. **273:**2487-2504. doi: 10.1111/j.1742-4658.2006.05256.x.

91. **Blanco, S., L. Klimcakova, F. M. Vega, and P. A. Lazo.** 2006. The subcellular localization of vaccinia-related kinase-2 (VRK2) isoforms determines their different effect on p53 stability in tumour cell lines. Febs J. **273:**2487-2504. doi: 10.1111/j.1742-4658.2006.05256.x.

92. **Wiebe, M. S., R. J. Nichols, T. P. Molitor, J. K. Lindgren, and P. Traktman.** 2010. Mice Deficient in the Serine/Threonine Protein Kinase VRK1 Are Infertile Due to a Progressive Loss of Spermatogonia. Biology of Reproduction. **82:**182-193. doi: 10.1095/biolreprod.109.079095.

93. **Kang, T., D. Park, Y. H. Choi, K. Kim, H. S. Yoon, and K. Kim.** 2007. Mitotic Histone H3 Phosphorylation by Vaccinia-Related Kinase 1 in Mammalian Cells. Molecular and Cellular Biology. **27:**8533-8546. doi: 10.1128/MCB.00018-07.

94. **Molitor, T. P., and P. Traktman.** 2014. Depletion of the protein kinase VRK1 disrupts nuclear envelope morphology and leads to BAF retention on mitotic chromosomes. Mol. Biol. Cell. **25:**891-903. doi: 10.1091/mbc.E13-10-0603.

95. **Monsalve, D. M., T. Merced, I. F. Fernandez, S. Blanco, M. Vazquez-Cedeira, and P. A. Lazo.** 2013. Human VRK2 modulates apoptosis by interaction with Bcl-xL and regulation of BAX gene expression. Cell. Death Dis. **4:**e513. doi: 10.1038/cddis.2013.40.

96. **Li, L. Y., M. Y. Liu, H. M. Shih, C. H. Tsai, and J. Y. Chen.** 2006. Human cellular protein VRK2 interacts specifically with Epstein-Barr virus BHRF1, a homologue of Bcl-2, and enhances cell survival. J. Gen. Virol. **87:**2869-2878. doi: 87/10/2869 [pii].

97. **Teferi, W. M., K. Dodd, R. Maranchuk, N. Favis, and D. H. Evans.** 2013. A whole-genome RNA interference screen for human cell factors affecting myxoma virus replication. J. Virol. **87:**4623-4641. doi: 10.1128/JVI.02617-12.

98. **Nichols, R. J., M. S. Wiebe, and P. Traktman.** 2006. The vaccinia-related kinases phosphorylate the N' terminus of BAF, regulating its interaction with DNA and its retention in the nucleus. Mol. Biol. Cell. **17:**2451-2464. doi: 10.1091/mbc.E05-12-1179.

99. **Furukawa, K., S. Sugiyama, S. Osouda, H. Goto, M. Inagaki, T. Horigome, S. Omata, M. McConnell, P. A. Fisher, and Y. Nishida.** 2003. Barrier-to-autointegration factor plays crucial roles in cell cycle progression and nuclear organization in Drosophila. Journal of Cell Science. **116:**3811-3823. doi: 10.1242/jcs.00682.

100. **Puente, X. S., V. Quesada, F. G. Osorio, R. Cabanillas, J. Cadinanos, J. M. Fraile, G. R. Ordonez, D. A. Puente, A. Gutierrez-Fernandez, M. Fanjul-Fernandez, N. Levy, J. M. Freije, and C. Lopez-Otin.** 2011. Exome sequencing and functional analysis identifies BANF1 mutation as the cause of a hereditary progeroid syndrome. Am. J. Hum. Genet. **88:**650-656. doi: 10.1016/j.ajhg.2011.04.010.

101. **Paquet, N., J. K. Box, N. W. Ashton, A. Suraweera, L. V. Croft, A. J. Urquhart, E. Bolderson, S. D. Zhang, K. J. O'Byrne, and D. J. Richard.** 2014. Nestor-Guillermo Progeria Syndrome: a biochemical insight into Barrier-to-Autointegration Factor 1, alanine 12 threonine mutation. BMC Mol. Biol. **15:**27. doi: 10.1186/s12867-014-0027-z.

102. **Jamin, A., A. Wicklund, and M. S. Wiebe.** 2014. Cell and Virus Mediated Regulation of the Barrier-to-Autointegration Factor's Phosphorylation State Controls its DNA Binding, Dimerization, Subcellular Localization, and Antipoxviral Activity. J. Virol. **88:**5342-5355. doi: 10.1128/JVI.00427-14.

103. **Puente, X. S., L. M. Sanchez, C. M. Overall, and C. Lopez-Otin.** 2003. Human and mouse proteases: a comparative genomic approach. Nat. Rev. Genet. **4:**544-558. doi: 10.1038/nrg1111 [doi].

104. **Todd, A. E., C. A. Orengo, and J. M. Thornton.** 2002. Sequence and structural differences between enzyme and nonenzyme homologs. Structure. **10:**1435-1451. doi: S0969212602008614 [pii].

105. **Pils, B., and J. Schultz.** 2004. Inactive enzyme-homologues find new function in regulatory processes. J. Mol. Biol. **340:**399-404. doi: 10.1016/j.jmb.2004.04.063 [doi].

106. **Eyers, P. A., and J. M. Murphy.** 2013. Dawn of the dead: protein pseudokinases signal new adventures in cell biology. Biochem. Soc. Trans. **41:**969-974. doi: 10.1042/BST20130115 [doi].

107. **Hammaren, H. M., A. T. Virtanen, and O. Silvennoinen.** 2015. Nucleotide-binding mechanisms in pseudokinases. Biosci. Rep. **36:**e00282. doi: 10.1042/BSR20150226 [doi].

108. **Ejaz, S.** 2017. Transcription and translation of APOL1 variants. Biosci. Rep. **37:**10.1042/BSR20170647. Print 2017 Oct 31. doi: BSR20170647 [pii].

109. **Magnuson, B., E. K. Rainey, T. Benjamin, M. Baryshev, S. Mkrtchian, and B. Tsai.** 2005. ERp29 triggers a conformational change in polyomavirus to stimulate membrane binding. Mol. Cell. **20:**289-300. doi: S1097-2765(05)01600-X [pii].

110. **Walczak, C. P., and B. Tsai.** 2011. A PDI family network acts distinctly and coordinately with ERp29 to facilitate polyomavirus infection. J. Virol. **85:**2386-2396. doi: 10.1128/JVI.01855-10 [doi].

111. **He, S., J. Zhao, S. Song, X. He, A. Minassian, Y. Zhou, J. Zhang, K. Brulois, Y. Wang, J. Cabo, E. Zandi, C. Liang, J. U. Jung, X. Zhang, and P. Feng.** 2015. Viral pseudo-enzymes activate RIG-I via deamidation to evade cytokine production. Mol. Cell. **58:**134-146. doi: 10.1016/j.molcel.2015.01.036 [doi].

112. **Howard, S. T., and G. L. Smith.** 1989. Two early vaccinia virus genes encode polypeptides related to protein kinases. J. Gen. Virol. **70:**3187-3201.

113. **Banham, A. H., and G. L. Smith.** 1992. Vaccinia virus gene B1R encodes a 34-kDa serine/threonine protein kinase that localizes in cytoplasmic factories and is packaged into virions. Virology. **191:**803-812.

114. **Banham, A. H., and G. L. Smith.** 1993. Characterization of vaccinia virus gene B12R. J. Gen. Virol. **74:**2807-2812. doi: 10.1099/0022-1317-74-12-2807 [doi].

115. **Tscharke, D. C., P. C. Reading, and G. L. Smith.** 2002. Dermal infection with vaccinia virus reveals roles for virus proteins not seen using other inoculation routes. J. Gen. Virol. **83:**1977-1986. doi: 10.1099/0022-1317-83-8-1977 [doi].

116. **Senkevich, T. G., E. V. Koonin, and B. Moss.** 2011. Vaccinia virus F16 protein, a predicted catalytically inactive member of the prokaryotic serine recombinase superfamily, is targeted to nucleoli. Virology. **417:**334-342. doi: 10.1016/j.virol.2011.06.017 [doi].

117. **De Silva, F. S., and B. Moss.** 2003. Vaccinia Virus Uracil DNA Glycosylase Has an Essential Role in DNA Synthesis That Is Independent of Its Glycosylase Activity: Catalytic Site Mutations Reduce Virulence but Not Virus Replication in Cultured Cells. J Virol. **77:**159-166.

118. **Reiterer, V., P. A. Eyers, and H. Farhan.** 2014. Day of the dead: pseudokinases and pseudophosphatases in physiology and disease. Trends Cell Biol. **24:**489-505. doi: 10.1016/j.tcb.2014.03.008 [doi].

119. **Zou, J., C. Zhang, J. Marjanovic, M. V. Kisseleva, P. W. Majerus, and M. P. Wilson.** 2012. Myotubularin-related protein (MTMR) 9 determines the enzymatic activity, substrate specificity, and role in autophagy of MTMR8. Proc. Natl. Acad. Sci. U. S. A. **109:**9539-9544. doi: 10.1073/pnas.1207021109 [doi].

120. **Kang, T. H., and K. T. Kim.** 2006. Negative regulation of ERK activity by VRK3-mediated activation of VHR phosphatase. Nat. Cell Biol. **8:**863-869. doi: 10.1038/ncb1447.

121. **Berger, M. B., J. M. Mendrola, and M. A. Lemmon.** 2004. ErbB3/HER3 does not homodimerize upon neuregulin binding at the cell surface. FEBS Lett. **569:**332-336. doi: 10.1016/j.febslet.2004.06.014 [doi].

122. **McKay, M. M., A. K. Freeman, and D. K. Morrison.** 2011. Complexity in KSR function revealed by Raf inhibitor and KSR structure studies. Small GTPases. **2:**276-281. doi: 10.4161/sgtp.2.5.17740 [doi].

123. **Reiterer, V., D. Fey, W. Kolch, B. N. Kholodenko, and H. Farhan.** 2013. Pseudophosphatase STYX modulates cell-fate decisions and cell migration by spatiotemporal regulation of ERK1/2. Proc. Natl. Acad. Sci. U. S. A. **110:**E2934-43. doi: 10.1073/pnas.1301985110 [doi].

124. **Howard, S. T., and G. L. Smith.** 1989. Two Early Vaccinia Virus Genes Encode Polypeptides Related to Protein Kinases. Journal of General Virology. **70:**3187-3201. doi: 10.1099/0022-1317-70-12-3187.

125. **Traktman, P., M. K. Anderson, and R. E. Rempel.** 1989. Vaccinia virus encodes an essential gene with strong homology to protein kinases. J. Biol. Chem. **264:**21458-21461.

126. **Mostoslavsky, G., A. J. Fabian, S. Rooney, F. W. Alt, and R. C. Mulligan.** 2006. Complete correction of murine Artemis immunodeficiency by lentiviral vector-mediated gene transfer. Proc. Natl. Acad. Sci. U. S. A. **103:**16406-16411. doi: 0608130103 [pii].

127. **Olson, A. T., A. B. Rico, Z. Wang, G. Delhon, and M. S. Wiebe.** 2017. Deletion of the Vaccinia Virus B1 Kinase Reveals Essential Functions of This Enzyme Complemented Partly by the Homologous Cellular Kinase VRK2. J. Virol. **91:**e00635-17. doi: e00635-17 [pii].

128. **Esposito, J., K. Brechling, G. Baer, and B. Moss.** 1987. Vaccinia virus recombinants expressing rabiesvirus glycoprotein protect against rabies. Virus Genes. **1:**7-21.

129. **Chakrabarti, S., J. R. Sisler, and B. Moss.** 1997. Compact, synthetic, vaccinia virus early/late promoter for protein expression. BioTechniques. **23:**1094-1097.

130. **Delhon, G., E. R. Tulman, C. L. Afonso, Z. Lu, A. de la Concha-Bermejillo, H. D. Lehmkuhl, M. E. Piccone, G. F. Kutish, and D. L. Rock.** 2004. Genomes of the Parapoxviruses Orf Virus and Bovine Papular Stomatitis Virus. Journal of Virology. **78:**168-77.

131. **Evans, E., and P. Traktman.** 1987. Molecular genetic analysis of a vaccinia virus gene with an essential role in DNA replication. Journal of Virology. **61:**3152-3162.

132. **Traktman, P., P. Sridhar, R. C. Condit, and B. E. Roberts.** 1984. Transcriptional mapping of the DNA polymerase gene of vaccinia virus. J. Virol. **49:**125-131.

133. **Greseth, M. D., K. A. Boyle, M. S. Bluma, B. Unger, M. S. Wiebe, J. A. Soares-Martins, N. T. Wickramasekera, J. Wahlberg, and P. Traktman.** 2012. Molecular genetic and biochemical characterization of the vaccinia virus I3 protein, the replicative single-stranded DNA binding protein. J. Virol. **86:**6197-6209. doi: 10.1128/JVI.00206-12; 10.1128/JVI.00206-12.

134. **Boyle, K. A., M. D. Greseth, and P. Traktman.** 2015. Genetic confirmation that the H5 protein is required for vaccinia virus DNA replication. J. Virol. **89:**6312-6327. doi: JVI.00445-15 [pii].

135. **Skoko, D., M. Li, Y. Huang, M. Mizuuchi, M. Cai, C. M. Bradley, P. J. Pease, B. Xiao, J. F. Marko, R. Craigie, and K. Mizuuchi.** 2009. Barrier-to-autointegration factor (BAF) condenses DNA by looping. Proc. Natl. Acad. Sci. U. S. A. **106:**16610-16615. doi: 10.1073/pnas.0909077106.

136. **Lorenzetti, D., C. Poirier, M. Zhao, P. A. Overbeek, W. Harrison, and C. E. Bishop.** 2014. A transgenic insertion on mouse chromosome 17 inactivates a novel immunoglobulin superfamily gene potentially involved in sperm-egg fusion. Mamm. Genome. **25:**141-148. doi: 10.1007/s00335-013-9491-x [doi].

137. **Zhang, X., C. Dong, X. Sun, Z. Li, M. Zhang, Z. Guan, and M. Duan.** 2014. Induction of the cellular miR-29c by influenza virus inhibits the innate immune response through protection of A20 mRNA. Biochem. Biophys. Res. Commun. **450:**755-761. doi: 10.1016/j.bbrc.2014.06.059 [doi].

138. **Lin, J., J. Xia, Y. T. Chen, K. Y. Zhang, Y. Zeng, and Q. Yang.** 2017. H9N2 avian influenza virus enhances the immune responses of BMDCs by down-regulating miR29c. Vaccine. **35:**729-737. doi: S0264-410X(16)31287-7 [pii].

139. **Molitor, T. P., and P. Traktman.** 2013. Molecular genetic analysis of VRK1 in mammary epithelial cells: depletion slows proliferation in vitro and tumor growth and metastasis in vivo. Oncogenesis. **2:**e48. doi: 10.1038/oncsis.2013.11; 10.1038/oncsis.2013.11.

140. **López-Sánchez, I., M. Sanz-García, and P. A. Lazo.** 2009. Plk3 Interacts with and Specifically Phosphorylates VRK1 in Ser342, a Downstream Target in a Pathway That Induces Golgi Fragmentation. Molecular and Cellular Biology. **29:**1189-1201. doi: 10.1128/MCB.01341-08.

141. **Vinograd-Byk, H., T. Sapir, L. Cantarero, P. A. Lazo, S. Zeligson, D. Lev, T. Lerman-Sagie, P. Renbaum, O. Reiner, and E. Levy-Lahad.** 2015. The spinal muscular atrophy with pontocerebellar hypoplasia gene VRK1 regulates neuronal migration through an amyloid-ß precursor protein-dependent mechanism. Journal of Neuroscience. **35:**936-42. doi: 10.1523/JNEUROSCI.

142. **Kang, T. H., D. Y. Park, W. Kim, and K. T. Kim.** 2008. VRK1 phosphorylates CREB and mediates CCND1 expression. J. Cell. Sci. **121:**3035-41. doi: 10.1242/jcs.026757.

143. **Valbuena, A., I. López-Sánchez, and P. A. Lazo.** 2008. Human VRK1 Is an Early Response Gene and Its Loss Causes a Block in Cell Cycle Progression. Plos One. **3:**e1642.

144. **Lancaster, O. M., C. F. Cullen, and H. Ohkura.** 2007. NHK-1 phosphorylates BAF to allow karyosome formation in the Drosophila oocyte nucleus. J. Cell Biol. **179:**817-824. doi: 10.1083/jcb.200706067.

145. **Shin, J., G. Chakraborty, N. Bharatham, C. Kang, N. Tochio, S. Koshiba, T. Kigawa, W. Kim, K. T. Kim, and H. S. Yoon.** 2011. NMR solution structure of human vaccinia-related kinase 1 (VRK1) reveals the C-terminal tail essential for its structural stability and autocatalytic activity. The Journal of Biological Chemistry. **286:**22131-22138. doi: 10.1074/jbc.M110.200162.

146. **Brown, S., W. Levinson, and J. A. Spudich.** 1976. Cytoskeletal elements of chick embryo fibroblasts revealed by detergent extraction. J. Supramol. Struct. **5:**119-130. doi: 10.1002/jss.400050203 [doi].

147. **Lenk, R., L. Ransom, Y. Kaufmann, and S. Penman.** 1977. A cytoskeletal structure with associated polyribosomes obtained from HeLa cells. Cell. **10:**67-78. doi: 0092-8674(77)90141-6 [pii].

148. **Pasdar, M., and W. J. Nelson.** 1988. Kinetics of desmosome assembly in Madin-Darby canine kidney epithelial cells: temporal and spatial regulation of desmoplakin organization and stabilization upon cell-cell contact. II. Morphological analysis. J. Cell Biol. **106:**687-695.

149. **He, S., J. M. Sun, L. Li, and J. R. Davie.** 2005. Differential intranuclear organization of transcription factors Sp1 and Sp3. Mol. Biol. Cell. **16:**4073-4083. doi: E05-05-0388 [pii].

150. **Livingston, C. M., N. A. DeLuca, D. E. Wilkinson, and S. K. Weller.** 2008. Oligomerization of ICP4 and rearrangement of heat shock proteins may be important for herpes simplex virus type 1 prereplicative site formation. J. Virol. **82:**6324-6336. doi: 10.1128/JVI.00455-08 [doi].

151. **Margalit, A., A. Brachner, J. Gotzmann, R. Foisner, and Y. Gruenbaum.** 2007. Barrier-to-autointegration factor--a BAFfling little protein. Trends Cell Biol. **17:**202-208. doi: 10.1016/j.tcb.2007.02.004.

152. **Margalit, A., J. Liu, A. Fridkin, K. L. Wilson, and Y. Gruenbaum.** 2005. A lamin-dependent pathway that regulates nuclear organization, cell cycle progression and germ cell development. Novartis found. Symp. **264:**231-40; discussion 240-5.

153. **Haraguchi, T., T. Koujin, M. Segura-Totten, K. K. Lee, Y. Matsuoka, Y. Yoneda, K. L. Wilson, and Y. Hiraoka.** 2001. BAF is required for emerin assembly into the reforming nuclear envelope. J. Cell. Sci. **114:**4575-4585.

154. **Haraguchi, T., T. Kojidani, T. Koujin, T. Shimi, H. Osakada, C. Mori, A. Yamamoto, and Y. Hiraoka.** 2008. Live cell imaging and electron microscopy reveal dynamic processes of BAF-directed nuclear envelope assembly. J. Cell. Sci. **121:**2540-2554. doi: 10.1242/jcs.033597.

155. **McCraith, S., T. Holtzman, B. Moss, and S. Fields.** 2000. Genome-wide analysis of vaccinia virus protein–protein interactions. Proceedings of the National Academy of Sciences. **97:**4879-4884. doi: 10.1073/pnas.080078197.

156. **Tolonen, N., L. Doglio, S. Schleich, and J. Krijnse Locker.** 2001. Vaccinia virus DNA replication occurs in endoplasmic reticulum-enclosed cytoplasmic mini-nuclei. Mol. Biol. Cell. **12:**2031-2046.

157. **Cepeda, V., and M. Esteban.** 2014. Novel insights on the progression of intermediate viral forms in the morphogenesis of vaccinia virus. Virus Res. **183:**23-29. doi: 10.1016/j.virusres.2014.01.016 [doi].

158. **Tooze, J., M. Hollinshead, B. Reis, K. Radsak, and H. Kern.** 1993. Progeny vaccinia and human cytomegalovirus particles utilize early endosomal cisternae for their envelopes. Eur. J. Cell Biol. **60:**163-178.

159. **Sivan, G., A. S. Weisberg, J. L. Americo, and B. Moss.** 2016. Retrograde Transport from Early Endosomes to the trans-Golgi Network Enables Membrane Wrapping and Egress of Vaccinia Virus Virions. J. Virol. **90:**8891-8905. doi: 10.1128/JVI.01114-16 [doi].

160. **Wang, S., and S. Shuman.** 1995. Vaccinia virus morphogenesis is blocked by temperature-sensitive mutations in the F10 gene, which encodes protein kinase 2. J. Virol. **69:**6376-6388.

161. **Szajner, P., A. S. Weisberg, and B. Moss.** 2004. Evidence for an essential catalytic role of the F10 protein kinase in vaccinia virus morphogenesis. J. Virol. **78:**257-265.

162. **Szajner, P., A. S. Weisberg, and B. Moss.** 2004. Physical and functional interactions between vaccinia virus F10 protein kinase and virion assembly proteins A30 and G7. J. Virol. **78:**266-274.

163. **Punjabi, A., and P. Traktman.** 2005. Cell Biological and Functional Characterization of the Vaccinia Virus F10 Kinase: Implications for the Mechanism of Virion Morphogenesis. Journal of Virology. **79:**2171-2190. doi: 10.1128/JVI.79.4.2171-2190.

164. **Greseth, M. D., D. C. Carter, S. S. Terhune, and P. Traktman.** 2017. Proteomic Screen for Cellular Targets of the Vaccinia Virus F10 Protein Kinase Reveals that Phosphorylation of mDia Regulates Stress Fiber Formation. Mol. Cell. Proteomics. **16:**S124-S143. doi: 10.1074/mcp.M116.065003 [doi].

165. **Novy, K., S. Kilcher, U. Omasits, C. K. E. Bleck, C. Beerli, J. Vowinckel, C. K. Martin, M. Syedbasha, A. Maiolica, I. White, J. Mercer, and B. Wollscheid.** 2018. Proteotype profiling unmasks a viral signalling network essential for poxvirus assembly and transcriptional competence. Nat. Microbiol. **3:**588-599. doi: 10.1038/s41564-018-0142-6 [doi].

166. **Stuart, C. A., E. K. Zhivkoplias, T. G. Senkevich, L. S. Wyatt, and B. Moss.** 2018. RNA polymerase mutations selected during experimental evolution enhance replication of a hybrid vaccinia virus with an intermediate transcription factor subunit replaced by the myxoma virus ortholog. J. Virol. JVI.01089-18. doi: JVI.01089-18 [pii].

167. **Esposito, J. J., S. A. Sammons, A. M. Frace, J. D. Osborne, M. Olsen-Rasmussen, M. Zhang, D. Govil, I. K. Damon, R. Kline, M. Laker, Y. Li, G. L. Smith, H. Meyer, J. W. Leduc, and R. M. Wohlhueter.** 2006. Genome sequence diversity and clues to the evolution of variola (smallpox) virus. Science. **313:**807-812. doi: 1125134 [pii].

168. **Coulson, D., and C. Upton.** 2011. Characterization of indels in poxvirus genomes. Virus Genes. **42:**171-177. doi: 10.1007/s11262-010-0560-x [doi].

169. **Feschenko, V. V., and S. T. Lovett.** 1998. Slipped misalignment mechanisms of deletion formation: analysis of deletion endpoints. J. Mol. Biol. **276:**559-569. doi: S0022-2836(97)91566-7 [pii].

170. **Lovett, S. T.** 2004. Encoded errors: mutations and rearrangements mediated by misalignment at repetitive DNA sequences. Mol. Microbiol. **52:**1243-1253. doi: 10.1111/j.1365-2958.2004.04076.x [doi].

171. **Dobson, B. M., and D. C. Tscharke.** 2015. Redundancy complicates the definition of essential genes for vaccinia virus. J. Gen. Virol. **96:**3326-3337. doi: 10.1099/jgv.0.000266 [doi].

172. **Wen, Y., E. Behiels, and B. Devreese.** 2014. Toxin-Antitoxin systems: their role in persistence, biofilm formation, and pathogenicity. Pathog. Dis. **70:**240-249. doi: 10.1111/2049-632X.12145 [doi].

173. **Goeders, N., and L. Van Melderen.** 2014. Toxin-antitoxin systems as multilevel interaction systems. Toxins (Basel). **6:**304-324. doi: 10.3390/toxins6010304 [doi].

174. **Harms, A., D. E. Brodersen, N. Mitarai, and K. Gerdes.** 2018. Toxins, Targets, and Triggers: An Overview of Toxin-Antitoxin Biology. Mol. Cell. **70:**768-784. doi: S1097-2765(18)30003-0 [pii].

175. **Unterholzner, S. J., B. Poppenberger, and W. Rozhon.** 2013. Toxin-antitoxin systems: Biology, identification, and application. Mob Genet. Elements. **3:**e26219. doi: 10.4161/mge.26219 [doi].

176. **McLaughlin, R. N.,Jr, and H. S. Malik.** 2017. Genetic conflicts: the usual suspects and beyond. J. Exp. Biol. **220:**6-17. doi: 10.1242/jeb.148148 [doi].

177. **Burt, A., and A. Crisanti.** 2018. Gene Drive: Evolved and Synthetic. ACS Chem. Biol. **13:**343-346. doi: 10.1021/acschembio.7b01031 [doi].

178. **Ben-David, E., A. Burga, and L. Kruglyak.** 2017. A maternal-effect selfish genetic element in Caenorhabditis elegans. Science. **356:**1051-1055. doi: 10.1126/science.aan0621 [doi].

179. **Nuckolls, N. L., M. A. Bravo Nunez, M. T. Eickbush, J. M. Young, J. J. Lange, J. S. Yu, G. R. Smith, S. L. Jaspersen, H. S. Malik, and S. E. Zanders.** 2017. Wtf Genes are Prolific Dual Poison-Antidote Meiotic Drivers. Elife. **6:**10.7554/eLife.26033. doi: 10.7554/eLife.26033 [doi].

180. **Hansen, S., M. Vulic, J. Min, T. J. Yen, M. A. Schumacher, R. G. Brennan, and K. Lewis.** 2012. Regulation of the Escherichia coli HipBA toxin-antitoxin system by proteolysis. PLoS One. **7:**e39185. doi: 10.1371/journal.pone.0039185 [doi].

181. **Otsuka, Y.** 2016. Prokaryotic toxin-antitoxin systems: novel regulations of the toxins. Curr. Genet. **62:**379-382. doi: 10.1007/s00294-015-0557-z [doi].

182. **Burt, A., and R. Trivers.** 2006. Genes in conflict: the biology of selfish genetic elements. The Belknap Press of Harvard University Press, Cambridge, Mass.; London. doi: 10.4159/9780674029118.

183. **Ember, S. W., H. Ren, B. J. Ferguson, and G. L. Smith.** 2012. **Vaccinia virus protein C4 inhibits NF-κB activation and promotes virus virulence**. The Journal of General Virology. **93:**2098-2108. doi: 10.1099/vir.0.045070-0.

184. **Unterholzner, L., R. P. Sumner, M. Baran, H. Ren, D. S. Mansur, N. M. Bourke, F. Randow, G. L. Smith, and A. G. Bowie.** 2011. Vaccinia virus protein C6 is a virulence factor that binds TBK-1 adaptor proteins and inhibits activation of IRF3 and IRF7. PLoS Pathog. **7:**e1002247. doi: 10.1371/journal.ppat.1002247 [doi].

185. **Fahy, A. S., R. H. Clark, E. F. Glyde, and G. L. Smith.** 2008. Vaccinia virus protein C16 acts intracellularly to modulate the host response and promote virulence. J. Gen. Virol. **89:**2377-2387. doi: 10.1099/vir.0.2008/004895-0 [doi].

186. **Benfield, C. T., D. S. Mansur, L. E. McCoy, B. J. Ferguson, M. W. Bahar, G. L. Smith, J. M. Grimes, D. I. Stuart, S. C. Graham, and G. L. Smith.** 2011. Mapping the IkappaB kinase beta (IKKbeta)-binding interface of the B14 protein, a vaccinia virus inhibitor of IKKbeta-mediated activation of nuclear factor kappaB. The Journal of Biological Chemistry. **286:**20727-20735. doi: 10.1074/jbc.M111.231381.

187. **Teferi, W. M., M. A. Desaulniers, R. S. Noyce, M. Shenouda, B. Umer, and D. H. Evans.** 2017. The vaccinia virus K7 protein promotes histone methylation associated with heterochromatin formation. PLoS One. **12:**e0173056. doi: 10.1371/journal.pone.0173056 [doi].

188. **Ferguson, B. J., C. T. Benfield, H. Ren, V. H. Lee, G. L. Frazer, P. Strnadova, R. P. Sumner, and G. L. Smith.** 2013. Vaccinia virus protein N2 is a nuclear IRF3 inhibitor that promotes virulence. J. Gen. Virol. **94:**2070-2081. doi: 10.1099/vir.0.054114-0 [doi].

189. **Yuwen, H., J. H. Cox, J. W. Yewdell, J. R. Bennink, and B. Moss.** 1993. Nuclear localization of a double-stranded RNA-binding protein encoded by the vaccinia virus E3L gene. Virology. **195:**732-744. doi: S0042-6822(83)71424-8 [pii].

190. **Vega, F. M., A. Sevilla, and P. A. Lazo.** 2004. p53 Stabilization and accumulation induced by human vaccinia-related kinase 1. Mol. Cell. Biol. **24:**10366-10380. doi: 10.1128/MCB.24.23.10366-10380.

191. **Sevilla, A., C. R. Santos, R. Barcia, F. M. Vega, and P. A. Lazo.** 2004. c-Jun phosphorylation by the human vaccinia-related kinase 1 (VRK1) and its cooperation with the N-terminal kinase of c-Jun (JNK). Oncogene. **23:**8950-8959.

192. **Sevilla, A., C. R. Santos, F. M. Vega, and P. A. Lazo.** 2004. Human Vaccinia-related Kinase 1 (VRK1) Activates the ATF2 Transcriptional Activity by Novel Phosphorylation on Thr-73 and Ser-62 and Cooperates with JNK. Journal of Biological Chemistry. **279:**27458-27465. doi: 10.1074/jbc.M401009200.

193. **Moura, D. S., I. Campillo-Marcos, M. Vazquez-Cedeira, and P. A. Lazo.** 2018. VRK1 and AURKB form a complex that cross inhibit their kinase activity and the phosphorylation of histone H3 in the progression of mitosis. Cell Mol. Life Sci. **75:**2591-2611. doi: 10.1007/s00018-018-2746-7 [doi].

194. **Hirota, T., J. J. Lipp, B. H. Toh, and J. M. Peters.** 2005. Histone H3 serine 10 phosphorylation by Aurora B causes HP1 dissociation from heterochromatin. Nature. **438:**1176-1180. doi: nature04254 [pii].

195. **Barcia, R., S. López-Borges, F. M. Vega, and P. A. Lazo.** 2002. Kinetic Properties of p53 Phosphorylation by the Human Vaccinia-Related Kinase 1. Arch. Biochem. Biophys. **399:**1-5. doi: 10.1006/abbi.2001.2746.

196. **Vega, F. M., P. Gonzalo, M. L. Gaspar, and P. A. Lazo.** 2003. Expression of the VRK (vaccinia-related kinase) gene family of p53 regulators in murine hematopoietic development. FEBS Lett. **544:**176-180.

197. **Blanco, S., C. Santos, and P. A. Lazo.** 2007. Vaccinia-Related Kinase 2 Modulates the Stress Response to Hypoxia Mediated by TAK1. Molecular and Cellular Biology. **27:**7273-7283. doi: 10.1128/MCB.00025-07.

198. **Fernandez, I. F., L. G. Perez-Rivas, S. Blanco, A. A. Castillo-Dominguez, J. Lozano, and P. A. Lazo.** 2012. VRK2 anchors KSR1-MEK1 to endoplasmic reticulum forming a macromolecular complex that compartmentalizes MAPK signaling. Cell Mol. Life Sci. **69:**3881-93. doi: 10.1007/s00018-012-1056-8.

199. **Boudeau, J., D. Miranda-Saavedra, G. J. Barton, and D. R. Alessi.** 2006. Emerging roles of pseudokinases. Trends Cell Biol. **16:**443-452. doi: S0962-8924(06)00175-9 [pii].

200. **Valbuena, A., A. Suárez-Gauthier, F. López-Rios, A. López-Encuentra, S. Blanco, P. L. Fernández, M. Sánchez-Céspedes, and P. A. Lazo.** 2007. Alteration of the VRK1-p53 autoregulatory loop in human lung carcinomas. Lung Cancer. **58:**303-309. doi: 10.1016/j.lungcan.2007.06.023.

201. **Liu, Z. C., K. Cao, Z. H. Xiao, L. Qiao, X. Q. Wang, B. Shang, Y. Jia, and Z. Wang.** 2017. VRK1 promotes cisplatin resistance by up-regulating c-MYC via c-Jun activation and serves as a therapeutic target in esophageal squamous cell carcinoma. Oncotarget. **8:**65642-65658. doi: 10.18632/oncotarget.20020 [doi].

202. **Renbaum, P., E. Kellerman, R. Jaron, D. Geiger, R. Segel, M. Lee, M. C. King, and E. Levy-Lahad.** 2009. Spinal Muscular Atrophy with Pontocerebellar Hypoplasia Is Caused by a Mutation in the VRK1 Gene. The American Journal of Human Genetics. **85:**281-289. doi: 10.1016/j.ajhg.2009.07.006.

203. **Vinograd-Byk, H., P. Renbaum, and E. Levy-Lahad.** 2018. Vrk1 partial Knockdown in Mice Results in Reduced Brain Weight and Mild Motor Dysfunction, and Indicates Neuronal VRK1 Target Pathways. Sci. Rep. **8:**11265-018-29215-x. doi: 10.1038/s41598-018-29215-x [doi].

204. **Chan, K. L., P. S. North, and I. D. Hickson.** 2007. BLM is required for faithful chromosome segregation and its localization defines a class of ultrafine anaphase bridges. Embo J. **26:**3397-3409. doi: 7601777 [pii].

205. **Wyatt, H. D., S. Sarbajna, J. Matos, and S. C. West.** 2013. Coordinated actions of SLX1-SLX4 and MUS81-EME1 for Holliday junction resolution in human cells. Mol. Cell. **52:**234-247. doi: 10.1016/j.molcel.2013.08.035 [doi].

206. **Germann, S. M., V. Schramke, R. T. Pedersen, I. Gallina, N. Eckert-Boulet, V. H. Oestergaard, and M. Lisby.** 2014. TopBP1/Dpb11 binds DNA anaphase bridges to prevent genome instability. J. Cell Biol. **204:**45-59. doi: 10.1083/jcb.201305157 [doi].